PREPARATION OF NANOPARTICLE-BASED ELICITORS AND THEIR ABILITY TO CONTROL CASSAVA LEAF SPOT DISEASE

NGUYEN HUY HOANG

A Thesis Submitted in Partial Fulfillment of the Requirements for the

Degree of Master of Science in Crop Science

Suranaree University of Technology

Academic Year 2021

การผลิตและการเตรียมอนุภาคนาโนอิลิซิเตอร์และความสามารถในการควบคุมโรคใบจุดมันสำปะหลัง

เหงียน ฮุ่ย ฮวง

วิทยานิพนธ์นี้เป็นส่วนหนึ่งของการศึกษาตามหลักสูตรปริญญาวิทยาศาสตรมหาบัณฑิต
สาขาวิชาพืชศาสตร์
มหาวิทยาลัยเทคโนโลยีสุรนารี
ปีการศึกษา 2564

PREPARATION OF NANOPARTICLE-BASED ELICITORS AND THEIR ABILITY TO CONTROL CASSAVA LEAF SPOT DISEASE

Suranaree University of Technology has approved this thesis submitted in partial fulfillment of the requirements for a Master's Degree.

Thesis Examining Committee

(Asst. Prof. Dr. Thitiporn Machikowa)
Chairperson

(Asst. Prof. Dr. Natthiya Buensanteai)
Member (Thesis Advisor)

(Asst. Prof. Dr. Anyanee Kamkaew)
Member (Thesis Co-advisor)

(Dr. Wanploy Jinagool)
Member

(Dr. Toan Le Thanh)
Member

(Assoc. Prof. Dr. Chatchai Jothityangkoon)
Vice Rector for Academic Affaire
and Quality Assurance

(Prof. Dr. Neung Teaumroong)
Dean of Institute of Agricultural
Technology

เหงียน ฮุ่ย ฮวง: การผลิตและการเตรียมอนุภาคนาโนอิลิซิเตอร์และความสามารถในการควบคุมโรคใบจุดมันสำปะหลัง (PREPARATION OF NANOPARTICLE-BASED ELICITORS AND THEIR ABILITY TO CONTROL CASSAVA LEAF SPOT DISEASE) อาจารย์ที่ปรึกษา : ผู้ช่วยศาสตราจารย์ ดร.ณัฐธิญา เบือนสันเทียะ, 258 หน้า

อัลเทอร์นาเรีย/มันสำปะหลัง/ใบจุด/อนุภาคนาโน/ตัวกระตุ้น

วัตถุประสงค์ของการศึกษานี้คือ (1) เพื่อตรวจหาเชื้อราสาเหตุโรคใบจุดมันสำปะหลังในประเทศไทย (2) เพื่อสังเคราะห์อิลิซิเตอร์อนุภาคนาโนที่มีประสิทธิภาพในการต่อต้านโรคใบจุดมันสำปะหลัง และ (3) เพื่อประเมินวิธีการใช้อิลิซิเตอร์อนุภาคนาโนในการลดโรคใบจุดมันสำปะหลังในสภาพโรงเรือนตาข่าย เริ่มจากเชื้อราสาเหตุโรคใบจุดมันสำปะหลังถูกตรวจสอบและจำแนกตามตามวิธีการของ Koch's postulates ผลการศึกษาพบว่า สามารถแยกเชื้อราบริสุทธิ์และจำแนกเชื้อราได้ทั้งหมดจำนวน 36 ไอโซเลต จากใบพืชสาเหตุโรคใบจุดจำนวน 16 ตัวอย่าง ในจำนวนนี้ มีเชื้อราที่แยกได้ 23 ไอโซเลต ที่แสดงความรุนแรงในการก่อให้เกิดโรค โดยทำให้เกิดจุดแผลเน่าในใบพืชด้วยวิธีการ detached leaves ไอโซเลตที่มีความรุนแรงในการก่อโรคมากที่สุดนั้น ทำให้เกิดแผลเน่าขนาด 28.35-32.72 × 25.70-29.70 มม. และ 26.86-30.57 × 19.20-24.05 มม. โดยคิดเป็น 30.4 และ 34.8% ของพื้นที่ใบทั้งหมด ตามลำดับ ลักษณะทางสัณฐานวิทยาและการจัดลำดับของโมเลกุลบริเวณ ITS region สามารถจำแนกได้ว่าเป็นเชื้อรา *Alternaria alternata* จำนวน 14 ไอโซเลต และ *Alternaria solani* จำนวน 9 ไอโซเลต ซึ่ง *A. alternata* นั้น มีความรุนแรงในการก่อให้เกิดโรคใบจุดมันสำปะหลังสูงกว่า *A. solani* จากการทดสอบความสามารถในการก่อให้เกิดโรค พบว่า *A. alternata* ก่อให้เกิดอาการแผลตายและแผลใหม้บนใบมันสำปะหลัง เทคนิค Synchrotron (SR) Fourier-Transform Infrared Spectroscopy (FTIR) ถูกนำมาใช้ในการตรวจสอบการเปลี่ยนแปลงของสารประกอบทางชีวเคมีของเนื้อเยื่อใบบริเวณชั้น epidermis และชั้น mesophyll เมื่อมีการเข้าทำลายของเชื้อรา *A. alternata* ผลการศึกษาพบว่า ปริมาณของ pectins, polysaccharides, celluloses, hemicelluloses เพิ่มขึ้น ส่วนปริมาณของ lipids, proteins, phenolics, ligins, carbohydrate ลดลงสำหรับการทดลองการสังเคราะห์อิลิซิเตอร์อนุภาคนาโนโดยใช้ Chitosan (CS) (0.4% หรือ 0.5%) และ pentasodium triphosphate (0.2% หรือ 0.5%) กับ salicylic acid (SA) 0.05, 0.1 and 0.2% หรือ silver nitrate 1, 2, 3 mM ถูกนำมาเตรียม CS-NP-loaded SA จำนวน 3 สูตร ได้แก่ N1, N2, N3 และ CS-NP-loaded silver จำนวน 3 สูตร ได้แก่ N4, N5, N6 ตามลำดับ NPs ทั้งหมด 6 สูตร ได้ผ่านการพิสูจน์แล้วว่าไม่เป็นพิษต่อใบมันสำปะหลัง โดยสูตร CS-NP-loaded

SA (N3) และ CS-NP-loaded silver (N6) มีประสิทธิภาพสูงกว่าสูตรอื่นๆ (N1, N2, และ N4, N5) ในการลดความรุนแรงและดัชนีการเกิดโรคใบจุด นอกจากนี้ สูตร N3 ที่ความเข้มข้น 400 ppm และ N6 ที่ความเข้มข้น 200, 400, 800 ppm สามารถลดความรุนแรงของโรคได้เท่ากับ 68.9-73.6% หรือ 37.0-37.7% โดยขึ้นอยู่กับระยะเวลาในการทดสอบและความหนาแน่นของเชื้อราสาเหตุโรค และส่งเสริมการเจริญเติบโตของพืชได้สูงกว่าหรือเทียบเท่ากับการใช้สารเคมีกำจัดโรคพืชเชิงพาณิชย์ (pyraclostrobin และ flutriafol) หรือ อนุภาคนาโน zinc oxide ภายใต้สภาพโรงเรือนตาข่าย ในการอธิบายลักษณะเฉพาะของอนุภาค พบว่าเส้นผ่านศูนย์กลางของอนุภาคแบบไฮโดรไดนามิคของ N3 และ N6 เท่ากับ 89.86 ± 9.04 และ 249.67 ± 23.97 นาโนเมตร ในขณะที่ดัชนีการกระจายหลายตัวเท่ากับ 0.36 ± 0.02 และ 0.53 ± 0.03 ศักย์ซีตาเท่ากับ 22.27 ± 1.01 และ 13.53 ± 0.74 mV ตามลำดับ กลุ่มฟังก์ชันและสัณฐานวิทยา รูปแบบทรงกลมและโครงสร้างที่มีรูพรุน เมื่อทำการตรวจสอบและยืนยันโดย FTIR และกล้องจุลทรรศน์อิเล็กตรอนแบบส่องกราด (Field Emission Scanning Electron Microscope) ตามลำดับ จากนั้น ทำการศึกษาประสิทธิภาพของสูตร N3 ที่ความเข้มข้น 400 ppm และสูตร N6 ที่ความเข้มข้น 200, 400, 800 ppm ในการลดการเกิดโรคใบจุดในมันสำปะหลังทั้งก่อนและหลังใช้ ในสภาพโรงเรือนตาข่าย และประเมินความรุนแรงในการก่อให้เกิดโรคของเชื้อรา *A. alternata* หลังจากได้รับการทดสอบด้วยสูตร CS-NP ด้วยวิธีการ detached leaves ผลการศึกษาพบว่าค่าเฉลี่ยความรุนแรงของโรคก่อนและหลังการทดสอบนั้นไม่มีความแตกต่างทางสถิติ ในขณะที่ค่าเฉลี่ยความรุนแรงของโรคที่ทดสอบด้วย CS-NP นั้นอยู่ที่ 26.77-28.11% ใกล้เคียงกับ flutriafol (28.65%) ซึ่งน้อยกว่าอนุภาคนาโน zinc oxide เชิงพาณิชย์ (32.58%) การทดสอบด้วยสูตร N3 ความเข้มข้น 400 ppm และสูตร N6 ความเข้มข้น 200 ppm สามารถยับยั้งการงอกของโคนิเดียได้ 32.51 และ 23.25% ตามลำดับ การแช่ชิ้นส่วนเส้นใยของ *A. alternata* ในสูตรสารข้างต้น สามารถลดการเจริญเติบโตของเส้นใยและความรุนแรงในการก่อให้เกิดแผลเน่าได้ 42.26 และ 51.11% ยิ่งไปกว่านั้น การแช่ในสารข้างต้นนี้ทำให้มี อัตราของเซลล์ตายต่อเซลล์ที่ยังมีชีวิตสูงกว่าการแช่ในอนุภาคนาโน zinc oxide เชิงพาณิชย์ แต่ต่ำกว่าใน flutriafol สรุปได้ว่า CS-NP loaded SA (N3) ที่ความเข้มข้น 400 ppm และ CS-NP loaded silver (N6) ที่ความเข้มข้น 200 ppm นั้น สามารถนำมาใช้ในการจัดการกับโรคใบจุดในมันสำปะหลังได้

สาขาวิชาเทคโนโลยีการผลิตพืช
ปีการศึกษา 2564

ลายมือชื่อนักศึกษา .....
ลายมือชื่ออาจารย์ที่ปรึกษา .....
ลายมือชื่ออาจารย์ที่ปรึกษาร่วม .....

NGUYEN HUY HOANG: PREPARATION OF NANOPARTICLE-BASED ELICITORS AND THEIR ABILITY TO CONTROL CASSAVA LEAF SPOT DISEASE. THESIS ADVISOR : ASST. PROF. DR. NATTHIYA BUENSANTEAI, 258 PP.

Alternaria/CASSAVA/LEAF SPOT/NANOPARTICLE/ELICITOR

The objectives of this study were (1) to detect fungal pathogen associated with leaf spot disease on cassava in Thailand, (2) to synthesize effective nanoparticle (NP) - based elicitors against cassava leaf spot disease, and (3) to evaluate the application method of NP elicitors to reduce cassava leaf spot disease at net-house conditions. First, the fungal pathogen causing leaf spot disease on cassava plants was detected and identified following Koch's postulates. The results showed that 36 fungal isolates were isolated and purified from 16 leaf spot samples. Among these, 23 fungal isolates showed virulent activities by causing rot lesions on detached leaves assay. The most and highly virulent fungal isolate caused rot lesions with sizes 28.35-32.72 × 25.70-29.70 mm and 26.86-30.57 × 19.20-24.05 mm, accounting for 30.4 and 34.8% of total leaf area, respectively. The morphology and molecular sequencing on ITS region identified 14 isolates of *Alternaria alternata* and 9 isolates of *Alternaria solani,* the causal agents of cassava leaf spot disease in Thailand. The *A. alternata* was found to be more virulent than *A. solani*. In the pathogenicity test, *A. alternata* caused necrotic spot lesions and blight symptoms on cassava leaves. In addition, Synchrotron (SR) Fourier-Transform Infrared Spectroscopy (FTIR) was used to determine the biochemical changes in the epidermis and mesophyll tissues of leaves infected by *A. alternata*. The results showed an increase in pectins, polysaccharides, celluloses, and hemicelluloses and a decrease in lipids, proteins, phenolics, ligins, and carbohydrate components. Moreover, the chitosan (CS) (0.4%) and pentasodium triphosphate (TPP) (0.2%) were mixed with salicylic acid (SA) at 0.05, 0.1 and 0.2% to prepare three formulations of CS-NP-loaded SA named N1, N2, N3, respectively. Similarly, CS (0.5%) and TPP (0.5%) were mixed with silver nitrate at 1, 2, 3 mM to prepare three formulations of CS-NP-loaded silver named N4, N5, N6, respectively. The six NPs

formulations were proved to be non-toxic to cassava leaves. The CS-NP-loaded SA (N3) and CS-NP-loaded silver (N6) were more effective than the other remaining formulations (N1, N2, and N4, N5) in reducing disease severity and disease index of leaf spots. Furthermore, the N3 at 400 ppm and N6 at 200, 400, 800 ppm could reduce disease severity at 68.9-73.6% or 37.0-37.7%, depending on treatment time and pathogen density and could enhance plant growth higher than or equally to commercial fungicides (pyraclostrobin and flutriafol) or zinc oxide NPs under net house conditions. In characterization, the hydrodynamic diameters of N3 and N6 were 89.86 ± 9.04 and 249.67 ± 23.97 nm while polydispersity index was 0.36 ± 0.02 and 0.53 ± 0.03, and the zeta potential was 22.27 ± 1.01 and 13.53 ± 0.74 mV, respectively. The functional group and morphology as spherical forms and porous architecture were confirmed by FTIR and Field Emission Scanning Electron Microscope, respectively. After that, the effectiveness of pre- and post-treatments of N3 at 400 ppm and N6 at 200, 400, 800 ppm on reducing cassava leaf spot at net house conditions and the potential virulence of *A. alternata* treated by the CS-NP formulations in detached leaves were evaluated. The results showed that the disease severities of pre- and post-treatments were not significant while the disease severities of CS-NP treatments were 26.77-28.11% similar to flutriafol (28.65%), which are significantly lower than commercial zinc oxide NP (32.58%). The N3 400 ppm and N6 200 ppm treatments could inhibit *A. alternata* conidial germination by 32.51 and 23.25%, respectively. The soaking of *A. alternata* plugs into these two treatments could reduce mycelial growth and their potential virulence causing rot lesions by 42.26 and 51.11%, respectively. Furthermore, the soaking of these two treatments caused a higher cell death/live rate than one of the commercial zinc oxide NPs but lower than one of the flutriafol. In conclusion, CS-NP loaded SA (N3) at 400 ppm and CS-NP loaded silver (N6) at 200 ppm are a promising solution in cassava leaf spot management.

School of Crop Production Technology
Academic Year 2021

Student's Signature .....
Advisor's Signature .....
Co-advisor's Signature .....

ACKNOWLEDGEMENT

To my mother and my father, who gave birth to me, my whole life is devoted to my life and career.

This Thesis cannot be completed without support Suranaree University of Technology (SUT OROG Scholarship [M6201616; No. 67/2562]). I would like to express my sincerest appreciation and deepest gratitude to all the following individuals:

My advisor, Asst. Prof. Dr. Natthiya Buensanteai, for giving me an opportunity to study Master Degree at Suranaree University of Technology, as well as Her vision and support for my research. My co-advisor, Asst. Prof. Dr. Anyanee Kamkaew, for support my works related chemistry field. Dr. Toan Le Thanh, for His guidance and help in carrying out the research. Dr. Sopone Wongkaew, for His suggestions on my experiment, proposal, and Thesis.

Asst. Prof. Dr. Thitiporn Machikowa, Dr. Wanploy Jinagool, and Asst. Prof. Dr. Sodchol Wonprasaid for their valuable comments and suggestions during my comprehensive, proposal and Thesis examination. Dr. Kanjana Thumanu, Dr. Supatcharee Siriwong for training FTIR techniques at Synchrotron Light Research Institute (SLRI), Thailand. Ms. Hataikan Tongjareon and CIA staffs, for their encouragement, and care during my years at Suranaree University of Technology.

Dr. Chanon Saengchan, Dr. Narendra Kumar Papathoti, Dr. Rungthip Sangpueak, Dr. Wannaporn Thepbandit, Ms. Dusadee Kiddeejing, Ms. Kansinee Laemchiab, Ms. Kodchaphon Tonpho, Ms. Nattaya Thongprom, Ms. Parichat Numparditsub, Ms. Supaluk Tamphimai, Mr. Akkawat Tharapreuksapong, Mr. Nattapol Prasert, Ms. Oratai Nachin, and all members of Plant Pathology and Bio Pesticide Lab, for supporting materials and techniques in experiment.

Ms. Chadapon Chaiyapan, Ms. Jongjit Treekoon, Ms. Tanaporn Jaichopsanthia, Ms. Pimvipa Arom, Ms. Anusara Saeng-ngam, Ms. Pichaya Nokphutsa, Ms. Rattanaporn Toemkhunthod, Ms. Thai Ngoc Oanh, Ms. Minh Thu for helping my experiments and collecting data.

Bioactive Agro Industry Co., Ltd and CS Tapioca Research & Innovation Co., Ltd. for supporting fund experiments.

Mr. Nguyen Huy Hoang for His efforts, persist and believes in himself in his work until successful.

Nguyen Huy Hoang

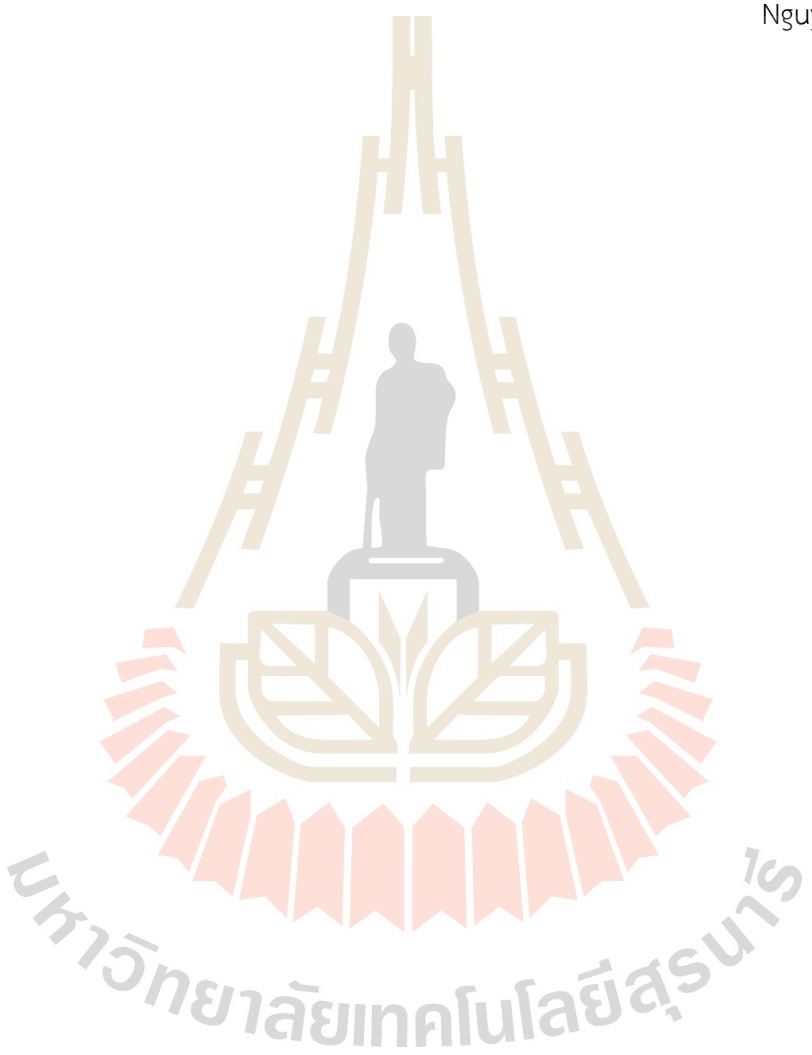

CONTENTS

CONTENTS (Continued)

Page

CONTENTS (Continued)

Page

CONTENTS (Continued)

Page

CONTENTS (Continued)

Page

CONTENTS (Continued)

Page

LIST OF TABLES

Table **Page**

LIST OF TABLES (Continued)

Table **Page**

LIST OF FIGURES

Figure **Page**

LIST OF FIGURES (continued)

Figure **Page**

LIST OF FIGURES (continued)

Figure **Page**

LIST OF FIGURES (continued)

Figure **Page**

LIST OF FIGURES (continued)

Figure **Page**

LIST OF FIGURES (continued)

Figure **Page**

LIST OF ABBREVIATIONS

°C	=	Degree Celsius
µL	=	Microliter (s)
µm	=	Micrometer (s)
min	=	Minute (s)
mL	=	Milliliter (s)
mM	=	Millimolar (s)
nm	=	Nanometer (s)
ha	=	Hectare
mV	=	millivolt
CS	=	Chitosan
D. R.	=	Democratic republic
DAI	=	Days after inoculation
DAP	=	Days after planting
DLS	=	Dynamic light scattering
DMRT	=	Duncan's multiple range test
FAO	=	Food and Agriculture Organization
FAOSTAT	=	Food and Agriculture Organization Corporate Statistical Database
FTIR	=	Fourier-transform infrared spectroscopy
ITS	=	Internal transcribed spacer
NP	=	Nanoparticle
PCA	=	Principal component analysis
PCR	=	Polymerase chain reaction
PDI	=	Polydispersity index
PI	=	Propidium iodide
ROS	=	Reactive oxygen species

LIST OF ABBREVIATIONS (Continued)

SA	=	Salicylic acid
SEM	=	Scanning electron microscope
SR	=	Synchrotron
TEM	=	Transmission electron microscopy
TPP	=	Sodium tripolyphosphate
U. R.	=	United republic
UV	=	Ultra violet
XRD	=	X-Ray Diffraction

CHAPTER I

INTRODUCTION

1.1 Background of the selected topic

The cassava (*Manihot esculenta* Crantz) plant and its tapioca are an important food source for world food security, especially in developing countries. Cassava is used in the production of food, industry, and animal feed. It is called "the 21st-century crop" as well as "food of the poor" (Henry and Hershey, 2002; Food and Agriculture Organization (FAO), 2013; Uchechukwu-Agua *et al*., 2015). The cassava plant originates from Latin America, its area and production are dominated by Africa but brings foreign currency to Southeast Asian countries. Thailand's cassava acreage and production reached 1.34 million hectares and 30.84 million tons in 2017, which has increased by 1.15 folds over the previous ten years. Although, Thailand's acreage and production account for only 5.45 and 11.04% of the world, the quantity and value of Thailand are between 58.5-81.2 and 44.4-56.7% in the world export market, respectively. Furthermore, this is Thailand's key export crop (FAOSTAT, 2020). Cassava can tolerate drought or nutrient-poor soil, so it also has a role at water-deficient farming areas. However, the biotic damages from diseases, insects, weeds or adverse environmental factors severely affect the growth of cassava, leading to loss of yield. Currently, twenty-eight types of diseases on cassava caused by fungi, viruses, bacteria and phytoplasma have been recorded. Among them, cassava mosaic disease, cassava brown streak disease, and bacterial blight disease can result in up to 90, 70, and 75% of yield reductions, respectively (Neuenschwander, 2008; Obiazi and Ojobor, 2013; McCallum *et al*., 2017). On cassava, there are many types of leaf spot diseases including cassava brown leaf spot, cassava white spot disease (*Cercospora caribaea* or *Passarola manihotis*), and cassava diffuse/blight leaf spot (*Cercospora vicosae* or *Passarola*

vicosae). Cassava brown leaf spot disease is commonly known to be caused by *Cercospora henningsii*, or *Cercosporidium henningsii* (Hillocks and Wydra, 2002; Reddy, 2015; McCallum *et al*., 2017). Besides, it has been reported to be caused by a variety of fungi with different names including *Mycosphaerella manihotis* in Colombia (Teri *et al*., 1980), *Cercospora henningsii* in Ghana (Ayesu-Offei and Antwi-Boasiako, 1996), *C. henningsii* [*Mycosphoraella henningsii*] in India (Prabakar and Raguchander, 2000), *Passalora henningsii* in China and Brazil (Pei *et al*., 2014; de Freitas *et al*., 2017), *Clarohilum henningsii* in Indonesia and Brazil (Hidayat *et al*., 2020; Julião *et al*., 2020), combination of 3 fungi *Colletotrichum*, *Alternaria*, and *Cladosporium* in Kenya (Ng'ang'a *et al*., 2019). The disease causes a loss of up to 30% of cassava yield. However, the disease is often neglected until a recent outbreak in Brazil (Julião *et al*., 2020). It is now possible to implement cultural methods, chemical methods, and host resistance to control and manage these cassava diseases. Fungicides containing copper, benomyl, thiophanate, carbendazim, flutriafol, cyproconazole, pyraclostrobin, thiophanate-methyl, tebuconazole, and azoxystrobin can control pathogens with varying degrees of efficacy. Hence, the fungicide is a popular method to reduce the damage of the cassava leaf spot. Also, the cassava cultivars Sri Prakash and Sri Visakam are recommended to resist cassava brown leaf spot disease in India (Prabakar and Raguchander, 2000; Reddy, 2015; Julião *et al*., 2020). Besides, each individual of plant had an innate immune system against adverse environmental factors including abiotic and biotic stresses, which differed levels depending on the cultivar and adverse factors. The plant's immune system can be artificially induced by the elicitor. Elicitors are biotic or abiotic compounds, which activate defense mechanisms and innate immunity in plants against pathogens and stress conditions. The elicitors may be chemical, microbial, chitosan (CS), plant extracts, algal extracts, composts, biochar. As such, applying appropriate elicitors could aid plants against pathogens, as well as cassava leaf spot disease (Burketova *et al*., 2015; Corwin and Kliebenstein, 2017). In previous, the salicylic acid formulations including RS and Zacha11 have able to reduce anthracnose, root rot disease and also enhance stem height, root length, and the

number of roots on cassava (Saengchan *et al*., 2021; Sangpueak *et al*., 2021). In recent years, nanotechnology has been applied to many fields in agriculture including nanofertilizers, nanobiotechnology, nanomaterials, nanosensors, nanopesticides to improve crop yield and quality, especially to build sustainable agriculture (Shang *et al*., 2019). Nanoparticles (NPs) are used as protectants (silver, gold, copper, titanium dioxide, CS) or carriers (CS, silica, solid lipid, layered double hydroxide) of active compounds (insecticides, fungicides, herbicides, RNA-interference) to protect plants against bacteria, fungi, viruses, insects. Superior features of NPs are improvement of shelf-life, target at site-specific uptake, and increase of solubility. Furthermore, it reduces soil leaching and toxicity (Worrall *et al*., 2018). NPs in the form of nutrients and non-nutrients are provided to plants through leaves or roots to improve plant health as well as control plant diseases. Foliar spray of silver NPs at 50-70 ppm on tomato plants reduced disease severity caused by *Tomato mosaic virus* and *Potato virus Y* from 3.9-4.8 and 2.2-4.5 folds, respectively. It also increases chlorophyll content, total soluble protein, activities of peroxidase and polyphenol oxidase (Noha *et al*., 2018). Also, CS-NP loaded salicylic acid (SA) at 0.01-0.16% can inhibit *Fusarium verticillioides* mycelium growth at 62.2-100% and spore germination at 48.3-60.5% under *in-vitro* conditions. And it acts as an elicitor, able to activate the defense system of the maize plants to reduce post-flowering stalk rot disease at 40.5 to 59.47% and increase yield by 1.3 to 1.5 folds when compared with the control at field conditions (Kumaraswamy *et al*., 2019). CS-NP loaded copper at 0.1% have been able to inhibit mycelium growth of *Alternaria alternata*, *Macrophomina phaseolina* and *Rhizoctonia solani* at 89.5, 63.0 and 60.1%, higher than CS-NP loaded saponin at 0.1% and CS-NP at 0.06 or 0.1%, are 80.9, 66.2, 27.7% and 78.3, 66.2, 27.7 or 82.2, 87.6, 34.4%, respectively. In addition, both CS-NPs, CS-NP loaded copper and CS-NP loaded saponin at 0.06% inhibited the germination of *A. alternata* at 84.4, 83.3 and 78.3%, respectively (Saharan *et al*., 2013). There are two approaches to synthesize NPs including top-down and bottom-up methods, which result in NPs with different sizes, shapes and functions. Some synthetic NPs for use as a pesticide are not too difficult to implement, such as

sol-gel processes, green synthesis by microorganisms or plant extracts (Singh *et al*., 2018). The ionic gelation technique for the production of micro-particles or NPs is based on the electrostatic interaction between ions with different charges which was discovered by Calvo *et al*. (1997). This system can load additional macromolecules or drugs as a delivery system to improve biological activity or efficiency. The method is simple, fast, economical, easy to implement, and does not use organic solvents, but it is important to select materials and optimize the process to produce suitable effective NPs (Du *et al*., 2009; Debnath *et al*., 2011; Koukaras *et al*., 2012; Kunjachan *et al*., 2014; Giri, 2016; Pedroso-Santana and Fleitas-Salazar, 2020).

The cassava leaf spot was a complex disease. The recent year control method of cassava leaf spot disease was used synthetic pesticides. However, the application of NPs on cassava plants to control or manage cassava diseases in general and cassava leaf spots is not yet available. This study was carried out to detect fungal pathogen associated with leaf spot disease on cassava in Thailand, to prepare the NP-based elicitors and to evaluate its effectiveness for the management of cassava leaf spots.

1.2 Research objectives of this study

1.2.1 To detect fungal pathogen associated with leaf spot disease on cassava in Thailand.

1.2.2 To synthesize effective NP elicitors against cassava leaf spot disease.

1.2.3 To evaluate the application method of NP elicitors on the reduction of cassava leaf spot disease at net-house conditions.

1.3 Research hypotheses of this study

1.3.1 The fungal pathogen can be detected from cassava leaf spot disease in Thailand.

1.3.2 The proposed NP elicitors can be synthesized, reproducible and can effectively control cassava leaf spot disease.

1.3.3 The suitable method of applying NP elicitors can reduce cassava leaf spot disease at net-house conditions.

1.4 Significance and designed paths of this study

1.4.1 Significance of this study

The leaf spot was a common, important and complex disease on cassava. The fungal pathogens of the disease were different in many reports in the world. A commonly known white leaf spot is caused by *C. caribaea* (*P. manihotis*) or *P. manihotis* while diffuse or blight leaf spot is *C. vicosae* or *P. vicosae*, and the brown leaf spot is *C. henningsii* or *C. henningsii* (Reddy, 2015; de Freitas *et al*., 2017; McCallum *et al*., 2017). However, brown leaf spot has been reported by many other names including *M. manihotis* in Colombia (Teri *et al*., 1980), *C. henningsii* in Ghana (Ayesu-Offei and Antwi-Boasiako, 1996), *C. henningsii* (*M. henningsii*) in India (Prabakar and Raguchander, 2000), *P. henningsii* in China and Brazil (Pei *et al*., 2014; de Freitas *et al*., 2017), *Colletotrichum*, *Alternaria*, *Cladosporium* in Kenya (Ng'ang'a *et al*., 2019) and *C. henningsii* in Indonesia and Brazil (Hidayat *et al*., 2020; Julião *et al*., 2020). Thus, the first objective of this study was to detect fungal pathogen associated with cassava leaf spot disease in Thailand. Fungicides containing copper, benomyl, thiophanate, carbendazim, flutriafol, cyproconazole, pyraclostrobin, thiophanate-methyl, tebuconazole, and azoxystrobin can control pathogens with varying degrees of efficacy. The flutriafol was shown a high effective control brown leaf spot disease in Brazil (Julião *et al*., 2020). However, the chemical fungicide was not a sustainable control method because of the toxic risks to the environment and humans. In recent years, application of nanotechnology to build sustainable agriculture was a trend. Nano-fungicides, nano-fertilizers, and nano-stimulants can be applied to control diseases and improve plant growth. Hence, the second and third objectives of this

study were to synthesize effective NP elicitors and to evaluate the application method on reducing leaf spot disease on cassava plants.

1.4.2 Designed paths of this study

This study was divided into three main parts including fifteen successive experiments that were described in chapter III, IV, and V.

In chapter III, the fungal pathogens were isolated from leaf spot samples collected from cassava fields in Nakhon Ratchasima, Thailand. Then, the virulence of fungal pathogen was tested by the detached leaf method. The virulent fungal strains were identified by sequencing Internal transcribed spacer (ITS) region and morphology characters. The most virulent fungal strain was used for pathogenicity test. Moreover, the Synchrotron (SR) Fourier-transform infrared spectroscopy (FTIR) was used to detect biochemical changes in diseased tissues of cassava leaves.

Interestingly, the experiment studies on management of leaf spot disease by NP elicitors was carried out according to reverse research model. In chapter IV, six CS-NP loaded SA or silver were synthesized by ionic gelation method. Then, these at 6 concentrations including 25, 50, 100, 200, 400, 800 ppm were used to evaluate potential reducing leaf spot as elicitors at net house conditions. One effective CS-NP loaded SA and CS-NP loaded silver at 6 concentrations were used to evaluate plant growth promoting. Besides, these formulations were characterized by detecting size, morphology, and function group interaction to confirm that was NPs. The most effective treatments for reducing disease were used for experiments presented on chapter IV.

In chapter V, the most effective treatments were tested their potential on reducing disease by pre- and post- inoculation at net-house conditions. The lower concentration with similar effectiveness was used to evaluate the ability on inhibiting conidial germination, mycelium growth and their virulent, cell live/death.

1.5 Scopes and limitation of this study

The purpose of this study is to detect fungal pathogen associated with leaf spot disease on cassava in Thailand, and to synthesize formulation elicitor-based NPs with different composition ratios. The study is also to evaluate the effects of prototype formulations on the inhibition of pathogens, as well as the control or management of leaf spot disease in cassava cv. Pirun 2 including application method, and application rate. Furthermore, the effectiveness of elicitor on cassava productivity was also be assessed at net-house conditions.

The limitation of this study is only the most virulent fungal pathogen was used to perform pathogenicity test and management by formulation elicitor-based NPs.

1.6 Expected results of this study

1.6.1 The detection of fungal pathogen associated with cassava leaf spot disease in Thailand.

1.6.2 The potential formula of elicitors NPs against cassava leaf spot disease effectively.

1.6.3 The application method of using elicitors of NPs effectively to reduce cassava leaf spot disease under net-house conditions.

1.7 References

Ayesu-Offei, E. N., & Antwi-Boasiako, C. (1996). Production of microconidia by *Cercospora henningsii* Allesch, cause of brown leaf spot of cassava (*Manihot esculenta* Crantz) and tree cassava (*Manihot glaziovii* Muell.-Arg.). *Annals of Botany*, 78(5): 653-657. doi:10.1006/anbo.1996.0173.

Burketova, L., Trda, L., Ott, P. G., & Valentova, O. (2015). Bio-based resistance inducers for sustainable plant protection against pathogens. *Biotechnology Advances*, 33(6): 994-1004. doi:10.1016/j.biotechadv.2015.01.004.

Calvo, P., Remunan - Lopez, C., Vila - Jato, J. L., & Alonso, M. J. (1997). Novel hydrophilic chitosan - polyethylene oxide nanoparticles as protein carriers. *Journal of Applied Polymer Science*, 63(1): 125-132. doi: 10.1002/(SICI)1097-4628(19970103)63:1<125::AID-APP13>3.0.CO;2-4.

Corwin, J. A., & Kliebenstein, D. J. (2017). Quantitative resistance: more than just perception of a pathogen. *The Plant Cell*, 29(4): 655-665. doi:10.1105/tpc.16.00915.

de Freitas, J. P. X., Diniz, R. P., de Oliveira, S. A. S., da Silva Santos, V., & de Oliveira, E. J. (2017). Inbreeding depression for severity caused by leaf diseases in cassava. *Euphytica*, 213(9): 1-12. doi:10.1007/s10681-017-1995-0.

Debnath, S., Kumar, R. S., & Babu, M. N. (2011). Ionotropic gelation–a novel method to prepare chitosan nanoparticles. *Research Journal of Pharmacy and Technology*, 4(4): 492-495.

Du, W. L., Niu, S. S., Xu, Y. L., Xu, Z. R., & Fan, C. L. (2009). Antibacterial activity of chitosan tripolyphosphate nanoparticles loaded with various metal ions. *Carbohydrate Polymers*, 75(3): 385-389. doi:10.1016/j.carbpol.2008.07.039.

FAOSTAT (2020). Rankings. Commodities by country. Retrieved from http://www.fao.org/faostat/en/#rankings/commodities_by_country_exports

Food and Agriculture Organization (FAO). (2013). *Save and Grow: Cassava: a guide to sustainable production intensification*. Rome: Food and Agriculture Organization of the United Nations.

Giri, T. K. (2016). Alginate containing nanoarchitectonics for improved cancer therapy. In Holban A. M. & Grumezescu A. M. (Eds.). *Nanoarchitectonics for Smart Delivery and Drug Targeting* (1st ed., pp. 565-588). Oxford: William Andrew. doi:10.1016/B978-0-323-47347-7.00020-3.

Henry, G. & Hershey, C. (2002). Cassava in South America and the Caribbean. In Hillocks, R. J., Thresh, J. M. & Bellotti, A. (Eds.). *Cassava: Biology, Production and Utilization* (1st ed, pp. 17-40). Cali, Colombia: CABI.

Hidayat, I., Hastuty, A., & Ramadhani, I. (2020). A molecular phylogenetic study of *Clarohilum henningsii* (Mycosphaerellaceae, Fungi) on cassava from Indonesia

based on the ITS rDNA sequence. *Journal of Microbial Systematics and Biotechnology*, 2(1): 40-45. doi:10.37604/jmsb.v2i1.43.

Hillocks, R. J. & Wydra, K. (2002). Bacterial, fungal and nematode diseases. In R. J. Hillocks, J. M. Thresh & A. Bellotti (Eds.). *Cassava: Biology, Production and Utilization*, (1st ed, pp. 261-280). Cali, Colombia: CABI.

Julião, E. C., Santana, M. D., Freitas-Lopes, R. D. L., Vieira, A. D. P., de Carvalho, J. S. B., & Lopes, U. P. (2020). Reduction of brown leaf spot and changes in the chlorophyll a content induced by fungicides in cassava plants. *European Journal of Plant Pathology*, 157(2): 433–439. doi:10.1007/s10658-020-02001-0.

Koukaras, E. N., Papadimitriou, S. A., Bikiaris, D. N., & Froudakis, G. E. (2012). Insight on the formation of chitosan nanoparticles through ionotropic gelation with tripolyphosphate. *Molecular Pharmaceutics*, 9(10): 2856-2862. doi:10.1021/mp300162j.

Kumaraswamy, R. V., Kumari, S., Choudhary, R. C., Sharma, S. S., Pal, A., Raliya, R., Biswas, P., & Saharan, V. (2019). Salicylic acid functionalized chitosan nanoparticle: a sustainable biostimulant for plant. *International Journal of Biological Macromolecules*, 123: 59-69. doi:10.1016/j.ijbiomac.2018.10.202.

Kunjachan, S., Jose, S., & Lammers, T. (2014). Understanding the mechanism of ionic gelation for synthesis of chitosan nanoparticles using qualitative techniques. *Asian Journal of Pharmaceutics*, 4(2): 148-153. doi:10.4103/0973-8398.68467.

McCallum, E. J., Anjanappa, R. B., & Gruissem, W. (2017). Tackling agriculturally relevant diseases in the staple crop cassava (*Manihot esculenta*). *Current Opinion in Plant Biology*, 38: 50-58. doi:10.1016/j.pbi.2017.04.008.

Neuenschwander P. (2008). Cassava Mealybug, *Phenacoccus manihoti* Matile-Ferrero (Hemiptera: Pseudococcidae). In Capinera, J. L. (Eds.). *Encyclopedia of Entomology* (1st ed, pp. 760-764). Dordrecht: Springer.

Ng'ang, P. W., Miano, D. W., Wagacha, J. M., & Kuria, P. (2019). Identification and characterization of causative agents of brown leaf spot disease of cassava in Kenya. *Journal of Applied Biology and Biotechnology*, 7(6): 1-7. doi:10.7324/JABB.2019.70601.

Noha, K., Bondok, A. M., & El-Dougdoug, K. A. (2018). Evaluation of silver nanoparticles as antiviral agent against ToMV and PVY in tomato plants. *Middle East Journal of Applied Sciences*, 8(01): 100-111.

Obiazi, C. C., & Ojobor, S. A., 2013. Production challenges of cassava and prospects. *Journal of Biology, Agriculture and Healthcare*, 3(14): 31-35.

Pedroso-Santana, S., & Fleitas-Salazar, N. (2020). Ionotropic gelation method in the synthesis of nanoparticles/microparticles for biomedical purposes. *Polymer International*, 69(5): 443-447. doi:10.1002/pi.5970.

Pei, Y. L., Shi, T., Li, C. P., Liu, X. B., Cai, J. M., & Huang, G. X. (2014). Distribution and pathogen identification of cassava brown leaf spot in China. *Genetics and Molecular Research*, 13(2): 3461-3473. doi:10.4238/2014.April.30.7.

Prabakar, K., & Raguchander, T. (2000). Fungicidal control of cassava brown leaf spot caused by *Cercospora henningsii* Allescher. *Madras Agricultural Journal*, 87(7/9), 537-538.

Reddy, P. P. (2015). Cassava, *Manihot esculenta*. In Reddy, P. P. (Ed.). *Plant Protection in Tropical Root and Tuber Crops* (1st ed, pp. 17-81). New Delhi: Springer India.

Saengchan, C., Phansak, P., Le Thanh, T., Papathoti, N. K., & Buensanteai, N. (2021). Efficacy of salicylic acid and a *Bacillus* bioproduct in enhancing growth of cassava and controlling root rot disease. *Journal of Plant Protection Research*, 61(3): 302-310. doi:10.24425/jppr.2021.137952.

Saharan, V., Mehrotra, A., Khatik, R., Rawal, P., Sharma, S. S., & Pal, A. (2013). Synthesis of chitosan based nanoparticles and their *in vitro* evaluation against phytopathogenic fungi. *International Journal of Biological Macromolecules*, 62: 677-683. doi:10.1016/j.ijbiomac.2013.10.012.

Sangpueak, R., Phansak, P., Thumanu, K., Siriwong, S., Wongkaew, S., & Buensanteai, N. (2021). Effect of salicylic acid formulations on induced plant defense against cassava anthracnose disease. *The Plant Pathology Journal*, 37(4): p.356. doi:10.5423/PPJ.OA.02.2021.0015.

Shang, Y., Hasan, M., Ahammed, G. J., Li, M., Yin, H., & Zhou, J. (2019). Applications of nanotechnology in plant growth and crop protection: a review. *Molecules*, 24(14): 2558. doi:10.3390/molecules24142558.

Singh, J., Dutta, T., Kim, K. H., Rawat, M., Samddar, P., & Kumar, P. (2018). 'Green'synthesis of metals and their oxide nanoparticles: applications for environmental remediation. *Journal of Nanobiotechnology*, 16(1): 1-24. doi:0.1186/s12951-018-0408-4.

Teri, J. M., Thurston, H. D., & Lozano, J. C. (1980). Effect of brown leaf spot and cercospora leaf blight on cassava productivity. *Tropical Agriculture*, 57(3): 239-243.

Uchechukwu-Agua, A. D., Caleb, O. J., & Opara, U. L. (2015). Postharvest handling and storage of fresh cassava root and products: a review. *Food and Bioprocess Technology*, 8(4): 729-748. doi:10.1007/s11947-015-1478-z.

Worrall, E. A., Hamid, A., Mody, K. T., Mitter, N., & Pappu, H. R. (2018). Nanotechnology for plant disease management. *Agronomy*, 8(12): 285. doi:10.3390/agronomy8120285.

CHAPTER II

LITERATURE REVIEW

2.1 Cassava plants

2.1.1 Plant taxonomy and distribution

Manihot esculenta Crantz belongs to the order Euphorbiales, family Euphorbiaceae, genus *Manihot* was domesticated from wild cassava from 5000-7000 BC, which was found to have originated from the Amazon region (Allem, 2002). It was brought from Latin America (New World) to other regions by European explorers (Henry and Hershey, 2002). In the world, it is often called cassava, or tapioca, Brazilian arrowroot (English), yuca (Spanish), and manioc (French). Besides, it is referred to as "มัน สำปะหลัง" or "khoai mì" in Thailand and Vietnam, respectively (CABI, 2020). Cassava is a tropical plant that can tolerate drought and acidity. This 21st-century crop has an important impact on developing countries and especially water-restricted regions such as sub-Saharan Africa, which has resulted in also known as "food of the poor" (Henry and Hershey, 2002; Food and Agriculture Organization (FAO), 2013).

2.1.2 Usage of cassava

Cassava is used in the production of food, industry, and animal feed. The two main parts used are the root tubers and the young leaves. Regarding food, cassava root is used to produce dough, tapioca, chips, starch, and high-quality cassava flour. Starch can be applied in manufacturing industries such as plywood, paper, beverage, textiles, sweeteners, fructose, amylose-free "waxy" starch, alcohol, monosodium glutamate, bio-fuel, and animal feed (**Figure 2.1**). In addition, cassava young leaves are used as food or in combination with pellets as an animal feed (FAO, 2013; Uchechukwu-Agua *et al*., 2015).

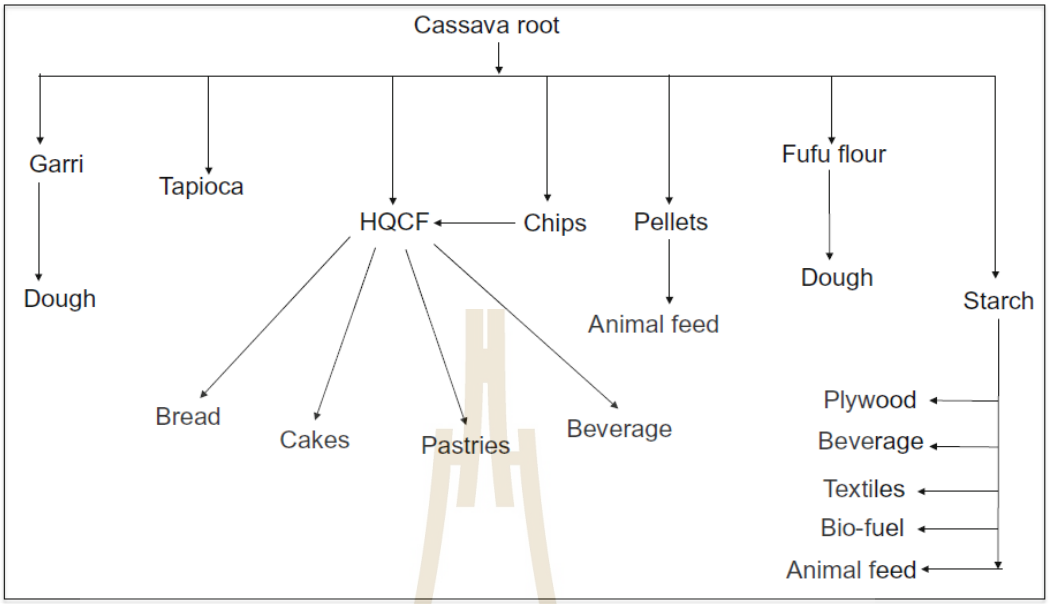

Figure 2.1 Different products derived from cassava tubers. *Note*: HQCF: high-quality cassava flour. Source: Uchechukwu-Agua *et al*., 2015.

2.1.3 Growth and development characteristics

The growing cycle of cassava is usually 12 months. Cassava stalk will germinate in the first 2 weeks period after being deeped into the soil. Leaves and root systems begin to form and develop 15 to 90 days after planting (DAP). Canopy including branching habit and plant architecture is established and developed (maximum growth rate leaves and stems) in stage of 90 - 180 DAP. Then, carbohydrates are vigorously synthesized and transported to the roots (tubers) in stage of 180 - 300 DAP. After that, the leaves fall and the roots stop their vegetative growth that changes to dormancy at 300 to 360 DAP (**Figure 2.2**) (Alves, 2002).

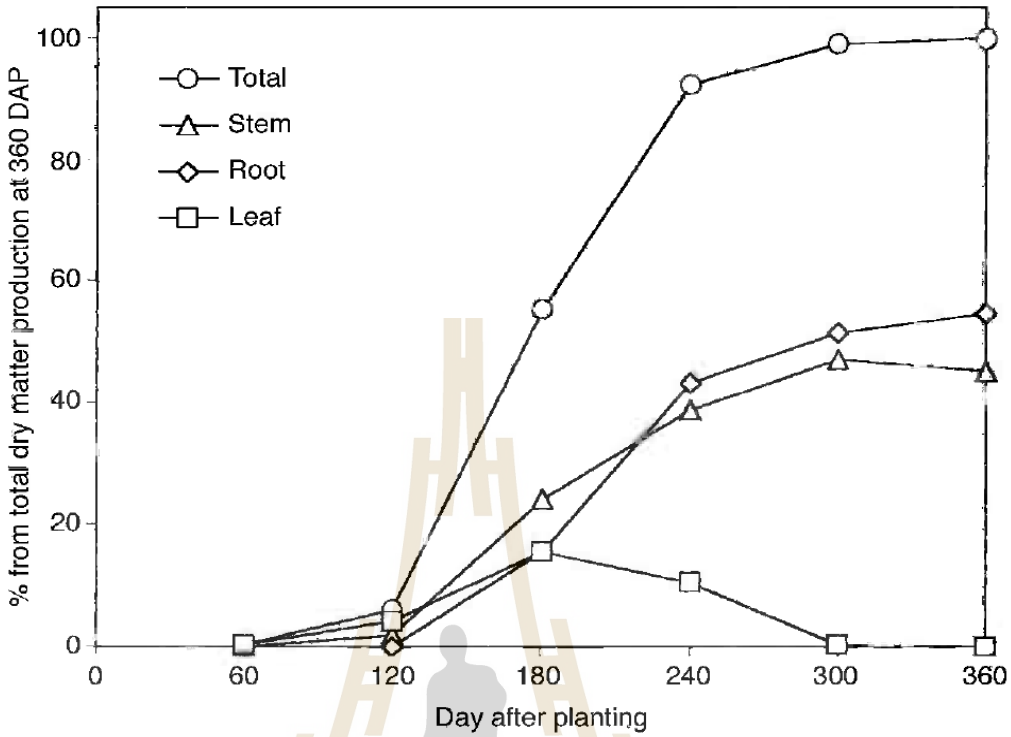

Figure 2.2 Growth of cassava plant during the first cycle (12 months). *Note*: DAP: days after planting. Source: Alves (2002).

2.1.4 Cassava cultivation story

The cassava-related data for 10 years (2007-2017) from The Food and Agriculture Organization Corporate Statistical Database (FAOSTAT) was used and analyzed to visualize cassava cultivation as well as answer the question "How important is cassava?". The results are shown in the following parts.

2.1.4.1 Cassava acreage and production

In 2017, the worldwide cassava area reached 24.57 million hectares, mainly concentrated in African countries including Nigeria, Democratic Republic (D. R.) of the Congo, Mozambique, Ghana, United Republic (U. R.) of Tanzania, Côte d'Ivoire, Angola and Southeast Asia including Thailand, Indonesia, and Vietnam. The top two growers were Nigeria (6.63 million ha) and the D. R. of the Congo (3.81 million ha), higher than the third grower - Thailand (1.34 million tons) at 4.9 and 2.8 folds, respectively (Figure

2.3 and 2.4). Nigeria's cassava production also on the top one of the world with 59.4 million tons, which accounts for 21.25% of the market share, but only higher than the two countries followed by D. R. of the Congo (31 million tons, accounting for 11.11%) and Thailand (30.8 million tons, accounting for 11.04%) at 1.9 folds (Figure 2.5 and 2.6). That shows that the productivity problem of this country or in other words is the productivity improvement of Thailand.

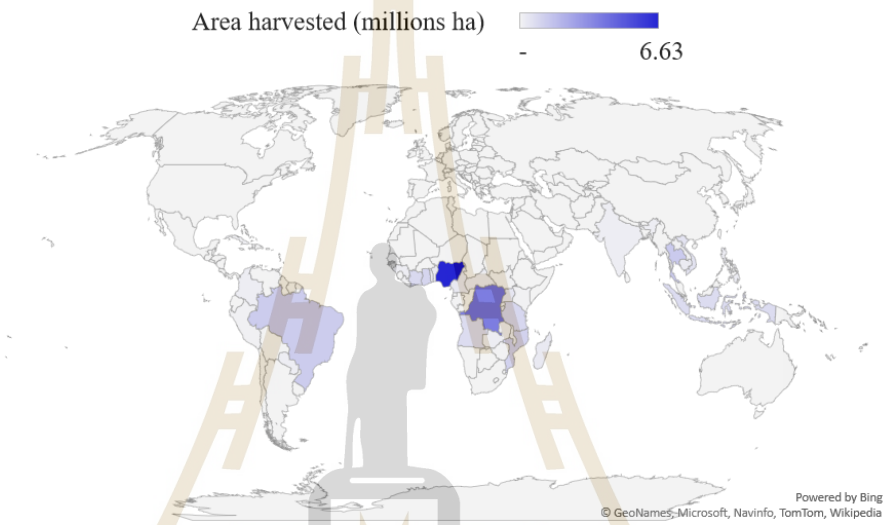

Figure 2.3 The global cassava area in 2017. Source: FAOSTAT (2020).

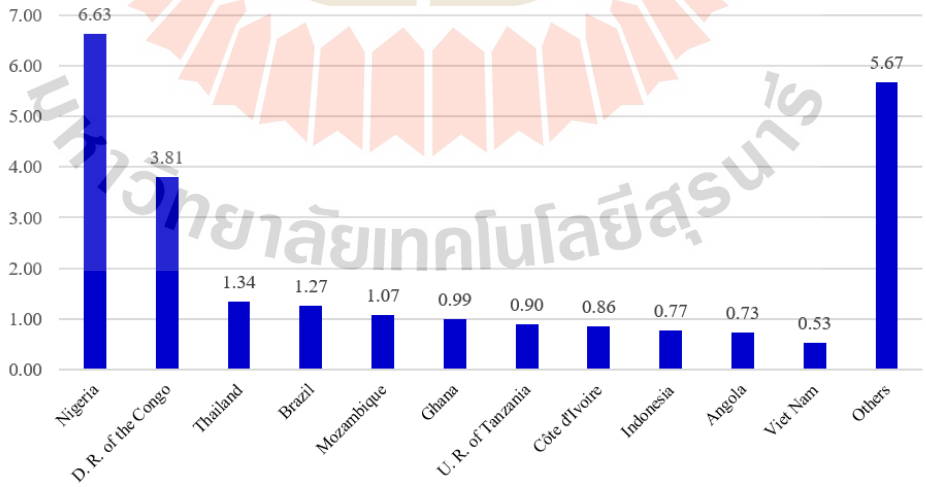

Figure 2.4 Top 10 countries leading the cassava cultivation area in 2017. Source: FAOSTAT (2020).

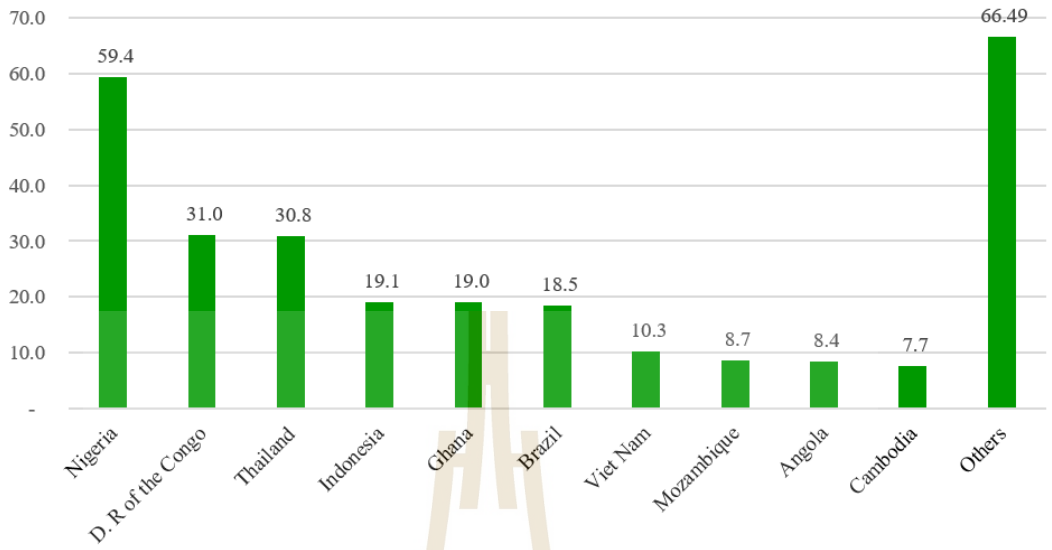

Figure 2.5 Top 10 countries leading in cassava production in 2017. Source: FAOSTAT (2020)

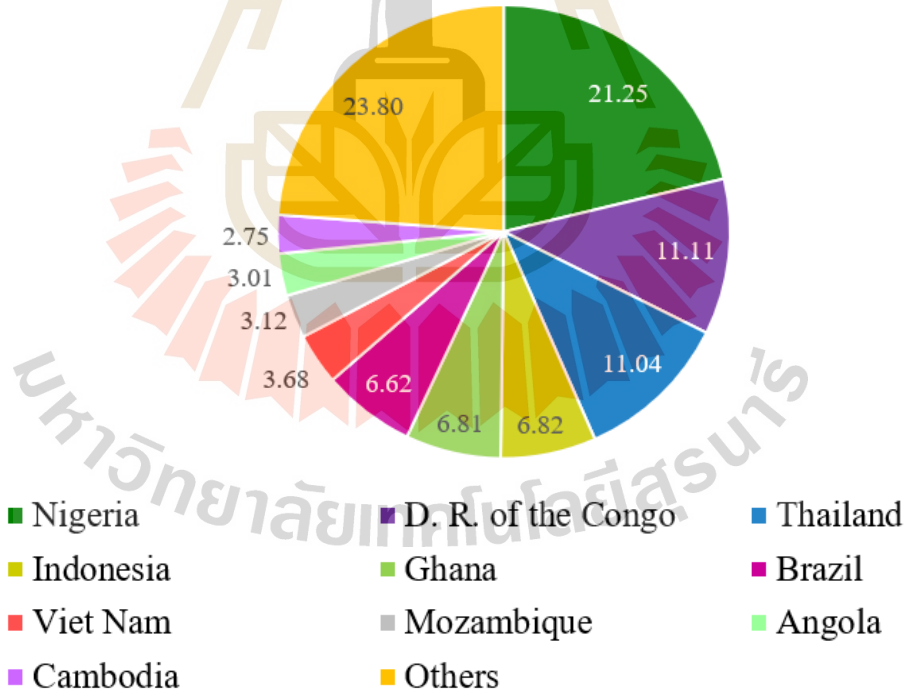

Figure 2.6 The market share of cassava production in 2017. Source: FAOSTAT (2020).

In the period of 2007-2017, the cultivated area of cassava increased from 19.06 to 24.57 million ha. It increased continuously each year in the period of 2007-2013 and increased - decreased alternately in the period of 2013-2017. In 2012, the cultivated area of cassava reached 25.41 million ha, an increase of 24.0% compared to 2011 (20.5 million ha). This highlight is because the area of the D. R. of the Congo and Nigeria has increased from 1.85 to 4.06 and 4.12 to 6.4 million ha, which increased by 119.5 and 55.3 percent, respectively. Thailand's cassava acreage increased by 14.5% after 10 years (**Figure 2.7**, **Table 2.1**).

On the other hand, cassava production increased from 226.97 to 279.3 million tons during this period. It increased continuously every year in the period of 2007-2015 and decreased continuously for two years thereafter. Nigeria was always the production leader during this period and kept a big gap behind. In 2012, cassava production reached 277.68 million tons, which increased by 10.6% compared to 2011 (251.82 million tons). The noteworthy point at this time was that the cassava production of the D. R. of the Congo reached 33.03 million tons, an increase of 119.9% over the previous year, and remained the top 2 until 2017. Also, the production of Thailand and Nigeria also increased by 36.2% and 10.3% from a year earlier, respectively. Thailand's cassava production increased by 14.6% after 10 years, and is consistently in the top 4 (**Figure 2.8**, **Table 2.2**).

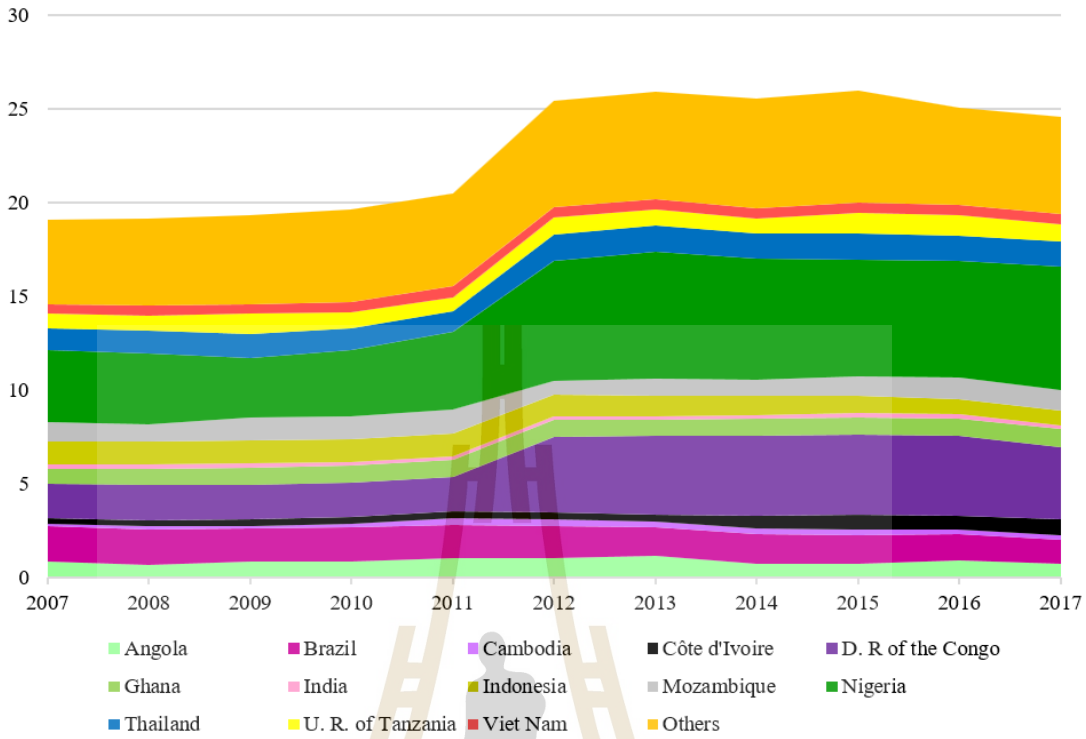

Figure 2.7 The status of cassava cultivation area (millions ha) in the period of 2007-2017. Source: FAOSTAT (2020).

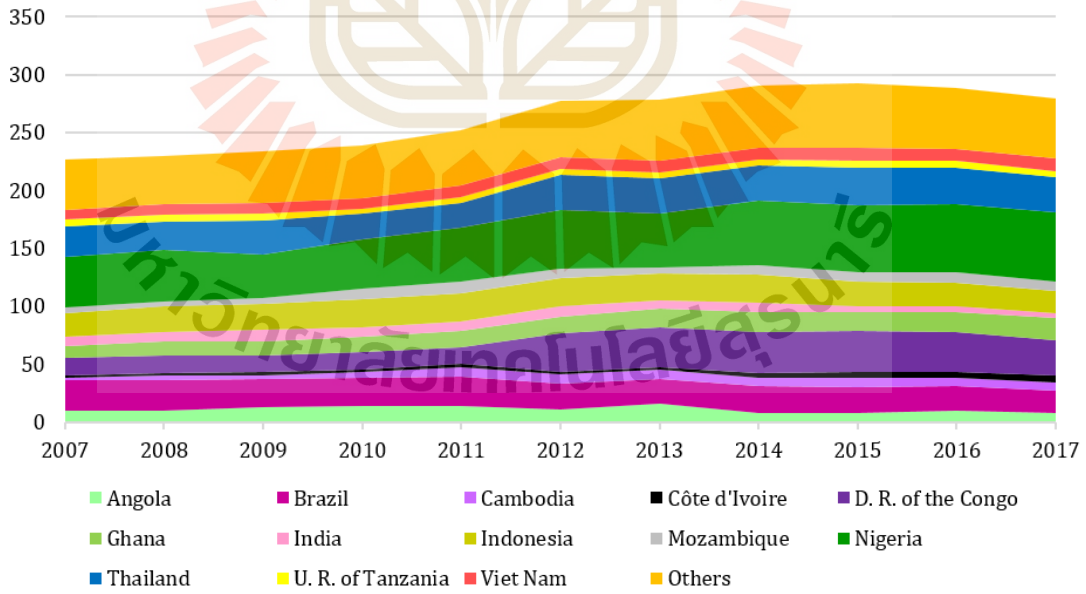

Figure 2.8 The status of cassava production (million tons) in the period of 2007-2017. Source: FAOSTAT (2020).

Table 2.1 The status of cassava cultivation area (millions ha) in the period of 2007-2017. Source: FAOSTAT (2020).

Country	2007	2008	2009	2010	2011	2012	2013	2014	2015	2016	2017
Angola	0.84	0.68	0.85	0.89	1.07	1.06	1.17	0.76	0.76	0.90	0.73
Brazil	1.89	1.89	1.76	1.79	1.73	1.69	1.53	1.57	1.51	1.40	1.27
Cambodia	0.11	0.18	0.16	0.20	0.37	0.34	0.31	0.30	0.28	0.29	0.28
Côte d'Ivoire	0.32	0.33	0.34	0.35	0.35	0.37	0.37	0.65	0.79	0.72	0.86
D. R. of the Congo	1.85	1.85	1.85	1.85	1.85	4.06	4.17	4.29	4.29	4.25	3.81
Ghana	0.80	0.84	0.89	0.88	0.89	0.87	0.88	0.89	0.92	0.94	0.99
India	0.26	0.27	0.28	0.23	0.22	0.23	0.21	0.23	0.21	0.20	0.20
Indonesia	1.20	1.19	1.18	1.18	1.18	1.13	1.07	1.00	0.95	0.82	0.77
Mozambique	0.99	0.95	1.25	1.25	1.29	0.76	0.93	0.87	0.99	1.18	1.07
Nigeria	3.88	3.78	3.13	3.48	4.12	6.40	6.74	6.46	6.22	6.17	6.63
Thailand	1.17	1.18	1.33	1.18	1.14	1.36	1.39	1.35	1.43	1.38	1.34
U. R. of Tanzania	0.78	0.84	1.08	0.87	0.74	0.95	0.86	0.80	1.09	1.06	0.90
Viet Nam	0.50	0.55	0.51	0.50	0.56	0.55	0.54	0.55	0.57	0.57	0.53
Others	4.47	4.58	4.71	4.94	4.97	5.63	5.75	5.83	5.95	5.16	5.19
Total	19.06	19.12	19.31	19.61	20.50	25.41	25.92	25.55	25.97	25.04	24.57

Table 2.2 The status of cassava production (million tons) in the period of 2007-2017. Source: FAOSTAT (2020).

Country	2007	2008	2009	2010	2011	2012	2013	2014	2015	2016	2017
Angola	9.73	10.06	12.83	13.86	14.33	10.64	16.41	7.64	7.73	9.85	8.40
Brazil	26.54	26.70	24.40	24.97	25.35	23.04	21.48	23.25	23.06	21.04	18.50
Cambodia	2.22	3.68	3.50	4.25	8.03	7.61	7.55	7.73	7.63	7.64	7.67
Côte d'Ivoire	2.34	2.53	2.26	2.31	2.36	2.41	2.44	4.24	5.09	4.55	5.37
D. R. of the Congo	15.00	15.01	15.05	15.01	15.02	33.03	33.92	34.87	34.93	34.57	31.02
Ghana	10.22	11.35	12.23	13.50	14.24	14.55	15.99	17.80	17.21	17.80	19.01
India	8.23	9.06	9.62	8.06	8.08	8.75	7.24	8.14	4.37	4.34	4.17
Indonesia	19.99	21.59	22.04	23.92	24.04	24.18	23.94	23.44	21.80	20.26	19.05
Mozambique	4.96	3.84	5.67	9.74	10.09	8.20	4.30	8.27	8.10	9.10	8.70
Nigeria	43.41	44.58	36.82	42.53	46.19	50.95	47.41	56.33	57.64	59.57	59.35
Thailand	26.92	25.16	30.09	22.01	21.91	29.85	30.23	30.02	32.36	31.16	30.84
U. R. of Tanzania	5.20	5.39	5.92	4.55	4.65	5.46	4.76	4.99	5.89	5.64	5.01
Viet Nam	8.19	9.31	8.53	8.60	9.90	9.74	9.76	10.21	10.74	10.91	10.27
Others	44.03	41.82	44.83	46.00	47.62	49.28	53.04	54.01	56.46	52.08	51.94
Total	226.97	230.08	233.79	239.30	251.82	277.68	278.45	290.94	293.01	288.50	279.30

2.1.4.2 Cassava exports and Thailand's position of cassava production

Cassava is used as a major food source in African countries. In addition, cassava products such as cassava dried (cassava chip and cassava pellet), cassava starch, cassava flour are exported as a foreign currency income, especially in Southeast Asian countries. In the period of 2007-2017, Southeast Asian countries, especially Thailand, dominate the export markets of cassava dried and cassava starch. In 2017, the quantity and value of exports of cassava dried reached 9.2 million tons and 1.9 billion USD, which increased by 24.4 and 124.5% compared to 2007, respectively (**Figure 2.9**, **Table 2.3** and **2.4**). Furthermore, the quantity and value of exports of cassava starch reached 5.2 million tons and $ 1.8 billions that has increased by 230.9 and 308.8% after 10 years, respectively (**Figure 2.10**, **Table 2.5** and **2.6**). The increase in a value higher than the increase in the quantity indicated that the price of cassava increased after ten years. Besides, Thailand's annual export quantity of cassava dried and cassava starch accounts for 63.2 - 77.2% and 58.5 - 91.5% of the total world quantity, higher than the second country which is Vietnam from 1.9 - 4.3 and 1.5 - 8.9 folds, respectively. On the other hand, the export quantity of cassava flour ranged from 36.6 - 107.38 thousand tons (increased 193.4%) with a value of 46.6 - 65.57 million USD (increased 40.7%) in the period of 2014 - 2017, which is much lower than cassava dried and cassava starch. Thailand still dominates the export quantity, which accounts for 72.6 - 82.6% of the annual export quantity. However, Thailand only accounts for 27.2 - 44.4% of the annual export value. On the other hand, Peru only accounts for 3.1 - 7.2% of the export quantity, but it accounts for 23.5 - 58.0% of the value in the export market (**Figure 2.11**, **Table 2.7** and **2.8**). This shows that Peru's cassava flour price is much higher than that of Thailand.

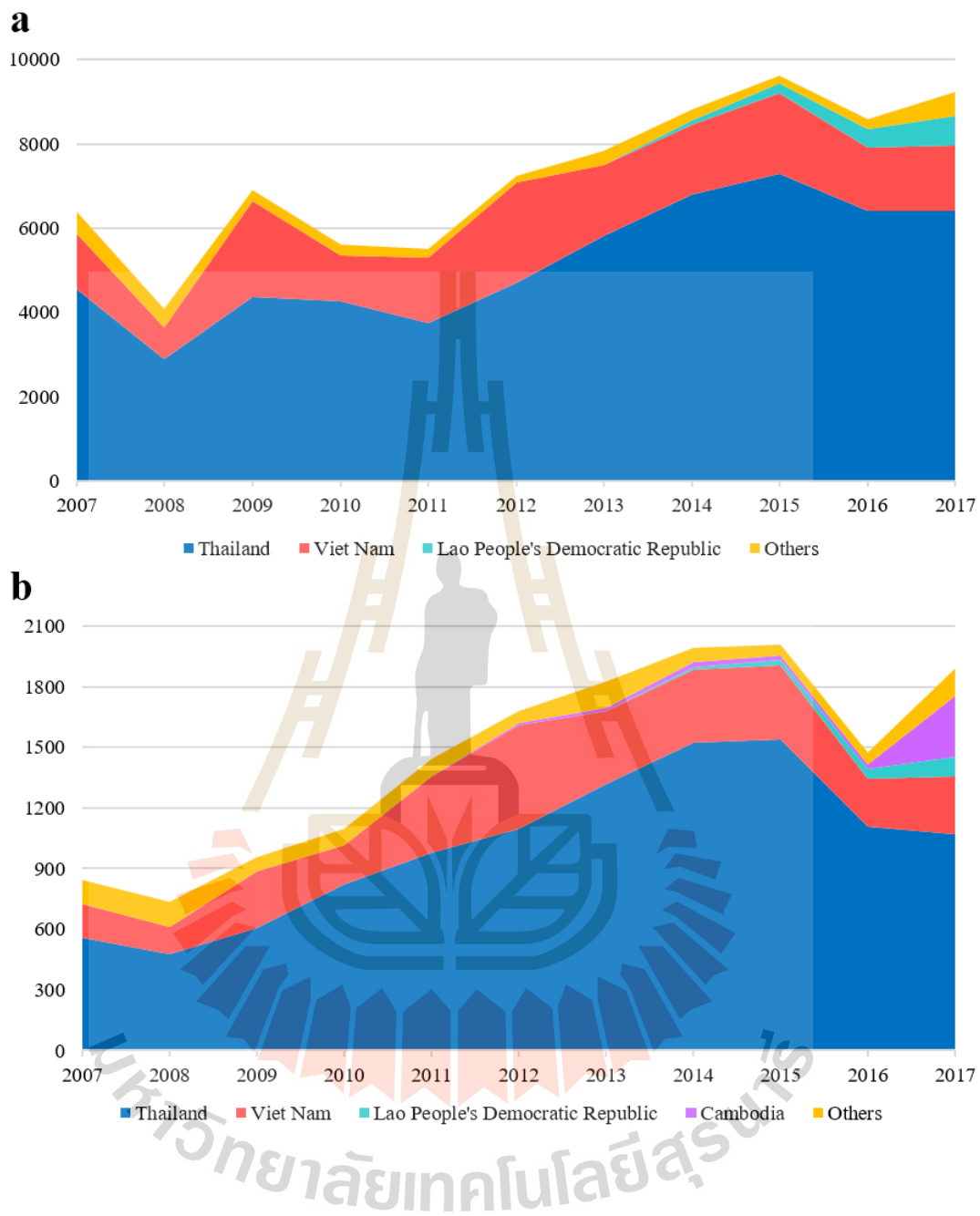

Figure 2.9 (a) The status of dried cassava export quantity (thousand tons) in the period of 2007-2017. (b) The status of dried cassava export value (millions USD) in the period of 2007-2017. Source: FAOSTAT (2020).

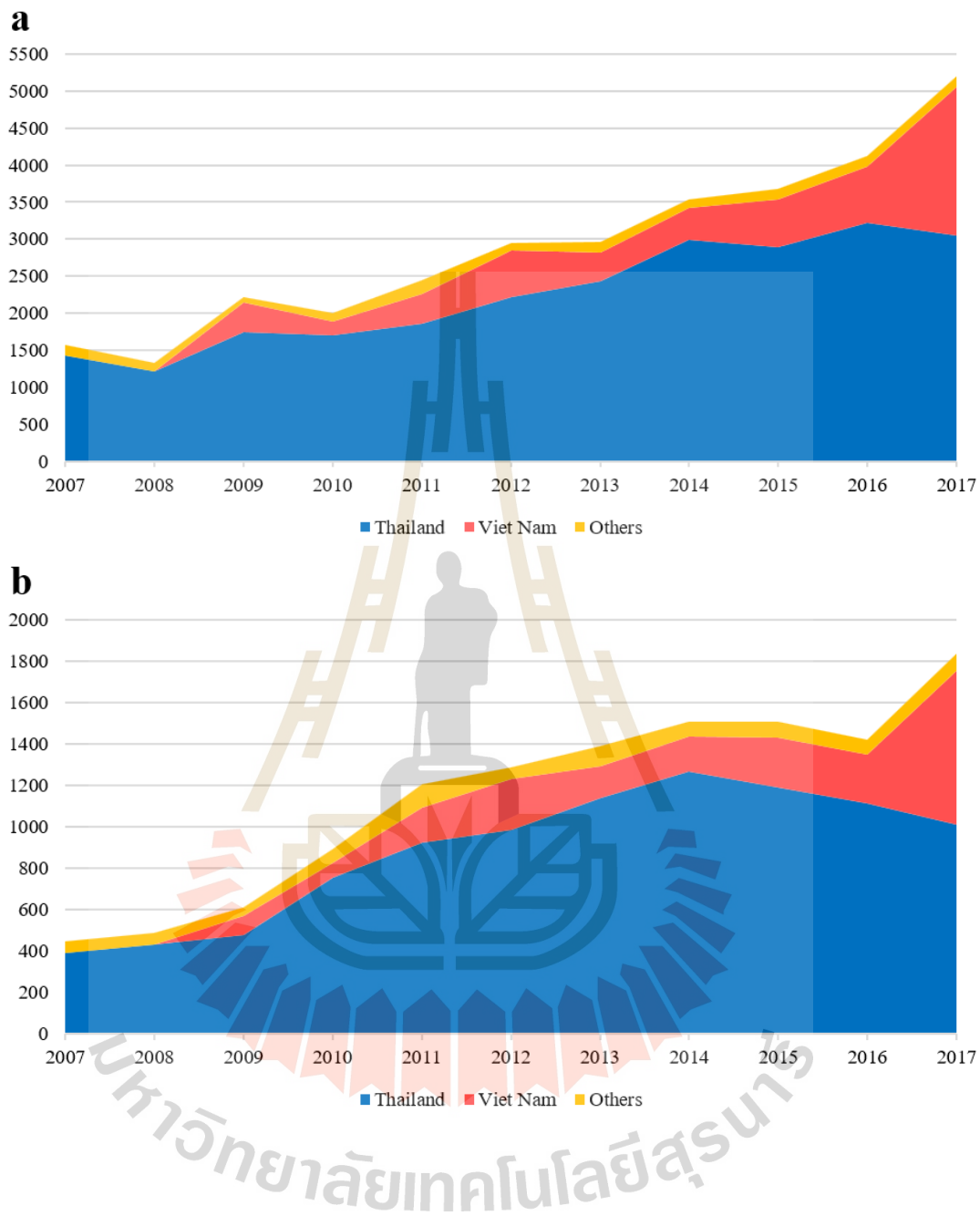

Figure 2.10 (a) The status of starch cassava export quantity (thousand tons) in the period of 2007-2017. (b) The status of starch cassava export value (millions USD) in the period of 2007-2017. Source: FAOSTAT (2020).

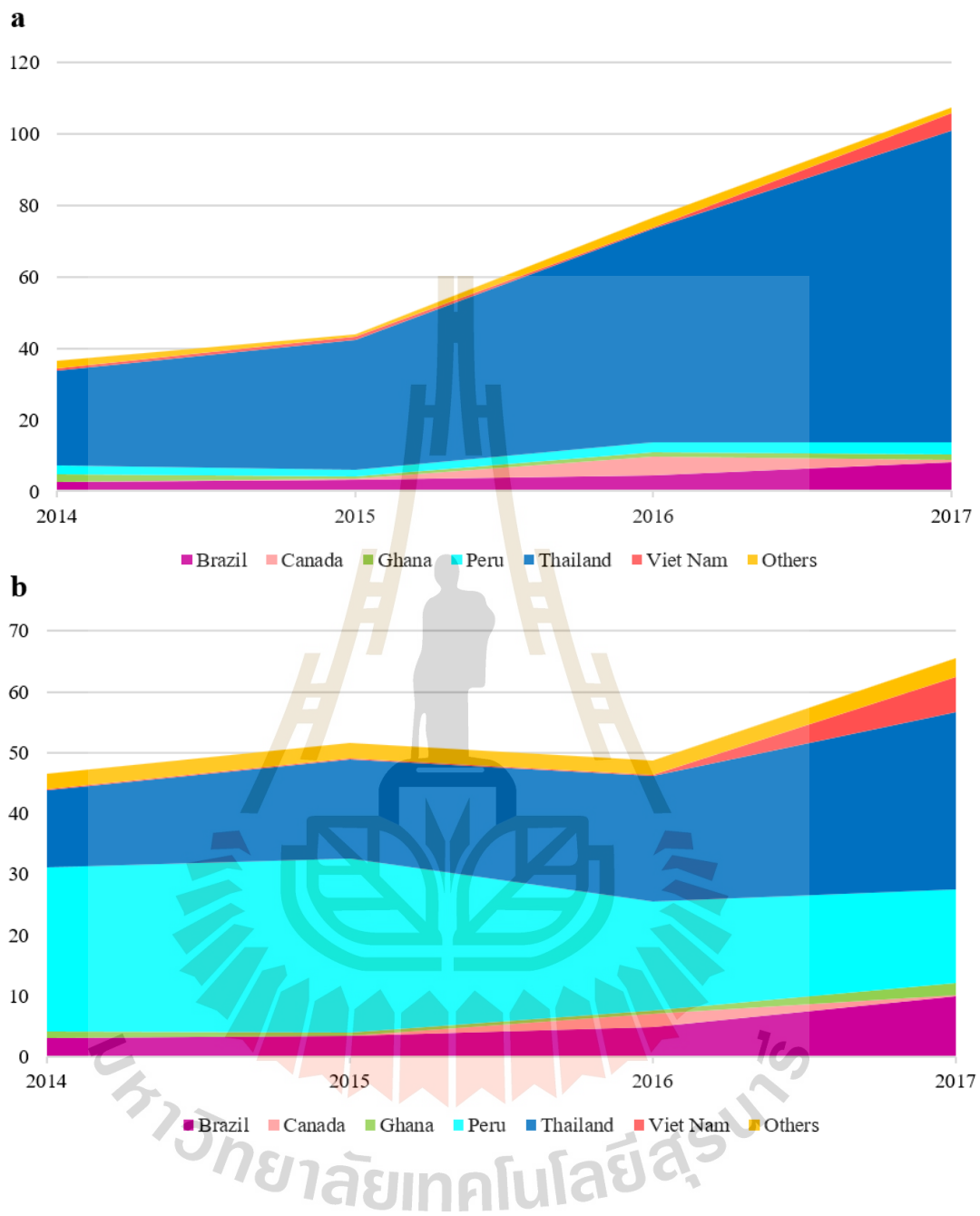

Figure 2.11 (a) The status of cassava flour export quantity (thousand tons) in the period of 2007-2017. (b) The status of flour cassava export value (millions USD) in the period of 2007-2017. Source: FAOSTAT (2020).

Table 2.3 The status of dried cassava export quantity (thousand tons) in the period of 2007-2017. Source: FAOSTAT (2020).

Country	2007	2008	2009	2010	2011	2012	2013	2014	2015	2016	2017
Thailand	4558.81	2882.85	4357.29	4273.38	3735.21	4697.24	5816.94	6800.26	7299.02	6417.99	6402.29
Viet Nam	1316.56	753.34	2294.13	1070.99	1567.17	2386.34	1689.61	1662.51	1913.81	1504.46	1561.15
Lao People's D. R.	0.00	0.00	0.00	0.00	0.00	0.00	0.00	95.79	214.88	435.88	685.50
Cambodia	0	0	0	2.4	9.35	35.159	59.952	98.412	117.526	97	396.214
Others	518.11	449.48	237.64	253.56	193.84	117.71	276.88	148.64	72.74	127.31	188.41
Total	6393.47	4085.66	6889.06	5600.33	5505.57	7236.45	7843.38	8805.60	9617.96	8582.63	9233.56

Table 2.4 The status of dried cassava export value (millions USD) in the period of 2007-2017. Source: FAOSTAT (2020).

Country	2007	2008	2009	2010	2011	2012	2013	2014	2015	2016	2017
Thailand	556.78	477.64	605.20	819.29	978.59	1095.24	1317.65	1522.76	1538.73	1108.95	1071.33
Viet Nam	166.34	133.92	281.74	195.70	375.03	513.65	363.71	358.78	365.29	234.43	285.33
Lao People's D. R.	0.00	0.00	0.00	0.00	0.00	0.00	0.00	14.18	28.51	50.37	94.93
Cambodia	0.00	0.00	0.00	0.42	2.29	8.08	13.59	23.29	22.21	21.33	304.84
Others	118.08	126.58	67.38	81.02	83.52	62.94	132.06	73.91	52.32	61.13	131.83
Total	841.21	738.14	954.31	1096.42	1439.43	1679.90	1827.01	1992.92	2007.06	1476.21	1888.25

Table 2.5 The status of starch cassava export quantity (thousand tons) in the period of 2007-2017. Source: FAOSTAT (2020).

Country	2007	2008	2009	2010	2011	2012	2013	2014	2015	2016	2017
Thailand	1422.10	1216.76	1743.07	1694.25	1861.06	2208.22	2428.55	2993.45	2886.98	3216.16	3046.08
Viet Nam	0.00	0.00	397.45	189.48	392.88	640.98	382.19	428.78	640.33	761.99	2004.39
Others	150.28	113.73	78.87	119.20	196.95	102.68	147.14	114.54	146.45	144.88	152.58
Total	1572.39	1330.49	2219.39	2002.92	2450.89	2951.88	2957.88	3536.77	3673.75	4123.03	5203.06

Table 2.6 The status of starch cassava export value (millions USD) in the period of 2007-2017. Source: FAOSTAT (2020).

Country	2007	2008	2009	2010	2011	2012	2013	2014	2015	2016	2017
Thailand	390.88	432.29	475.33	752.51	922.29	983.17	1139.14	1267.67	1190.68	1112.43	1007.92
Viet Nam	0	0	92.37	74.49	169.45	245.06	154.41	165.58	241.28	237.62	745.59
Others	57.63	56.08	45.01	62.71	114.36	59.07	94.67	72.83	75.84	71.87	80.15
Total	448.51	488.37	612.71	889.70	1206.1	1287.3	1388.21	1506.08	1507.8	1421.92	1833.66

Table 2.7 The status of cassava flour export quantity (thousand tons) in the period of 2007-2017. Source: FAOSTAT (2020).

Country	2014	2015	2016	2017
Brazil	2.48	3.33	4.45	8.20
Canada	0.08	0.05	5.13	0.50
Ghana	2.05	0.82	1.39	1.55
Peru	2.64	1.89	2.68	3.38
Thailand	26.57	36.36	59.62	87.20
Viet Nam	0.60	0.65	0.59	4.94
Others	2.17	0.91	2.54	1.62
Total	36.60	44.00	76.39	107.38

Table 2.8 The status of cassava flour export value (millions USD) in the period of 2007-2017. Source: FAOSTAT (2020).

Country	2014	2015	2016	2017
Brazil	3.03	3.43	4.84	9.97
Canada	0.04	0.07	2.28	0.22
Ghana	1.12	0.47	0.56	2.00
Peru	27.01	28.63	17.83	15.40
Thailand	12.69	16.32	20.68	29.09
Viet Nam	0.19	0.20	0.19	5.86
Others	2.53	2.43	2.41	3.04
Total	46.60	51.54	48.78	65.57

Export quantities of Thailand's cassava dried, starch, and flour were the largest in the world, which accounts for 69.3, 58.5, and 81.2% of the export market in 2017, respectively. Although the export value still ranks first in the market with 56.7, 55.0, and 44.4%, respectively, they are still lower than the export quantitative market share (**Figures 2.12, 2.13** and **2.14**). This shows that the cassava selling price of Thailand is

lower than those of other countries. On the other hand, export quantities of cassava dried, starch, and flour in Thailand increased by 40.4, 114.2, and 228.2% in the period of 2007 - 2017 or 2014 - 2017, respectively. Similarly, the value of exports increased by 92.4, 157.9, and 129.2%. This shows that Thailand has focused more on producing and exporting higher value-added products such as cassava starch and flour (**Figure 2.9, 2.10** and **2.11**, **Table 2.3** to **2.8**).

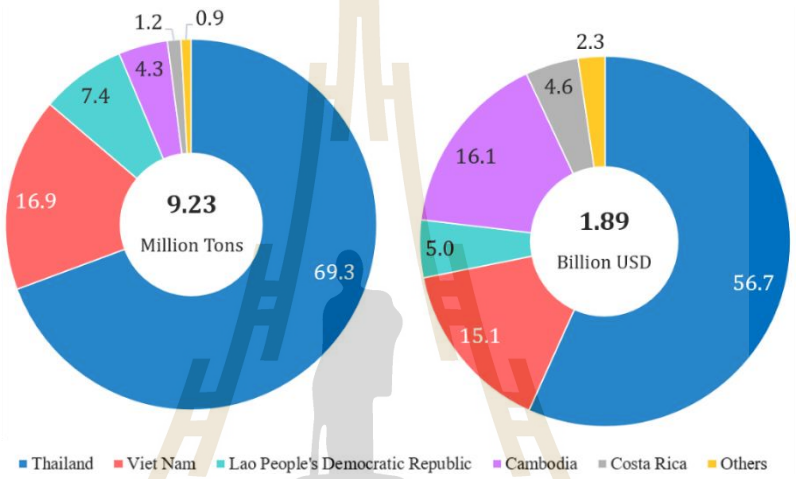

Figure 2.12 Top 5 countries leading in cassava dried market share of export quantity (left) and value (right) in 2017. Source: FAOSTAT (2020).

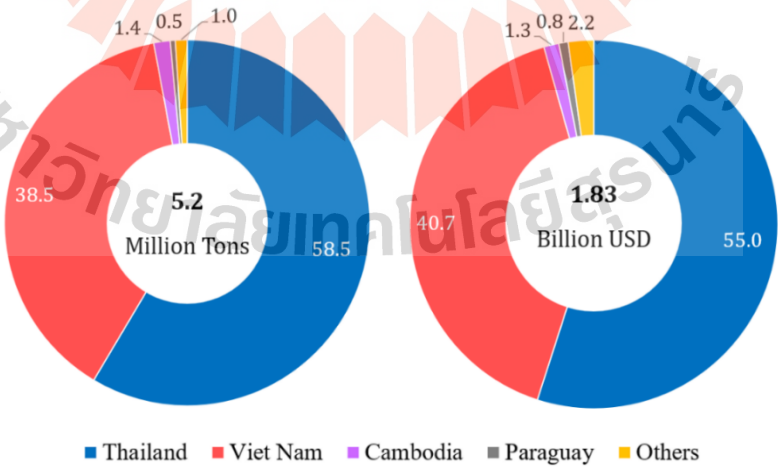

Figure 2.13 Top 4 countries leading in cassava starch market share of export quantity (left) and value (right) in 2017. Source: FAOSTAT (2020).

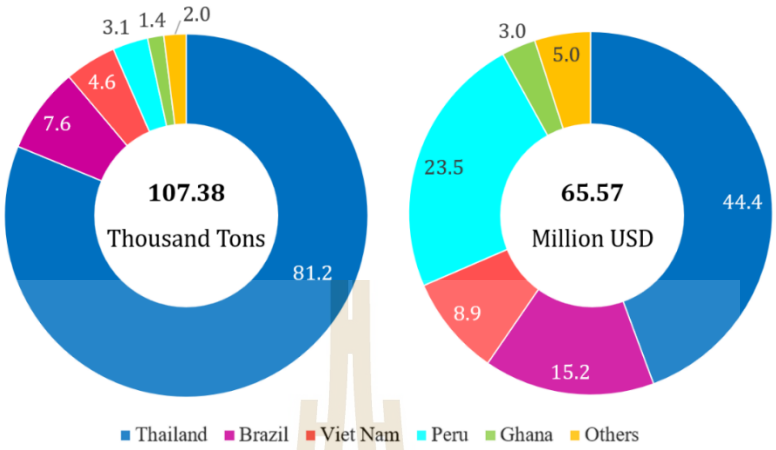

Figure 2.14 Top 5 countries leading in cassava flour market share of export quantity (left) and value (right) in 2017. Source: FAOSTAT (2020).

In 2017, cassava dried and cassava starch is Thailand's key crop exports with 6.4 and 3.05 million tons, which is only lower than rice milled 1.6 and 3.3 folds, respectively. But in terms of export value, cassava dried or starch brings foreign currency lower than rubber natural dry, rice milled, rubber natural, sugar refined, sugar raw centrifugal (**Figure 2.15**, **Table 2.9**).

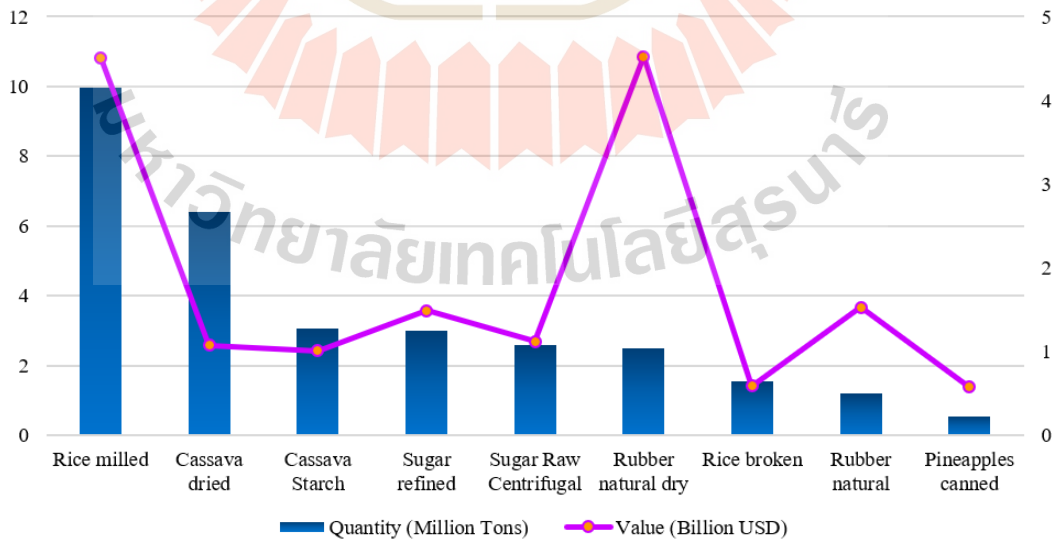

Figure 2.15 The quantity and value of Thailand's key commodities exported in 2017. Source: FAOSTAT (2020).

Table 2.9 The quantity and value of Thailand's key commodities exported in 2017. Source: FAOSTAT (2020).

Commodities	Quantity (Million Tons)	Value (Billion USD)
Rice milled	9.97	4.51
Cassava dried	6.40	1.07
Cassava starch	3.05	1.01
Sugar refined	3.00	1.48
Sugar raw centrifugal	2.59	1.12
Rubber natural dry	2.48	4.52
Rice broken	1.54	0.59
Rubber natural	1.19	1.53
Pineapples canned	0.53	0.57

2.1.5 Problem of cassava production

There are many biotic and abiotic stress factors, diseases, insects or weeds that could affect the growth of cassava, leading to a decrease in their yield. The cassava plant prefers airy and porous soils. It is drought tolerant but very sensitive and unsuitable under poorly drained, heavy or saline soils. In addition, pathogenic microorganisms including fungi, bacteria and viruses also attack and damage cassava. According to a review of McCallum *et al*. (2017), there are six types of viral diseases including cassava mosaic disease, cassava brown streak disease, cassava common mosaic disease, cassava vein mosaic disease, cassava green mottle disease, cassava symptomless diseases; six bacterial diseases including cassava bacterial blight, cassava bacterial angular leaf spot, cassava bacterial stem rot, cassava bacterial wilt, cassava bacterial stem gall, cassava sudden wilt; thirteen fungal diseases including cassava anthracnose disease, cassava diffuse/blight leaf spot, cassava brown leaf spot, cassava white leaf spot, cassava ring leaf spot, cassava superelongation disease, cassava ash disease, cassava rust, cassava stem rot, cassava root rot, cassava dry root rot, cassava stem and root rot, cassava bud necrosis; and 3 types of phytoplasma including cassava

acantholysis, cassava witches' broom, and cassava frogskin disease that have been reported in cassava. Among them, cassava mosaic disease, cassava brown streak disease, and bacterial blight can result in up to 90, 70 and 75% yield reductions, respectively. Nematodes could cause a loss of 6% of annual cassava production. Also, approximately 200 arthropod species have been reported to attack cassava, many of which have been adapted to biochemical defense mechanisms including laticifers and cyanogenic compounds. Cassava mealybug (*Phenacoccus manihoti*) suck the growing tip and leaf back, which can lose up to 100% of leaf yield and 80% of root yield. On the other hand, whitefly (*Bemisia tabaci*) is a vector of the *Cassava mosaic virus*, which supports the disease outbreak in many cassava growing areas. Weeds compete for nutrition, being a host for insects and pathogens, which is also a cause of yield loss in cassava fields (Neuenschwander, 2008; Obiazi and Ojobor, 2013; McCallum *et al*., 2017).

2.1.6 Important diseases on cassava

The pathogens cause diseases, resulting in loss of yield and quality of cassava. There are at least 28 known diseases in this crop (McCallum *et al*., 2017). In particular, many diseases commonly appear and cause damage to many varieties of cassava plants in many areas of the world.

2.1.6.1 Cassava bacterial blight disease

Cassava bacterial blight disease caused by *Xanthomonas axonopodis* pv. *manihotis* usually appears on the leaf and canopy top. Symptoms of the disease are dark, and angular spots. Then, leaf infected - usually from the head or border of the leaf lobe becomes blight and necrotic. The top part of the canopy usually dies first (**Figure 2.16**) (Abdulai *et al*., 2018). *X. axonopodis* pv. *manihotis* usually remains on cassava stems to infect the next crop. Furthermore, this pathogen can survive on

weeds for up to 5 months without showing harmful symptoms. The disease can be spread by the insect vector, grasshopper *Zonocerus variegatus* (Fanou *et al*., 2018).

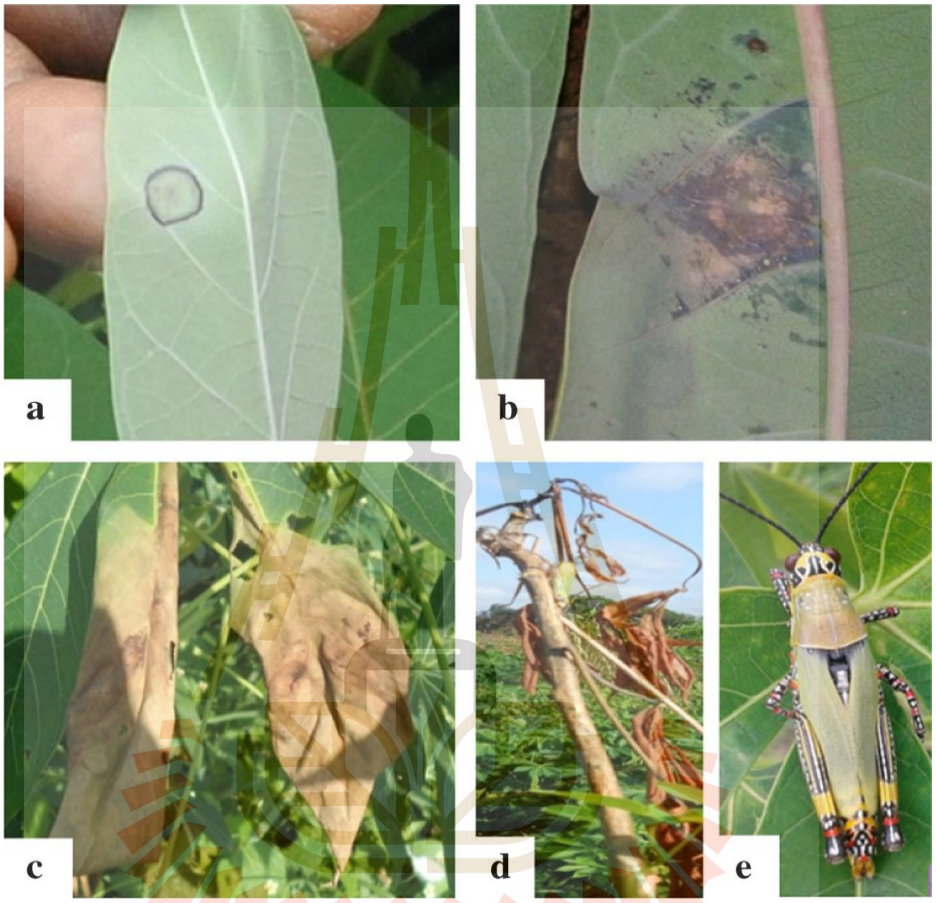

Figure 2.16 Cassava Bacterial Blight symptoms. (a) initial symptoms on leaf, (b) water-soaked angular leaf spots, (c) blighted leaves, (d) cassava die-back, (e) vector (*Zonocerus variegatus*). Source: Abdulai *et al*. (2018).

2.1.6.2 Cassava anthracnose disease

Anthracnose is an important cassava disease caused by *Colletotrichum gloesporioides* f.sp. *manihotis* in Tanzania and *C. gloeosporioides*, *C. capsica*, *C. lindemuthianum*, *C. aeschynomene*, and *C. boninense* in Thailand. Symptoms are characterized by brown concave spots on leaf blades and elliptical spots on leaf stalks.

The infected leaves could turn yellow and fall off. More seriously, an entire plant could lose all its leaves and die (**Figure 2.17**). This disease has been reported in many cassava growing regions in Tanzania and Thailand (Magdalena *et al*., 2012; Sangpueak *et al*., 2018).

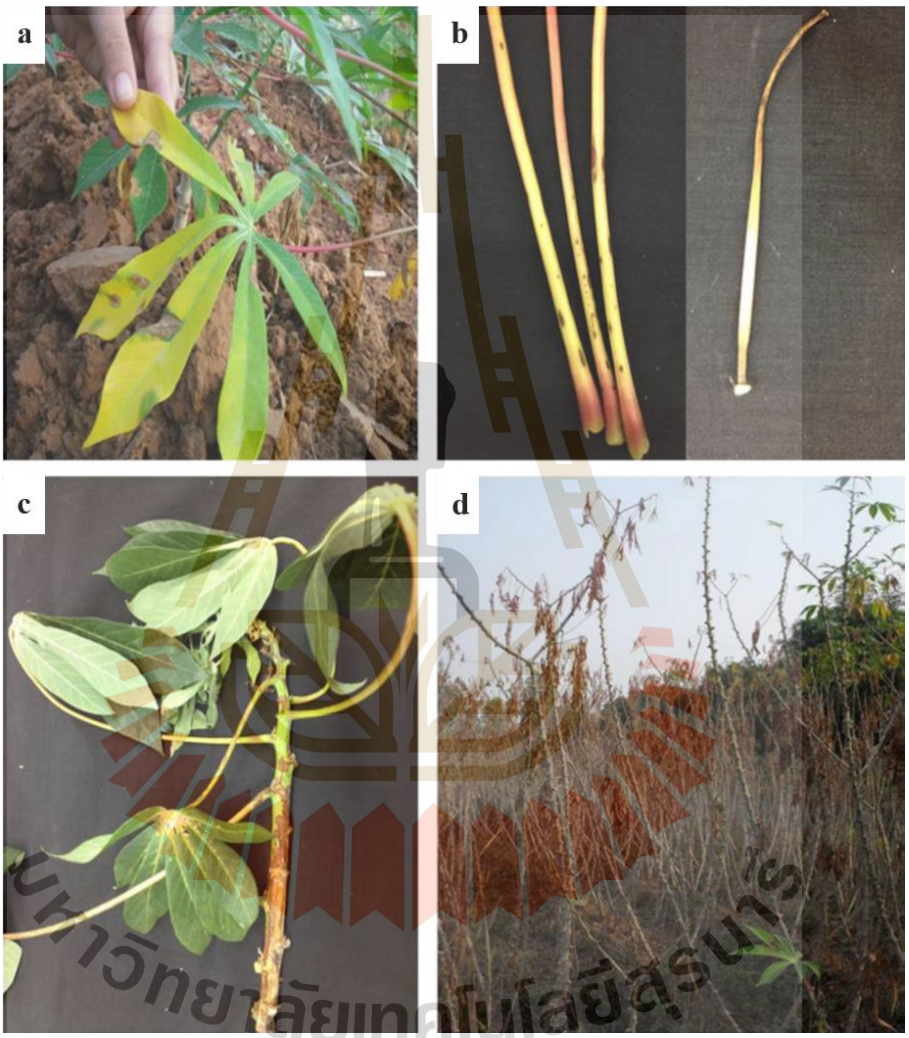

Figure 2.17 Symptoms of anthracnose found on cassava plants in major growing areas (a) brown sunken spots on leaves (b) elliptical lesions on petioles or at the leaf-blade base (c) patches of necrotic lesions on young stem (d) defoliation in heavily infected plants. Source: Sangpueak *et al*. (2018).

2.1.6.3 Cassava root rot disease

Cassava root rot disease was serious damage in many cassava cultivation area. The disease caused by many fungi including *Lasiodiplodia theobromae*, *L. euphorbicola*, *Neoscytalidium dimidiatum*, *Sclerotium rolfsii*, *Fusarium* spp., *Phytopthora* sp., which lead to loss 80-100% root yield. The typical symptoms were stem and root becoming discoloration, offensive odor, blackening and decaying. The vascular of infected roots and stems were turning to dark-browning (**Figure 2.18**) (Sangpueak *et al*., unpublish).

Figure 2.18 Symptoms of stem and root black rot in cassava. (a-c) Plants wilting, (d-g) Root rot, (h-j) Black fungal structures erupting from the bark of the plants. Source: Sangpueak *et al*. (unpublish).

2.1.6.4 Cassava mosaic disease

Cassava mosaic disease was firstly recorded in Tanzania in 1894. Subsequently, the disease was reported in other cassava growing areas in Sub-Saharan such as Cameroon, Kenya, and Malawi (Alabi *et al*., 2011). The disease is spread to the Indian subcontinent. Cassava mosaic disease has been recorded in Southeast Asian countries such as Cambodia and Vietnam since 2016 (Minato *et al*., 2019). This disease is caused by many viruses of the *Geminiviridae* family, genus *Begomovirus*. *African cassava mosaic virus* and *East African cassava mosaic virus* mainly cause this disease in African countries (Alabi *et al*., 2011). *Indian cassava mosaic virus* and *Sri Lanka cassava mosaic virus* have been known to cause disease in the Indian subcontinent (Saunders *et al*., 2002). Studies of Uke *et al*. (2018), and Minato *et al*. (2019) showed that cassava mosaic disease in Southeast Asia is caused by the *Sri Lanka cassava mosaic virus*. The characteristic symptoms of the disease are mosaic, deformed, and curl patches appearing on the leaf surface. Diseased plants grow poorly, become yellow and stunted (**Figure 2.19**). The virus is transmitted by whitefly *Bemisia tabaci* or cassava stalk. Moreover, the virus can survive in cassava plants without symptoms (Minato *et al*., 2019).

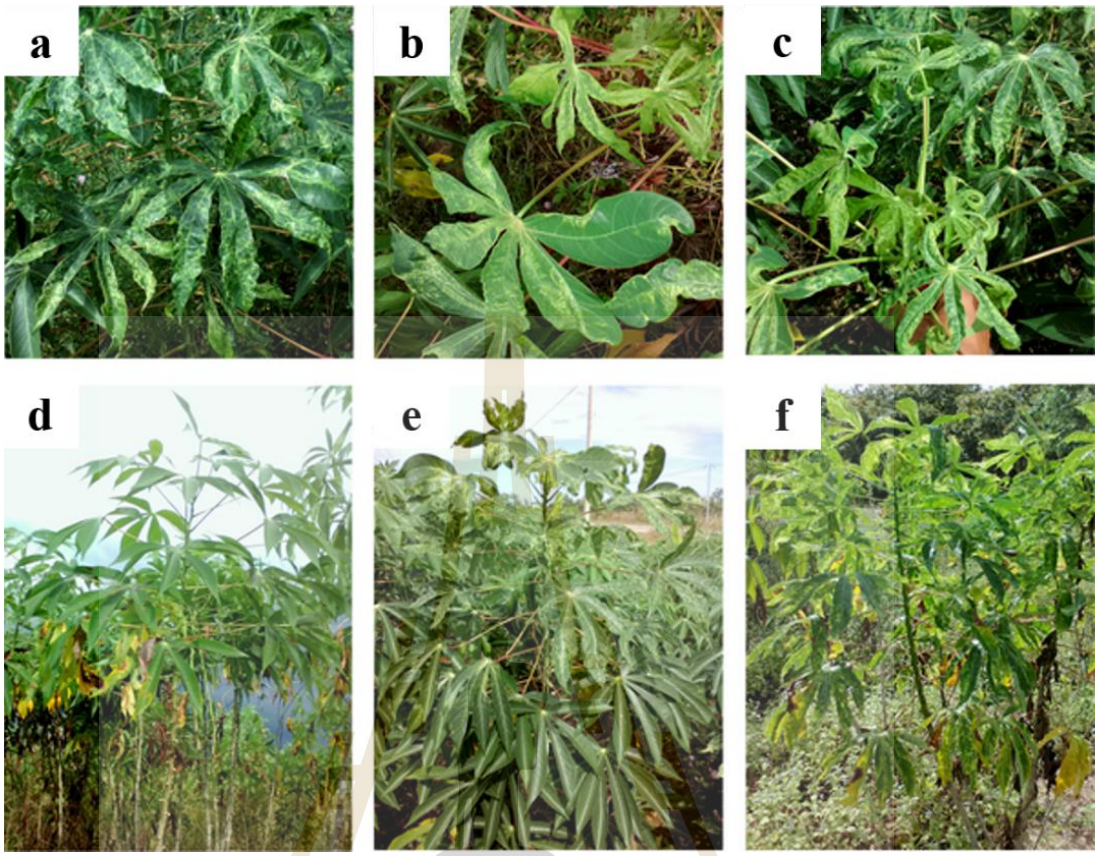

Figure 2.19 Symptoms were observed on SLCMV positive plants identified in Cambodia. (a-c) Typical CMD symptoms on leaves, (a) Mosaic, (b) Deformation, and (c) Curl, (d) Asymptomatic plant testing positive by PCR for SLCMV infection, (e) Plant with mosaic symptoms only on upper leaves, (f) Plant with systemic mosaic symptoms. Source: Minato *et al*. (2019).

2.1.6.5 Cassava leaf spot disease and their control

Cassava brown leaf spot is the name of a cassava disease to distinguish it from cassava white spot disease (**Figure 2.20**) caused by *Cercospora caribaea* or *Passarola manihotis* and cassava diffuse/blight leaf spot caused by *Cercospora vicosae* or *Passarola vicosae* (**Figure 2.21**) (Hillocks and Wydra, 2002; de Freitas *et al*., 2017). Cassava brown leaf spot disease is commonly known to be caused by the fungus *Cercospora henningsii*, or *Cercosporidium henningsii* (Hillocks and Wydra, 2002; Reddy, 2015; McCallum *et al*., 2017). Also, it has been reported to be caused by a variety of fungi with different names including *Mycosphaerella manihotis* in Colombia (Teri *et al*., 1980), *C. henningsii* in Ghana (Ayesu-Offei and Antwi-Boasiako, 1996), *C. henningsii* [*Mycosphoraella henningsii*] in India (Prabakar and Raguchander, 2000), *Passalora henningsii* in China and Brazil (Pei *et al*., 2014; de Freitas *et al*., 2017), *Clarohilum henningsii* in Indonesia and Brazil (Hidayat *et al*., 2020; Julião *et al*., 2020). In general, these spots are small yellowish spots initially, then develop into round or angular spots, brown or reddish-brown with a dark border of 3-12 mm (sometimes up to 15 mm) and surrounded by small pale yellow halo. These spots appear both above and below the leaf surface, and usually appear on older leaves than younger leaves, especially over 5 months old. The infected leaves turn yellow and fall off afterward (**Figure 2.22**). On the other hand, Ng'ang'a *et al*. (2019) reported cassava brown leaf disease in Kenya caused by a combination of the three fungi *Colletotrichum*, *Alternaria*, and *Cladosporium* (**Figure 2.23**). This disease causes a loss of up to 30% in cassava yield. The disease is often neglected until several recent outbreaks in Brazil (Julião *et al*., 2020).

Studies of Ayesu-Offei and Antwi-Boasiako (1996) showed that mature conidia of *C. henningsii* did not germinate but accumulate in the lesions. Under favorable conditions of the temperature at 25-32°C and the presence of free-water, the mature conidia sprout and fragment into multiple microconidia, which can germinate and form appressoria on both the upper and lower surfaces of the leaves. Furthermore,

according to Reddy (2015), the pathogen causes serious harm in warm, wet conditions, and spreads through the wind.

It is now possible to implement cultural methods, chemical methods, and host resistance to control or manage the disease. The planting spacing is kept suitable to create an open space in the field. The season crop can be designed so that 5 months of cassava does not coincide with the rainy season. Moreover, copper fungicides, benomyl, thiophanate, and carbendazim are also recommended to be sprayed at 3 months after planting to control the disease. Besides, the cassava varieties Sri Prakash and Sri Visakam are recommended to be resistant to cassava brown leaf spot disease in India (Prabakar and Raguchander, 2000; Reddy, 2015).

Furthermore, the study of the efficacy of six fungicides in the control of this disease showed that the active ingredient of flutriafol (commercial name Impact®) could effectively control the disease by reducing area under disease progress curve and rate of defoliation at 3.2 and 11 folds in the net-house conditions and at 3.7 and 4.5 folds in the field conditions compared with the control, respectively. Furthermore, Flutriafol treatment also increased chlorophyll content in leaves at 1.2 folds compared to the control but lower than pyraclostrobin (Comet®) and azoxystrobin (Priori®), which increased at 1.5 and 1.4 folds, respectively (Julião *et al*., 2020).

Figure 2.20 The symptoms of cassava white leaf spot disease. Source: Hillocks and Wydra (2002)

Figure 2.21 The symptoms of diffuse/blight leaf spot (*Cercospora vicosae*). Source: Hillocks and Wydra (2002).

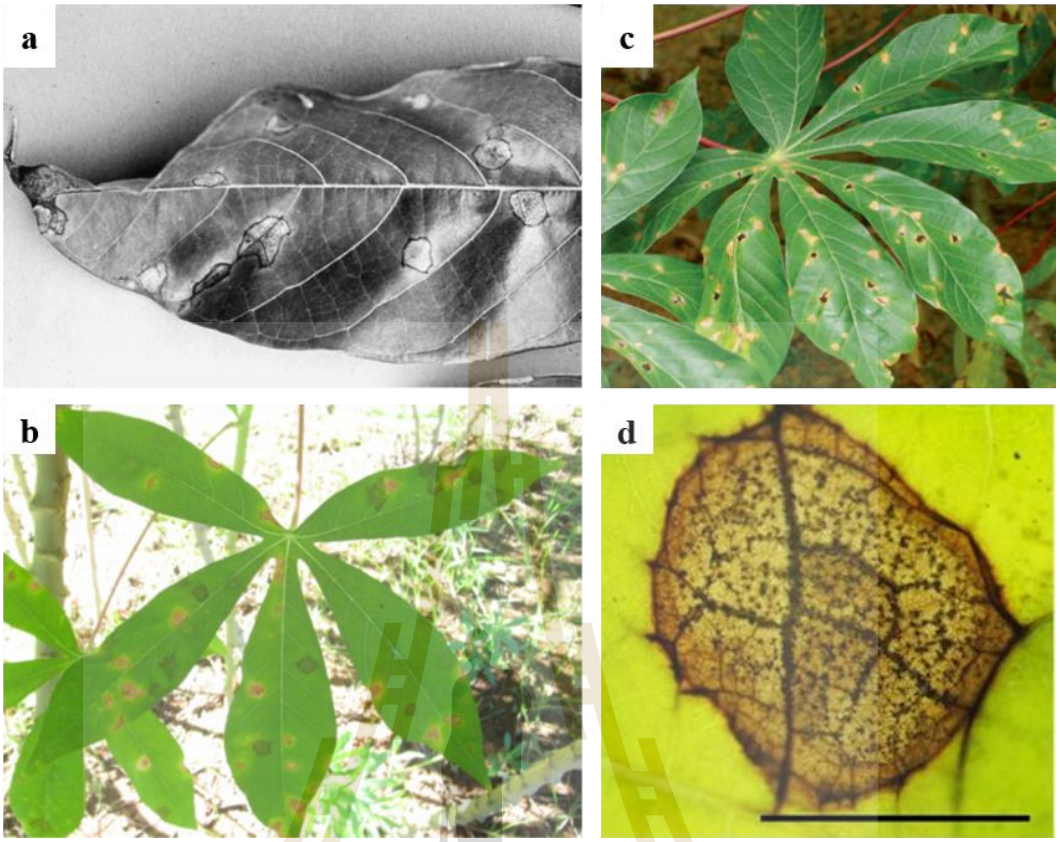

Figure 2.22 The symptoms of cassava brown leaf spot from many reports of (a) Hillocks and Wydra (2002), (b) Reddy (2015); (c) Pei *et al*. (2014), (d) Hidayat *et al*. (2020).

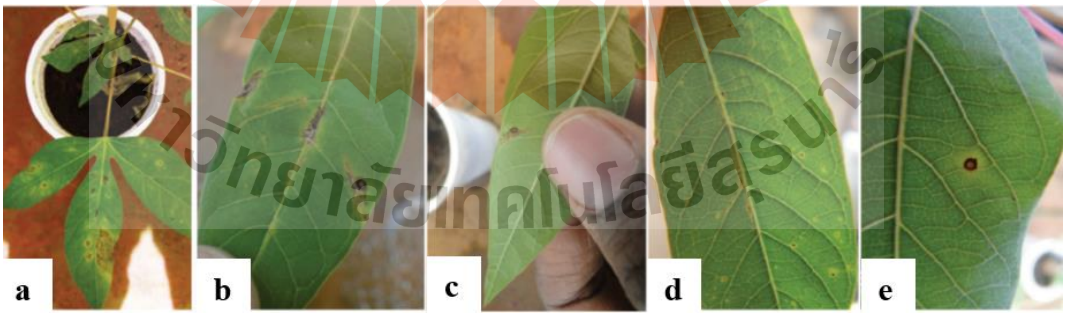

Figure 2.23 Foliar symptoms in cassava cultivar TME 204 upon inoculation with a combination of the three isolates of *Colletotrichum*, *Alternaria* and *Cladosporium*. (a - b) The front side of the leaf and (c - e) back side of the leaf. Source: Ng'ang'a *et al*. (2019).

2.2 Plant innate immunity and induced resistance

Each kind of plant has an innate immune system to counteract adverse environmental factors including abiotic and biotic stresses, which vary level depending on the cultivar and stress factors. The system can be enhanced by elicitors. Plant innate immune system has three stages including perception, signal transduction, and defense response. When pathogens attack plants, the receptors on the plasma membrane recognize damage or microbe/pathogen -associated molecular patterns. Then, signals were formed and transmitted to the nucleus by mitogen activated protein kinases (MAPK) cascade and transcription factors. Here, defense responses were active including Reactive oxygen species (ROS) production, callose deposition, and camalexin production against the pathogens (**Figure 2.24**) (Corwin and Kliebenstein, 2017). Plants respond to adverse conditions through changes in one or more levels of molecular, tissue, anatomical, and morphological traits. If the plants have good tolerance during pathogen attack, they would survive and grow. If the plants are susceptible to pathogen infection, they would die. This response depends on the host cultivar and the type of pathogen that attacks the plants.

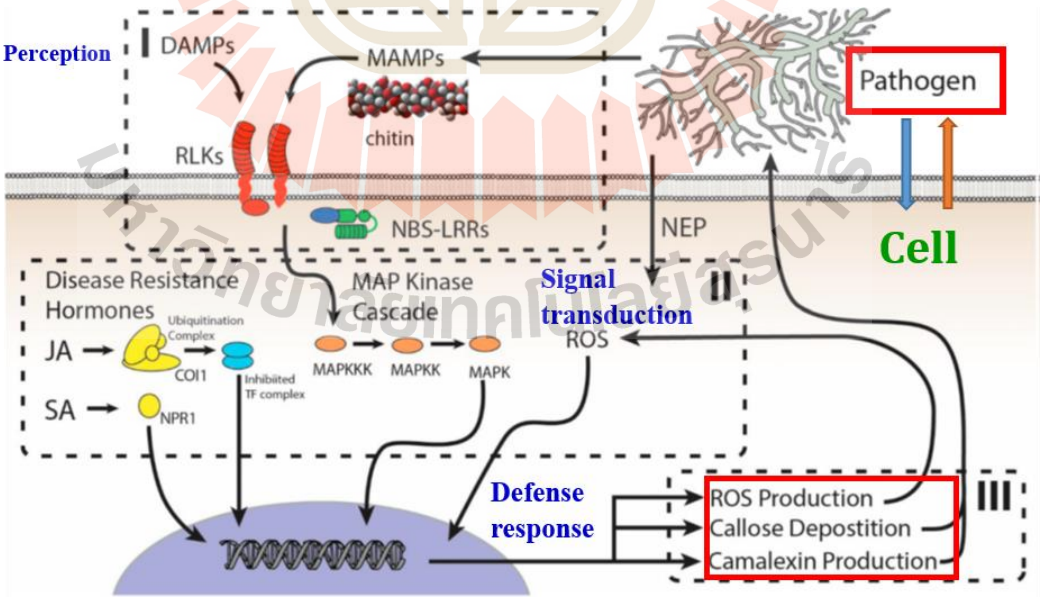

Figure 2.24 General Model for the Plant Innate Immune System. Source: Modified from Corwin and Kliebenstein (2017).

The plant's immune system can be artificially induced by elicitors. The elicitors are biotic or abiotic compounds, which activate defense mechanisms and innate immunity in plants against pathogens and stress conditions. The elicitors can be chemicals including acibenzolar-S-methyl/benzothiadiazole, probenazole, β-amino butyric acid, salicylic acid (SA); microbes including bacterial, fungal, mycorrhiza; chitosan (CS), poly- and oligoglucans, plant extracts, algal extracts including laminarins, ulvans, carrageenans, fucans; extracts of higher plants, composts, biochar, nanoparticles (NPs) including zinc oxide NP, silica NP, silver NP, CS-NP loaded SA. There are two types of stimulated plant resistance including systemic acquired resistance and induced systemic resistance, depending on the signaling pathway (SA for systemic acquired resistance, jasmonic acid and ethylene for induced systemic resistance) as well as the elicitors (**Figure 2.25**) (Burketova *et al*., 2015; Elbeshehy *et al*., 2015; El-Dougdoug *et al*., 2018; Cai *et al*., 2019; Kamaraswamy *et al*., 2019). As such, applying the right elicitors would aid plants against pathogens.

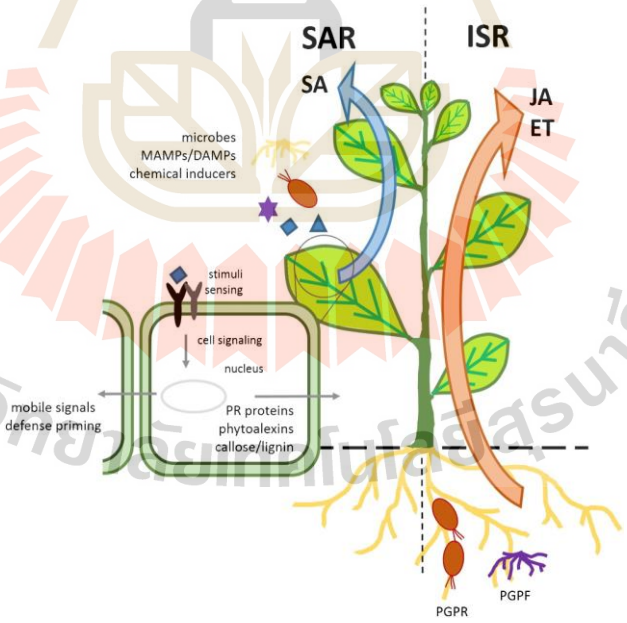

Figure 2.25 Scheme of different types of systemic resistance. *Note*: Systemic acquired resistance (SAR), Induced systemic resistance (ISR), plant-growth-promoting rhizobacteria (PGPR) or fungi (PGPF), Salicylic acid (SA), jasmonic acid (JA) and ethylene (ET). Source: Burketova *et al*. (2015).

2.3 Nanoparticles

2.3.1 What is nanoparticles

NPs is any material with at least one dimension in 1–100 nanometers (nm) range (**Figure 2.26**) (Dhasmana *et al*., 2017). NPs can exist in nature such as virus or viroid molecules, volcanic dust, and oceanic salt sprays, which are quite irregular and vary of sizes. Meanwhile, engineered NPs have uniform shape and size, including nanocubes, nanospheres, bipyramids, nanobars, nanorice angles, nanoplates (**Figure 2.27**). Furthermore, the important characteristics of NPs are their small size and large surface contact area, so they are applicable in many fields (Cobley *et al*., 2009; Elmer and White, 2018).

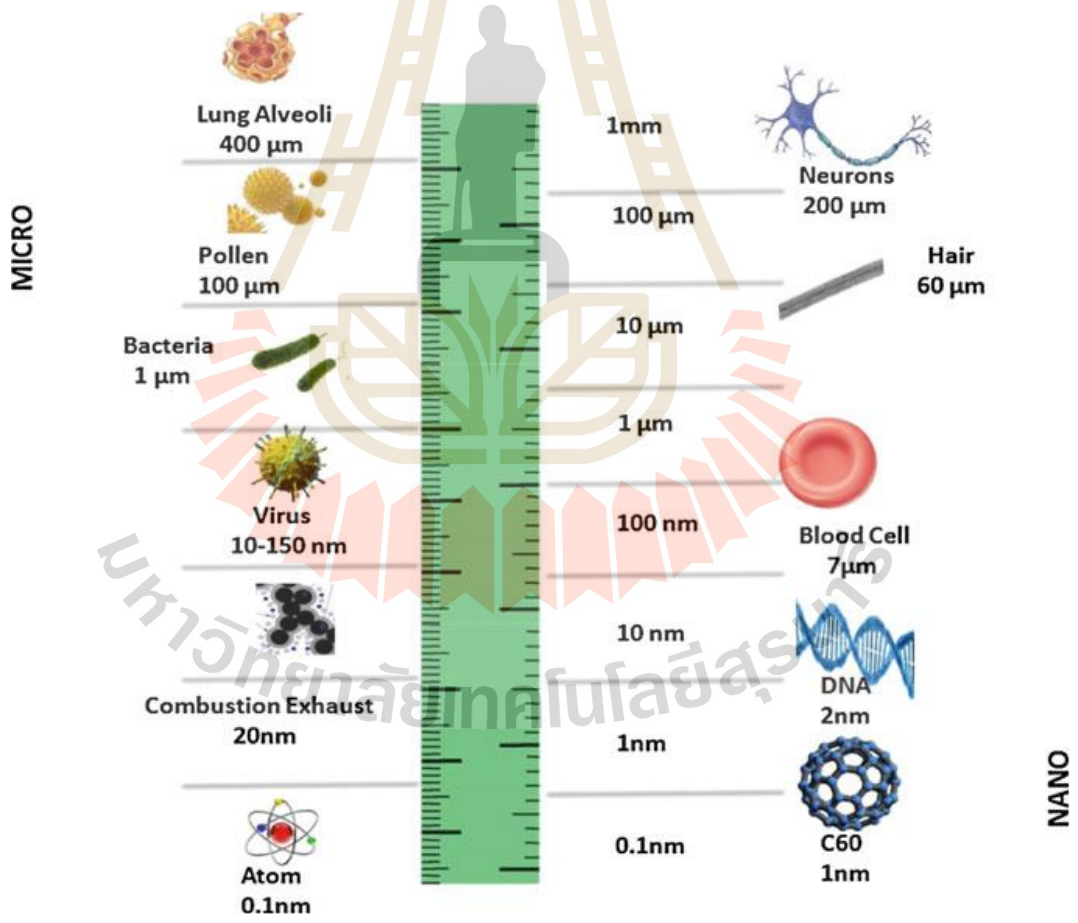

Figure 2.26 Scale of science from millimeter (mm) to nanometer (nm). Source: Dhasmana *et al*. (2017).

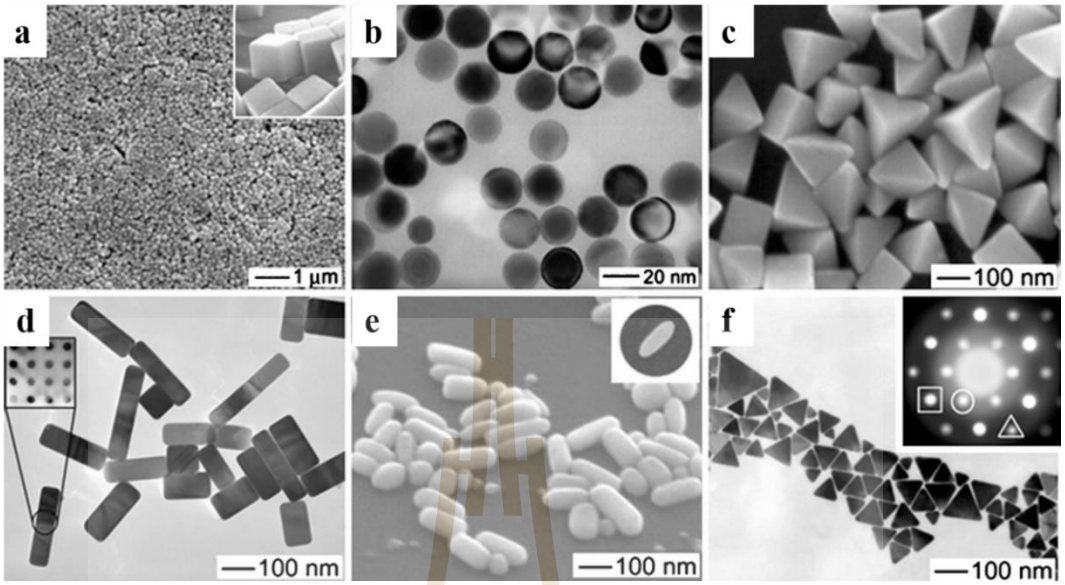

Figure 2.27 Electron microscope images of silver NPs in different shapes. Scanning electron microscope of nanocubes (a), right bipyramids (c), nanorice taken at a 45° angle (e), Transmission electron microscopy of nanospheres (b), nanobars (d), nanoplates (f). Source: Cobley *et al*. (2009).

2.3.2 Application of Nanoparticles in Agriculture and Plant Diseases

In recent years, nanotechnology has been applied in many fields in agriculture to improve the yield and quality of crops, especially to build sustainable agriculture. Nanofertilizers and nanobiotechnology can be used in improving crop yields by providing absorbable nutrients and genetic material, respectively. Furthermore, nanomaterials can be applied to the soil or supplied directly to the crop to increase soil health or crop health against adverse environmental factors such as drought, salinity, and UV-B stress. Also, highly sensitive and precise nanosensors have been used in prediction to make precise farming decisions. Moreover, nanopesticides have been applied to protect plants from pests (**Figure 2.28**) (Shang *et al*., 2019). NPs are used as protectants (silver, gold, copper, titanium dioxide, CS) or carriers (CS, silica, solid lipid, layered double hydroxide) of actives agents (insecticides, fungicides, herbicides, RNA-interference) to protect plants against bacteria, fungi, viruses, and insects. Highlights of

NPs are an improvement of shelf-life, a target on site-specific uptake, and an increase of solubility. Furthermore, it reduces soil leaching and toxicity (**Figure 2.29**) (Worrall *et al*., 2018).

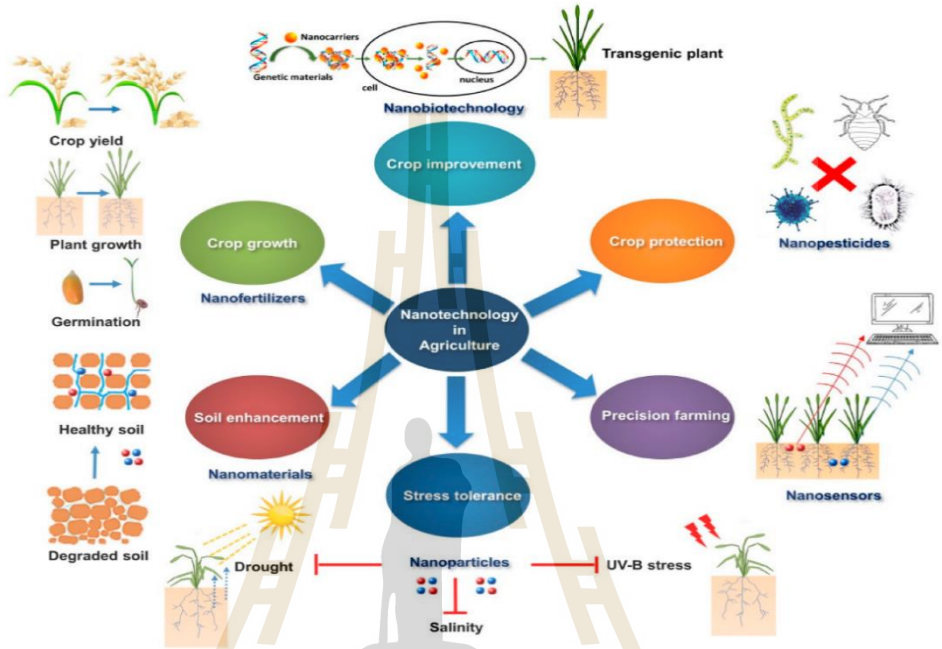

Figure 2.28 Applications of nanotechnology in agriculture. Source: Shang *et al*. (2019).

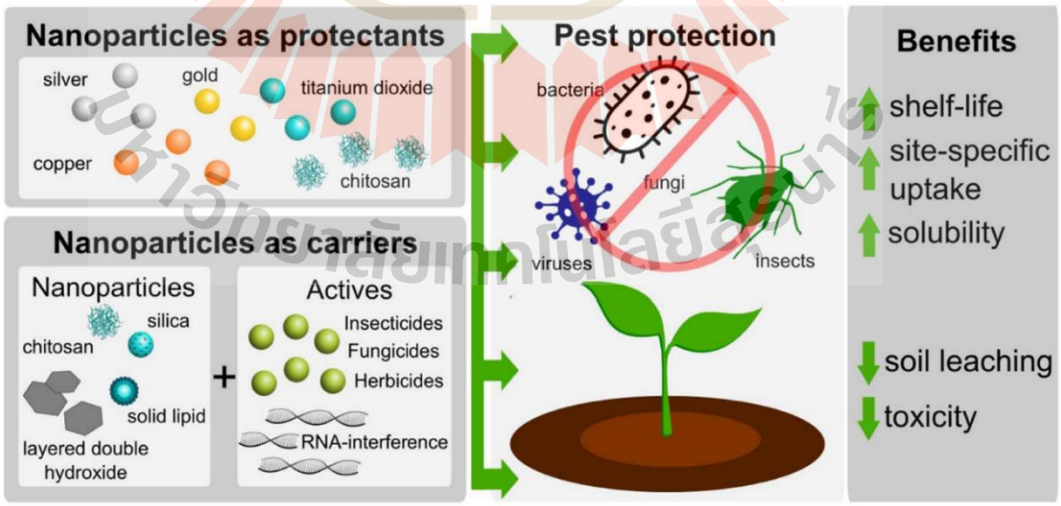

Figure 2.29 Nanomaterials as protectants or carriers to provide crop protection. Source: Worrall *et al*. (2018).

NPs in the form of nutrients and non-nutrients are provided to plants through the leaves or roots to improve plant health as well as control plant diseases. According to the review of Servin *et al*. (2015), micronutrient NPs (Cu, ZnO, MgO, ZnO) and non-micronutrient NPs (Ag) could improve plant growth and inhibit plant pathogens such as *Phoma destructive*, *Phytophthora infestans*, *Rhizopus stolonifera*, *Mucor plumbeus*, *Fusarium oxysporum*, *Botrytis cinerea*, *P. cubensis*, *Pseudomonas syringae* pv. *lachrymans*, *Colletotrichum* spp. (**Figure 2.30**).

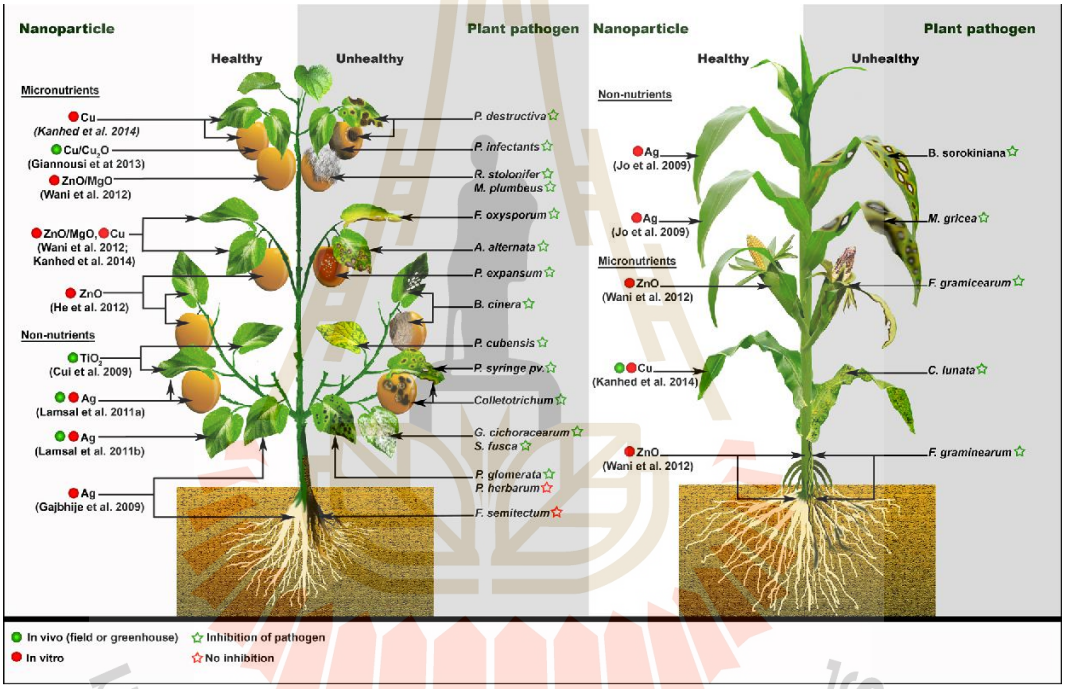

Figure 2.30 Effect of NP nutrients and non-nutrients on crop disease. Source: Servin *et al*. (2015).

In the study of Noha *et al*. (2018), applying foliar silver NPs at 50-70 ppm on tomatoes could increase chlorophyll content, total soluble proteins, activities of peroxidases and polyphenol oxidases when compared with non-treated control. Furthermore, silver NPs could directly inhibit and indirectly reduce disease severity caused by *Tomato mosaic virus* and *Potato virus Y* at 3.9-4.8 and 2.2-4.5 folds, respectively.

In the study of Kumaraswamy *et al*. (2019), CS-NP loaded SA at 0.01-0.16% synthesized by the ionic gelation method can inhibit *Fusarium verticillioides* mycelium growth at 62.2 - 100% and spore germination at 48.3-60.5% under *in vitro* conditions. Also, it could act as an elicitor to activate the maize plant defense system to reduce post-flowering stalk rot disease at 40.5 to 59.47% when compared with the control at field conditions. On the other hand, this kind of NPs promotes plant growth and increases yield by 1.3 to 1.5 folds when compared to the control (**Figure 2.31**).

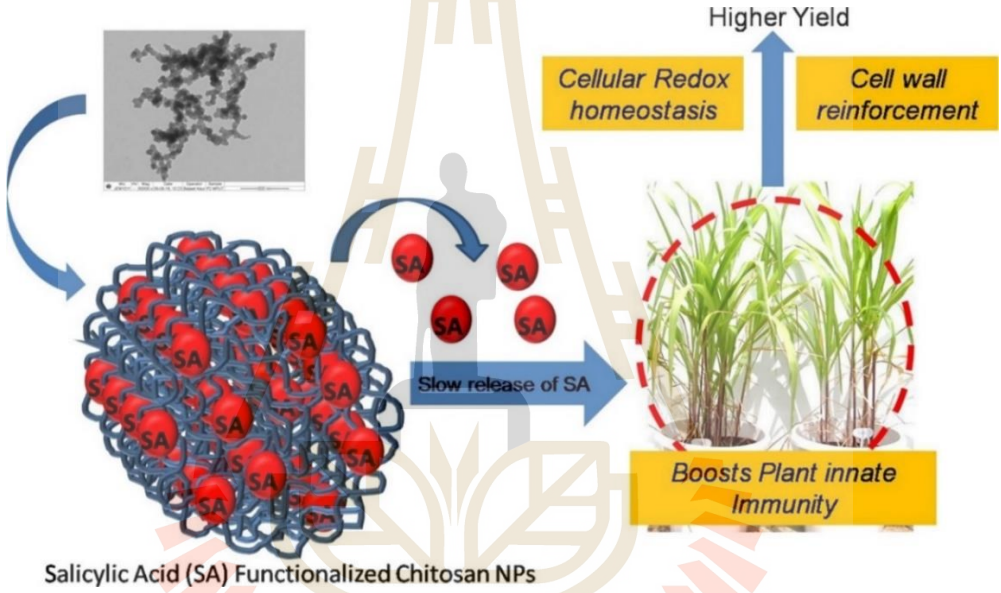

Figure 2.31 SA functionalized CS-NP: A sustainable biostimulant for plant. Source: Kumaraswamy *et al*. (2019).

Saharan *et al*. (2013) examined the antifungal activity of NPs synthesized according to the ionic gelation method. Results showed that CS-NP loaded copper at 0.1% was able to inhibit mycelium growth of *Alternaria alternata*, *Macrophomina phaseolina* and *Rhizoctonia solani* at 89.5, 63.0 and 60.1%, respectively, similar to CS-NP loaded saponin at 0.1% and along with CS-NPs at 0.1% are inhibit mycelium growth at 80.9, 66.2, 27.7% and 78.3, 66.2, 27.7 or 82.2, 87.6, 34.4%, respectively. Also, both CS-NPs, CS-NP loaded copper and CS-NP loaded saponin at 0.06% inhibited the germination of *A. alternata* at 84.4, 83.3, and 78.3%, respectively.

2.3.3 Approach to Nanoparticle Synthesis

There are two approaches to synthesize NPs including top-down and bottom-up methods. Those NPs come in different sizes, shapes and functions. The top-down methods are to synthesize NPs from bulk, including chemical etching, laser ablation, mechanical milling, ball milling, sputtering and electro-explosion. The bottom-up methods are to synthesize NPs from atoms or molecules, including chemical vapor deposition, sol-gel processes, laser pyrolysis, spray pyrolysis, atomic/molecule condensation, aerosol processes and green synthesis by microorganisms or plant extracts (**Figure 2.32**) (Singh *et al*., 2018). The CS-NPs, CS-NP loaded copper, CS-NP loaded saponin, CS-NP loaded SA in researches of Saharan *et al*. (2013) and Kumaraswamy *et al*. (2019) were synthesized by ionic gelation method (sol-gel processes).

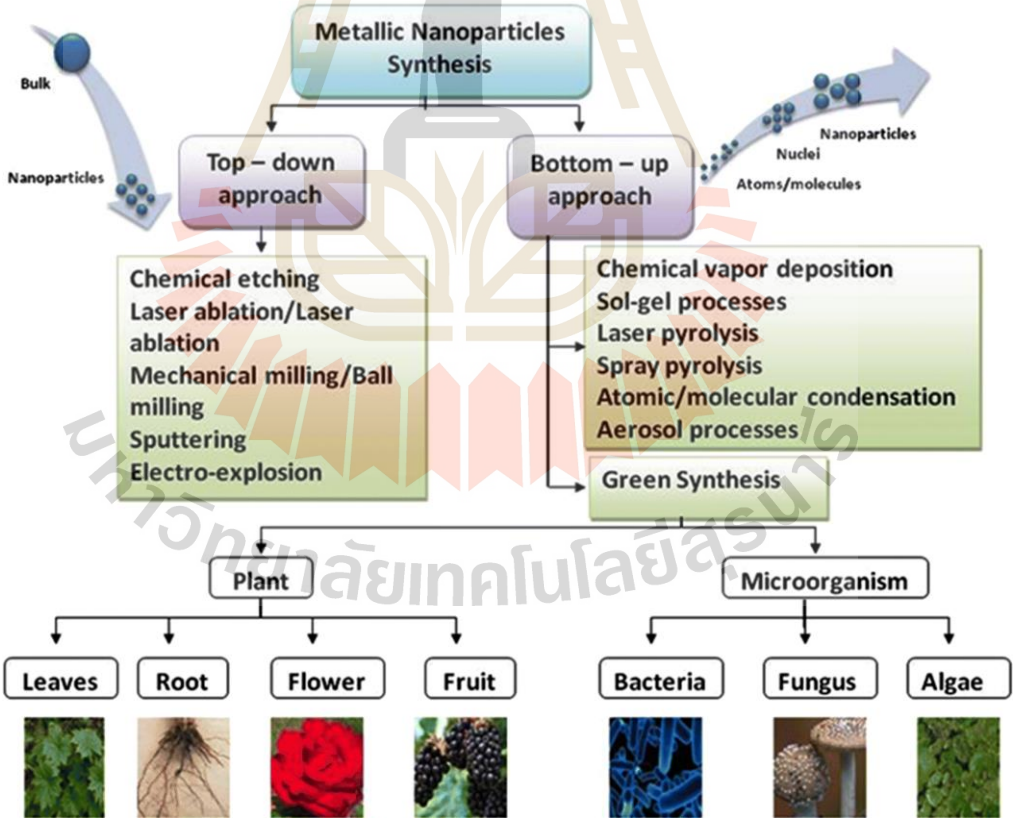

Figure 2.32 Different synthesis approaches available for the preparation of metal NPs. Source: Singh *et al*. (2018).

2.1.4 Ionic Gelation Method

In 1997, two publications by Calvo *et al*. about the synthesis of NPs by a method called ionic (ionotropic) gelation. There, sodium tripolyphosphate (TPP) solution is added to CS and/or diblock copolymer of ethylene oxide and propylene oxide under stirring conditions, leading to the formation of CS-NP particles, with the size 200-1000 nm and zeta potential 20-60 mV, depends on mass ratio CS/TPP or molecular weight of CS. This hydrogel formation is known due to the electrostatic interactions of the amino group of CS and the polyanion group of TPP. In addition, in these studies, bovine serum albumin (protein), tetanus, diphtheria toxoid (vaccine) were also successfully loaded into NPs (Calvo *et al*., 1997a; Calvo *et al*., 1997b). Since then (Dec, 2021), approximately 11,300 researches or review articles related to this method have been published according to the statistics of **Google Scholar (Figure 2.33)**. Interestingly, the number of articles has increased year by year, reaching the top in 2021 with 2020 publications. This shows the researchers' interest in the ionic gelation method and NPs.

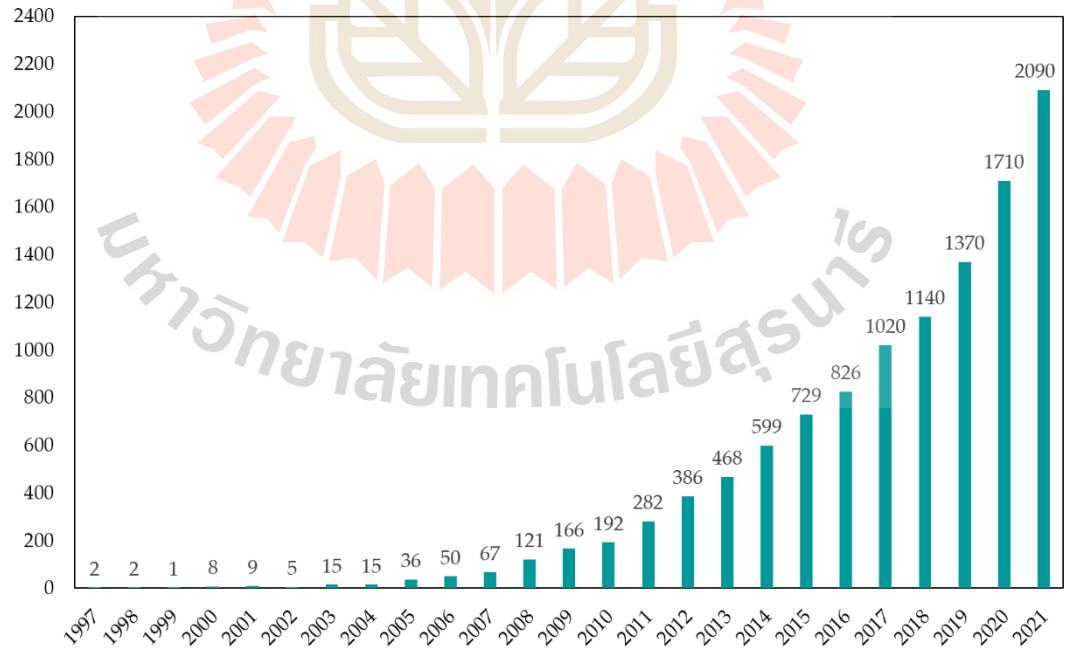

Figure 2.33 The number of articles in Google Scholar searched by key word “ionic gelation” + "nanoparticles". Source: Designed from Google Scholar.

In general, this is a method to form microparticles or NPs based on electrostatic interaction between or opposite charge type that contains at least one polymer under mechanical stirring conditions (Pedroso - Santana and Fleitas - Salazar, 2020). On the records of Racovită *et al*. (2009), Mudgil *et al*. (2012), and Pedroso - Santana and Fleitas - Salazar (2020), polymers including CS, carboxymethyl cellulose, collagen, dextran, fibrin, gelatin, gellan gum, hyaluronic acid, sodium alginate, pectin and anions including chloride salts (Ba, Ca, Mg, Cu, Zn, Co), sulfate salts (Na, Mg, or octyl-, lauryl-, hexadecyl-, cetostearyl-), polyphosphate salts (pyro-, tri-, tetra-, octa-, hexameta-), ferrocyanide and ferricyanide salts were used for synthesis of NPs. Among them, CS (polymer-cation) and TPP (anion) are most commonly used. Furthermore, drugs or bioactive molecules can be encapsulated into matrix of NPs to increase its efficacy.

CS is a natural polysaccharide, produced by the alkaline deacetylation of chitin, which possesses excellent characters including low toxic, cheap, biodegradability, biocompatibility, environmental non-toxicity, adsorption abilities (Kashyap *et al*., 2015; Malerba and Cerana, 2019; Chakraborty *et al*., 2020). With its superiority, CS is used in wastewater treatment, cosmetics, toiletries, food, beverages, agrochemicals, pharmaceuticals, and their production at the South-East Asian region which reaches 1.5 million tons per year (FAO, 2014; FAO, 2020). The properties of CS could be modified by chemical and/or mechanical processes by hydroxide and/or amide groups, respectively (Agarwal *et al*., 2015). TPP is also a safe material, commonly used in the synthesis of NPs by the ionic gelation method as a crosslinking agent (Pedroso - Santana and Fleitas - Salazar, 2020; U.S. Food and Drug Administration, 2021).

CS and TPP can be seen as a “legendary” pair of counter ions in the ionic gelation method because of their popularity in studies. Typically, cations and polyanions are released from dissolving CS and TPP in acetic acid and distilled water, respectively. When TPP is dripped into a CS solution, the polyanion (negative charge) bonds to an amino group (positive charge) by electrostatic interaction, which causes CS to undergo a gel ionization process leading to the formation of NPs that are usually

collected by centrifuge (Kashyap *et al*., 2015; Wang *et al*., 2016; Maluin and Hussein, 2020). The primary interaction in ionic crosslinking configuration is H-link and T-link. The H-link is interaction of O- and NH_3^+ in the same plane while the H-link is interaction of nonbrinding oxygen atom and NH_3^+ in different plane (**Figure 2.34**) (Koukaras *et al*., 2012; Pedroso - Santana and Fleitas - Salazar, 2020). The formation of NPs is influenced by CS concentration, CS molecular weight, CS/TPP ratio, drug or bioactive molecules concentration, pH, stirring, and centrifuge (time, speed) (Wang *et al*., 2016).

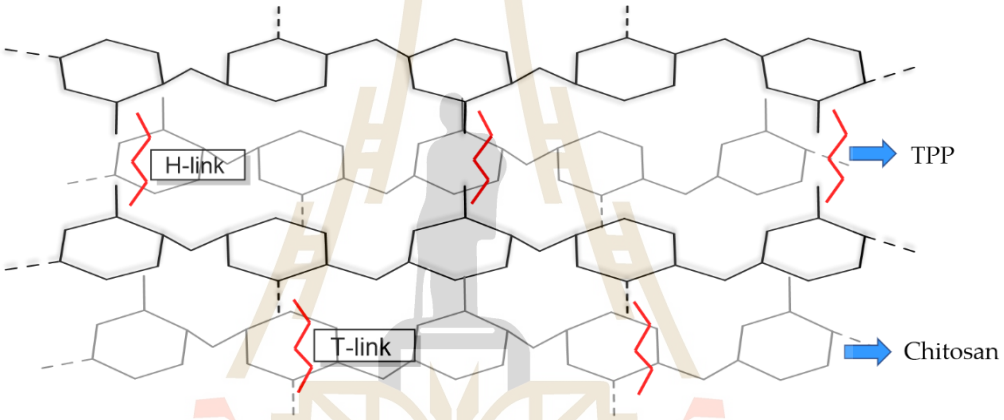

Figure 2.34 The electrostatic interactions between CS and TPP by an H-link configuration (in the same plane) and T-link configuration (in a different plane) in ionotropic gelation.

After the synthesis of NPs, their popular features include hydrodynamic diameter, zeta potential, polydispersity index (PDI), morphology, dry state diameter, interaction confirms, encapsulation efficiency (EE), loading capacity (LC), crystal phase, defined by dynamic light scattering (DLS), scanning electron microscope (SEM), transmission electron microscopy (TEM), fourier-transform infrared spectroscopy (FTIR), inductively coupled plasma atomic emission spectroscopy (ICP-OES), atomic absorption spectrometry (AAS), ultra violet visible (UV-Vis), x-ray diffraction techniques.

These features will vary, depending on the synthesis condition that is on detailed in **Table 2.10** and **Table 2.11**.

NPs is any material with at least one dimension in 1-100 nanometers (nm) range (Devi *et al*., 2020). However, the size of the NPs synthesized by the ionic gelation method is usually greater than 100 nm (Saharan *et al*. 2013, Kheiri *et al*. 2017, Bangun *et al*. 2018, Suryadi *et al*. 2019, Oh *et al*., 2019, Rodriguez *et al*. 2019). The characteristics of CS-NPs synthesized according to the ionic gelation method are presented in **Table 2.10**. In the synthesis, CS-NPs, mass ratios and volume ratios between CS and TPP are varied from 1:10 to 15:1 and 1:10 to 25:1 (Mohamed *et al*., 2018; Saharan *et al*., 2013; Bangun *et al*., 2018; Du *et al*., 2009). CS-NPs smaller than 100 nm are synthesized with CS and TPP mass-to-volume ratios reported in studies of Mohamed *et al*. (2018) with 2:5 and 1:10 (50 nm), Maluin *et al*. (2019) with 5:4 and 1:1 (2.3-7.5 nm), Manikandan and Sathiyabama (2016) with 6:1 and 3:1 (83.32 nm), Nadendla *et al*. (2018) with 5:1 and 5:1 (86.8 nm), Du *et al*. (2009) with 25:1 and 15:1 (53.99 nm). Similarly, CS-NPs larger than 100 nm were reported in studies of Kheiri *et al*. (2017) with 3:1 (180.9-595.7 nm), Saharan *et al*. (2013) with 1:10 and 1:1 (192.5 nm), Suryadi *et al*. (2019) with 10:1 and 5:1 (126.2-167.1 nm), 8:1 and 4:1 (493.3-573.1 nm), Oh *et al*. (2019) with 2:5 and 1:1 (100-1000 nm), Bangun *et al*. (2018) with 5:1 and 2:1 (238.17 nm), Rodriguez *et al*. (2019) with 5:1 and 1:2 (204.8-472.1 nm). The CS molecular weight also influences NPs formation. As reported by Kheiri *et al*. (2017), CS-NPs were synthesized from CS low molecular weight (161 kDa) of 180.9 nm in size, smaller when compared with a medium (300 kDa) and high (810 kDa) molecular weight of 309.9 and 339.4 nm, respectively. Suryadi *et al*. (2019) had various mass (10:1 and 8:1) and volume (5:1 and 4:1) ratio between CS and TPP with time stirring (60 and 30 min). Results showed that CS-NPs with longer stirring would have smaller sizes in the same mass ratios of 126.2, 167.1, 493.3, 573.1 nm for 10:1 and 5:1, 8:1, 4:1 (volume ratio), respectively. This is slightly different from the study of Bangun *et al*. (2018) when increasing mass ratio CS:TPP from 5:1 to 20:1 with the same volume ratio, the NPs size

increased from 238.17 to 1315.37 nm. Rodriguez *et al*. (2019) did a research with various sonicate times for 3, 5, 10, and 20 min, the results showed that the NPs size was decreased, which was 344.6, 472.1, 261.3, and 204.8 nm, respectively. In addition to centrifuge, Kheiri *et al*. (2017) adjusted the pH of the CS:TPP mixture to 4.5-5 to collect NPs. The results showed that the NPs size was greater than that of the centrifugation method for low (180.9 and 225.7 nm) and high (339.4 and 595.7 nm) CS molecular weight, and similar to medium molecular weight (309.9 and 301.5 nm), respectively. The PDI of CS-NPs ranged from 0.195 (Rodriguez *et al*., 2019) to 1.0 (Du *et al*., 2009). A low PDI shows a high uniform dispersion of the particles in the solution and vice versa (Clayton *et al*., 2016). CS-NPs have PDI 0.31-0.52 (Kheiri *et al*., 2017), 0.6 (Saharan *et al*., 2013), 0.44-0.69 (Suryadi *et al*., 2019), 0.20-0.57 (Rodriguez *et al*., 2019). Zeta potential is an effective electric charge on NPs surface, from -100 mV to 100 mV, only NPs stability (Selvamani, 2019). Zeta potential of CS-NPs at 21.7-45.6 mV (Kheiri *et al*., 2017), 45.3 mV (Saharan *et al*., 2013), -28 mV (Manikandan and Sathiyabama, 2016), 32.4 mV (Sathiyabama *et al*., 2016a), 20.8-27.8 mV (Suryadi *et al*., 2019), 51.37 mV (Du *et al*., 2009). CS-NPs were mostly spherical when observed under SEM or TEM (Mohamed *et al*., 2018; Maluin *et al*., 2019; Saharan *et al*., 2013; Manikandan and Sathiyabama, 2016; Nadendla *et al*., 2018; Sathiyabama *et al*., 2016a; Rodriguez *et al*., 2019) or spherical- like (Suryadi *et al*., 2019; Oh *et al*., 2019). Furthermore, sizes under TEM (dry state) which smaller than DLS (hydrodynamic size), were showed in the study of Maluin *et al*. (2019) with 1.5 nm, Manikandan and Sathiyabama (2016) with 20-50 nm, Sathiyabama *et al*. (2016a) with 10-30 nm, Oh *et al*. (2019) with 100 nm while DLS is 2.3-7.5, 83.32, 89.8, 100-1000 nm, respectively. In CS-NPs, the interaction between ammonium group of CS and polyphosphoric of TPP was determined by FTIR with peaks (cm^{-1}) of 3428, 1580 (Mohamed *et al*., 2018), 3288, 1647 (Maluin *et al*., 2019), 1636, 3410 (Saharan *et al*., 2013), 1648.84, 1527.35 (Manikandan and Sathiyabama, 2016), 1563 (Nadendla *et al*., 2018), 3421.2 (Bangun *et al*., 2018). The crystal phase of CS-NPs is amorphous, which has been identified by X-ray diffraction (Manikandan and Sathiyabama, 2016; Maluin *et al*., 2019). UV-Vis is not common in determining

properties of CS-NPs synthesized according to the ionic gelation method. As reported by Manikandan and Sathiyabama (2016) and Oh *et al*. (2019), CS-NPs absorb at wavelength 295 and 320 nm, respectively. Interestingly, Sathiyabama *et al*. (2016a) synthesized CS-NPs by CS and anionic protein of *Penicillium oxalicum* by mass and volume ratio by 7.5:0.108 and 5:2 under stirring for 30 min. Hydrodynamic size, dry state size, PDI, zeta potential, were 89.8 nm, 10-30 nm (spherical under SEM), 0.225, -37 mV, respectively. Besides, the peaks of 1602.8, 1564.18, and 1403.5 cm^{-1} characterize the binding of proteins and CS. Furthermore, these NPs absorb at wavelength 285 nm and are amorphous.

Table 2.10 Character of CS-NPs synthesized by ionic gelation method.

Mass ratio	Volume ratio	Condition synthesis	DLS	SEM, TEM	FTIR (cm^{-1})	UV (nm)	XRD	Reference
15:2	25:1	25 mL of 0.3% CS, 1 mL of 1% TPP; stirring 20 min, sonication 1.5 kW for 30 min, centrifuge 12,000 g for 10 min	53.99 nm PDI 1.0 51.37 mV	-	-	-	-	Du *et al*., 2009
1:10	1:1	0.1% CS and 1% TPP with ratio 1:1; 10,000 rpm for 10 min and ultrasonication	192.5 nm PDI 0.6 +45.33 mv	Spherical	1636, 3410: hydrogen bonding	-	-	Saharan *et al*., 2013
69.4:1	5:2	15 mL of 0.5% CS (pH 4.8) and 6 mL of 0.018% anionic protein of *Penicillium oxalicum*, stirring 30 min, centrifuge 10,000 G for 10 min	89.8 nm PDI 0.225 -37 mV	Spherical 10-30 nm	1602.8, 1564.18, 1403.5: binding of Protein and CS	285 nm	Amorphous	Sathiyabama and Parthasarathy, 2016
3:1	3:1	3 mL of 0.5% CS vary (a) low molecular weight (Mw = 161 kDa), (b) medium molecular weight (Mw = 300 kDa), (c) high molecular weight (Mw = 810 kDa), and 1 mL of 0.5% TPP, centrifuge 25,000 rpm for 30 min	(a) 180.9 nm, PDI 0.31, 45.6 mV (b) 309.9 nm, PDI 0.46, 33.2 mV (c) 339.4 nm, PDI 0.52, 21.7 mV	-	-		-	Kheiri *et al*., 2017

Mass ratio	Volume ratio	Condition synthesis	DLS	SEM, TEM	FTIR (cm^{-1})	UV (nm)	XRD	Reference
3:1	3:1	3 mL of 0.5% CS (pH 4.7-5) vary (d) low molecular weight (Mw = 161 kDa), (e) medium molecular weight (Mw = 300 kDa), (f) high molecular weight (Mw = 810 kDa), and 1 mL of 0.5% TPP, adjust pH to 4.5-5, discard supernatant to collect CS-NPs	(d) 225.7 nm, PDI 0.44, 33.4 mV (e) 301.5 nm, PDI 0.2, 20.2 mV (f) 595.7 nm, PDI 0.92, 16 mV	-	-	-	-	
2:5	1:10	CS 0.2%: TPP 0.05% (1:10), 25°C, pH 4	50 nm	Spherical	3428, 1580: hydrogen bonding between polyphosphoric of TPP and ammonium group of CS		-	Mohamed *et al*., 2018
6:1	3:1	0.5% CS (pH 5) and 0.25% TPP with ratio 3:1, 10,000 rpm for 10 min	83.32 nm PDI 0.31 -28 mV	Spherical 20-50 nm	1648.84, 1527.35: interaction between ammonium group of CS and polyphosphoric group of TPP	295 nm	Amorphous	Manikandan and Sathiyabama, 2016

Mass ratio	Volume ratio	Condition synthesis	DLS	SEM, TEM	FTIR (cm^{-1})	UV (nm)	XRD	Reference
5:1	5:1	5 mL of 0.1% CS (pH 5.5) and 1 mL of 0.1% TPP, 20,000 rpm for 30 min	86.8 nm +32.4 mV	Spherical	1563: interaction of amide and phosphate	-	-	Nadendla et al., 2018
5:1 10:1 15:1 20:1	2:1	10 mL of 0.1% TPP, 20 mL of CS vary at (a) 0.25%, (b) 0.5%, (c) 0.75% and (d) 1%; stirring 8 hours, sonication 45 min	(a) 238.17 nm (b) 575.2 nm (c) 706.01 nm (d) 1315.37 nm	-	3421.2: interaction between phosphate and NH_2	-	-	Bangun *et al*., 2018
5:4	1:1	0.25 g CS and 0.2 g TPP/40 mL, pH 3.6, 2% TWEEN 80, 40000 rpm for 10 min	bimodal particle with 2.3 and 7.5 nm	1.5 nm spherical	3288, 1647: hydrogen bonding between amino of CS and phosphate of TPP		Amorphous	Maluin *et al*., 2019
10:1 8:1	5:1 4:1	0.2% Hydrolyzed CS (by chitinase from *Burkholderia cepacia* E76) and 0.1% TPP with vary ratio (a) 5:1 and stirring 60 min, (b) 5:1 and stirring 30 min, (c) 4:1 and stirring 60 min, (d) 4:1 and stirring 30 min	(a) 126.2 nm, PDI 0.44, 27.8 mV (b) 167.1 nm, PDI 0.47, 25.4 mV (c) 493.3 nm, PDI 0.69, 22.9 mV (d) 573.1, PDI 0.54, 20.8 mV	Spherical-like	-	-	-	Suryadi *et al*., 2019

Mass ratio	Volume ratio	Condition synthesis	DLS	SEM, TEM	FTIR (cm^{-1})	UV (nm)	XRD	Reference
2:5	1:1	0.1% CS, 0.25% TPP with ratio 1:1, centrifuge 10,000 rpm for 10 min, ultrasonication 28% pulse for 100 s at 4°C	100-1000 nm	100 nm spherical-like High porous surface	1576: NH_2 bond (wagging) 1412: C-H bending vibration of alkyl group	320 nm	-	Oh *et al*., 2019
5:1	1:2	10 mL of 1% CS, 20 mL of 0.1% TPP, pH 5.5, stirring 1,000 rpm for 5 min, sonication 30% amplitude for vary (a) 3, (b) 5, (c) 10, (d) 20 min	(a) 344.6 nm, PDI 0.57, 44.1 mV (b) 472.1 nm, PDI 0.507, 42.9 mV (c) 261.3 nm, 0.195 PDI, 42.8 mV (d) 204.8 nm, 0.205 PDI, 36.0 mV	Globular	-	-	-	Rodriguez *et al*., 2019

Note: CS: Chitosan; DLS: Dynamic light scattering; FTIR: Fourier-transform infrared spectroscopy; NPs: Nanoparticles; PDI: polydispersity index; SEM: Scanning electron microscope; TEM: Transmission electron microscopy; TPP: Sodium tripolyphosphate; UV: Ultra violet visible; XRD: X-Ray Diffraction.

To improve application efficiency, CS-NPs can load drugs, bioactive molecules (active ingredients), depending on the purpose. These NPs were synthesized by adding drugs, bioactive molecules solution to CS and TPP during the gelation process (incorporation) or after that (incubation) (Kashyap *et al*., 2015; Malerba and Cerana, 2019; Maluin and Hussein, 2020; Devi *et al*., 2020). That is shown in **Table 2.11**. The active ingredient can be metal ions (Cu, Ag, Zn, Mn, Fe) (Du *et al*., 2009; Saharan *et al*., 2013), drugs (Gentamicin-SA complex, Ag-Furosemide complex) (Ji *et al*., 2011; Rodriguez *et al*., 2019), proteins (Harpin from *P. syringae* pv. *syringae*), agrochemicals (Hexaconazole) (Maluin *et al*., 2019), hormone (SA) (Kumaraswamy *et al*., 2019), other bio-molecules (saponin, thiamine, *Achillea melefolium* extract) (Saharan *et al*., 2013; Muthukrishnan *et al*., 2019; Kain and Kumar, 2020). The mass ratio between the active ingredients and the CS or TPP can be smaller or larger, which affects the characters of the NPs. Metal ions (Ag, Cu, Zn, Mn, Fe) are added to CS: TPP (1:10 or 15:2) at the rate such that the final ion concentration reaches 0.012% (Du *et al*., 2009; Saharan *et al*., 2013). Ag-Furosemide complex added with CS:TPP with ratios 0.005:10:2 and 0.01:10:2. The DLS of the two NPs were 210.5 nm, PDI 0.232, 41.5 mV; and 197.1 nm, PDI 0.234, 36.7 mV, respectively (Rodriguez *et al*., 2019). When changing the mass ratio TPP:CS by 1:3, 1:4, 1:5, 1:6, 1:7 (keeping the gentamicin-salicylic complex ratio), the DLS of NPs changed with decreasing size and increasing zeta potential that were 343.3 nm, PDI 0.41, 34.26 mV; 217.7 nm, PDI 0.275, 35.77 mV; 180.0 nm, PDI 0.235, 37.12 mV; 172.2 nm, PDI 0.308, 39.44 mV; 150.8 nm, 0.237 PDI, 42.43 mV, respectively (Ji *et al*., 2011). On the other hand, the results of various mass ratios between TPP and CS:Hexaconazole by 1:5:10, 2:5:10, 4:5:10, 8:5:10 showed that the size of the NPs decreased with respect to their ratios were 220.2, 164.2, 68.1, and 6.5-18.1 nm, respectively (Maluin *et al*., 2019). The Harpin protein (*P. syringae* pv. *syringae*) was also loaded into CS-NPs, with size at 133.7 nm and zeta potential at 48.6 mV, with an initial mass ratio of 1: 100: 20 (Nadendla *et al*., 2018). When adding SA to CS: TPP at the ratio 1: 4: 2, the DLS was 368.7 nm, PDI 0.1, +34.1 mV (Kumaraswamy *et al*., 2019). Saharan *et al*. (2013) and Muthukrishnan *et al*. (2019) added saponin and thiamine to CS:TPP

at the ratio 1:2:20 and 25:24:4, DLS of the two NPs were 373.9 nm (2 peaks), PDI 1.0, +31 mV and 596 nm, 37.7 mV, respectively. In a study by Kain and Kumar (2020), CS-NP loaded with *A. melefolium* extract by mix the extract (semi-solid form) with 0.1% CS solution to obtain 5, 10, 15, and 20% before adding 1% TPP solution. That led to form NPs with the size of 118 nm but containing 3 peaks (10, 122, and 712 nm). CS-NPs loaded metal ions have a compact polyhedron shape, while CS-NPs loaded saponin, SA, gentamicin-SA complex were spherical when observed under SEM and TEM (Ji *et al*., 2011; Saharan *et al*., 2013; Kumaraswamy *et al*., 2019). The size of CS-NPs loaded active ingredient when recorded under the TEM is sometimes larger than the size specified by DSL. CS-NPs loaded Hexaconazole with initial CS:TPP:Hexaconazole ratios of 5:1:10 and 5:2:10 had dried state sizes at 271.4 and 168.5 nm while DLS is 220.2 and 164.2 nm, respectively. However, at the ratio of 5:4:10 and 5:8:10, the TEM size were 32.3 and 8.1 nm compared with DLS at 68.1 and 6.5-18.1 nm (2 peaks), respectively (Maluin *et al*., 2019). Also, CS-NPs loaded thiamine was 596 nm by DLS but 10-60 nm by TEM that very different (Muthukrishnan *et al*., 2019). Not only using TPP as anions, Bocchetta (2020) also synthesized a novel conductive bio-composite membrane by combining CS and phosphotungstate anions on an aluminum substrate by the ionic gelation method. Interaction in these NPs can also be determined by FTIR. CS-NPs load Cu is characterized by peaks of 1631 and 1536 cm^{-1} for amide ($-CONH_2$) and primary amide ($-NH_2$), respectively (Saharan *et al*., 2013). Peaks of 1345 and 1095 cm^{-1} feature harpin protein assigned to C-N and C-O stretch (Nadendla *et al*., 2018). Peaks of 3218 and 3430 cm^{-1} characterize a hydrogen bonding between three chemicals in CS-NPs loaded Hexaconazole (Maluin *et al*., 2019). CS-NPs loaded saponin characterized by peak 3430 cm^{-1} for the hydrogen bonding between saponin and CS, 1536 cm^{-1} for amide linkage between saponin and CS-NPs (Saharan *et al*., 2013). The peak at 1317 cm^{-1} features interaction between -COOH of SA with primary amide ($-NH_2$) of CS in a CS-NPs loaded SA (Kumaraswamy *et al*., 2019). In CS-NPs loaded Gentamicin-SA complex, a peak at 3423 cm^{-1} characterizes the hydrogen bonding between -OH group bending of gentamicin and CS while two peaks of 1542,

1637 cm^{-1} for interaction between NH_3^+ of CS and TPP, 1300 cm^{-1} for CN bending between COOH of SA and primary amide of CS (Ji *et al*., 2011). And the peak of 1657 cm^{-1} characterizes the binding of thiamine and CS in these NPs (Muthukrishnan *et al*., 2019). The crystal phase of the NPs could also be identified by the X-ray diffraction technique. CS-NPs loaded silver-furosemide complex was amorphous while the crystalline peak of Hexaconazole was clearly embedded in the amorphous phase of CS (Maluin *et al*., 2019). In addition, peak 2θ of 10°-20° and 18°-30° recognized for SA and CS, respectively (Kumaraswamy *et al*., 2019). UV-Vis is seldom used, only CS-NPs loaded with 267 nm absorption thiamine was reported by Muthukrishnan *et al*. (2019). In general, the main steps for synthesizing and building the CS-NPs loaded active ingredients by the ionic gelation method are shown in **Figure 2.35**. Parameters can be optimized to suit each laboratory's conditions.

Table 2.11 Characteristics of CS-NPs loaded active ingredients synthesized by ionic gelation method.

NPs	Mass ratio	Volume ratio	Condition synthesis	DLS	SEM, TEM	FTIR (cm^{-1})	UV (nm)	XRD	Reference
CS-NP loaded mental ion (Ag, Cu, Zn, Mn, Fe)	15:2	25:1	25 mL of 0.3% CS, 1 mL of 1% TPP, salt solution at 0.3% added to mixture to ion final concentration 0.012%; stirring 20 min, sonication 1.5 kW for 30 min, centrifuge 12000 g for 10 min	(Ag) 90.29 nm, 92.05 mV (Cu) 121.9 nm, 88.69 mV (Zn) 210.9 nm, 86.65 mV (Mn) 102.3 nm, 75.74 mV (Fe) 95.81 nm, 71.42 mV	-	-	-		Du *et al*., 2009
CS-NP loaded copper (Cu)	1:10	1:1	0.1% CS and 1% TPP with ratio 1:1, added 0.01% $CuSO_4$ to final concentration of Cu^{2+} 0.012% in mixture, 10000 rpm for 10 min and ultrasonication	196.4 nm PDI 0.5 +88 mv	Compact polyhedron	1631: -$CONH_2$ 1536: -NH_2	-	-	Saharan *et al*., 2013

NPs	Mass ratio	Volume ratio	Condition synthesis	DLS	SEM, TEM	FTIR (cm^{-1})	UV (nm)	XRD	Reference
CS-NP loaded Silver-Furosemide complex	10:2:0.01	1:2	10 mL of 1% CS, 20 mL of 0.1% TPP, pH 5.5, stirring 1000 rpm for 5 min, sonication 30% amplitude for 10 min. (a) 5, (a) 10 mg Silver-Furosemide complex was mix with TPP solution	(a) 210.5 nm, PDI 0.232, 41.5 mV (b) 197.1 nm, PDI 0.234, 36.7 mV	-	-	-	Amorphous	Rodriguez *et al*., 2019
CS-NP loaded Harpin (*P. syringae* pv. *syringae*)	100:20:1	10:2:1	5 mL of 0.1% CS (pH 5.5) and 1 mL of 0.1% TPP, 0.5 mL of 0.01% Harpin, 20000 rpm for 30 min	133.7 nm +48.6 mV	-	1345, 1095: Harpin assigned to C-N stretch and C-O stretch in CS-NP loaded Harpin	-	-	Nadendla *et al*., 2018
CS-NP loaded Hexaconazole	5:1:10 5:2:10 5:4:10 5:8:10	5:2:5	100 mL of 0.5% CS and 100 mL of 1% Hexaconazole, 2% TWEEN 80, 40 mL of TPP vary at (a) 0.25%, (b) 0.5%, (c) 1% and (d) 2%	(a) 220.2 nm (b) 164.2 nm (c) 68.1nm (d) 2 peaks (6.5 and 18.1 nm)	(a) 271.4 nm (b) 168.5 nm (c) 32.3 nm (d) 8.1 nm	3218: hydrogen bonding of 3 chemicals	-	Crystalline of hexaconazole clear embedded in amorphous phase of CS	Maluin *et al*., 2019

NPs	Mass ratio	Volume ratio	Condition synthesis	DLS	SEM, TEM	FTIR (cm^{-1})	UV (nm)	XRD	Reference
CS-NP loaded saponin	2:20:1	10:10:1	0.1% CS, 1% TPP and 0.5% saponin with ratio 10:10:1, 10000 rpm for 10 min and ultrasonication	373.9 nm (2 peaks) PDI 1.0 +31 mV	Spherical	1560: amide linkage between saponin and CS-NPs 3430: hydrogen bonding between saponin and CS		-	Saharan *et al*., 2013
CS-NP loaded SA	4:2:1	1:1:1	0.4% CS, 0.2% TPP and 0.1% SA with ratio 1:1:1	368.7 nm PDI 0.1 +34.1 mV	Spherical and porous	1541, 1639: acetoxy group of SA 1317: interaction between –COOH group of SA with primary amide of CS		Peak at 2θ of 10°-20° denoted SA peak 2θ of 18°-30° confides CS	Kumaraswamy *et al*., 2019
CS-NP loaded gentamicin and SA	-	-	0.1% SA and 0.2% gentamicin with ratio 3:2, 0.2% CS (pH 5). A mass TPP solution added into CS with ratio vary at (a)	(a) 343.3 nm, PDI 0.41, 34.26 mV (b) 217.7 nm, PDI 0.275, 35.77 mV	-	-	-	-	Ji *et al*., 2011

NPs	Mass ratio	Volume ratio	Condition synthesis	DLS	SEM, TEM	FTIR (cm^{-1})	UV (nm)	XRD	Reference
			1:3, (b) 1:4, (c) 1:5, (d) 1:6, (e) 1:7; stirring 1 hour, centrifuge 16000 rpm for 30 min	(c) 180.0 nm, PDI 0.235, 37.12 mV (d) 172.2 nm, PDI 0.308, 39.44 mV (e) 150.8 nm, PDI 0.237, 42.43 mV					
-	-		CS/TPP ratio 4:1, pH 5.0, drug to polymer ratio 1:4, feed ratio of SA to gentamicin 1.5:1.0).	180 nm PDI 0.235 37.12 mV	Spherical 200 nm	3423: hydrogen bonding between -OH bending of gentamicin and CS 1542, 1637: interaction between NH_3^+ of CS and TPP 1300: C-N bending (interaction between -COOH of SA and primary amide of CS)	-	-	

NPs	Mass ratio	Volume ratio	Condition synthesis	DLS	SEM, TEM	FTIR (cm^{-1})	UV (nm)	XRD	Reference
CS-NP loaded Thiamine	24:4:25	24:8:25	375 mg Thiamine/75 mL, 360 mg CS/72 mL and 60 mg TPP/24 mL, stirring overnight, centrifuge 10,000 g for 30 min	596 nm 37.7 mV	10-60 nm	1657: binding of Thiamine to CS	267 nm	-	Muthukrishnan *et al*., 2019
CS-NP loaded *Achillea melefolium* extract	1:5:-	2:1:-	*A. millefolium* extract (semi solid form) added into 10 mL of 0.1% CS to obtain final concentration at 20%, 5 mL of 1% TPP, stirring 2 h and centrifuge 10,000 x g for 10 min	118 nm with 3 peaks (10, 122 and 712 nm)	Spherical 4.15-100 nm	3281.73, 2163.36 and 1636.78: interaction in NP	417 nm	-	Kain *et al*., 2020

Note: CS: Chitosan; DLS: Dynamic light scattering; FTIR: Fourier-transform infrared spectroscopy; NPs: Nanoparticles; PDI: polydispersity index; SEM: Scanning electron microscope; TEM: Transmission electron microscopy; TPP: Sodium tripolyphosphate; UV: Ultra violet visible; XRD: X-Ray Diffraction.

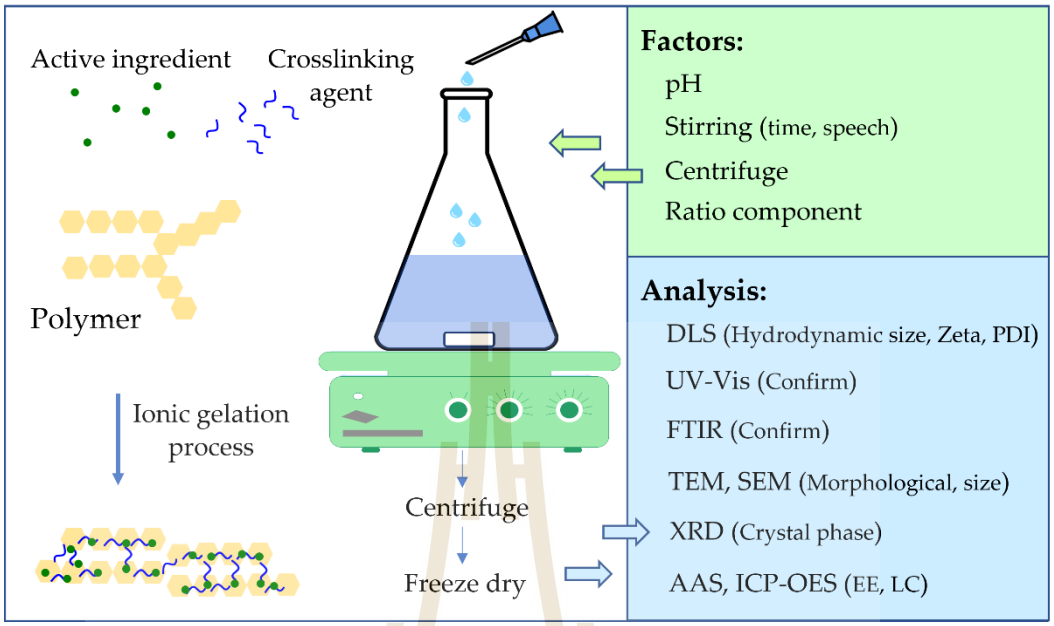

Figure 2.35 The schematic representation of NPs synthesized and characterized by ionic gelation method.

The ionic gelation method requires simple, easy-to-find, expensive materials and equipment, so it can be done easily, mildly, quickly in normal laboratories. In addition, the mechanism based on electrostatic interaction instead of chemical reaction leads to no need to use organic solvents, thus avoiding potential toxicity of chemicals or reagents. However, the disadvantage of this method is that it is not easy to produce uniformly sized NPs and researches on other polymers (not CS) is limited (Racovită *et al*., 2009; Kashyap *et al*., 2015; Pedroso - Santana and Fleitas - Salazar, 2020; Maluin and Hussein, 2020).

2.4 Application of chitosan nanoparticles based ionic gelation method in plant disease management

With its advantages, CS-NPs synthesized according to the ionic gelation method has been applied in many fields including pharmaceuticals, new materials, and agriculture (nanopesticides, nanofertilizers, nanoherbicides) (Ji *et al*., 2011; Kashyap *et*

al., 2015; Rodriguez *et al*., 2019; Bocchetta, 2020; Malerba and Cerana, 2019; Maluin and Hussein, 2020).

On management of plant diseases, CS-NPs could be applied as protectants (nano pesticides) and carriers (fungicides, insecticides, herbicides, plant hormones, elicitors, nucleic acids) (Kashyap *et al*., 2015; Worrall *et al*., 2018; Das and Pattanayak, 2020). In particular, using CS-NPs as the delivery system is of special interest because it can load, protect the ingredients surrounding the environment and release them to the target site uptake of the plants (Kashyap *et al*., 2015). In addition, with the basic properties of NPs being small size and high contact area, CS-NPs or CS-NPs loaded active ingredients could be easily penetrated and permeated into the membrane of phytopathogens or enhanced plant tissues uptake that resulted in an increased control or defense response activity, respectively (Maluin and Hussein, 2020). Therefore, these NPs can be used directly and indirectly to manage plant diseases.

Studies using CS-NPs synthesis by ionic gelation method in plant disease management are shown in **Table 2.12** and **Figure 2.36.**

2.4.1 Chitosan nanoparticles

2.4.1.1 Directly

Under *in vitro* conditions, Kheiri *et al*. (2017) determined that the minimum inhibitory concentration of CS-NPs prepared by centrifuge and pH change method at 0.05 and 0.09% could inhibit growth of *Fusarium graminearum* at 31.97% and 29.67%, respectively. Furthermore, Kheiri *et al*. (2017) also showed that CS-NPs from CS low molecular weight which has a higher inhibitory effect than CS height, molecular weight at the same concentration. CS-NPs may or may not inhibit pathogens. CS-NPs may inhibit mycelial growth of *Pyricularia grisea* (65%) at 0.1% (Sathiyabama and Manikandan, 2016), *C. gloeosporioides* (85.7%) (Suryadi *et al*., 2019), *C. gloeosporioides* (37.8%), *Phytophthora capsica* (50.7%), *Sclerotinia sclerotiorum* (39.5%), *F. oxysporum* (50.3%), *Gibberella fujikuori* (56.3%) at 0.5% (Oh *et al*., 2019), *P. grisea* (92%), *Alternaria solani* (87%), *F. oxysporum* (72%) with amount of 100 µg (Sathiyabama and

Parthasarathy, 2016), *A. alternata* (80.1-82.2%), *R. solani* (32.2-34.4%) at 0.06-0.1%, *M. phaseolina* (84%) at 0.1% (Saharan *et al*., 2013), *A. solani* (10, 70%) at 0.03, 0.04 % (Popova *et al*., 2020), *Alternaria tenuis* (67.67%), *Aspergillus niger* (62.75%), *Aspergillus terreus* (74.67%), *Baeuvaria bassiana* (76.08%), *F. graminearum* (60.37%), *F. oxysporum* (66.60%), *Sclerotium rolfsii* (37.41%) at 800 ppm and the zearalenone produced by *F. graminearum* (Abdel-Aliem at al., 2019). Furthermore, CS-NPs at 0.014% (in acetate buffer), the lysis zone diameter of *Clavibacter michiganensis* and *F. graminearum* were 29.5 and 20.0 mm while CS was 22.5 and 18.0 mm, respectively (Popova *et al*., 2020). Moreover, 0.2 ml of CS-NP at 125 ppm could inhibit mycelium of *F. graminearum* by 44.3% that higher than fungicide (8-hydroxy quinoline) at 42.33% (Abdel-Aliem at al., 2019). In addition, CS-NPs also inhibited spore germination of *C. gloeosporioides* (61.2%) (Suryadi *et al*., 2019), *A. alternata* (84.4-87.1) at 0.06-0.1% (Saharan *et al*., 2013). On the other hand, CS-NPs do not inhibit mycelial growth, spore germination, and sporulation of *P. grisea* even at a concentration of 0.1% (Sathiyabama and Manikandan, 2016; Manikandan and Sathiyabama, 2016). A study by Oh *et al*. (2019) showed that OD_{600nm} of *Erwinia carotovora* subsp. *carotovora* strains 113114, 113154, YKB133061 and *Xanthomonas campestris* pv. *vesicatoria* strain 11154 were reduced by 41.3, 55.5, 48.5, 52.1% when treated with CS-NPs at 0.5%; but interestingly, they were also reduced by 64.7, 76.3, 78.0, 73.8% when treating CS-NPs at 0.05%, respectively. Furthermore, CS-NPs at 2 ml/L inhibited anthracnose disease at 87.5 and 75% for chili, at 50 and 10% for papaya by the prevent and curative treatments under *in vivo* conditions, respectively (Suryadi *et al*., 2019).

2.4.1.2 Indirectly

Pre-treatment of CS-NPs at 0.1% reduced sheath blight and blast in rice caused by *R. solani* and *P. grisea* by 92.78% and 100%, respectively, under detach leaves assay (Manikandan and Sathiyabama, 2016; Divya *et al*., 2020).

In the greenhouse trial, CS-NPs are capable of induced plants of rice, finger millet, wheat against pathogens attacks (Sathiyabama and Manikandan, 2016; Kheiri *et*

al., 2017; Divya *et al*., 2020). The sheath blight disease was reduced by 75.01% compared with CS at 44.82%. Moreover, the peroxidase, phenylalanine ammonia-lyase, chitinases activity also increased by 19, 1.5, 1.9 folds, respectively (Divya *et al*., 2020). In the study of Sathiyabama and Manikandan (2016), the symptom and disease incidence of blast delayed 10 days and decreased at 2.8 folds, respectively, that were influenced by an increase of peroxidase activity by 1.6 folds and ROS activity. Spray of CS-NPs at 0.05% after infection of *F. graminearum* leads to reduce area under the disease progress curve at 28 days after inoculation (DAI) by 2.2 folds compared to the water control. The NPs caused structural damage in mycelium and cell pathogen but could also increase superoxide and H_2O_2 content (Kheiri *et al*., 2017).

2.4.2 Chitosan nanoparticles loaded active ingredients

2.4.2.1 Directly

The effect of controlling or enhancing the immunity of plants is different, depending on the same CS-NPs and the type of active ingredient. The EC_{50} of 4 formulate CS-NPs loaded Hexaconazole to control *Ganoderma boninense* is 8.0-18.4 ppb, which is 21.4 and 1534.5 ppb lower than Hexaconazole and CS-NPs, respectively. Similarly, fiducial limit (lower-upper) were 6.0-10.9 to 13.0-32.8 ppb while Hexaconazole and CS-NPs were 16.7-27.3, 494.0-13280.4 ppb (Maluin *et al*., 2019).

CS-NPs loaded Cu could inhibit mycelial growth of *Curvularia lunata* by 50.0 and 52.7% at 0.12 and 0.16% (Choudhary *et al*., 2017c), *A. solani* and *F. oxysporum* by 84.2 and 60.1% at 0.1% (Saharan *et al*., 2015), *A. alternata* and *R. solani* by 82.1-89.5% and 62.5-63.0% at 0.06-0.1%, *M. phaseolina* by 60.1% at 0.1% (Saharan *et al*., 2013), respectively. These NPs also inhibited spore germination of *A. solani* and *F. oxysporum* by 73.3 and 79.9% at 0.1% (Saharan *et al*., 2015), *A. alternata* by 83.3-87.4% at 0.06-0.1% (Saharan *et al*., 2013). CS-NPs loaded Zn inhibited mycelial growth and spore germination of *C. lunata* by 47.7-65.2% and 50.5-73.3% at 0.08-0.16% (Choudhary *et al*., 2019). In addition, the mixture of CS-NPs (ionic gelation) and Cu-NPs (chemical

reduction) could inhibit the mycelial growth of *F. oxysporum* by 61.94-100% at 0.05-0.2% (Mohamed *et al*., 2018). CS-NPs loaded SA could evade mycelial growth by 62.2-100% and spore germination of *F. verticillioides* by 48.3-60.5% at 0.08-0.16% (Kumaraswamy *et al*., 2019). CS-NPs loaded saponin inhibited mycelial growth of *A. alternata* by 78.3-80.9% and *R. solani* by 27.7% at 0.06-0.1% and spore germination of *A. alternata* by 78.3-82.9% at 0.1% (Saharan *et al*., 2013). On the other hand, CS-NPs loaded thiamine did not inhibit *F. oxysporum*, even at a concentration of 0.1% (Muthukrishnan *et al*., 2019).

Under greenhouse conditions, at 3 DAI, *A. solani* and *F. oxysporum*, CS-NPs loaded Cu (0.1 and 0.12%) was foliar sprayed and applied to soil lead to reduced early blight (84.2 and 87.7%) and fusarium wilt (49.9 and 61.1%), respectively (Saharan *et al*., 2015). Furthermore, priming maize seeds into these NPs (0.02-0.14%) for 4 and 8 hours combined with foliar spraying after *F. verticillioides* infected could reduce post-flowering stalk rot disease by 38.2-48.1% and 24.8-49.6%, respectively (Choudhary *et al*., 2017a). These treatments could reduce disease severity by 23.5-33.9% and 2.55-15.8% for 4 and 8 hours priming at field conditions.

2.4.2.2 Indirectly

Previously, harpin protein (from *Erwinia amylovora*) was known for its ability to induce systemic acquired resistance in plants (Dong *et al*., 1999). With the same amount (20 µg), CS-NPs loaded harpin protein (from P. *syringae* pv. *syringae*) could enhance cell death, necrotic lesions, and also H_2O_2 accumulation faster and stronger than harpin protein only (Nadendla *et al*., 2018). Furthermore, treatment of these NPs reduced fungal biomass (5 folds), lesion diameter (12 folds), and caused failing colonization of *R. solani* in tomato leaves compared with the control. Peroxidase and phenylalanine ammonia-lyase activity also steadily increased up to 72 hours. And interestingly, the transcriptome changes including defense response, signal transduction, transport, transcription, photosynthesis, housekeeping, and aromatic biosynthesis were enhanced more than 2 folds at 24, 48, 72 hours after spraying.

At greenhouse conditions, pre-treated CS-NPs loaded Cu (0.04-0.16%) could reduce leaf spot disease (*C. lunata*) in maize by 43.86-48.48%. Moreover, this treatment increased superoxide dismutases (1.8-2.2 folds), peroxidase (1.5-2.1 folds), phenylalanine ammonia-lyase (1.3-2.0 folds), polyphenol oxidase (1.1-1.2 folds) (Choudhary *et al*., 2017c). Furthermore, CS-NPs loaded Zn also induced superoxide dismutases, phenylalanine ammonia-lyase, polyphenol oxidase, H_2O_2 activity by 1.2-2.0, 2.0-3.0, 17.24-49.37, 1.5-2.6 folds when compared with the control, respectively. The H_2O_2 and lignin localization were also increased, leading to reduce maize leaf spot (*C. lunata*) by 32.3-50.77% (Choudhary *et al*., 2019).

A hormone-elicitor is the SA that has been loaded into CS-NPs. The maize was pre-treated with these NPs at 0.01-0.16% could suppressed post-flowering stalk rot disease (37.33-49.5%) caused by *F. verticillioides*. Furthermore, at 2 and 3 days after spraying NPs, superoxide dismutases (1.8 and 3.2 folds), peroxidase (7.0 and 4.6 folds), catalase (3.1 and 2.6 folds), phenylalanine ammonia-lyase (2.0 and 1.7 folds), polyphenol oxidase (1.7 and 2.0 folds), superoxide anion (1.1 and 1.1 folds), H_2O_2 (17.5 and 37.0 folds), and lignin accumulation were increased (Kumaraswamy *et al*., 2019).

Although CS-NPs loaded thiamine did not inhibit fungi at *in vitro* conditions, pre-treatment of these NPs (0.1%) at 3 days before infection of *F. oxysporum* on chickpea could reduce cell death in 2 DAI compared with the control. Furthermore, polyphenol oxidase, peroxidase, β-1,3-glucanase, chitinase, chitosanase, and protease were increased by 2.1, 2.0, 1.4, 1.4, 1.4, 1.1 folds in leaves and 2.0, 1.3, 1.1, 1.3, 1.3, 1.1 folds in roots, respectively (Muthukrishnan *et al*., 2019).

On the other hand, in the study of Swati (2020), CS-NPs loaded Cu at 0.12-0.06% was treated before and after an infection of *Xanthomonas axonopodis* pv. *glycine* could reduce bacterial pustule disease in soybean by 40.6-49.7%, respectively. Interestingly, the low concentration is more effective. In addition, application of the mixture of CS-NPs (ionic gelation) and Cu-NPs (chemical reduction) to date palm root zone could increase plant immunomodulatory including total phenols (1.1-1.5 folds),

phenoloxidases (1.1-2.0 folds), peroxidase (1.6-3.0 folds), which lead to reducing disease by 16.2-59.3% (Mohamed *et al*., 2018).

At field conditions, CS-NPs loaded Cu, Zn and SA is effective in reducing disease by inducing plant defense system in maize and soybean (Choudhary *et al*., 2017c; Choudhary *et al*., 2019; Kumaraswamy *et al*., 2019; Swati, 2020). Treatment CS-NPs loaded Cu (0.06%) reduced bacterial pustule disease by 51.3%. In addition, these NPs at 0.01-0.08% reduced maize leaf spot disease by 27.72-28.53% while at 0.12-0.16% reduced 30.42-33.8% (Choudhary *et al*., 2017c). On the other hand, CS-NPs loaded Zn at 0.01-0.16% reduced this disease by 25.42-39.67% (Choudhary *et al*., 2019). CS-NPs loaded SA at 0.01-0.16% could reduce post-flowering stalk rot by 40.5-59.47% (Kumaraswamy *et al*., 2019).

Table 2.12 The CS-NPs synthesized by ionic gelation used in plant disease management.

NPs	Plant	Pathogen	Summary research	Reference
CS-NPs with DLS (83.32 nm, PDI 0.31, -28 mV), HRTEM (20-50 nm)	Rice	*P. grisea* /Blast	***In vitro*:** Treat CS-NPs not cause inhibit mycelial and spore germination even 0.1%. **Detach leaves assay:** painting brush 500 µL onto surface each leave. After 24 hours, inoculate with similar method. Treat CS-NPs 0.1% could cause no blast symptom up to 10 DAI (suppression 100%).	Manikandan and Sathiyabama, 2016
CS-NPs described as Manikandan and Sathiyabama (2016)	Fingermillet	*P. grisea* / Blast	***In vitro*:** CS-NPs at 0.1% could inhibited nearly 65% mycelial growth and did not sporulate compared with the control. **Greenhouse:** seed soaking overnight, foliar spraying at 20 and 30 DAP, inoculate at 30 DAP. Treat CS-NPs could delay symptom by 10 days, and decreased disease incidence 2.8 folds. Moreover, treat CS-NPs could increase dry weight (148.8%), yield (93.2%), peroxidase (1.6 folds) and ROS activity.	Sathiyabama and Manikandan, 2016
CS-NPs with DLS (9.8 nm, PDI 0.225, -37 mV), HRTEM (10-30 nm)	Chickpea	*P. grisea* *A. solani* *F. oxysporum*	***In vitro*:** CS-NPs with amount 100 µg could inhibited mycelial growth of *P. grisea*, *A. solani*, *F. oxysporum* were 92, 87 and 72%, respectively. **Seeding:** Treat NPs could increase seedling vigor index (57.1%), number lateral root (133.3%), dry weight (200%).	Sathiyabama and Parthasarathy, 2016

NPs	Plant	Pathogen	Summary research	Reference
CS-NPs Centrifuge method with DLS (180.9 nm, PDI 0.31, 45.6 mV) pH change method with DLS (225.7 nm, PDI 0.44, 33.4 mV)	Wheat	*F. graminearum* / Head blight	***In vitro*:** CS-NPs synthesized by CS low molecular weight could highly inhibit pathogens than low molecular weight and high molecular weight at the same concentration. MIC of CS-NPs prepared by centrifuge and pH change method were 0.05% and 0.09% with 31.97% and 29.67%, respectively. **Greenhouse:** Spraying after inoculate The area under the disease progress curve at 28 DAI of treatment CS-NPs 0.05% was reduced 2.2 folds compared with the control. The CS-NPs could cause structural damage in mycelium and cell pathogen, increase superoxide, H_2O_2 content	Kheiri *et al*., 2017
CS-NPs with DLS (126.2 nm, PDI 0.44, 27.8 mV)	Chilli Papaya	*C. gloeosporioides* / Anthracnose	***In vitro*:** CS-NPs could inhibit mycelial growth (85.7%) and spore germination (61.2%). ***In vivo*:** preventive (soaking onto CS-NPs 2 mL/L for 60 min before inoculate), curative (soaking onto spore suspension for 15 min following air-dried and soaking onto CS-NPs for 60 min). Inhibition rate of preventive and curative treatment were 87.5% and 75% for chilli, 50% and 10% for papaya.	Suryadi *et al*., 2019
CS-NPs with size 100 nm	Tomato	*C. gloeosporioides*, *Ph. capsici*, *S. sclerotiorum*, *F. oxysporum*,	***In vitro*:** CS-NPs at 0.5% could inhibit mycelial growth of *C. gloeosporioides*, *P. capsici*, *S. sclerotiorum*, *F. oxysporum*, *G. fujikuori* by 37.8, 50.7, 39.5, 50.3, 56.3% at day 10 (except S. sclerotiorum was at day 5), respectively.	Oh *et al*., 2019

NPs	Plant	Pathogen	Summary research	Reference
		G. fujikuori, *E. carotovora* subsp. *carotovora*, *X. campestris* pv. *vesicatoria*	CS-NPs at 0.5% could reduce OD_{600nm} of *E. carotovora* subsp. *carotovora* strains 113114, 113154, YKB133061 and *X. campestris* pv. *vesicatoria* strain 11154 by 41.3, 55.5, 48.5, 52.1, respectively, Interesting, CS-NPs at 0.05% similarly reduce 64.7, 76.3, 78.0, 73.8%, respectively.	
CS-NPs	Rice	*R. solani* / Sheath blight	**Detach leaves assay:** Pre-treated CS-NPs and CS at 0.1% could reduce disease leaf area 92.78% and 78.89%, respectively. **Greenhouse:** Seed treat 2 hours, soil amended and foliar spraying 15 and 30 DAP, inoculate 45 DAP. The disease was suppressed 75.01% and 44.82% when treated with CS-NPs and CS, respectively. peroxidase, phenylalanine ammonia-lyase, chitinase activity were increased 19, 1.5, 1.9 folds, respectively.	Divya *et al*., 2020
CS-NPs with DLS (47 nm, PDI 0.45, 26.8 mV)	Tomato Cereal	*C. michiganensis* /Bacterial canker *A. solani* /Leaf spot *F. graminearum* /Head blight and root rot	***In vitro*:** lysis zone diameter of *C. michiganensis* and *F. graminearum* treated CS-NPs at 0.014% (in acetate buffer) were 29.5 and 20 mm, respectively. Similar, CS were 22.5 and 18.0 mm. CS-NPs at 0.03 and 0.04% (in acetate buffer) inhibited mycelial of *A. solani* by 10 and 70% compared with CS, respectively.	Popova *et al*., 2020

NPs	Plant	Pathogen	Summary research	Reference
CS-NPs with DLS (192.5 nm, PDI 0.6, +45.33 mv), CS-NPs loaded saponin with DLS (373.9 nm (2 peaks), PDI 1.0, +31 mV), CS-NPs loaded copper (Cu) with DLS (196.4 nm, PDI 0.5, +88 mV)		*A. alternata* *M. phaseolina* *R. solani*	***In vitro*:** CS-NPs, CS-NPs loaded saponin, and CS-NPs loaded copper at 0.06-0.1% could inhibit mycelial growth of *A. alternate* (80.1-82.2, 78.3-80.9, and 82.1-89.5%) and *R. solani* (32.2-34.4, 27.7, and 62.5-63.0%) respectively. For *M. phaseolina*, 3 NPs at 0.1% could inhibit 84, 66.2, and 60.1%, respectively. Moreover, 3 NPs at 0.06-0.1% could inhibit *A. alternata* spore germination 84.4-87.1, 78.3-82.9, and 83.3-87.4%, respectively.	Saharan *et al*., 2013
CS-NPs loaded copper (Cu) with DLS (374.3 nm, PDI 0.33, 22.6 mV), TEM (150 nm)	Tomato	*A. solani* /Early blight *F. oxysporum* /Wilt	**Seeding:** Treat CS-NPs loaded Cu at 0.08, 0.1, 0.12% could increase seedling vigor index (33.9, 33.7, 24.3%), fresh weight (18.9, 21.6, 16.2%), dry weight (20.0, 26.7, 13.3%), respectively. ***In vitro*:** CS-NPs loaded Cu at 0.1% could inhibit mycelium growth, spore germination of *A. solani* and *F. oxysporum* were 84.2%, 60.1% and 73.3%, 79.9%, respectively. **Greenhouse:** Spraying at 3-4 DAI (*A. solani*); apply to soil at 3 DAI (*F. oxysporum*). NPs at 0.1 and 0.12% could reduce early blight at 84.2% and 87.7%, fusarium wilt at 49.9% and 61.1%, respectively.	Saharan *et al*., 2015
CS-NPs loaded copper (Cu) with DLS (295.4 nm), PDI 0.28, 19.6 mV)	Maize	*F. verticillioides* / Post flowering stalk rot	**Greenhouse:** Inoculate before planting by mix with soil, seed treat for 4, 8 hours, spraying at 45 and 65 DAP.	Choudhary *et al*., 2017a

NPs	Plant	Pathogen	Summary research	Reference
			NP treatment at 0.02-0.14% could reduce disease severity 38.2-48.1 % and 24.8-49.6% for treat seed at 4 and 8 hours, respectively. **Field:** similar greenhouse experiments except inoculate at flowering stage. NP treatment at 0.02-0.14% could reduce disease severity 23.5-33.9% and 2.55-15.8% for treat seed at 4 and 8 hours, respectively.	
CS-NPs loaded copper (Cu) with DLS (361.3 nm, PDI 0.2, 22.1 mV)	Maize	*C. lunata* /Leaf spot	***In vitro*:** CS-NPs loaded Cu at 0.12 and 0.16% could inhibit mycelial growth at 50.0 and 52.7%, respectively. **Greenhouse:** Seed treat 4 hours, foliar spraying 35 DAP, inoculate 45 DAP. Treat CS-NPs loaded Cu at 0.01-0.08% could increase plant height (15.9-47.0%), stem diameter (82.9-102.9%), root length (9.5-15.8%), root number (20.9-46.3%), chlorophyll content (67.3-182.6%). But treat at 0.16% could reduce root length (9.8%) and chlorophyll content (4.6-9.7%) although the difference was non-significant. Moreover, treat NPs at 0.04-0.16 could increase superoxide dismutases (1.8-2.2 folds), peroxidase (1.5-2.1 folds), phenylalanine ammonia-lyase (1.3-2.0 folds), polyphenol oxidase (1.1-1.2 folds, which also reduced disease severity 43.86-48.48%. **Field:** Treat CS-NPs loaded Cu at 0.01-0.08% could reduce disease severity 27.72-28.53%. Similarly, NPs at 0.12-0.16% reduced 30.42-	Choudhary *et al*., 2017c

NPs	Plant	Pathogen	Summary research	Reference
			33.88%, and also increased grain yield (25.4-29.3%), 100 grain weight (14.4-16.9%).	
CS-NPs with DLS (86.8 nm, 32.4 mV) CS-NPs load Harpin (*Pseudomonas syringae* pv. *syringae*) DLS (133.7 nm, 48.6 mV)	Tomato	*R. solani*	***In planta*:** Treat amount 20 µg of CS-NPs load Harpin could enhance cell death, necrotic lesion and also H_2O_2 accumulation faster and stronger than Harpin protein only. Moreover, treat this NPs could reduce fungal biomass (5 folds), lesion diameter (12 folds) and failed colonization in leaves when compared with control. For mechanism, peroxidase and phenylalanine ammonia-lyase activity could be steady increased up to 72 hours. The transcriptome change including defense response, signal transduction, transport, transcription, photosynthesis, housekeeping and aromatics biosynthesis were enhanced more than 2 folds at 24, 48, 72 hours after spraying.	Nadendla *et al*., 2018
CS-NPs 50 nm	Date palm	*Fusarium oxysporum* / Vascular wilt	Mix CS-NPs (ionic gelation method) and Cu-NPs (chemical reduction method) to obtain copper-CS nanocomposition (CuCs) ***In vitro*:** CuCs at 0.05-0.2% could inhibite 61.94-100% mycelial growth. **Greenhouse:** Apply 50 mL of CuCs to root zone of seeding Treated CuCs could increase plant immunomodulatory including total phenol (1.1-1.5 folds), phenoloxidase (1.1-2.0 folds), peroxidase (1.6-3.0 folds), which lead to reduce disease 16.2-59.3%.	Mohamed *et al*., 2018

NPs	Plant	Pathogen	Summary research	Reference
CS-NPs (DLS 180 nm with range 500-800 nm)	Ground nut oil seed	*A. tenuis* *A. niger* *A. terreus* *B. bassiana* *F. graminearum* *F. oxysporum* *S. rolfsii*	***In vitro*:** CS-NP at 800 ppm could inhibit mycelial growth of *A. tenuis, A. niger, A. terreus, B. bassiana, F. graminearum, F. oxysporum, S. rolfsii* by 67.67, 62.75, 74.67, 76.08, 60.37, 66.60, 37.41%, respectively. Moreover, 0.2 ml of CS-NP at 125 ppm could inhibit *F. graminearum* by 44.3% that higher than fungicide (8-hydroxy quinoline) was 42.33%. In addition, the CS-NP at 800 ppm could reduce zearalenone secreted by *F. graminearum.*	Abdel-Aliem *et al*., 2019
CS-NPs loaded zinc (Zn) with DLS (387 nm, PDI 0.22, 34 mV), TEM/SEM (200-300 nm, spherical)	Maize	*C. lunata* / Leaf spot	***In vitro*:** NPs could inhibit mycelium growth at 47.7-65.2% at 0.08-0.16% and spore germination 50.5-73.3% at 0.01-0.16%. **Greenhouse:** Seed treat 4 hours, foliar spraying 35 DAP, inoculate 45 DAP. The superoxide dismutases, phenylalanine ammonia-lyase, polyphenol oxidase, H_2O_2 activity could be increased at 1.2-2.0, 2.0-3.0, 17.24-49.37, 1.5-2.6 folds when compared with the control, respectively. H_2O_2 and lignin localization were also increased. The DS was reduced 32.3-50.77%. The plant height, stem diameter, root length were increased 30.3-60.3, 66.3-237.5, 2.7-61.1%, respectively. **Field:** The DS was reduced at 25.42-39.67%.	Choudhary *et al*., 2019

NPs	Plant	Pathogen	Summary research	Reference
CS-NPs loaded salicylic acid (SA) with DLS (368.7 nm, PDI 0.1, 34.1 mV)	Maize	*F. verticillioides* / Post-flowering stalk rot	***In vitro*:** CS-NPs loaded SA treatment at 0.08-0.16% could evade mycelial growth at 62.2-100% and spore germination at 48.3-60.5%. **Greenhouse:** Seed treat 4 hours, foliar spraying 55 DAP, inoculate 60 DAP. NP treatment at 0.01-0.16% could reduce disease severity at 37.33-49.5%, and increase leaf area (160.6-224.7%), shoot length (38.5-76.9%), root length (66.9-111.5%), root length (59.6-91.8%), stem diameter (22.8-53.9%), total chlorophyll (54.2-141.4%). Moreover, at 2 and 3 days after spraying NPs, superoxide dismutases (1.8 and 3.2 folds), peroxidase (7.0 and 4.6 folds), catalase (3.1 and 2.6 folds), phenylalanine ammonia-lyase (2.0 and 1.7 folds), polyphenol oxidase (1.7 and 2.0 folds), superoxide anion (1.1 and 1.1 fold), H_2O_2 (17.5 and 37.0 folds), and lignin accumulation also were increased. **Field:** NP treatment could reduce disease severity at 40.5-59.47%. At 0.08%, days to 50% tasseling was early by 4 days. Moreover, the plant height (25.5%), ear height (12.1%), cob length (44.8%), test weight (71.1%) and grain yield (48.3%) were also increased.	Kumaraswamy *et al*., 2019
CS-NPs with DLS (bimodal particle with 2.3 and 7.5 nm), TEM (1.5 nm),	Oil palm	*G. boninense*	***In vitro*:** EC_{50} of hexaconazole, CS-NPs and 4 formulate CS-NPs load hexaconazole were 21.4, 1534.5 and 8.0 to 18.4 ppb. Similar, fiducial limit (lower-upper) were 16.7-27.3, 494.0-13280.4 and 6.0-10.9 to 13.0-32.8 ppb, respectively.	Manikandan *et al*., 2019

NPs	Plant	Pathogen	Summary research	Reference
CS-NPs loaded Hexaconazole as described Maluin *et al*., 2019				
CS-NPs loaded Thiamine with DLS (596 nm, 37.7 mV), HRTEM (10-60 nm)	Chickpea	*Fusarium oxysporum* / Wilt	**Seeding:** soaking seed overnight at 0.1% could increase seedling vigor index by 64.2% and Indole-3-acetic acid content by 10 folds. ***In vitro***: CS-NPs loaded Thiamine not inhibit fungi even 0.1%. **Greenhouse:** Spraying 12 DAP, inoculate 15 DAP NP treatment at 0.1% could reduce cell death in 2 DAI compared with the control. Moreover, shoot length, number of leaves per plant, fresh weight, dry weight, number of secondary root per plant also were increased by 15.3, 14.4, 37.7, 20.0, 52.8%, respectively. In leaves, polyphenol oxidase, peroxidase, β-1,3-glucanase, chitinase, chitosanase, protease were increased by 2.1, 2.0, 1.4, 1.4, 1.4, 1.1 folds, respectively. In root, this enzyme activity were increased 2.0, 1.3, 1.1, 1.3, 1.3, 1.1 folds, respectively.	Muthukrishnan *et al*., 2019
CS-NPs loaded copper (Cu) with DLS (314 nm, PDI 0.48, 19.5 mV)	Soybean	*X. axonopodis* pv. *glycine* /Bacterial pustule	**Greenhouse:** Seed treat 4 hours, foliar spraying at trifoliate stage and after disease occurrence, inoculate 35 DAP CS-NPs loaded Cu at 0.12-0.06% could reduce disease 40.6-49.7%. NP treatment at 0.06% could increase plant height (56.8%), root length	Swati, 2020

NPs	Plant	Pathogen	Summary research	Reference
			(40.3%), pod number (7.2%). NP treatment at 0.02% could increase root weight (46.8%), nodule number (44.2%), nodule weight (125.8%). **Field:** CS-NPs load Cu treatment at 0.06% could reduce disease at 51.3% and increase root length (60.9%), root weight (46.8%), pod number (29.7%).	

Note: DAI: Days after inoculate; DAP: Days after planting; HRTEM: High-resolution transmission electron microscopy; NPs: Nanoparticles; PDI: polydispersity index; ROS: Reactive oxygen species; SEM: Scanning electron microscope; TEM: Transmission electron microscopy.

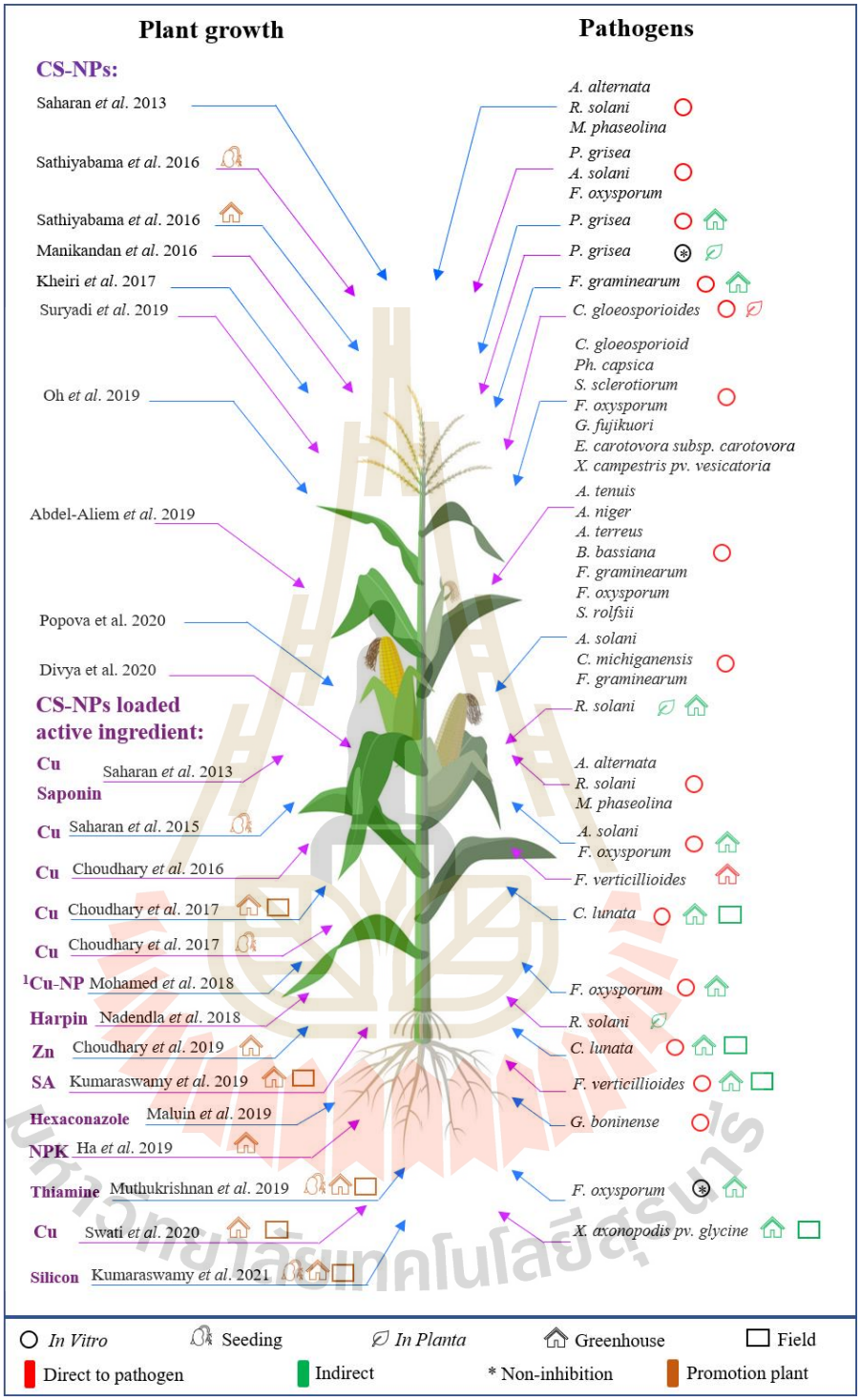

Figure 2.36 The application of CS-NPs and CS-NPs loaded active ingredients synthesized by ionic gelation method in plant disease management and enhancing plant growth. *Note*: [1] Mixture of CS-NP (ionic gelation method) and Cu-NP (chemical reduction method).

2.4.3 Plant growth promotion

A concern for any agrochemical is the safety of the plant, environment, farmers and consumers. In recent reviews, NP is a biosafety solution. However, nanotoxicological still has to be noticed (Elemike *et al*., 2019; Ashraf *et al*., 2021). When applying NP to plant, they will enter the tissues and cause positive and negative impacts depending on the size, shape and concentration. NPs usually enhance shoot elongation, root elongation, seed germination at low concentration and in contrast at high concentration (Hassanisaadi *et al*., 2022). When applied to soil, the NP can cause negative impacts on soil microflora but will be less than agrochemical apply (Ur Rahim *et al*., 2021). On the other hand, the amount of agrochemical and fertilizer applied to agriculture would be reduced if they were replaced by NPs, which lead to reduce their toxicity. Usually, the safety-by-design principle is applied to screen potential risk from materials, methods synthesis to NP formulation (Zielińska *et al*., 2020). As mentioned above, ionic gelation method and CS – a natural polymer are friendly, safe and biodegradable solutions.

In addition to its ability to directly inhibit the pathogens or induce plant defense system against diseases, CS-NPs or CS-NPs loaded active ingredients have the ability to stimulate plant growth. At this time, it acts as a fertilizer or nutrient, which affects plant physiological processes including nutrient uptake, cell division, cell elongation, enzymatic activation, synthesis of protein that lead to increase yield (Chakraborty *et al*., 2020). Efficiency depends on both the CS-NPs and the active ingredient, even when it releases all the active ingredients because the main component of CS is nitrogen, which takes 9-10% (Agarwal *et al*., 2015). Furthermore, the rich positive charge of CS leads to increase affinity toward the plant cell membrane, which could enhance reactivity in the plant system (Maluin and Hussein, 2020).

Several types of NPs presented in **Table 2.12** have been shown to stimulate plant growth.

In the seeding stage, CS-NPs increased the seeding vigor index (57.1%), the number of lateral roots (133.3%), and dry weight (200%) of chickpea (Sathiyabama and Parthasarathy, 2016). Additionally, the chickpea seeds were soaked with CS-NPs loaded thiamine at 0.1% overnight lead to the seeding vigor index increased by 64.2%, with indole-3-acetic acid content increased by 10 folds (Muthukrishnan *et al*., 2019). Treatment CS-NPs loaded Cu at 0.08, 0.1 and 0.12% increased seedling vigor index (33.9, 33.7, 24.3%), fresh weight (18.9, 21.6, 16.2%), dry weight (20.0, 26.7, 13.3%) in tomato, respectively (Saharan *et al*., 2015). Additionally, CS-NPs loaded Cu at 0.01-0.16% could increase seeding vigor index (15.6-48.6%), fresh weight (7.1-11.4%), dry weight (21.4-57.1%) in maize seedings, which were related to increasing α-amylase and proteases at day 5 and 7, respectively (Choudhary *et al*., 2017b).

At greenhouse conditions, the dry weight and yield of finger millet were increased by 148.8% and 93.2% when treated with CS-NPs, respectively (Sathiyabama and Manikandan, 2016). The plant height, stem height, and root length of maize was increased by 30.3-60.3, 66.3-237.5, 2.7-61.1% when treated with CS-NPs loaded Zn at 0.01-0.16%, respectively (Choudhary *et al*., 2019). In chickpea, the shoot length, number of leaves per plant, fresh weight, dry weight and number of secondary roots per plant increased by 15.3, 14.4, 37.7, 20.0, 52.8%, respectively, when sprayed with CS-NPs loaded thiamine at 0.1% (Muthukrishnan *et al*., 2019). In addition, CS-NPs loaded Cu at 0.06% could increase plant height (56.8%), root length (40.3%), and pod number (7.2%). NPs treatment at 0.02% could increase root weight (46.8%), nodule number (44.2%), nodule weight (125.8%) at greenhouse conditions and also increase root length (60.9%), root weight (46.8%), pod number (29.7 %) in soybean at field conditions (Swati, 2020). Furthermore, this NPs at 0.01-0.08% could increase plant height (15.9-47.0%), stem diameter (82.9-102.9%), root length (9.5-15.8%), root number (20.9-46.3%), chlorophyll content (67.3-182.6%) at greenhouse conditions and increased grain yield (25.4-29.3%), 100 grain weight (14.4-16.9%) in maize at field conditions (Choudhary *et al*., 2017c). Hovever, the treatment at 0.16% could reduce

root length (9.8%) and chlorophyll content (4.6-9.7%) although the difference was no significance. The CS-NPs loaded SA at 0.01-0.16% increased leaf area (160.6-224.7%), shoot length (38.5-76.9%), root length (66.9-111.5%), root number (59.6-91.8%), stem diameter (22.8-53.9%), total chlorophyll (54.2-141.4%) in maize at greenhouse conditions. Besides, the treatment of these NPs at 0.08%, days to 50% tasselling was early by 4 days at field conditions. Moreover, the plant height (25.5%), ear height (12.1%), cob length (44.8%), test weight (71.1%), and grain yield (48.3%) were also increased (Kumaraswamy *et al*., 2019). Ha *et al*. (2019) synthesized CS-NPs loaded NPK (ionic gelation) with slow-release N (66.7%), P (3.1%), K (57.7%) for 240 hours. The leaf number, leaf area, plant height, and stem diameter of coffee were increased at 22.8, 46.9, 12.7, 28.3% when treated these NPs at 30 ppm, respectively. This synthesized CS-NPs loaded NPK improved N (17.04%), P (13.1%), K (67.5%), chlorophyll (30.68%), carotenoid (21.4%) content and photosynthesis rate (71.7%) in the coffee leaves. Another nano fertilizer as CS-NPs loaded silicon at 0.04-0.12% could increase the seeding vigor index in maize seeding by 167.5-285.2%. Furthermore, foliar spraying could induce antioxidant defense enzyme activity, equilibrated cellular redox, and balancing superoxide anion and H_2O_2 in leaf lead to homeostasis. In the field trial, the yield and test weight of maize was increased by 186.6 and 77.1% by treated CS-NPs loaded silicon at 0.08 and 0.04%, respectively (Kumaraswamy *et al*., 2021).

2.4.4 Conclusion and Future perspectives

Discovered since 1997, the studies on NPs synthesized by ionic gelation method have only received attention in the last ten years. The researches on using these NPs in plant disease management has only been interested in the last five years. With the advantage of being easy to implement, both CS-NP and CS-NP loaded active ingredients (Cu, saponin, harpin protein, Zn, SA, hexaconazole, NPK, thiamine, silicon) are effective in plant disease management and enhance plant growth depending on the concentrations and application method by direct or indirect mechanisms. CS-NP

loaded active ingredients is the “drug delivery system” model. The effectiveness of disease management and enhanced plant growth of CS-NP or CS-NP depend on the mechanism of CS (carrier) and active ingredients (drug). At higher concentrations, CS-NP or CS-NP loaded active ingredients are effective in directly inhibiting phytopathogens. This can be applied to control when the disease has broken out. In addition, CS-NP and CS-NP loaded active ingredients at lower concentrations can indirectly reduce disease through activation of plant's innate immunity, including stimulating cell death, H_2O_2 accumulation, oxidative burst (O_2^-), enzymes (**β**-1,3-glucanase, catalase, chitinase, chitosanase, peroxidase, phenoloxidases, phenoloxidases, phenylalanine ammonia-lyase, polyphenol oxidase, protease, superoxide dismutases) and secondary metabolites (total phenols, lignin). Moreover, their treatment could enhance transcriptome changes including defense response, signal transduction, transport, transcription, photosynthesis, housekeeping, and aromatic biosynthesis. In the nature, plant diseases often have seasonal outbreaks. Periodical pre-treat CS-NP or CS-NP loaded active ingredients at sensitive periods can prevent disease and reduce the consequences of disease outbreaks. Furthermore, CS-NP and CS-NP loaded active ingredient can enhance indole-3-acetic acid, **α**-amylase, protease, chlorophyll, carotenoid content, photosynthesis rate that led to increase plant growth, yield, and quality. When plants grow well, their health is enhanced, they can better tolerance diseases. In particular, CS-NP and CS-NP loaded active ingredients have nano size and positive charge, which are able to easily penetrate cells or stick to plant surfaces. Besides, the active ingredient could be slowly released to plant easily absorbed and no waste. The CS (carrier) as a nitrogen source enhances cell division, cell elongation, enzymatic activation, and synthesis of protein. These preeminent characteristics lead to CS-NP or CS-NP loaded active ingredient being more effective than CS or active ingredients single. The, CS-NP loaded active ingredients are more interested in evaluating effectiveness at greenhouse and filed conditions. Most of the studies are interested in fungal diseases (*Alternaria* spp., *Aspergillus* spp., *B. bassiana*, *C. gloeosporioides*, *C. lunata*, *Fusarium* spp., *G. boninense*, *G. fujikuori*, *M. phaseolina*,

P. capsici, *P. grisea*, *R. solani*, *S. sclerotiorum*, *S. rolfsii*) and bacteria (*C. michiganensis*, *E. carotovora* subsp. *carotovora*, *Xanthomonas* spp.,) than viruses, phytoplasma, viroid, nematode. Many crops including chickpea, chilli, date palm, fingermillet, maize, papaya, rice, soybean, tomato, wheat have been evaluated in *in vivo* or greenhouse conditions. However, field experiments are still limited as only maize (with CS-NP loaded Cu, Zn, SA, and Silicon) and soybean (with CS-NP loaded Cu) that have been evaluated for manage post flowering stalk rot, Curvularia leaf spot, and bacterial pustule disease and/or enhancing plant growth.

Nanotechnology is the trend of the future. Easy access and dissemination of nano pesticides are essential, especially in developing areas. Since 2019, 5 of 7 studies of NPs were performed in field conditions that have shown interest in CS-NPs synthesized by the ionic gelation method. In the future, new active ingredients can be loaded into CS-NPs or new polymers with anion by ionic gelation methods and used to improve crop yields. A hypothesis is proposed that “mixing CS and TPP under stirring conditions will lead to CS-NP formation” then, character or not, they are still NPs and possess the superiority of NPs. Therefore, the "legendary" pairs of counter ions are CS and TPP can be studied for immediate application in fields in developing regions where advanced research facilities are limited to building sustainable agriculture

2.5 Reference

Abdel-Aliem, H. A., Gibriel, A. Y., Rasmy, N. M., Sahab, A. F., El-Nekeety, A. A., & Abdel-Wahhab, M. A. (2019). Antifungal efficacy of chitosan nanoparticles against phytopathogenic fungi and inhibition of zearalenone production by *Fusarium graminearum*. *Comunicata Scientiae*, 10(3): 338-345. doi:10.14295/cs.v10i3.1899.

Abdulai, M., Basım, H., Basım, E., Baki, D., & Öztürk, N. (2018). Detection of *Xanthomonas axonopodis* pv. *manihotis*, the causal agent of cassava bacterial blight diseases in cassava (*Manihot esculenta*) in Ghana by polymerase chain reaction.

European Journal of Plant Pathology, 150(2): 471-484. doi:10.1007/s10658-017-1297-3.

Agarwal, M., Nagar, D. P., Srivastava, N., & Agarwal, M. K. (2015). Chitosan nanoparticles-based drug delivery: An update. *International Journal of Advanced Multidisciplinary Research*, 2(4): 1-13.

Alabi, O. J., Kumar, P. L., & Naidu, R. A. (2011). Cassava mosaic disease: A curse to food security in subSaharan Africa. *APSnet Features*. Retrieved from https://www.apsnet.org/edcenter/apsnetfeatures/Pages/cassava.aspx

Allem, A. C. (2002). The origins and taxonomy of cassava. In Hillocks, R. J., Thresh, J. M. & Bellotti, A. (Eds.). *Cassava: Biology, Production and Utilization* (1st ed, pp. 1-16), Cali, Colombia: CABI.

Alves, A. A. C. (2002). Cassava botany and physiology. In Hillocks, R. J., Thresh, J. M. & Bellotti, A. (Eds.). *Cassava: Biology, Production and Utilization* (1st ed, pp. 67-89), Cali, Colombia: CABI.

Ayesu-Offei, E. N., & Antwi-Boasiako, C. (1996). Production of microconidia by *Cercospora henningsii* Allesch, cause of brown leaf spot of cassava (*Manihot esculenta* Crantz) and tree cassava (*Manihot glaziovii* Muell.-Arg.). *Annals of Botany*, 78(5): 653-657. doi:10.1006/anbo.1996.0173.

Bangun, H., Tandiono, S., & Arianto, A. (2018). Preparation and evaluation of chitosan-tripolyphosphate nanoparticles suspension as an antibacterial agent. *Journal of Applied Pharmaceutical Science*, 8(12): 147-156. doi:10.7324/JAPS.2018.81217.

Bocchetta, P. (2020). Ionotropic gelation of chitosan for next-generation composite proton conducting flat structures. *Molecules*, 25(7): 1632. doi:10.3390/molecules25071632.

Burketova, L., Trda, L., Ott, P. G., & Valentova, O. (2015). Bio-based resistance inducers for sustainable plant protection against pathogens. *Biotechnology Advances*, 33(6): 994-1004. doi:10.1016/j.biotechadv.2015.01.004.

CABI (2020). *Manihot esculenta* (cassava). Retrieved from https://www.cabi.org/isc/datasheet/32401

Cai, L., Liu, C., Fan, G., Liu, C., & Sun, X. (2019). Preventing viral disease by ZnONPs through directly deactivating TMV and activating plant immunity in *Nicotiana benthamiana*. *Environmental Science: Nano*, 6(12): 3653-3669. doi:10.1039/C9EN00850K.

Calvo, P., Remunan-Lopez, C., Vila-Jato, J. L., & Alonso, M. J. (1997). Novel hydrophilic chitosan-polyethylene oxide nanoparticles as protein carriers. *Journal of Applied Polymer Science*, 63(1): 125-132. doi:10.1002/(SICI)1097-4628(19970103)63:1<125::AID-APP13>3.0.CO;2-4

Calvo, P., Remuñan-López, C., Vila-Jato, J. L., & Alonso, M. J. (1997b). Chitosan and chitosan/ethylene oxide-propylene oxide block copolymer nanoparticles as novel carriers for proteins and vaccines. *Pharmaceutical Research*, 14(10): 1431-1436. doi:10.1023/A:1012128907225.

Chakraborty, M., Hasanuzzaman, M., Rahman, M., Rahman Khan, M., Bhowmik, P., Mahmud, N. U., Tanveer, M. & Islam, T., (2020). Mechanism of plant growth promotion and disease suppression by chitosan biopolymer. *Agriculture*, 10(12): p.624. doi:10.3390/agriculture10120624.

Choudhary, M. K., Joshi, A., Sharma, S. S., & Saharan, V., (2017a). Effect of laboratory synthesized Cu-Chitosan nanocomposites on control of PFSR disease of maize caused by *Fusarium verticillioids*. *International Journal of Current Microbiology and Applied Sciences*, 6: 1656-1664. doi:10.20546/ijcmas.2017.608.199.

Choudhary, R. C., Joshi, A., Kumari, S., Kumaraswamy, R. V., & Saharan, V. (2017b). Preparation of Cu-chitosan nanoparticle and its effect on growth and enzyme activity during seed germination in maize. *Journal of Pharmacognosy and Phytochemistry*, 6(4): 669-673.

Choudhary, R. C., Kumaraswamy, R. V., Kumari, S., Sharma, S. S., Pal, A., Raliya, R., Biswas, P., & Saharan, V. (2019). Zinc encapsulated chitosan nanoparticle to promote maize crop yield. *International Journal of Biological Macromolecules*, 127: 126-135. doi:10.1016/j.ijbiomac.2018.12.274.

Choudhary, R. C., Kumaraswamy, R. V., Kumari, S., Sharma, S. S., Pal, A., Raliya, R., Biswas, P., & Saharan, V., (2017c). Cu-chitosan nanoparticle boost defense responses

and plant growth in maize (*Zea mays* L.). *Scientific Reports*, 7(1): 1-11. doi:10.1038/s41598-017-08571-0.

Clayton, K. N., Salameh, J. W., Wereley, S. T., & Kinzer-Ursem, T. L. (2016). Physical characterization of nanoparticle size and surface modification using particle scattering diffusometry. *Biomicrofluidics*, 10(5): 054107. doi:10.1063/1.4962992.

Cobley, C. M., Skrabalak, S. E., Campbell, D. J., & Xia, Y. (2009). Shape-controlled synthesis of silver nanoparticles for plasmonic and sensing applications. *Plasmonics*, 4(2): 171-179. doi:10.1007/s11468-009-9088-0.

Corwin, J. A., & Kliebenstein, D. J. (2017). Quantitative resistance: more than just perception of a pathogen. *The Plant Cell*, 29(4): 655-665. doi:10.1105/tpc.16.00915.

Das, S., & Pattanayak, S. (2020). Nanotechnological approaches in sustainable agriculture and plant disease management. In Das, S. K. *Organic Agriculture*. (1st ed, 18 pp). London: IntechOpen. doi: 10.5772/intechopen.92463

de Freitas, J. P. X., Diniz, R. P., de Oliveira, S. A. S., da Silva Santos, V., & de Oliveira, E. J. (2017). Inbreeding depression for severity caused by leaf diseases in cassava. *Euphytica*, 213(9): 1-12. doi:10.1007/s10681-017-1995-0.

Devi, K. A., Prajapati, D., Kumar, A., Pal, A., Bhagat, D., Singh, B. R., Adholeya, A., & Saharan, V. (2020). Smart Nano-Chitosan for Fungal Disease Control. In Fraceto, L. F., de Castro, V. L. S. S., Grillo, R., Ávila, D., Oliveira, C. H., & Lima, R. (Eds). *Nanopesticides* (1st ed, pp. 23-47). Cham: Springer.

Dhasmana, A., Firdaus, S., Singh, K. P., Raza, S., Jamal, Q. M. S., Kesari, K. K., Rahman, Q., & Lohani, M. (2017). Nanoparticles: Applications, Toxicology and Safety Aspects. In K. Kesari (Eds.) *Perspectives in Environmental Toxicology* (1st ed, pp. 47-70). Cham: Springer.

Divya, K., Thampi, M., Vijayan, S., Varghese, S., & Jisha, M. S. (2020). Induction of defence response in *Oryza sativa* L. against *Rhizoctonia solani* (Kuhn) by chitosan nanoparticles. *Microbial Pathogenesis*, 149: p.104525. doi:10.1016/j.micpath.2020.104525.

Dong, H., Delaney, T. P., Bauer, D. W., & Beer, S. V. (1999). Harpin induces disease resistance in *Arabidopsis* through the systemic acquired resistance pathway

mediated by salicylic acid and the NIM1 gene. *The Plant Journal*, 20(2): 207-215. doi:10.1046/j.1365-313x.1999.00595.x.

Du, W. L., Niu, S. S., Xu, Y. L., Xu, Z. R., & Fan, C. L. (2009). Antibacterial activity of chitosan tripolyphosphate nanoparticles loaded with various metal ions. *Carbohydrate Polymers*, 75(3): 385-389. doi:10.1016/j.carbpol.2008.07.039.

Elbeshehy, E. K., Elazzazy, A. M., & Aggelis, G. (2015). Silver nanoparticles synthesis mediated by new isolates of *Bacillus* spp., nanoparticle characterization and their activity against *Bean Yellow Mosaic Virus* and human pathogens. *Frontiers in Microbiology*, 6: 453. doi:10.3389/fmicb.2015.00453.

Elmer, W., & White, J. C. (2018). The future of nanotechnology in plant pathology. *Annual Review of Phytopathology*, 56: 111-133. doi:10.1146/annurev-phyto-080417-050108.

Fanou, A. A., Zinsou, V. A., & Wydra, K. (2018). Cassava bacterial blight: A devastating disease of cassava. In: Waisundara V. Y. (Ed). *Cassava* (1st ed, pp. 13-36). Rijeka: IntechOpen. doi: 10.5772/intechopen.71527

FAOSTAT (2020). Crops and livestock products. Retrieved from http://www.fao.org/faostat/en/#data/TP

FAOSTAT (2020). Crops. Retrieved from http://www.fao.org/faostat/en/#data/QC

FAOSTAT (2020). Rankings. Commodities by country. Retrieved from http://www.fao.org/faostat/en/#rankings/commodities_by_country_exports

Food and Agriculture Organization (FAO). (2013). *Save and Grow: Cassava: a guide to sustainable production intensification*. Rome: Food and Agriculture Organization of the United Nations.

Food and Agriculture Organization of the United Nations (FAO). (2014). *The State of World Fisheries and Aquaculture. Opportunities and Challenges*. Rome: Food and Agriculture Organization of the United Nations.

Food and Agriculture Organization of the United Nations (FAO). (2020). *The State of World Fisheries and Aquaculture 2020. Sustainability in Action*. Rome: Food and Agriculture Organization of the United Nations. doi:10.4060/ca9229en

Ha, N. M. C., Nguyen, T. H., Wang, S. L., & Nguyen, A. D. (2019). Preparation of NPK nanofertilizer based on chitosan nanoparticles and its effect on biophysical

characteristics and growth of coffee in green house. *Research on Chemical Intermediates*, 45(1): 51-63. doi:0.1007/s11164-018-3630-7.

Henry, G. & Hershey, C. (2002). Cassava in South America and the Caribbean. In Hillocks, R. J., Thresh, J. M. & Bellotti, A. (Eds.). *Cassava: Biology, Production and Utilization* (1st ed, pp. 17-40). Cali, Colombia: CABI.

Hidayat, I., Hastuty, A., and Ramadhani, I. (2020). A molecular phylogenetic study of *Clarohilum henningsii* (Mycosphaerellaceae, Fungi) on cassava from Indonesia based on the ITS rDNA sequence. *Journal of Microbial Systematics and Biotechnology*, 2(1): 40-45. doi:10.37604/jmsb.v2i1.43.

Hillocks, R. J. & Wydra, K. (2002). Bacterial, fungal and nematode diseases. In Hillocks, R. J., Thresh, J. M. & Bellotti, A. (Eds.). *Cassava: Biology, Production and Utilization* (1st ed, pp. 261-280), Cali, Colombia: CABI.

Ji, J., Hao, S., Wu, D., Huang, R., & Xu, Y. (2011). Preparation, characterization and *in vitro* release of chitosan nanoparticles loaded with gentamicin and salicylic acid. *Carbohydrate Polymers*, 85(4): 803-808. doi:10.1016/j.carbpol.2011.03.051.

Julião, E. C., Santana, M. D., Freitas-Lopes, R. D. L., Vieira, A. D. P., de Carvalho, J. S. B., & Lopes, U. P. (2020). Reduction of brown leaf spot and changes in the chlorophyll a content induced by fungicides in cassava plants. *European Journal of Plant Pathology*, 157(2): 433–439. doi:10.1007/s10658-020-02001-0.

Kain, D., & Kumar, S. (2020). Synthesis and characterization of chitosan nanoparticles of *Achillea millefolium* L. and their activities. *F1000Research*, 9: 1297. doi:10.12688/f1000research.26446.1.

Kashyap, P. L., Xiang, X., & Heiden, P. (2015). Chitosan nanoparticle based delivery systems for sustainable agriculture. *International Journal of Biological Macromolecules*, 77: 36-51. doi:10.1016/j.ijbiomac.2015.02.039.

Kheiri, A., Jorf, S. M., Malihipour, A., Saremi, H., & Nikkhah, M. (2017). Synthesis and characterization of chitosan nanoparticles and their effect on Fusarium head blight and oxidative activity in wheat. *International Journal of Biological Macromolecules*, 102: 526-538. doi:10.1016/j.ijbiomac.2017.04.034.

Koukaras, E. N., Papadimitriou, S. A., Bikiaris, D. N., & Froudakis, G. E. (2012). Insight on the formation of chitosan nanoparticles through ionotropic gelation with

tripolyphosphate. *Molecular Pharmaceutics*, 9(10): 2856-2862. doi:10.1021/mp300162j.

Kumaraswamy, R. V., Kumari, S., Choudhary, R. C., Sharma, S. S., Pal, A., Raliya, R., Biswas, P., & Saharan, V. (2019). Salicylic acid functionalized chitosan nanoparticle: a sustainable biostimulant for plant. *International Journal of Biological Macromolecules*, 123: 59-69. doi:10.1016/j.ijbiomac.2018.10.202.

Kumaraswamy, R. V., Saharan, V., Kumari, S., Choudhary, R. C., Pal, A., Sharma, S. S., Rakshit, S., Raliya, R., & Biswas, P. (2021). Chitosan-silicon nanofertilizer to enhance plant growth and yield in maize (*Zea mays* L.). *Plant Physiology and Biochemistry*, 159: 53-66. doi:10.1016/j.plaphy.2020.11.054

Magdalena, N. M. W., Ernest, R. M., & Robert, B. M. (2012). An outbreak of anthracnose caused by *Colletotrichum gloesporioides* f. sp. *manihotis* in cassava in North Western Tanzania. *American Journal of Plant Sciences*, 3: 596-598. doi:10.4236/ajps.2012.35072.

Malerba, M., & Cerana, R. (2019). Recent applications of chitin-and chitosan-based polymers in plants. *Polymers*, 11(5): p.839. doi:10.3390/polym11050839.

Maluin, F. N., & Hussein, M. Z. (2020). Chitosan-based agronanochemicals as a sustainable alternative in crop protection. *Molecules*, 25(7): p.1611. doi:10.3390/molecules25071611.

Maluin, F. N., Hussein, M. Z., Yusof, N. A., Fakurazi, S., Idris, A. S., Zainol Hilmi, N. H., & Jeffery Daim, L. D. (2019). Preparation of chitosan–hexaconazole nanoparticles as fungicide nanodelivery system for combating Ganoderma disease in oil palm. *Molecules*, 24(13): p.2498. doi:10.3390/molecules24132498.

Manikandan, A., & Sathiyabama, M. (2016). Preparation of chitosan nanoparticles and its effect on detached rice leaves infected with *Pyricularia grisea*. *International Journal of Biological Macromolecules*, 84: 58-61. doi:10.1016/j.ijbiomac.2015.11.083.

McCallum, E. J., Anjanappa, R. B., & Gruissem, W. (2017). Tackling agriculturally relevant diseases in the staple crop cassava (*Manihot esculenta*). *Current Opinion in Plant Biology*, 38: 50-58. doi:10.1016/j.pbi.2017.04.008.

Minato, N., Sok, S., Chen, S., Delaquis, E., Phirun, I., Le, V. X., Burra, D. D., Newby, J. C., Wyckhuys, K. A., & de Haan, S. (2019). Surveillance for *Sri Lankan cassava mosaic virus* (SLCMV) in Cambodia and Vietnam one year after its initial detection in a single plantation in 2015. *Plos One*. 14(2): p.e0212780. doi:10.1371/journal.pone.0212780.

Mohamed, E. A., Gaber, M. H., & Elsharabasy, S. F. (2018). Evaluating the *in vivo* efficacy of copper-chitosan nanocomposition for treating vascular wilt disease in date palm. *International Journal of Environment, Agriculture and Biotechnology*, 3(2): p.239085. doi:10.22161/ijeab/3.2.17.

Mudgil, M., Gupta, N., Nagpal, M., & Pawar, P. (2012). Nanotechnology: a new approach for ocular drug delivery system. *International Journal of Pharmacy and Pharmaceutical Sciences*, 4(2): 105-112.

Muthukrishnan, S., Murugan, I., & Selvaraj, M. (2019). Chitosan nanoparticles loaded with thiamine stimulate growth and enhances protection against wilt disease in Chickpea. *Carbohydrate Polymers*, 212: 169-177. doi:10.1016/ j.carbpol.2019.02.037.

Nadendla, S. R., Rani, T. S., Vaikuntapu, P. R., Maddu, R. R., & Podile, A. R. (2018). $Harpin_{Pss}$ encapsulation in chitosan nanoparticles for improved bioavailability and disease resistance in tomato. *Carbohydrate Polymers*, 199: 11-19. doi:10.1016/j.carbpol.2018.06.094.

Neuenschwander, P. (2008). Cassava Mealybug, *Phenacoccus manihoti* Matile-Ferrero (Hemiptera: Pseudococcidae). In Capinera, J. L. (Eds.). *Encyclopedia of Entomology* (1st ed, pp. 760-764). Dordrecht: Springer.

Ng'ang, P. W., Miano, D. W., Wagacha, J. M., & Kuria, P. (2019). Identification and characterization of causative agents of brown leaf spot disease of cassava in Kenya. *Journal of Applied Biology and Biotechnology*, 7(6): 1-7. doi:10.7324/JABB.2019.70601.

Noha, K., Bondok, A. M., & El-Dougdoug, K. A. (2018). Evaluation of silver nanoparticles as antiviral agent against ToMV and PVY in tomato plants. *Middle East Journal of Applied Sciences*, 8(01): 100-111.

Obiazi, C. C., & Ojobor, S. A. (2013). Production challenges of cassava and prospects. *Journal of Biology, Agriculture and Healthcare*, 3(14): 31-35.

Oh, J. W., Chun, S. C. & Chandrasekaran, M. (2019). Preparation and *in vitro* characterization of chitosan nanoparticles and their broad-spectrum antifungal action compared to antibacterial activities against phytopathogens of tomato. *Agronomy*, 9(1): p.21. doi:10.3390/agronomy9010021.

Pedroso-Santana, S., & Fleitas-Salazar, N. (2020). Ionotropic gelation method in the synthesis of nanoparticles/microparticles for biomedical purposes. *Polymer International*, 69(5): 443-447. doi:10.1002/pi.5970.

Pei, Y. L., Shi, T., Li, C. P., Liu, X. B., Cai, J. M., & Huang, G. X. (2014). Distribution and pathogen identification of cassava brown leaf spot in China. *Genetics and Molecular Research*, 13(2): 3461-3473. doi:10.4238/2014.April.30.7.

Popova, E. V., Zorin, I. M., Domnina, N. S., Novikova, I. I., & Krasnobaeva, I. L. (2020). Chitosan–tripolyphosphate nanoparticles: Synthesis by the ionic gelation method, properties, and biological activity. *Russian Journal of General Chemistry*, 90(7): 1304-1311. doi:10.1134/S1070363220070178.

Prabakar, K., & Raguchander, T. (2000). Fungicidal control of cassava brown leaf spot caused by *Cercospora henningsii* Allescher. *Madras Agricultural Journal*, 87(7/9), 537-538.

Racoviţă, S., Vasiliu, S., Popa, M., & Luca, C. (2009). Polysaccharides based on micro- and nanoparticles obtained by ionic gelation and their applications as drug delivery systems. *Revue Roumaine de Chimie*, 54(9): 709-718.

Reddy, P. P. (2015). Cassava, *Manihot esculenta*. In Reddy, P. P. (Ed.). *Plant Protection in Tropical Root and Tuber Crops* (1st ed, pp. 17-81). New Delhi: Springer India.

Rodriguez, V. A., Bolla, P. K., Kalhapure, R. S., Boddu, S. H. S., Neupane, R., Franco, J., & Renukuntla, J. (2019). Preparation and characterization of furosemide-silver complex loaded chitosan nanoparticles. *Processes*, 7(4): p.206. doi:10.3390/pr7040206.

Saharan, V., Mehrotra, A., Khatik, R., Rawal, P., Sharma, S. S., & Pal, A. (2013). Synthesis of chitosan based nanoparticles and their *in vitro* evaluation against

phytopathogenic fungi. *International Journal of Biological Macromolecules*, 62: 677-683. doi:10.1016/j.ijbiomac.2013.10.012.

Saharan, V., Sharma, G., Yadav, M., Choudhary, M. K., Sharma, S. S., Pal, A., Raliya, R., & Biswas, P. (2015). Synthesis and *in vitro* antifungal efficacy of Cu–chitosan nanoparticles against pathogenic fungi of tomato. *International Journal of Biological Macromolecules*, 75: 346-353. doi:10.1016/j.ijbiomac.2015.01.027.

Sangpueak, R., Duchanee, R., Saengchan, C., Papathoti, N. K., Hoang, N. H., Wongkeaw, S., and Buensanteai, N. Occurrence of Cassava Black Stem and Root Rot Disease in Thailand (*Manuscript, Unpublish*)

Sangpueak, R., Phansak, P., & Buensanteai, N. (2018). Morphological and molecular identification of *Colletotrichum* species associated with cassava anthracnose in Thailand. *Journal of Phytopathology*, 166(2): 129-142. doi:10.1111/jph.12669.

Sathiyabama, M., & Manikandan, A. (2016). Chitosan nanoparticle induced defense responses in fingermillet plants against blast disease caused by *Pyricularia grisea* (Cke.) Sacc. *Carbohydrate Polymers*, 154: 241-246. doi:10.1016/ j.carbpol.2016.06.089.

Sathiyabama, M., & Parthasarathy, R. (2016). Biological preparation of chitosan nanoparticles and its *in vitro* antifungal efficacy against some phytopathogenic fungi. *Carbohydrate Polymers*, 151: 321-325. doi:10.1016/j.carbpol.2016.05.033.

Saunders, K., Salim, N., Mali, V. R., Malathi, V. G., Briddon, R., Markham, P. G., & Stanley, J. (2002). Characterisation of *Sri Lankan cassava mosaic virus* and *Indian cassava mosaic virus*: evidence for acquisition of a DNA B component by a monopartite begomovirus. *Virology*. 293(1): 63-74. doi:10.1006/viro.2001.1251.

Selvamani, V. (2019). Stability studies on nanomaterials used in drugs. In Shyam, S. M., Shivendu, R., Nandita, D., Raghvendra, K. M., & Sabu, T. (Eds). *Characterization and Biology of Nanomaterials for Drug Delivery: Nanoscience and Nanotechnology in Drug Delivery* (1st ed, pp. 425-444). Amsterdam: Elsevier.

Servin, A., Elmer, W., Mukherjee, A., De la Torre-Roche, R., Hamdi, H., White, J. C., Bindraban, P., & Dimkpa, C. (2015). A review of the use of engineered nanomaterials to suppress plant disease and enhance crop yield. *Journal of Nanoparticle Research*, 17(2): 1-21. doi:10.1007/s11051-015-2907-7.

Shang, Y., Hasan, M., Ahammed, G. J., Li, M., Yin, H., & Zhou, J. (2019). Applications of nanotechnology in plant growth and crop protection: a review. *Molecules*, 24(14): 2558. doi:10.3390/molecules24142558.

Singh, J., Dutta, T., Kim, K. H., Rawat, M., Samddar, P., & Kumar, P. (2018). 'Green'synthesis of metals and their oxide nanoparticles: applications for environmental remediation. *Journal of Nanobiotechnology*, 16(1): 1-24. doi:0.1186/s12951-018-0408-4.

Suryadi, Y., Priyatno, T. P., Samudra, I., Susilowati, D. N., Sriharyani, T. S., & Syaefudin, S. (2019). Control of anthracnose disease (*Colletotrichum gloeosporioides*) using nano chitosan hydrolyzed by chitinase derived from *Burkholderia cepacia* Isolate E76. *Jurnal AgroBiogen*, 13(2): 111–122. doi:10.21082/jbio.v13n2.2017.p111-122.

Swati, K.J.A.J. (2020). Cu-chitosan nanoparticle induced plant growth and antibacterial activity against bacterial pustule disease in soybean (*Glycine max* (L.)). *Journal of Pharmacognosy and Phytochemistry*, 9(1): 450-455.

Teri, J. M., Thurston, H. D., & Lozano, J. C. (1980). Effect of brown leaf spot and Cercospora leaf blight on cassava productivity. *Tropical Agriculture*, 57(3): 239-243.

U.S. Food and Drug Administration, 2021. *Title 21-Food and drugs. Chapter I-Food and drug administration. Subchapter B - Food for human consumption. Part 182-Substances generally recognized as safe*. Retrieved from https://www.accessdata.fda.gov/scripts/cdrh/cfdocs/cfcfr/CFRSearch.cfm?fr=182.6810

Uchechukwu-Agua, A. D., Caleb, O. J., & Opara, U. L. (2015). Postharvest handling and storage of fresh cassava root and products: a review. *Food and Bioprocess Technology*, 8(4): 729-748. doi:10.1007/s11947-015-1478-z.

Uke, A., Hoat, T. X., Quan, M. V., Liem, N. V., Ugaki, M., & Natsuaki, K. T. (2018). First report of *Sri Lankan cassava mosaic virus* infecting cassava in Vietnam. *Plant Disease*, 102(12): 2669. doi:10.1094/PDIS-05-18-0805-PDN.

Wang, H. L., Cui, X. Y., Wang, X. W., Liu, S. S., Zhang, Z. H., & Zhou, X. P. (2016). First report of *Sri Lankan cassava mosaic virus* infecting cassava in Cambodia. *Plant Disease*, 100(5): 1029. doi:10.1094/PDIS-10-15-1228-PDN.

Wang, Y., Li, P., Truong-Dinh Tran, T., Zhang, J., & Kong, L. (2016). Manufacturing techniques and surface engineering of polymer based nanoparticles for targeted drug delivery to cancer. *Nanomaterials*, 6(2): p.26. doi:10.3390/nano6020026.

Worrall, E. A., Hamid, A., Mody, K. T., Mitter, N., & Pappu, H. R. (2018). Nanotechnology for plant disease management. *Agronomy*, 8(12): 285. doi:10.3390/agronomy8120285.

CHAPTER III

IDENTIFICATION OF *ALTERNARIA* SPP. ASSOCIATED WITH CASSAVA LEAF SPOT DISEASE IN THAILAND

ABSTRACT

Cassava leaf spot is a complex disease that has been reported to be caused by a variety of fungi species. The objectives of this research were to determine (1) the fungi associated to leaf spot disease on cassava plants in Thailand and (2) biochemical changes in tissues when the fungal agent infected cassava. The results showed that 36 fungal isolates were isolated from 16 leaf spot samples. Of these, 23 fungal isolates showed virulent activity by causing rot lesions on detached leaves assay. The most and highly virulent fungal isolate caused rot lesions with sizes 28.35-32.72 ×25.70-29.70 mm and 26.86-30.57 × 19.20-24.05 mm, accounting for 30.4 and 34.8%, respectively. The morphology and molecular sequencing on ITS region identified 14 isolates of *Alternaria alternata* and 9 isolates of *Alternaria solani* isolates. The *A. alternata* showed to be more virulent than *A. solani*. In the pathogenicity test, *A. alternata* caused necrotic spot lesions and blight symptoms on cassava leaves. Synchrotron Fourier-transform infrared spectroscopy was used to determine the biochemical changes in the epidermis and mesophyll tissues of cassava leaves when *A. alternata* was infected. The results showed an increase in pectins, polysaccharides, celluloses, hemicelluloses and an decrease in lipids, proteins, phenolics, ligins, carbohydrate component.

Keywords: *Alternaria*; cassava; FTIR; leaf spot; virulence

3.1 Introduction

Cassava (*Manihot esculenta* Crantz) is an important crop and also a crutial source of food, feed and industrial materials in the world. Cassava tuber and leaves are used as sources of carbohydrates and proteins or vitamins (A, C), mineral salts for humans and sometimes as feed for animals, especially in poor areas. In addition, this is the main raw material source for starch, ethanol, biofuel, flour, glucose, modified starches (Balagopalan, 2002; Food and Agriculture Organization, 2013; Guira *et al*., 2017).

The plant is grown in many African countries but is mainly exported from Southeast Asian countries. Cassava is a Thailand's staple crop, with a production area of 1.39 million hectares and an output of 31.08 million tons in 2019, which accounts for 5.04 and 10.24% worldwide, respectively. These figures are lower than those of Nigeria and Congo (FAOSTAT, 2021a). However, Thailand is the world's leading exporter of cassava products. The output of cassava dried, flour and starch were exported to reach 1.76, 0.03 and 2.66 million tons with the value of 524.20, 21.19 and 1219.67 million USD, respectively (FAOSTAT, 2021b).

Cassava growth and development are influenced by climatic factors, soil, pests, weeds and diseases. The plants are sensitive to clay, salty soils, and excessive water condition (Obiazi and Ojobor, 2013). According to the review of McCallum *et al*. (2017), cassava diseases include 6 types of viral diseases, 6 types of bacterial diseases, 13 types of fungal diseases, 3 types of phytoplasma diseases caused by more than 50 species of phytopathogens. Among them, cassava mosaic disease (*African Cassava Mosaic Virus, East African Mosaic Virus, South African Cassava Mosaic Virus, Indian Cassava Mosaic Virus, Sri Lanka Cassava Mosaic Virus*), cassava brown streak disease (*Cassava Brown Streak Virus, Ugandan Brown Streak Virus*), and bacterial blight (*Xanthomonas axonopodis* pv. *manihotis*) can result in up to 90, 70 and 75% yield reductions, respectively (McCallum *et al*., 2017; Abdulai *et al*., 2018, Uke *et al*., 2018;

Minato *et al*., 2019). Furthermore, nematodes could cause an average loss of 6% of annual cassava production.

There are three types of symptomatic leaf spots including brown leaf spot, white leaf spot, and diffuse or blight leaf spot described on cassava. The diffuse or blight leaf spot features larger spots with no clear outline, while brown leaf spot and white leaf spot both feature with angular brown spots with yellow halo and circular-angular white or yellowish-brown spots with small sunken, respectively (McCallum *et al*., 2017). Several types of fungi species have been identified as pathogens of the cassava leaf spot disease. A commonly known white leaf spot is caused by *Cercospora caribaea* (*Phaeoramularia manihotis*) or *Passarola manihotis* while the diffuse or blight leaf spot agent is *Cercospora vicosae* or *Passarola vicosae* and the brown leaf spot agent is *Cercospora henningsii* or *Cercosporidium henningsii* (Reddy, 2015; de Freitas *et al*., 2017; McCallum *et al*., 2017). However, the brown leaf spot has been reported by many causal agents including *Mycosphaerella manihotis* in Colombia (Teri *et al*., 1980), *C. henningsii* in Ghana (Ayesu-Offei and Antwi-Boasiako, 1996), *C. henningsii* (*Mycosphoraella henningsii*) in India (Prabakar and Raguchander, 2000), *Passalora henningsii* in China and Brazil (Pei *et al*., 2014; de Freitas *et al*., 2017), *Colletotrichum, Alternaria, Cladosporium* in Kenya (Ng'ang'a *et al*., 2019) and *Clarohilum henningsii* in Indonesia and Brazil (Hidayat *et al*., 2020; Julião *et al*., 2020) **(Table 3.1)**. Cassava brown leaf spot disease causes up to 30% loss in yield. However, it is often neglected until several recent outbreaks in Brazil (Julião *et al*., 2020). Under conditions of the temperature at 25-32℃ and the presence of free-water, the mature conidia of pathogen's sprout and fragment into multiple microconidia, which can germinate and form an appressorium on both the upper and lower surfaces of the leaves (Ayesu - Offei and Antwi-Boasiako, 1996). Additionally, according to Reddy (2015), the pathogen causes serious harm in warm, wet conditions, and spreads through the wind - similar to weather in tropical countries like Thailand.

Table 3.1 The record of cassava leaf spot disease.

Type of symptoms	Country	Pathogen	Reference
White leaf spot	World	*Cercospora caribaea* (*Phaeoramularia manihotis*) or *Passarola manihotis*	de Freitas *et al*., 2017; McCallum *et al*., 2017
Diffuse or blight leaf spot	World	*Cercospora vicosae* or *Passarola vicosae*	
Brown leaf spot	World	*Cercospora henningsii* or *Cercosporidium henningsii*	Reddy, 2015; McCallum *et al*., 2017
	Colombia	*Mycosphaerella manihotis*	Teri *et al*., 1980
	Ghana	*Cercospora henningsii*	Ayesu-Offei and Antwi-Boasiako, 1996
	India	*Cercospora henningsii* [*Mycosphoraella henningsii*]	Prabakar and Raguchander, 2000
	China	*Passalora henningsii*	Pei *et al*., 2014
	and Brazil		de Freitas *et al*., 2017
	Kenya	*Colletotrichum*, *Alternaria*, *Cladosporium*	Ng'ang'a *et al*. (2019)
	Indonesia	*Clarohilum henningsii*	Hidayat *et al*., 2020
	and Brazil		Julião *et al*., 2020

The identification of a causal plant pathogen is usually based on the Koch postulate (Agios, 2005; Burgess *et al*., 2008). The fungal pathogen is classified and identified based on the common morphological features of colony, conidia and common molecular biology as sequencing internal transcribed spacer (ITS) region based on polymerase chain reaction (PCR) primers (Barnett and Hunter, 1987; White *et al*., 1990). For example, cassava anthracnose disease (*Colletotrichum gloeosporioides*,

C. capsici, *C. lindemuthianum*, *C. aeschynomene*, *C. boninense*, *C. plurivorum*, *C. karstii*, *C. fructicola* and *C. siamense*), tomato black spot (*Alternaria alternata*), cassava leaf spot (*Passalora henningsii*, *Colletotrichum*, *Alternaria*, *Cladosporium*, *Clarohilum henningsii*) and rice leaf spot (*Bipolaris sorokiniana*, *Curvularia hawaiiensis, Curvularia geniculata, Curvularia eragrostidis, Curvularia aeria* and *Curvularia lunata*) were identified by this method (Pei *et al*., 2014; Kusai *et al*., 2016; Liu *et al*., 2018; Sangpueak *et al*., 2018; Mohammadi and Bahramikia, 2019; Ng'ang'a *et al*. 2019; Hidayat *et al*., 2020).

In addition to mechanical forces, the chemical compounds produced by phytopathogens are a harmful weapon that attacks the host plants. Metabolites including toxins, enzymes, growth regulators, and polysaccharides produced by phytopathogens play a crutial role in the interaction between host-plant and phytopathogens, including the formation of disease symptoms (Agrios, 2005). In previous studies, *Alternaria* spp., *Curvularia* spp., *Bipolaris* spp. and *Cochliobolus* spp. are known to secrete mycotoxins such as tenuazonic acid, alternariol, alternariol monomethyl ether, α- and β-dehydrocurvularin, HC Toxin ($C_{21}H_{32}N_4O_6$), bipolaroxin, sorokinianin, carbotoxine, victorin, ophiobolin, curvularin, cytochalasin B that can necrotic plant tissues similar to leaf spot, or leaf blight symptoms (Davis *et al*., 1997; Jiang *et al*., 2008; Manamgoda *et al*., 2011; Andersen *et al*., 2013; Wight *et al*., 2013; Meena *et al*., 2017).

Synchrotron Fourier-transform infrared spectroscopy (SR-FTIR) is a technique for molecular chemical determination in solid, liquid, and biological samples with the advantages of rapid, direct, non-destructive and non-invasive (Yu, 2005). Previously, SR-FTIR has been studied to determine the altered biochemical components or compounds in potato plants infected by *Colletotrichum coccodes*, *Rhizoctonia*, *Helminthosporium* and *Phytophtora infestans*; cassava plants primed by *Bacillus subtilis* CaSUT007, chilli plants induced by *Bacillus subtilis* D604 to resist anthracnose disease, and rice plants induced by salicylic acid against *Xanthomonas oryzae* pv.

oryzae (Yu, 2005; Taoutaou *et al*., 2010; Thumanu *et al*., 2015; Le Thanh *et al*., 2017; Thumanu *et al*., 2017). Furthermore, the combination of SR-FTIR microspectroscopy, cryo-section samples and multiple analysis could clarify the biochemical compound changes in each epidermis and mesophyll tissues with high spatial resolution (Thumanu *et al*., 2017).

The objectives of this research are to determine the fungal species is related to leaf spot disease on cassava in Thailand, and the biochemical changes in tissues when the fungal agent infected cassava.

3.2 Materials and methods

3.2.1 Sample collection and isolation of cassava leaf spot pathogen

Cassava leaf spot samples were collected from cassava fields at Mueang Nakhon Ratchasima and Seang Sang district, then isolated at Bio Pesticide Laboratory, Suranaree University of Technology, Nakhon Ratchasima, Thailand. The leaf spot lesion was cut into small pieces with a size of about 3 × 3 mm, dipped in 70% alcohol (VWR BDH chemical, USA) for 15 s to sterilize the surface, then washed with sterilized distilled water, and placed on a sterile paper towel until dry. Later, pieces of leaf lesions were placed on Petri plates containing water agar medium, which kept at room temperature for 3-6 days. Mycelia grow from these pieces were transferred to potato dextrose agar medium and re-cultured it until fungal colonies were pure. Mycelium of the pure isolates were grown in Eppendorf containing potato dextrose broth medium at a shaking around 300 rpm for 48 hours, which was added 20% glycerol solution (AMRESCO, USA) and stored at -80°C as a stock (Burgess *et al*., 2008; Sangpueak *et al*., 2018).

3.2.2 Screening virulent fungal isolates

The virulent of fungal isolates was evaluated by the detached leaf assay method as described by Pettitt *et al*. (2011), Zheng *et al*. (2015), Maizatul-Suriza *et al*. (2017), Sangpueak *et al*. (2018) with a slight modification. Briefly, the without disease leaves were obtained from the cassava fields rinsed under running water and surface sterilized with 70% alcohol. These leaves were then placed into the plastic boxes containing the tissue paper wetting sterilized water to maintain high humidity. A piece of potato dextrose agar sized 3-5 × 3-5 mm containing 7 days-old fungal colony was placed on the surface of the cassava leaf. The boxes were kept at 28 ± 2°C in the laboratory to evaluate virulent trait of the fungal pathogen by measuring diameter of rot lesions. The experiment was performed in a completely randomized design with 4 replications as 4 positions of a cassava leaf inoculating for each fungal isolate.

The length and width of rot lesions were averaged from 4 replications. Then, the score was visualized by heatmap analysis by using Expression function with Clustering Method (Average Linkage) and Distance Measurement Method (Eucledian) in Heatmapper software (Babicki *et al*., 2016).

3.2.3 Morphological characterization

The virulent fungal isolates were cultured onto potato dextrose agar medium and kept at 28 ± 2°C up to three weeks. The morphological characters including colony, spore shape were used to identify fungi species. In addition, the size (length and width) of 30 conidia were measured by using light microscope and stage micrometer (Kusai *et al*., 2016; Sangpueak *et al*., 2018).

3.2.4 DNA extraction

The DNA of each pure fungal isolate was extracted using acetyl trimethylammonium bromide (CTAB) method as described by Mohammadi and

Bahramikia, (2018) with slight modification. The fungi were cultured on potato dextrose agar medium for 14 days at 28 ± 2°C. The colony was transferred to chilled porcelain mortar and ground by chilled pestle with liquid nitrogen until it was finely powdered. Next, 700 µL of CTAB buffer was added into the powder and further crushed, which was transferred to Eppendorf 1.5 mL and incubated at 65°C for 45 mins by using a water bath. The Eppendorf was then centrifuged at 14000 rpm, for 10 minutes at 4°C (Thermo Fisher Scientific, USA). Later, 600 µL of supernatant was mixed with 600 µL mixture of chloroform: isoamyl alcohol (24: 1) (VWR BDH chemical, USA), which was vortexed for 20 s and then centrifuged at 14000 rpm, for 10 minutes at 4°C. One volume of the aqueous phase was transferred to new Eppendorf, which added cold absolute ethanol (VWR BDH chemical, USA) (2 volumes) and then centrifuged at 10000 rpm for 10 minutes at 4°C. The pellet containing DNA was collected and washed with 600 µL of 70% ethanol by a centrifugation at 10000 rpm for 5 minutes. The DNA was air-dried overnight and resuspended in 25 µL TE buffer. The concentration of DNA was measured by using DeNovix DS-11 Series Spectrophotometer (DeNovix, USA). The eppendorf is stored at -20°C until use.

3.2.5 Polymerase chain reaction and DNA sequence analysis

The ITS region of fungi was amplified by priming pair ITS4 (TCCGTAGGTGAACCTGCGG) and ITS5 (GGAAGTAAAAGTCGTAACAAGG) or ITS1 (TCCGTAGGTGAACCTGCGG) and ITS4 (TCCGTAGGTGAACCTGCGG) (preliminary test) (White *et al*., 1990; Kusai *et al*., 2016; Mohammadi *et al*., 2019; Iturrieta-González *et al*., 2020; Hidayat *et al*., 2020). A reaction with a volume of 25 µL consisted of 0.2 µL of Taq DNA polymerase, 5 µL of 10 × buffer, 1 µL of 25 mM $MgCl_2$, 0.75 µL of 10 mm dNTP (i-Taq ™ DNA Polymerase kit, iNtRON Biotechnology, Inc., Korea), 0.5 µL of 10 µM primers, 1 µL of DNA template (100 ng / µL) and 16.05 µL of sterile distilled water. The PCR by Thermal cycler (Bio-Rad PCR mj mini, CA, USA) with an initial denaturation at 94°C for 5 min, 35 cycles of a denaturation step at 94°C for 30 s, an annealing step at

59°C for 30 s, and an extension step at 72°C for 30 s, and finished with a final extension step at 72°C for 7 min. The 3 µL of PCR product and 6X loading dye (vivantis, Malaysia) loaded onto 1% agarose gel (vivantis, Malaysia), which was electrophoresed with TBE buffer at 100 V for 25 minutes. The gel was stained with ethidium bromide (Invitrogen, USA) and observed under UV light by using the Gel documentation system (UVP GelDoc-It®², USA). The band of the PCR product was compared to the band size of 1 Kb Plus DNA Ladder (Invitrogen). Then, the PCR product was sent to Macrogen Inc. to conduct the sequence. The fungi were identified by using BLAST function in NCBI (https://blast.ncbi.nlm.nih.gov/Blast.cgi) (Mohammadi and Bahramikia, 2018; Sangpueak *et al*., 2018).

3.2.6 Pathogenicity test of *A. alternata* H-Vi 7 at net house conditions

The averaged 4 replications of the rot lesion size (length and width) in virulent test grouped by *A. alternata* and *A. solani* was visualized by using Excel to observe pathogenic distribution trends. Moreover, the data was analysed by Descriptive Statistics different between two fungal group following Principal Component Analysis (PCA) by using Unscramble X version 10.4 (CAMO, Norway) software.

The pathogenicity test was performed to evaluate the pathogenicity of *A. alternata* H-Vi 7 on cassava plants by Koch's postulate. The *A. alternata* H-Vi 7 on potato dextrose agar at 2-week-old was streaked by the sterile needle to enhance conidia production. Then, the sterilized distilled water was added into Petri plates to collect conidial suspension and adjusted to 1×10^5 conidia mL^{-1} (Pei *et al*., 2014). Cassava plant varieties cv. Pirun 2 at 30-45 days old without disease was used for pathogenicity test, which was previously prepared by planting a stalk soaked with 1% sodium hypochlorite for 2 min and washed with water in each pot containing sandy soil and keeping in a net-house (Sangpueak *et al*., 2021). The cassava plants were inoculated with *A. alternata* H-Vi 7 conidial suspension by two treatments including wounding and spraying.

For wounding treatment, the mature leaves were inoculated by dropping 25 µL of conidial suspension that had previously been punched with sterile needles. For spraying treatment, the cassava leaves were foliar sprayed with a conidial suspension until the water runoff. Sterilized water was used instead of conidia suspension as a control in both two treatments. After that, the plants were kept in humid conditions for 3-5 days by holding in the inoculation chamber and mist spray every day, then kept in a net house with shade. The plants were observed every day until 14 days for evaluating disease symptoms. The diseased tissues were incubated as shown in the isolation section to determine the presence of pathogens using light microscopy and re-isolated in agar medium. The experiment was performed in completely randomized design with 4 replications, one leaves in wounding treatment and one plant in spraying treatment as a replication (Pei *et al*., 2014).

3.2.7 Detection of biochemical component in cassava leaf spot tissues by SR-FTIR

The cassava plants including *A. alternata* H-Vi 7 inoculated one and control were prepared as spraying treatment. At 7 days after inoculation, the cassava leaves with the small symptoms were selected. The tissue area of early spot symptom was cut into 4 × 10 mm pieces, freezed in Tissue-Trek® optimal cutting temperature (OCT), and storaged at -80°C until use. The cassava leaves in control treatment were similarly prepared. The samples were cryosectioned with a thick 12 microns by using a Microm ™ HM 525 Cryostat (Thermo Fisher Scientific). The samples were put on infrared transparent BaF_2 windows (22 × 1 mm), and then all samples were placed inside on a desiccator to remove residual water before analyzed. The SR-FTIR spectra were collected in the mid-infrared region (Zohdi *et al*., 2015; Liyanage *et al*., 2017; Thumanu *et al* 2017). The IR spectra in a range of 4000 to 800 cm^{-1} were obtained and collected by 64 scans using the spectral resolution aperture (10 × 10 µm) of 4 cm^{-1} through a protocol including a 36x objective lens of an infrared microscope (Hyperion 2000,

Bruker), SR-FTIR (Hyperion 2000, Bruker Optics, Ettlingen, Germany), and a liquid nitrogen-cooled MCT D315 detector. The CytoSpec 2.06 (Cytospec Inc., NY, USA) and OPUS 7.5 (Bruker Optics Ltd, Ettlingen, Germany) software were used to monitor and analyse data. The biochemical traits in epidermis and mesophyll tissues between control and *A. alternata* H-Vi 7 inoculated one were analysed based on the IR spectra. The second derivative was generated using 13 smoothing points, and the effects of different sample thicknesses were normalized vectors. Then, the hierarchical cluster analysis (HCA) mapping including 15 × 15 M (control) and 10 × 10 M (*A. alternata* H-Vi 7 inoculated) was created into 2D image of 4 clusters to separate spectral ranges (1800-900 and 3000-2800 cm^{-1}) of epidermis and mesophyll tissues to characterize the biochemical components (Lasch *et al*., 2012; Thumanu *et al*., 2017; Siriwong *et al*., 2021). The Unscramble X version 10.4 (CAMO, Norway) software was used to analysis different biochemical components of epidermis and mesophyll tissues using PCA model based on the spectra of each cluster. Moreover, the function "Savitzky-Golay method" with third polynomial and 13 smoothing points was used to calculate the second spectra derivative. The sample was analysed at BL4.1 Infrared Spectroscopy and Imaging Station of the Synchrotron Light Research Institute (SLRI), Nakhon Ratchasima, Thailand, using licenced software tools.

3.3 Results

3.3.1 Fungal isolation and virulent test

In total, 16 leaf spot samples were collected from cassava fields in Soeng Sang and Mueang Nakhon Ratchasima District, Nakhon Ratchasima province, Thailand. As a result, 36 fungal isolates were isolated and purified for the virulent test by detach leaves assay method. The results showed that 23 fungal isolates expressed virulent by causing rot lesions with different levels, with lesion size from 17.17 ± 2.82 × 10.00 ± 0.94 mm (isolate HC-186) to 32.38 ± 2.18 × 19.70 ± 0.95 mm (isolate H-Vi 7) (**Table 3.2; Figure 3.1**) while the control had no rot lesion. The heatmap analysis showed 4

clusters corresponding to 4 virulent groups with least virulent (HC-186), moderately virulent (NH-36, NH-15, NH-28, HC-194, NH-1, NH-37, HC-193), highly virulent (HC-145, HC-132, HC-155, HC-149, NH-33, HC-184, NH-41, NH-23), most virulent (NH-32, HC- 172, H-Vi 9, NH-20, HC-156, H-Vi 7, HC-164) (**Figure 3.2**).

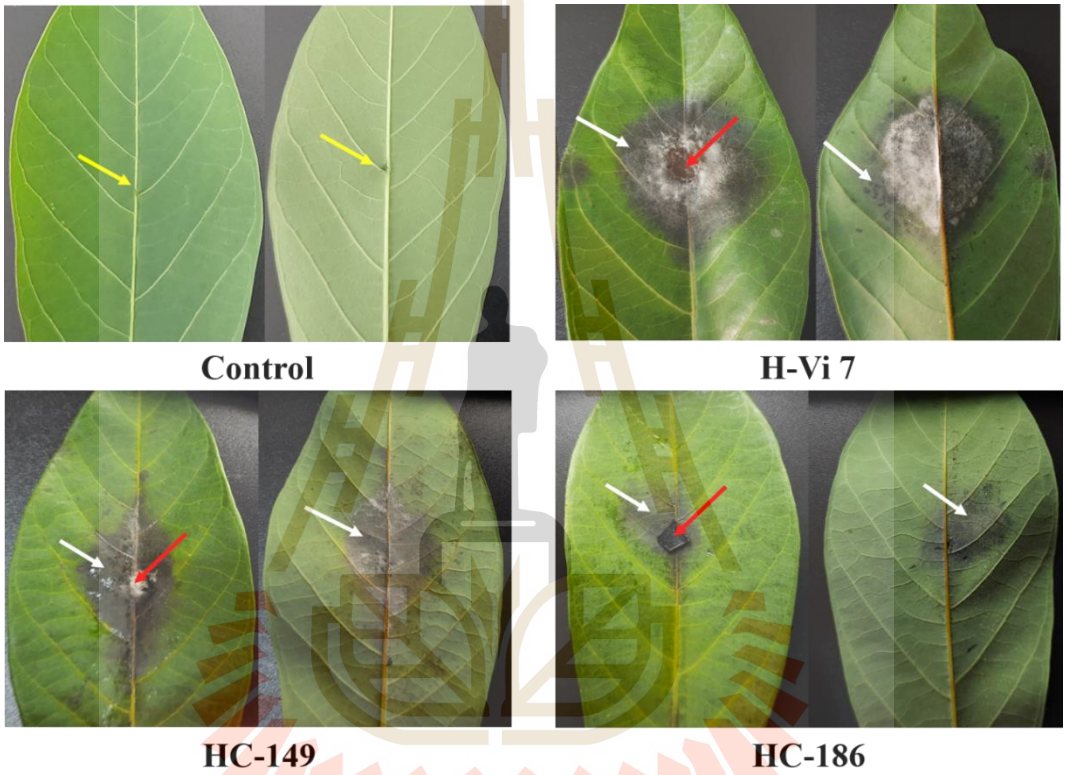

Figure 3.1 The rot lesion on detached leaves assay caused by *A. alternata* strains H-Vi 7, HC-149 and HC-186 compared with control. *Note*: The yellow arrow was injected needle position. The red arrow was the location of the fungal slice. The white arrow was rot lesion.

Table 3.2 The morphology, sequencing ITS region identification and lesion size of 23 virulent fungal isolates associated with cassava leaf spot disease in Thailand.

Strain	Morphology			Sequencing ITS region identification				Lesion size (mm)	
	Colonila group	Conidia size (μm) Length	Width	Species	Similar (%)	Reference	Accession Numbers	Length	Width
H-Vi 7	1	41.5 ± 7.1	8.4 ± 1.4	*A. alternata*	99.44	MK336603.1	OM736198	32.38 ± 2.18	29.70 ± 0.95
H-Vi 9	1	35.4 ± 4.4	7.8 ± 1.3	*A. alternata*	98.44	MZ350544.1	OM736197	29.83 ± 1.85	27.38 ± 0.76
HC-132	3	36.0 ± 8.1	13.5 ± 2.7	*A. alternata*	100	MW354931.1	OM736206	29.95 ± 4.80	20.33 ± 2.61
HC-156	3	35.8 ± 6.8	9.1 ± 1.5	*A. alternata*	100	MW354931.1	OM736202	31.48 ± 0.90	29.35 ± 0.99
HC-145	1	43.9 ± 5.0	10.5 ± 2.3	*A. alternata*	99.23	MK336603.1	OM736205	30.57 ± 3.18	22.20 ± 2.76
HC-149	1	43.8 ± 11.0	12.0 ± 2.1	*A. alternata*	99.45	MK336603.1	OM736204	26.99 ± 3.42	19.65 ± 2.61
HC-155-1	1	37.0 ± 5.7	7.2 ± 1.0	*A. alternata*	100	MW354931.1	OM736203	28.17 ± 2.96	19.20 ± 1.85
HC-164	1	44.7 ± 10.5	11.6 ± 2.0	*A. alternata*	100	MW354931.1	OM736201	32.72 ± 1.74	27.52 ± 1.40
HC-172	1	47.9 ± 10.6	9.3 ± 2.3	*A. alternata*	100	MW354931.1	OM736200	31.48 ± 2.42	25.75 ± 1.41
HC-184	1	46.1 ± 11.0	11.3 ± 1.8	*A. alternata*	99.81	MK336603.1	OM736199	27.43 ± 0.90	22.13 ± 0.74
NH-1	1	34.9 ± 7.5	10.6 ± 1.9	*A. alternata*	100	MZ350544.1	OM736196	24.00 ± 2.68	18.85 ± 1.01
NH-28	1	43.8 ± 7.1	9.1 ± 1.7	*A. alternata*	99.62	MW354931.1	OM736195	23.40 ± 1.85	21.25 ± 1.61
NH-32	1	37.1 ± 6.3	10.3 ± 2.1	*A. alternata*	100	MW354931.1	OM736194	30.93 ± 1.06	26.10 ± 2.20
NH-33	1	37.9 ± 8.4	10.5 ± 2.7	*A. alternata*	100	MW354931.1	OM736193	26.86 ± 1.50	22.20 ± 0.96

Table 3.2 The morphology, sequencing ITS region identification and lesion size of 23 virulent fungal isolates associated with cassava leaf spot disease in Thailand (**continued**).

Strain	Morphology			Sequencing ITS region identification				Lesion size (mm)	
	Colonila group	Conidia size (µm) Length	Width	Species	Similar (%)	Reference	Accession Numbers	Length	Width
HC-186	1	37.9 ± 8.7	8.5 ± 2.0	*A. solani*	100	KX452728.1	OM736211	17.17 ± 2.82	13.00 ± 0.94
HC-193	2	38.3 ± 8.2	11.3 ± 2.2	*A. solani*	99.81	KX452728.1	OM736210	24.05 ± 1.37	15.43 ± 2.75
HC-194	2	37.9 ± 7.7	10.4 ± 1.6	*A. solani*	99.63	KX452728.1	OM736209	23.49 ± 1.82	18.70 ± 1.00
NH-23	1	38.0 ± 9.6	7.2 ± 1.0	*A. solani*	99.82	KX452728.1	OM736215	24.78 ± 1.38	23.50 ± 0.64
NH-15	2	41.5 ± 6.9	10.3 ± 1.7	*A. solani*	100	KX452728.1	OM736208	22.95 ± 1.16	19.88 ± 0.59
NH-20	2	37.3 ± 6.8	8.5 ± 1.7	*A. solani*	99.82	KX452728.1	OM736207	28.35 ± 0.93	25.70 ± 1.10
NH-36	2	39.0 ± 10.4	8.9 ± 1.9	*A. solani*	99.63	KX452728.1	OM736214	21.70 ± 0.88	19.73 ± 0.48
NH-41	2	40.0 ± 9.0	11.0 ± 1.8	*A. solani*	99.63	KX452728.1	OM736212	27.00 ± 1.68	24.05 ± 1.25
NH-37	4	37.4 ± 8.9	10.1 ± 2.4	*A. solani*	99.63	KX452728.1	OM736213	24.95 ± 1.97	18.70 ± 0.93

Note: Group 1: gray color with cottony hyphae on upper surface medium and greenish-black on reverse side. Group 2: gray color with cottony hyphae on the upper surface medium, the colony is grayish white on reverse side, yellow pigment can be observed in agar medium and then slowly turns greenish-black in the center on reverse side. Group 3: slightly brownish gray without cottony hyphae on the upper surface medium, the colony is grayish-white on the edges, gradually changing to brown in the middle and greenish-black in the center of reverse side. Group 4: white-gray color with cottony hyphae on upper surface medium and greenish-black on reverse side. The edges and center of colony were darker than the middle one.

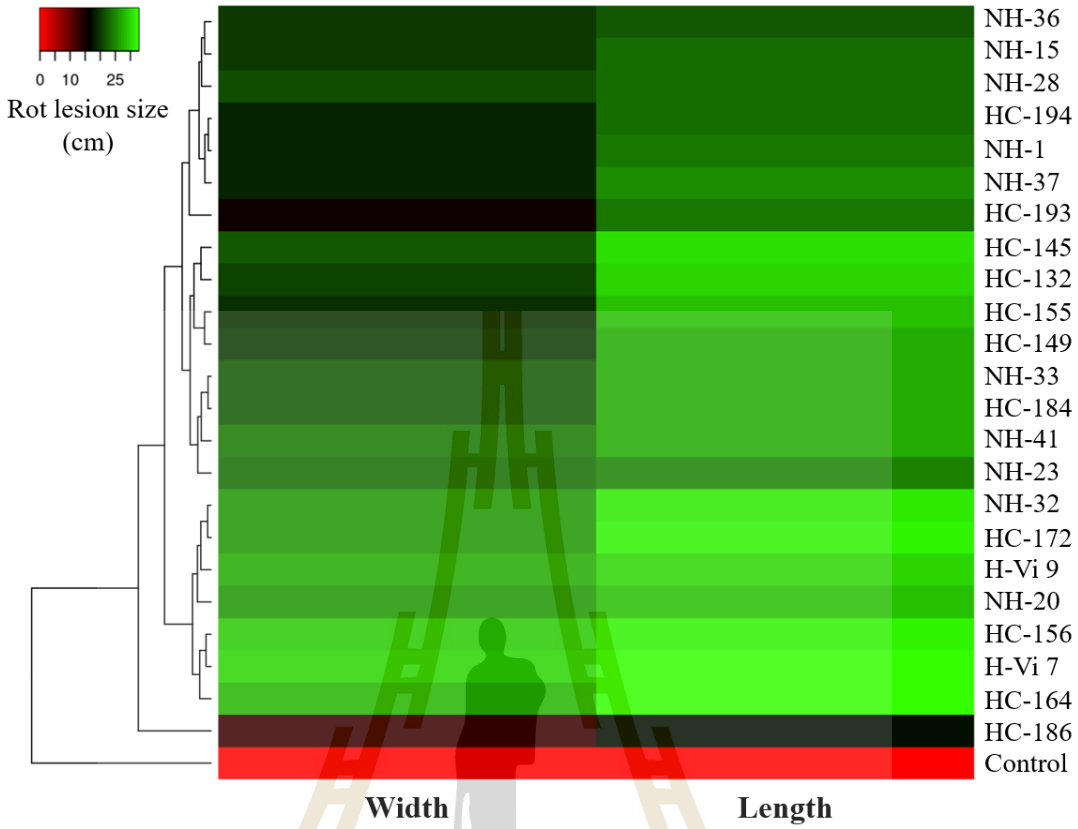

Figure 3.2 The heatmap of rot lesion size of 23 virulent fungal strains.

3.3.2 Morphological and molecular identification

In general, the mycelium of virulent fungal isolates are septate, white when young and turning dark in old age. The morphological colony is divided into 4 groups. In group 1, the fungal colony is gray color with cottony hyphae on upper surface medium and greenish-black on reverse side. In group 2, colony is gray color with cottony hyphae on the upper surface medium, the colony is grayish white on reverse side, yellow pigment can be observed in agar medium and then slowly turns greenish-black in the center on reverse side. In group 3, colony is slightly brownish gray without cottony hyphae on the upper surface medium, the colony is grayish-white on the edges, gradually changing to brown in the middle and greenish-black in the center of reverse side. In group 4, colony is white-gray color with cottony hyphae on upper surface medium and greenish-black on reverse side. The edges and center of colony

is darker than the middle one (**Figure 3.3 a**). The group 1 had the most fungal isolate (isolate 14) while group 2, 3, 4 accounted for 6, 2, 1 fungal isolates, respectively (**Table 3.2**). The conidia of all fungal isolates are yellow-brown when young and brown when mature, oval or ellipsoidal, one end tapering to the other. In particular, the conidia all have many transversal septa and at least one longitudinal septa. The conidia vary in size, from 34.9-47.9 × 7.2-13.5 µm (**Table 3.2; Figure 3.3 b**). All these characteristics suggest that the virulence fungal isolates belong to *Alternaria* genus.

The fungal isolate H-Vi 9 and NH-1 was amplified in the ITS region by ITS1/ITS4 primers and showed a fragment of 450 bps. Meanwhile, the remaining fungal isolates used ITS4/ITS5 showed the fragments at approximate 650 – 670 bps. All ITS DNA sequencing of fungal isolates have 98.11-100% similarity to *A. alternata* or *Alternaria solani*. The fungal isolates including HC-186, HC-193, HC-194, NH-23, NH-15, NH-20, NH-36, NH-41, and NH-37 were similar to the sequence of *A. solani* (accession number KX452728.1) at 99.45-100%. The seven fungal isolates (HC-132, HC-156, HC-149, HC-164, HC-172, NH-32, NH-33) were similar to *A. alternata* (accession number AY433814.1) at 99.45-99.63 %. Besides, the three fungal isolates (H-Vi 7, H-Vi 9, NH-28) were also similar to *A. alternata* (accession number KT223359.1) at 98.11-99.63%. The rest of fungal isolates including HC-145, HC-155-1, HC-184, NH-1 was similar at approximately 98.37-100% with *A. alternata* accession number KF747365.1, KT223345.1, MT446076.1, FJ809940.1, respectively (**Table 3.2**).

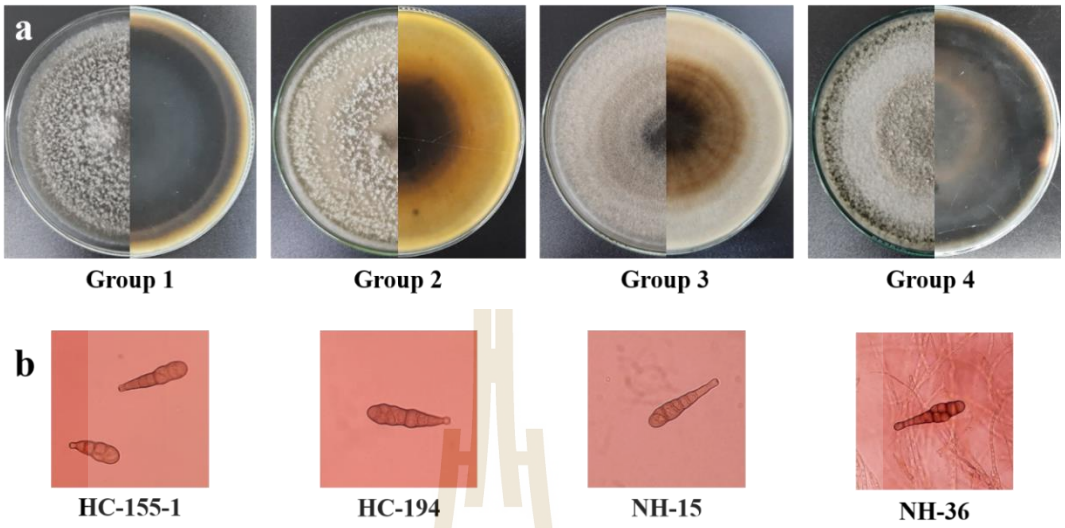

Figure 3.3 The colony upper and reverse sides (a) and conidia (b) of *Alternaria* isolated from cassava leaf spot disease. *Note*: **Group 1:** gray color with cottony hyphae on upper surface medium and greenish-black on reverse side. **Group 2:** gray color with cottony hyphae on the upper surface medium, the colony is grayish white on reverse side, yellow pigment can be observed in agar medium and then slowly turns greenish-black in the center on reverse side. **Group 3:** slightly brownish gray without cottony hyphae on the upper surface medium, the colony is grayish-white on the edges, gradually changing to brown in the middle and greenish-black in the center of reverse side. **Group 4:** white-gray color with cottony hyphae on upper surface medium and greenish-black on reverse side. The edges and center of colony was darker than the middle one.

3.3.3 Pathogenicity test of *A. alternata* H-Vi 7 at net house conditions

Fourteen *A. alternata* and nine *A. solani* fungal virulence isolates have been identified. The *A. alternata* group was associated with cassava leaf spot disease with higher toxicity than the *A. solani* group, leading to cause a larger lesion size (**Figure 3.4 a**). The PCA showed a different virulent based on rot lesion size between two group

fungi at 91% (PC1) and 9% (PC2) (**Figure 3.4 b**). The most virulent fungi *A. alternata* isolate H-Vi 7 was used to test for its ability to cause symptoms on cassava plants.

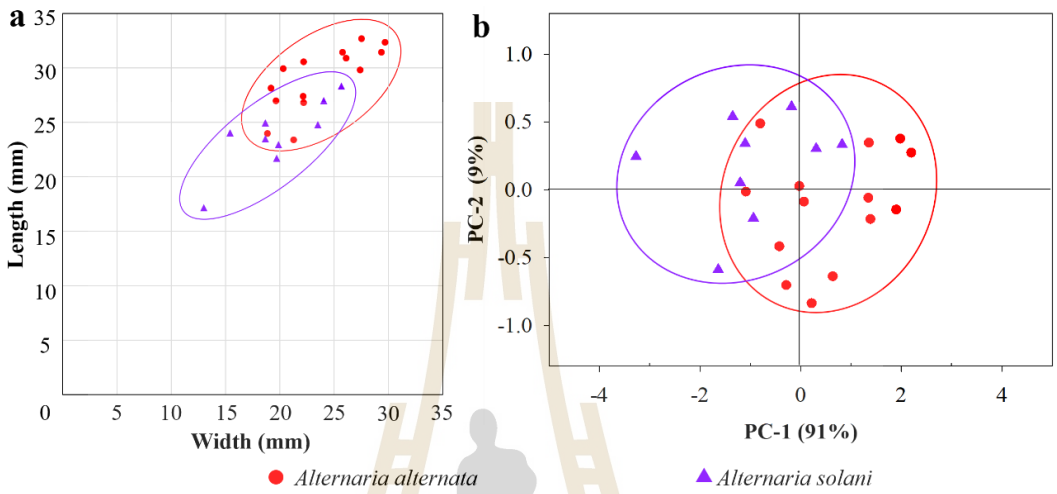

Figure 3.4 The trending distribution (a) and the PCA analysis (b) of rot lesion size separated by *A. alternata* and *A. solani* group.

In wounding treatment, the symptoms were nearly round or oval spots measuring 5.6-6.4 × 4.7-7.5 mm at 1 week after inoculation. The spot was initially water soaked, then turns yellow-brown, dark at the edges and bright in the center. Spots were concave and bold bordered on both upper and lower surfaces. Around the spot appeared a yellow halo. The *Alternaria* conidia can be observed on the leaf surface, especially the under leaf surface (**Figure 3.5 b-c**). As the disease progresses, the spot lesions may spread and turn into a blight symptom, the tissues tearing (**Figure 3.5 d**). The leaves of control treatment only show a brown dot at the inoculated sterile water site. This is just dead tissues of the leaf by the needle wound (**Figure 3.5 a**).

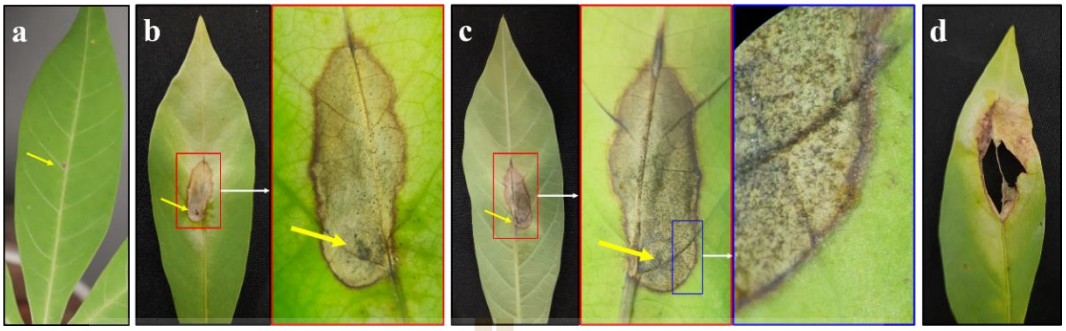

Figure 3.5 The symptoms of *A. alternata* H-Vi 7 in injecting treatment of pathogenicity test. (a) control, (b) spot lesion on upper leaves surface, (c) spot lesion on under leaves surface, (d) blight symptom. *Note*: The yellow arrow was injected needle position.

In spraying treatment, the fungi usually attacked the leaf margins and caused dark brown, water-soaked lesions at 4-5 days after inoculation (**Figure 3.6 b**). After 3-7 days, the symptom could be small round, brown spots, yellow halos or larger spots similar to the spot symptom of wounding treatment (**Figure 3.6 c**). Spots that were close together could coalesce to form a blight area at the leaf edge or tip. *Alternaria* conidia could also be seen on the surface of old diseased tissues as dusty black dots (**Figure 3.6 d-f**). When the disease was severe, the spots might tear or the entire leaf lobe might become blight symptoms (**Figure 3.6 g**). The leaves of control treatment showed no disease symptoms (**Figure 3.6 a**). The *A. alternata* in disease tissues was detected by observing conidia under light microscope and also re-isolated with the similar colony in potato dextrose agar medium.

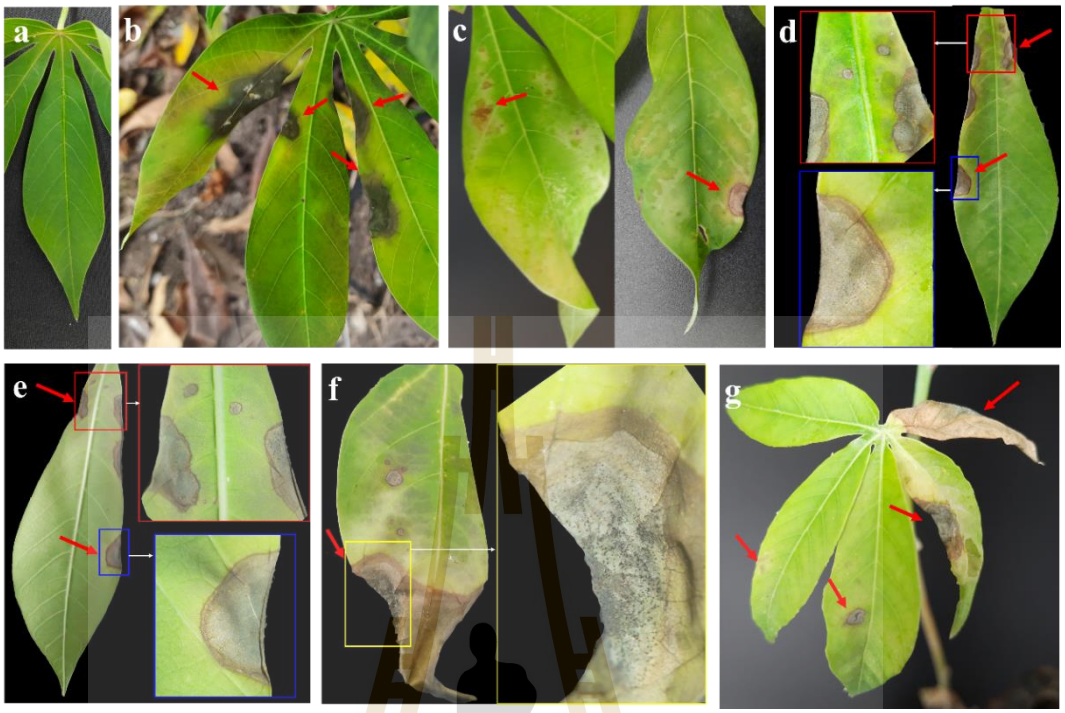

Figure 3.6 The symptoms of *A. alternata* H-Vi 7 in spraying treatment of pathogenicity test were indicated by red arrow. (a) control, (b) water-soaked lesion, (c) small and typical spot lesion, (d) spot lesion links to blight symptom formation on upper leaves surface, (e) spot lesion links to blight symptom formation on under leaves surface, (f) blight symptom with dark conidia on surface, (g) overview spot and blight symptom on cassava leaves.

3.3.4 Biochemical component in cassava leaf spot tissues by SR-FTIR

The SR-FTIR was applied to determine the changes on biochemical components in the epidermis and mesophyll tissues of cassava leaves infected *A. alternata* H-Vi 7 and control one without inoculation. The main bands related with lipids, proteins, lignins, polysaccharides occurred differently. The chemical mapping of cassava leaf cross-section was generated from the HCA of peaks obtained from SR-FTIR. That is used to classify the spectra according to the epidermis or mesophyll tissues of the control (**Figure 3.7 a-c**) and *A. alternata* H-Vi 7 infected one (**Figure 3.7**

d-f). The PCA is a multivariate model to visualize clustering spectra and identify variables spectra between control and *A. alternata* H-Vi 7 infected one. In epidermis tissues, the PC1 and PC2 loadings were explained by 22 and 10%, respectively (**Figure 3.8 a**). Similarly, in mesophyll tissues, the PC1 and PC2 loadings were 56 and 11%, respectively (**Figure 3.8 b**). Overall, the PCA score plot in mesophyll tissue (67%) was clearer than in epidermis tissues (32%). Loading plots were used to highlight biochemical contributions of cassava tissues, to define the spectral band variability associated with the second derivative of average spectra, and to analyze the score plot. The high positive loadings at 2946, 1735, 1733, 1471, 1469, 1342, 1278, 1276, 1143, 1112, 1058, 946 cm^{-1} were corresponded to the negative score plot of variable PC1 of *A. alternata* infected in epidermis and mesophyll tissues. Similarly, the high negative loadings at 2925, 1652, 1606, 1540, 1513, 1444, 1201, 1130, 1033, 993 cm^{-1} corresponded to the positive score plot of the variable PC1 of the control (**Figure 3.9**). The change in score of the second derivative average of 3000-2800 and 1800-900 cm^{-1} regions showed changes in components when the cassava tissues were attacked by *A. alternata* (**Figure 3.10** and **3.11**). The 3000-2800 cm^{-1} region corresponds to C-H asymmetric and symmetric stretching vibration of lipid group. The peak at 2946 cm^{-1} was higher than in *A. alternata* infected tissues, while the peaks at 2925 and 2917 cm^{-1} were on the opposite. The 1740-1700 cm^{-1} region corresponding to C=O esters showed that the peak of 1735 cm^{-1} was higher than in *A. alternata* infected tissues. In the wavelength of 1700-1500 cm^{-1}, the amide I (1654, 1652, 1608, 1606 cm^{-1}), amide II of proteins, phenolic group (1542, 1540 cm^{-1}), and C=C aromatic ring of lignins (1513 cm^{-1}) were decreased in *A. alternata* infected tissues. In the wavelength of 1470-1338 cm^{-1}, the peaks (1446, 1442, 1373, 1349 cm^{-1}) corresponding to C-H bending from CH_2 and CH_3 of mainly lipid and lignin were also lower in *A. alternata* infected tissues, except for the peak at 1342 cm^{-1} in mesophyll which was on the opposite. The wavelength of 1300-900 cm^{-1} is a major C-O-C region of polysaccharides but is very complex, which can be celluloses, hemicelluloses, pectins or carbohydrates. The peaks at 1203, 1201 cm^{-1} accounted for higher in control tissues while the peaks at

1147, 1143, 1112, 1110 cm^{-1} were on the opposite. For hemicellulose group, the peak at 1278 cm^{-1} was higher than in *A. alternata* infected tissues. The peak 1238 cm^{-1} was similar but only present in mesophyll tissues. For the carbohydrate group (C-O stretching vibration), the peaks at 1037, 1029, 993 cm^{-1} presented higher in control tissues while the peak at 950 cm^{-1} was opposite but only in the epidermis tissues (**Table 3.3**).

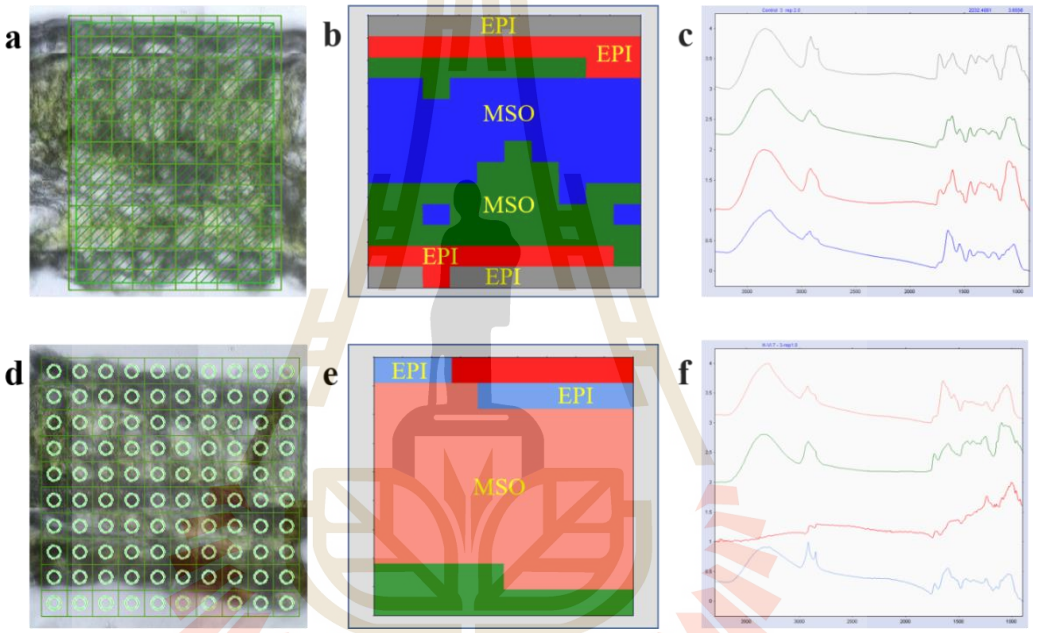

Figure 3.7 SR-FTIR transverse section, mapping, 2D Hierarchical cluster analysis mapping of control leaf (a, b, c) and *A. alternata* H-Vi 7 infected leaf (d, e, f). The area map was set 10x13 µm for control sample and 10x10 µm for *A. alternata* H-Vi 7 infected sample. *Note*: EPI: epidermis tissues; MSO: mesophyll tissues.

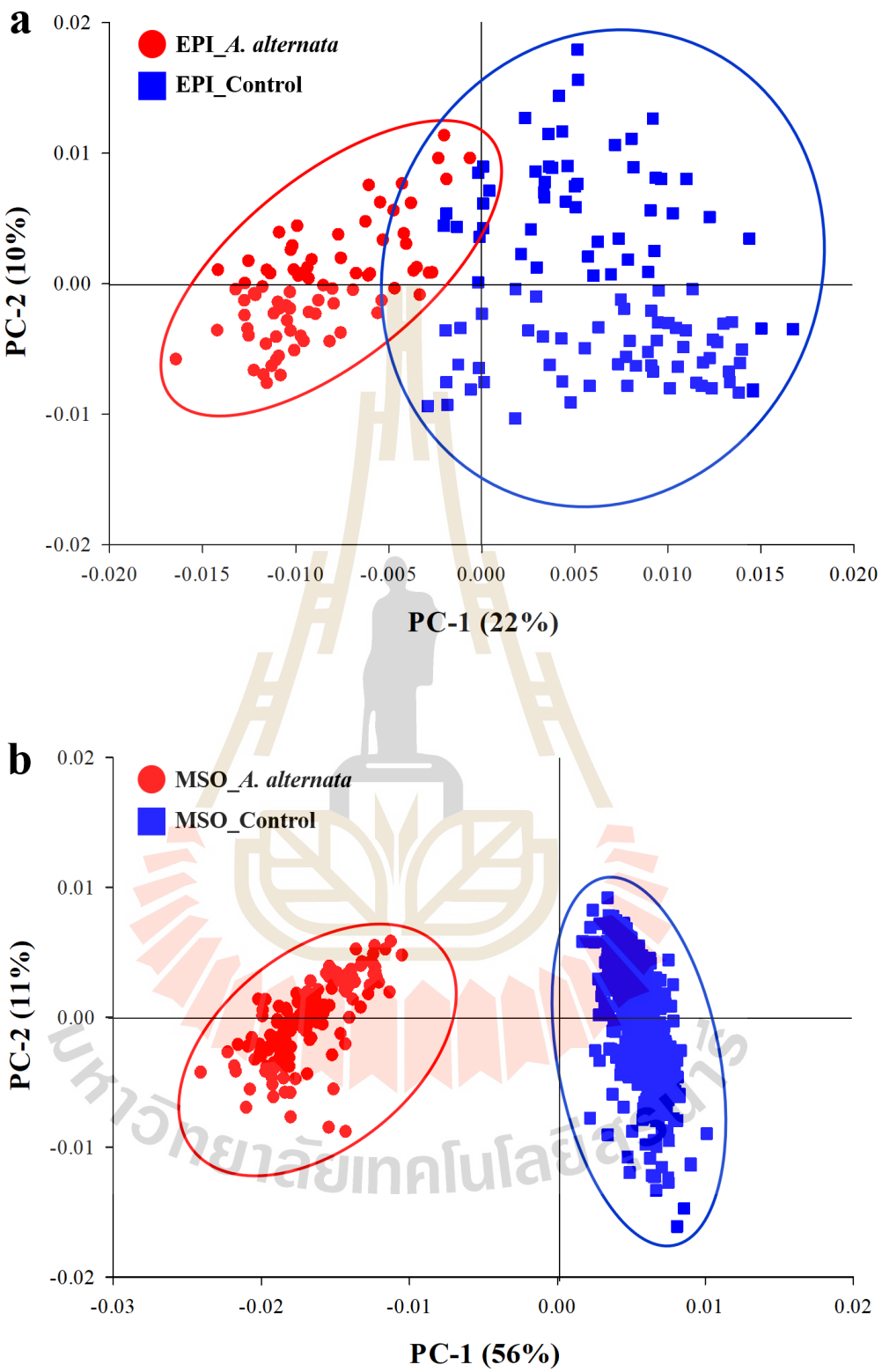

Figure 3.8 PCA analysis of the epidermis (a) and mesophyll (b) of cassava infected by *A. alternata* H-Vi 7 and control. *Note*: EPI: epidermis tissues; MSO: mesophyll tissues.

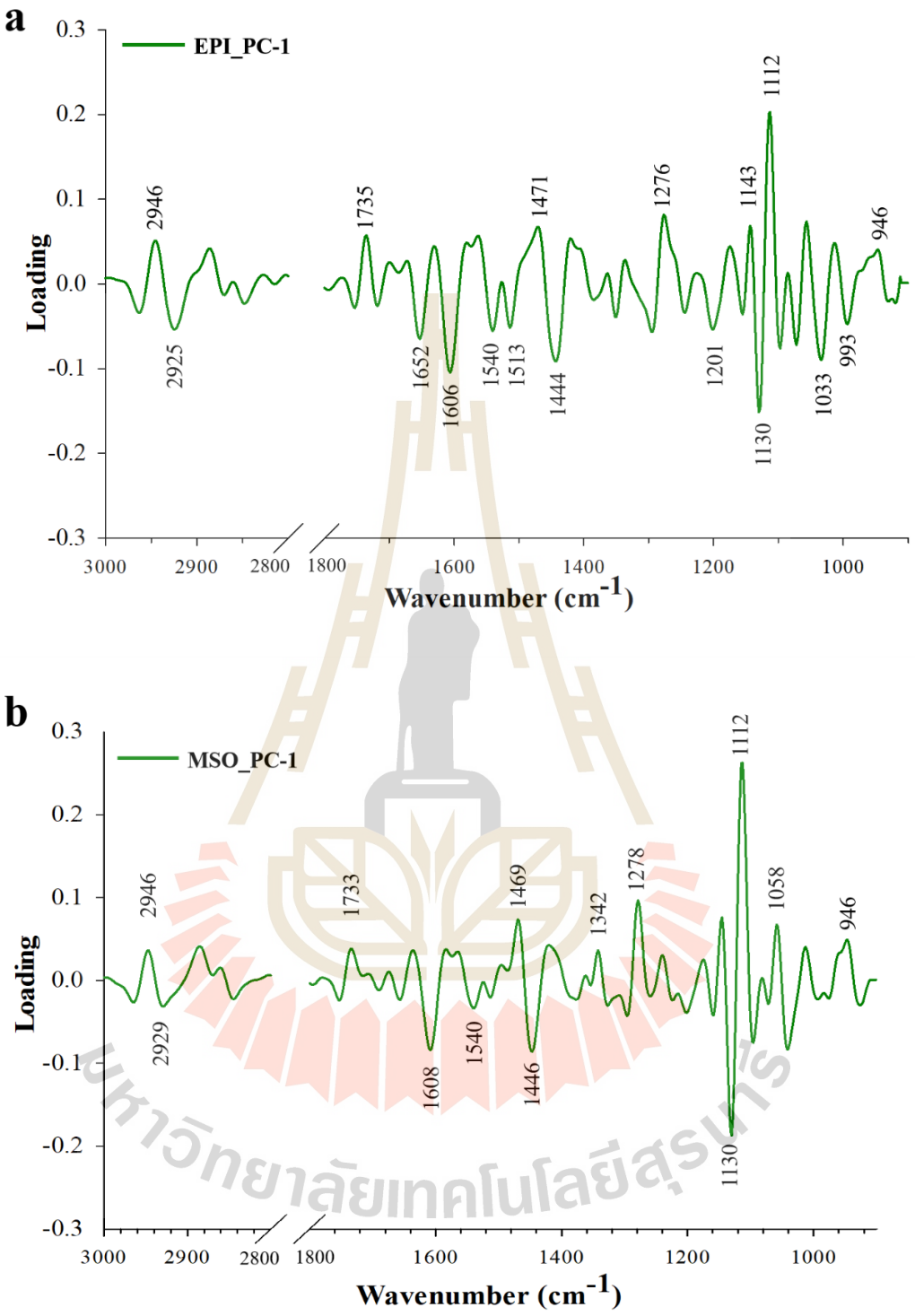

Figure 3.9 PC1 loading plot from PCA analysis of the epidermis (a) and mesophyll (b) of cassava infected by *A. alternata* H-Vi 7 and control. *Note*: EPI: epidermis tissues; MSO: mesophyll tissues.

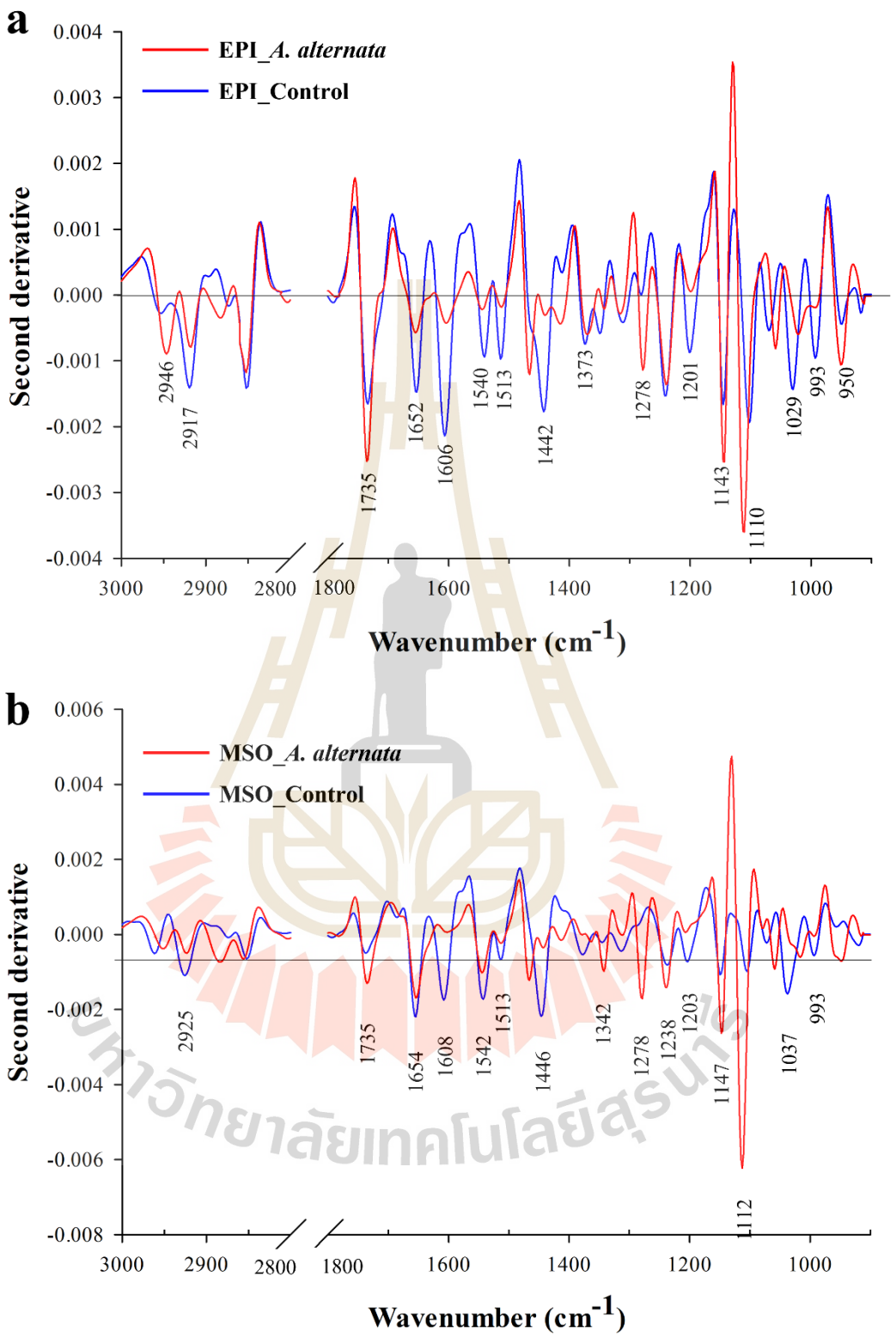

Figure 3.10 Representative second derivative average spectrum of the epidermis (a) and mesophyll (b) in cassava infected by *A. alternata* H-Vi 7 and control. *Note*: EPI: epidermis tissues; MSO: mesophyll tissues.

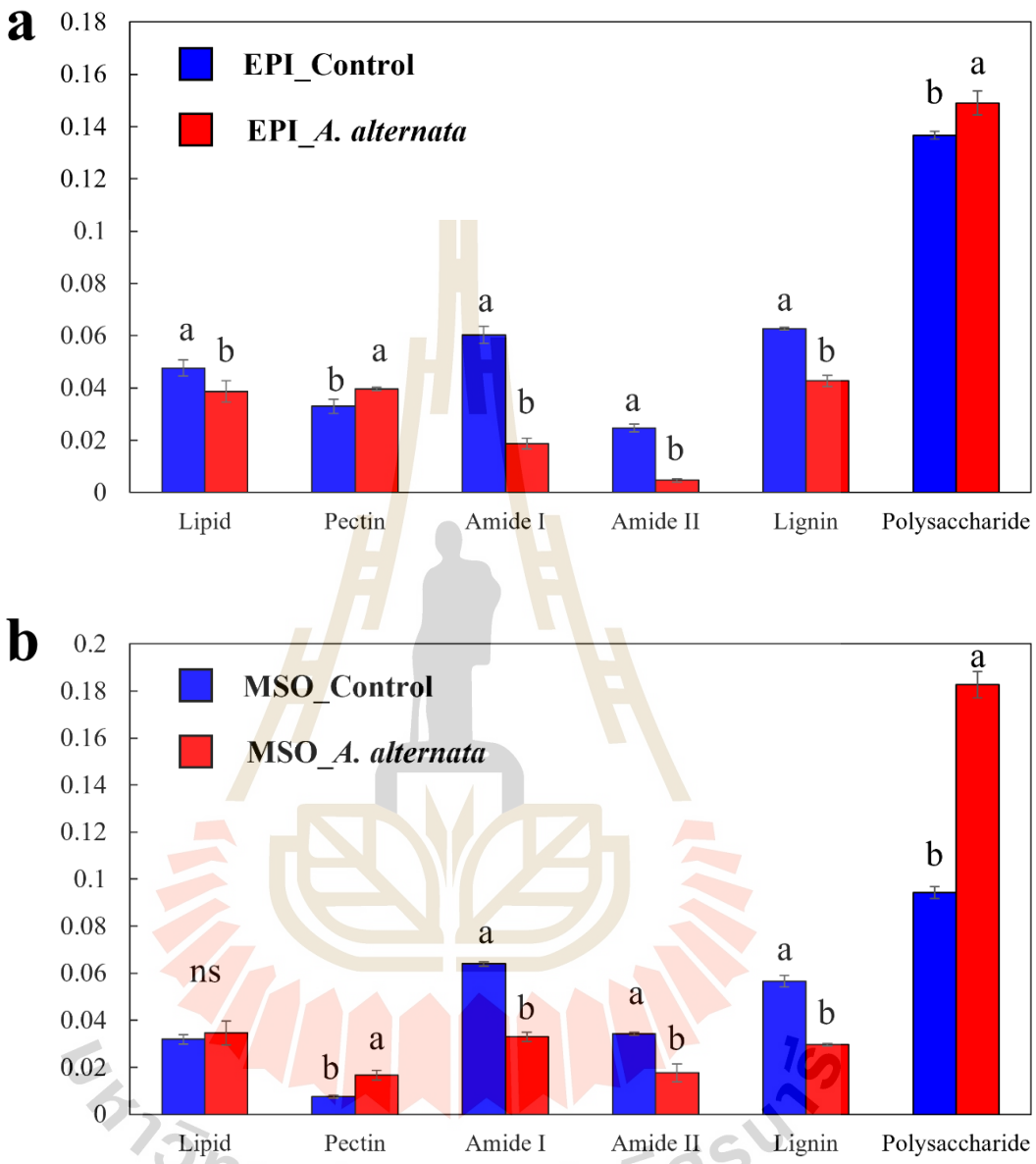

Figure 3.11 Integral areas of absorbance between 3000 and 900 cm^{-1} of the epidermis (a) and mesophyll (b) in cassava infected by *A. alternata* H-Vi 7 and control. *Note*: EPI: epidermis tissues; MSO: mesophyll tissues.

Table 3.3 The IR band assignment for plant tissue

Spectral ranges (cm^{-1})	Function group and components	Peaks on this research	References
3000-2800	C–H asymmetric and symmetric stretching vibration of mainly lipid groups with the little contribution of proteins	2946, 2925, 2917, 2882	Thepbandit *et al*., 2021; Le Thanh *et al*., 2017; Puttaso *et al*., 2020
1740-1700	Stretching vibration of C=O ester of bond lipids, lignins, pectins, or their esters		Le Thanh *et al*., 2017; Sangpueak *et al*., 2021; Thumanu *et al*., 2017
1740, 1738	C=O stretching of carbonyl/ alkyl ester compound of pectins		Lahlali *et al*., 2017; Wang et al., 2012
1737, 1730	C=O esters of lignins, and hemicelluloses/pectins	1735	Puttaso *et al*., 2020; Thumanu *et al*., 2017
1700-1600	C=O stretch (80%), C–N stretch (10%), N–H bending (10%) of Amide I of proteins	1654, 1652, 1608, 1606	Lahlali *et al*., 2017; Sangpueak *et al*., 2021; Le Thanh *et al*., 2017; Puttaso *et al*., 2020
1600-1500	N–H bend (60%), C–N stretch (40%) of Amide II of proteins		Sangpueak *et al*., 2021; Le Thanh *et al*., 2017
1580-1530	Phenolic group	1542, 1540	Lahlali *et al*., 2017
1525-1505	C=C aromatic ring of lignins	1513	Lahlali *et al*., 2017; Sangpueak *et al*., 2021; Thumanu *et al*., 2017; Puttaso *et al*., 2020; Skenderidis *et al*., 2019

Table 3.3 The IR band assignment for plant tissue (**continued**).

Spectral ranges (cm^{-1})	Function group and components	Peaks on this research	References
1470-1338	C–H bending from CH_2 and CH_3 of mainly lipids and lignins	1446, 1442, 1373, 1342	Le Thanh *et al.*, 2017; Sangpueak *et al.*, 2021
1300-900	Mainly C–O–C of polysaccharides; very complex and depends upon contributions from polysaccharides, celluloses, hemicelluloses, and pectins	1203, 1201, 1147, 1143, 1112, 1110	Sangpueak *et al.*, 2021; Le Thanh *et al.*, 2017; Thepbandit *et al.*, 2021; Thumanu *et al.*, 2017
1300-1200	C–C, C–O skeletal or C–O–C of hemicelluloses and lignins		Le Thanh *et al.*, 2017; Thumanu *et al.*, 2017
1275-1215	Hemicellulose group	1278, 1238	Lahlali *et al.*, 2017
1278, 1241	Hemicellulose group		Puttaso *et al.*, 2020
1105, 1103	C–O–C glycoside ether mainly hemicellulose		Le Thanh *et al.*, 2017; Thumanu *et al.*, 2015
1155	C–C ring celluloses		Le Thanh *et al.*, 2017; Thumanu *et al.*, 2015
1151	C–O–C asymmetric stretching, PO_2 stretching of celluloses		Lahlali *et al.*, 2017
1090-1043	Cellulose group		Lahlali *et al.*, 2017
1061	C–O–C asymmetric stretching of celluloses		Lahlali *et al.*, 2017

Table 3.3 The IR band assignment for plant tissue (**continued**).

Spectral ranges (cm^{-1})	Function group and components	Peaks on this research	References
1180-950	C–O stretching vibrations of carbohydrates	1037, 1029, 993, 950	Yu, 2005
1000-800	Vibration of the pyranose ring of Glucose, galactose and mannose		Lammers *et al*., 2009
1016, 991, 912	D-(+)-Glucose		Liu *et al*., 2021
1039, 990, 971, 953	D-(+)-Galactose		Liu *et al*., 2021
1034, 1016, 966, 949	D-(+)-Mannose		Liu *et al*., 2021
1050, 991, 940	D-(–)-Arabinose		Liu *et al*., 2021

3.4 Discussion

The results in the research showed that *Alternaria* was associated with leaf spot disease on cassava in Thailand. This is a genus of fungi that cause diseases on many kinds of plants. In the research of Meena *et al*. (2017), 48 isolates of *Alternaria* spp. isolated from tomato, brinjal, mustard, potato, cauliflower, pea, cabbage, spinach, onion, cicer, eichhornia, lantana, parthenium could cause black sunken necrotic lesions with many crops and were most infecting to tomato. The high pathogenic group accounted for 27.08% isolates, while moderate and less pathogenic ones were 35.41 and 37.5%, respectively. In our research, the most and highly virulent fungal isolate caused rot lesions with sizes 28.35-32.72 × 25.70-29.70 and 26.86-30.57 × 19.20-24.05 mm, accounting for 30.4 and 34.8%, respectively (**Figure 3.1 and 3.2**). The morphological characteristics of the fungi are diverse. The conidia are yellow-brown when young and brown when mature, oval or ellipsoidal, one end tapering to the other. And the transversal septa and at least one longitudinal septa in conidia of all

fungal isolates have been shown to belong to the *Alternaria* genus (Mmbaga *et al*., 2011; Siciliano *et al*., 2017; Basim *et al*., 2018). Combination with molecular sequencing ITS region identified the fungi were *A. alternata* and *A. solani* with 14 and 9 fungal isolates, respectively (**Table 3.2**). The morphological character of the two species is also complex. The colony of *A. alternata* belongs to group 1 and 3. While *A. solani* belongs to group 2 and 4, except isolates HC-186 and NH-23 belong to group 1 (**Figure 3.3**). Studies by Mmbaga *et al*. (2011), Basim *et al*. (2018), Elfar *et al*. (2018), and Aloi *et al*. (2021) also showed that the colony of *Alternaria* or *A. alternata* was complex in color and form. The *A. altenata* could cause more damaging than the *A. solani* isolates (**Figure 3.4**). In the research of Zheng *et al*. (2015), *A. alternata, A. solani* and *A. tenuissima* accounted for 18.6, 5.9 and 75.5% of the total 511 fungal isolates from potato foliar diseases in China. The fungal isolates also caused rot lesions with yellow halo but virulent was not significantly different between species. *A. alternata* caused small dark brown spots, which enlarged and coalesced to blight symptom on leaves and also sporadic necrotic lesions on petiole carob in Turkey (Basim *et al*., 2018). In the wild, the species composition of *Alternaria* is also complex. The *Alternaria* spp. (6 species) caused brown necrotic with concentric ring on detached leaves and moldy core on fruits of apple in Chile (Elfar *et al*., 2018). And 5 species of this genus caused leaf spot disease on cabbage, cauliflower, and rocket in Italy (Siciliano *et al*., 2017). Overall, these studies also agree that *A. alternata* could cause necrotic spots on leaves, which could expand to blight symptom with surrounding yellow halo. This is similar to the symptoms of *A. alternata* H-Vi 7 on cassava leaves in this research (**Figure 3.5 and 3.6**). Previously, the leaf spot disease on cassava has also been reported but is very complex. Brown leaf spot, white leaf spot, and diffuse or blight leaf spot are three types of spot symptom that have been reported. The commonly known agents are fungi of *Cercospora* (*Mycosphaerella*) and *Passalora* genus (Teri *et al*., 1980; Ayesu-Offei and Antwi-Boasiako, 1996; Prabakar and Raguchander, 2000; Pei *et al*., 2014; Reddy, 2015; de Freitas *et al*., 2017; McCallum *et al*., 2017). In 2018, Ng'ang'a *et al*. reported for the first time that *Alternaria*, *Colletotrichum*, *Cladosporium* caused brown

leaf spot disease on cassava in Kenya. In 2020, Hidayat *et al*. and Julião *et al*. recorded that *C. henningsii* caused this disease in Indonesia and Brazil, respectively. The present research is the first to document the damaging effects of *A. alternata* and *A. solani* on cassava in Thailand.

Each plant species possesses an innate defense system (structure and inductive immune) to protect themselves against biotic and abiotic stresses that various resistance level depending on the cultivar and stress factors (VanLoon *et al*., 2006; Corwin and Kliebenstein, 2017). The pathogens attacking plant produce elicitors and effectors such as peptides, metabolites, cell wall component (β-1,3-glucan, chitin), enzymes, toxins that were recognized by receptors on host plasma membrane. Then, the downstream regulatory was induced including signal generation and transmission to the nucleus by MAP kinase cascade and transcription factors. Here, physical and biochemical defense responses were active including reactive oxygen species production, callose deposition, programmed cell death, and camalexin production, defense related enzymes (β-1,3-glucanase, phenylalanine ammonia lyase, peroxidase, chitinase, chitosanase, polyphenol oxidase), phytoalexins, functional reinforcement of cell walls against the pathogens. The disease symptoms or hypersensitive response is the result of this interaction (Piasecka *et al*., 2015; Kushalappa *et al*., 2016; Appu *et al*., 2021).

In both wounding and spraying treatments, the *A. alternata* H-Vi 7 caused spots and blight necrotic lesions on cassava leaves. Symptoms vary in size but form similar including brown with dark brown rims, yellow halos, and dusty black dots as fungal conidia (**Figure 3.5 and 3.6**). Previously, both *Alternaria* spp. and *A. alternata* have been known to cause black sunken necrotic on tomato, mustard, brinjal and potato. Furthermore, these isolates were able to produce tenuazonic acid, alternariol, alternariol monomethyl ether and they were also able to induce symptoms similar to *Alternaria* fungi but to a lesser extent. Tenuazonic acid is produced by 75.0% of the total isolates, which is lower in alternariol (81.25%) and alternariol monomethyl ether

(95.83%) but causes a larger (more severe) necrotic area (Meena *et al*., 2017). In addition, *A. arborescens* and *A. alternata* have also been associated with symptoms of dark-red discoloration, soft to dry rot, wrinkling of the peel of pomegranate fruits and sporulating dark brown internal rots. All 42 *Alternaria* isolates produced tenuazonic acid and most of them secreted alternariol, alternariol monomethyl ether, altenuene or tentoxin (Aloi *et al*., 2021). The research of Mmbaga *et al*. (2011) also showed the cell-free culture of *A. alternata* induced wilting and necrotic lesions on lilac. During infection, *Alternaria* spp. produced primary and secondary metabolites with more than 70 mycotoxins including host specific (AK-, AF-, AC-toxin, ect.) and non-host specific that cause negative effects on chloroplast, mitochondria, plasma membrane, nucleus and Golgi bodies. The non-host specific mycotoxins such as tenuazonic acid, alternariol, alternariol monomethyl ether, tentoxin, altertoxins (ATX-I, -II and -III) and altenuene are more commonly produced by many *Alternaria* species with multiple hosts (Meena *et al*., 2017; Meena and Samal, 2019). The *Alternaria* toxin could perturb the sphingolipid (essential components in membrane) biosynthesis pathway, leading to necrotic cell death. Specifically, AAL toxin (*A. alternata* f.sp. *lycopersici*) – a sphinganine-analogous mycotoxin, could inhibite sphinganine N-acyltransferase, leading to accumulate 3-ketosphinganine and sphinganine, which causes susceptible tomato cell death (Takahashi *et al*., 2009). The production of this mycotoxin depends on many factors, notably water activity and temperature (Lee *et al*., 2015; Siciliano *et al*., 2017). At high a_w level (0.954), *A. alternata* isolated from tomato fruit blackmould lesions showed maximum production of alternariol (21°C), tenuazonic acid (21°C) and alternariol monomethyl ether (35°C) (Pose *et al*., 2010).

Necrotic and yellow-blight formation is the result of altered biochemical reactions when the plant host interacts with *Alternaria* fungi (**Figure 3.12**). The research of Meena *et al*. (2016) showed that *A. alternata* infecting tomato plant could induce a series of physical and biochemical changes, including an increase of H_2O_2 content (22 folds), lipid peroxidation (15.8 folds), enzyme activity of superoxide dismutase (5.9

folds), of catalase (23.0 folds), of peroxidase (13.1 folds), of glutathione reductase (33.4 folds) and a decrease of chlorophyll (42.88%) when compared with the heathy plants. The tenuazonic acid, alternariol, and alternariol monomethyl ether mycotoxin treatments also induced physical and biochemical changes in tomato plants similar to but weaker than *A. alternata* inoculation. The cellular damages were observed as increased malondialdehyde content and reduced chlorophylls that causes yellowing halo symptoms on leaves. Similarly, *A. alternata* infected chilli plants also increased abscisic acid, 6 amino acids (proline, glutamic acid, serine, arginine, glycine, lysine), soluble proteins, H_2O_2, lipid peroxidation, enzymes activity (superoxide dismutase, peroxidase, polyphenol oxidase), antioxidants (flavonoid, 2,2-diphenyl-1-picrylhydrazyl, total phenol), defense related proteins including *Capsicum annuum* ANTIMICROBIAL PROTEIN1 (*CaAMP1*), *Capsicum annuum* defensin protein precursor (*CADEF1*), *Capsicum annuum* pathogenesis-related protein 1 (*CaPR1*) and decrease chlorophylls, carotenoids, sugar content (Kazerooni *et al*., 2021). Interesting, alpha-D-galactoside, D-mannitol, D-erythropentitol, glycine, hexadecenoic acid, cinnamic acid, salicylic acid in groundnut resistance genotypes were found to be higher than susceptible ones when the plants were attacked by *A. alternata*. Myo-inositol, glucose, and fructose decreased in resistance genotypes but increased in susceptible ones. On the other hand, arabinofuranose, cinnamic acid, 2-butendioic acid, and linoleic acid were observed only in resistant genotypes. These results suggested that resistant genotypes had higher levels of cell wall synthesis and rigidity related compounds (Arabinofuranose) along with phenylropanoids (cinnamic, coumaric caffeic and salicylic acid) that may restrict pathogen entry (Mahatma *et al*., 2019). Similarly, when *Alternaria brassicicola* infected Brassicaceae and mustard plants also increased redox enzymes activity (superoxide dismutase, catalase, peroxidase, superoxide dismutase, peroxidase, phenylalanine ammonia lyase, polyphenol oxidase), total soluble proteins, abscisic acid, total phenol, proline, total amino acid, and decrease chlorophylls, carotenoids, total sugar, and relative water content. The magnitude of increase or decrease in resistance genotypes was greater than moderate or susceptible ones (Mallick *et al*.,

2015; Munir *et al*., 2020). Fungal infection caused denaturation and proteolysis leaf to enhancement of free amino acid content of host tissues (Meena *et al*., 2010).

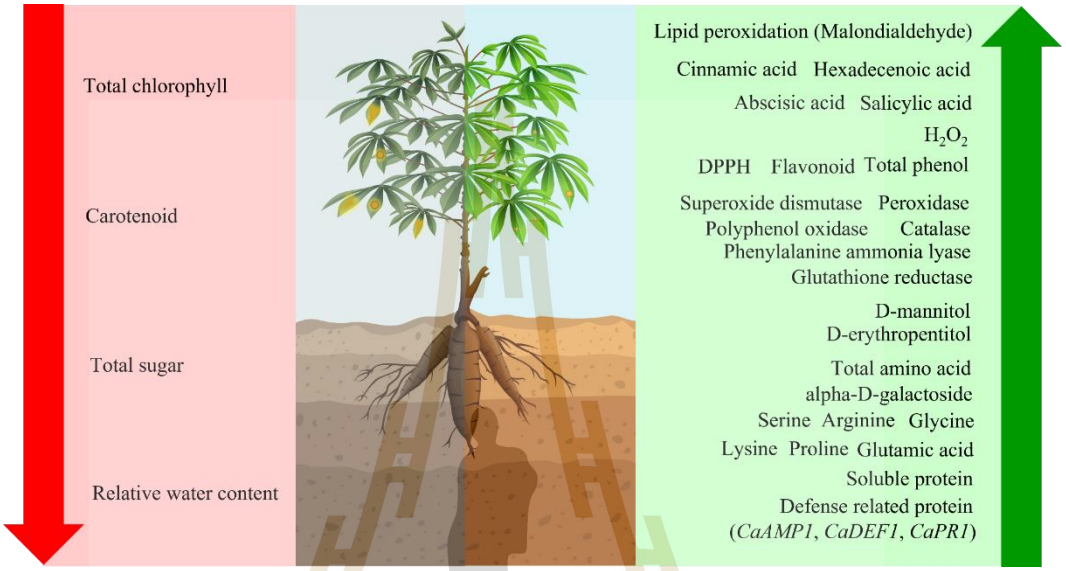

Figure 3.12 The change biochemical in *Alternaria* infected tissue plants (tomato, mustard, Brassicaceae germplasm, chilli, groundnut) compared with control that summarized from researches of Mallick et al. (2015), Meena et al. (2016), Mahatma et al. (2019) Munir et al. (2020), Kazerooni et al. (2021). The green (right) indicated increase. The red (left) indicated decrease.

These researches indicated that when being attacked, the plant could generate biochemical process to fight pathogens or *A. alternata*. Reactions are strong at first and weaken later – when energy is depleted. As the results, symptoms are the result of failure or "not being strong enough" in fighting the infection of pathogen. In this research, the tissues were collected at pre-symptom – that is, the fungi infected. The results of SR-FTIR analysis showed changes in lipids, proteins, lignins, and polysaccharide components in *A. alternata* infected tissues. The PC1 analysis showed

a difference of 22 and 56% between control and *A. alternata* infected tissues in epidermis and mesophyll, respectively. This may be due to the aggressive behavior of this fungi species, which firstly gets inside and secrete mycotoxins. Lipids are the main components of cell membranes, having the ability to store energy, protection communication, and structural support (Thepbandit *et al*., 2021). The lipids (C-H asymmetric and symmetric stretching) reduced in *A. alternata* infected tissues that may be due to the energizing immunity process. Similarly, most of the amide I, amide II of proteins, phenolics, lignins, carbohydrates were also reduced in *A. alternata* infected tissues. In plant innate immunity, the phenylalanine – an amino acid (amide) is a precursor of the phenylpropanoids, lignins in the phenylalanine ammonia lyase enzyme pathway (Lahlali *et al*., 2017; Thepbandit *et al*., 2021). When *A. alternata* attacks a plant, the phenylalanine ammonia lyase is induced (Mallick *et al*., 2015). That has a role to resist the attack of pathogens as physical barriers and biochemical processes. The peaks of 1735 cm^{-1} (C=O ester correspond to lignins, hemicelluloses, pectins), 1342 cm^{-1} (C–H bending from CH_2 and CH_3 of mainly lipids and lignins) increased in *A. alternata* infected tissues. This may be due to the formation of lignins from precursors of amino acids (proteins). Interestingly, the peaks (1147, 1143, 1112, 1110, 1278, 1238 cm^{-1}) related COC of polysaccharides including hemicelluloses, celluloses, pectins that is the major constituent in primary plant cell walls, and is increased in *A alternata* infected tissues. These components can be modified to make plant cells thicker and stronger, and play a crutial role in preventing pathogen infection (Malinovsky *et al*., 2014; Wan *et al*., 2021). On the other hand, the peaks of 1037, 1029, 993 cm^{-1} of carbohydrate group related sugar decreased in *A. alternata* infected tissues. This is also consistent with previous reports of *A. alternata* attacking plants where sugar provides energy for plant innate defense. And the reduced sugar is also the result of impaired photosynthesis as chlorophyll and carotenoids which are destroyed by mycotoxins (Mallick *et al*., 2015; Meena *et al*., 2016; Munir *et al*., 2020; Kazerooni *et al*., 2021). The changes in biochemical composition in the epidermis and mesophyll identified by SR-FTIR partly explained the infection of *A. alternata* with

cassava leaves. Previously, (Thumanu *et al*., 2015; Thumanu *et al*., 2017) used this technique to determine the promotion of plant growth treated by *Bacillus subtilis* or induced systemic resistance in cassava co-inoculated by *B. subtilis* and *Colectotrichum gloeosporioides* related with accumulation of pectin in cell walls.

3.5 Conclusion

In conclusion, *A. alternara* and *A. solani* were identified to be associated with leaf spot disease on cassava in Thailand. *A. alternata* was more common and damaging than *A. solani*. The *A. alternata* caused necrotic spot lesions and blight symptoms on cassava leaves. The *A. alternata* infection caused biochemical changes in the epidermis and mesophyll tissues including an increase in pectins, polysaccharides, celluloses, hemicelluloses and decrease in lipids, proteins, phenolics, lignins, carbohydrate component.

3.1 Reference

Abdulai, M., Basım, H., Basım, E., Baki, D., & Öztürk, N. (2018). Detection of *Xanthomonas axonopodis* pv. *manihotis*, the causal agent of cassava bacterial blight diseases in cassava (*Manihot esculenta*) in Ghana by polymerase chain reaction. *European Journal of Plant Pathology*, 150(2): 471-484. doi:10.1007/s10658-017-1297-3.

Agrios, G. (2005). *Plant Pathology* (5th ed). New York: Academic Press.

Aloi, F., Riolo, M., Sanzani, S. M., Mincuzzi, A., Ippolito, A., Siciliano, I., Pane, A., Gullino, M. L., & Cacciola, S. O. (2021). Characterization of *Alternaria* Species Associated with Heart Rot of Pomegranate Fruit. *Journal of Fungi*, 7(3): p.172. doi:10.3390/jof7030172.

Andersen, B., Hansen, M. E., & Smedsgaard, J. (2005). Automated and unbiased image analyses as tools in phenotypic classification of small-spored *Alternaria* spp. *Phytopathology*, 95(9): 1021-1029. doi:10.1094/PHYTO-95-1021.

Appu, M., Ramalingam, P., Sathiyanarayanan, A., & Huang, J. (2021). An overview of plant defense-related enzymes responses to biotic stresses. *Plant Gene*, 27 (2021): 100302. doi:10.1016/j.plgene.2021.100302.

Ayesu-Offei, E. N., & Antwi-Boasiako, C. (1996). Production of microconidia by *Cercospora henningsii* Allesch, cause of brown leaf spot of cassava (*Manihot esculenta* Crantz) and tree cassava (*Manihot glaziovii* Muell.-Arg.). *Annals of Botany*, 78(5): 653-657. doi:10.1006/anbo.1996.0173.

Babicki, S., Arndt, D., Marcu, A., Liang, Y., Grant, J. R., Maciejewski, A., & Wishart, D. S. (2016). Heatmapper: web-enabled heat mapping for all. *Nucleic Acids Research*, 44(Web Server issue): W147-W153. doi:10.1093/nar/gkw419.

Balagopalan, C., (2002). Cassava utilization in food, feed and industry. In Hillocks, R. J., Thresh, J. M. & Bellotti, A. (Eds.). *Cassava: Biology, Production and Utilization* (1st ed, pp. 301-318). Cali, Colombia: CABI.

Barnett, H. L., & Hunter, B. B. (1987). *Illustrated Genera of Imperfect Fungi* (1st ed). New York: Macmillan Publishing Co., and London: Collier Macmillan.

Basım, H., Basım, E., Baki, D., Abdulai, M., Öztürk, N., & Balkic, R. (2018). Identification and characterization of *Alternaria alternata* (Fr.) Keissler causing Ceratonia Blight disease of carob (*Ceratonia siliqua* L.) in Turkey. *European Journal of Plant Pathology*, 151(1): 73-86. doi:10.1007/s10658-017-1354-y.

Burgess, L. W., Phan, H. T., Knight, T. E., & Tesoriero, L. (2008). *Diagnostic Manual for Plant Diseases in Vietnam* (1st ed). Canberra: Australian Centre for International Agricultural Research (ACIAR).

Corwin, J. A., & Kliebenstein, D. J. (2017). Quantitative resistance: more than just perception of a pathogen. *The Plant Cell*, 29(4): 655-665. doi:10.1105/tpc.16.00915.

Davis, N. D., Diener, U. L., & Morgan-Jones, G. (1977). Tenuazonic acid production by *Alternaria alternata* and *Alternaria tenuissima* isolated from cotton. *Applied and Environmental Microbiology*, 34(2): 155-157.

de Freitas, J. P. X., Diniz, R. P., de Oliveira, S. A. S., da Silva Santos, V., & de Oliveira, E. J. (2017). Inbreeding depression for severity caused by leaf diseases in cassava. *Euphytica*, 213(9): 1-12. doi:10.1007/s10681-017-1995-0.

Elfar, K., Zoffoli, J. P., & Latorre, B. A. (2018). Identification and characterization of *Alternaria* species associated with moldy core of apple in Chile. *Plant Disease*, 102(11): 2158-2169. doi:10.1094/PDIS-02-18-0282-RE.

FAOSTAT, (2021a). *Crops and livestock products*. Retrieved from https://www.fao.org/faostat/en/#data/QCL

FAOSTAT, (2021b). *Countries by commodity*. Retrieved from https://www.fao.org/faostat/en/#rankings/countries_by_commodity_exports

Food and Agriculture Organization (FAO). (2013). *Save and Grow: Cassava: a guide to sustainable production intensification*. Rome: Food and Agriculture Organization of the United Nations.

Guira, F., Some, K., Kabore, D., Sawadogo-Lingani, H., Traore, Y., & Savadogo, A. (2017). Origins, production, and utilization of cassava in Burkina Faso, a contribution of a neglected crop to household food security. *Food Science & Nutrition*, 5(3): 415-423. doi:10.1002/fsn3.408.

Henry, G. & Hershey, C. (2002). Cassava in South America and the Caribbean. In Hillocks, R. J., Thresh, J. M. & Bellotti, A. (Eds.). *Cassava: Biology, Production and Utilization* (1st ed, pp. 17-40). Cali, Colombia: CABI.

Hidayat, I., Hastuty, A., & Ramadhani, I. (2020). A molecular phylogenetic study of *Clarohilum henningsii* (Mycosphaerellaceae, Fungi) on cassava from Indonesia based on the ITS rDNA sequence. *Journal of Microbial Systematics and Biotechnology*, 2(1): 40-45. doi:10.37604/jmsb.v2i1.43.

Iturrieta-González, I., Gené, J., Wiederhold, N., & García, D. (2020). Three new *Curvularia* species from clinical and environmental sources. *MycoKeys*, 68: 1-21. doi:10.3897/mycokeys.68.51667.

Jiang, S. J., Qiang, S., Zhu, Y. Z., & Dong, Y. F. (2008). Isolation and phytotoxicity of a metabolite from *Curvularia eragrostidis* and characterisation of its modes of action. *Annals of Applied Biology*, 152(1): 103-111. doi:10.1111/j.1744-7348.2007.00202.x.

Julião, E. C., Santana, M. D., Freitas-Lopes, R. D. L., Vieira, A. D. P., de Carvalho, J. S. B., & Lopes, U. P. (2020). Reduction of brown leaf spot and changes in the

chlorophyll a content induced by fungicides in cassava plants. *European Journal of Plant Pathology*, 157(2): 433–439. doi:10.1007/s10658-020-02001-0.

Kazerooni, E. A., Maharachchikumbura, S. S., Al-Sadi, A. M., Kang, S. M., Yun, B. W., & Lee, I. J. (2021). Biocontrol Potential of *Bacillus amyloliquefaciens* against *Botrytis pelargonii* and *Alternaria alternata* on *Capsicum annuum*. *Journal of Fungi*, 7(6): p.472. doi:10.3390/jof7060472.

Kusai, N. A., Azmi, M. M. Z., Zulkifly, S., Yusof, M. T., & Zainudin, N. A. I. M., (2016). Morphological and molecular characterization of *Curvularia* & related species associated with leaf spot disease of rice in Peninsular Malaysia. *Rendiconti Lincei*, 27(2): 205-214. doi:10.1007/s12210-015-0458-6.

Kushalappa, A. C., Yogendra, K. N., & Karre, S. (2016). Plant innate immune response: qualitative and quantitative resistance. *Critical Reviews in Plant Sciences*, 35(1): 38-55. doi:10.1080/07352689.2016.1148980.

Lahlali, R., Song, T., Chu, M., Yu, F., Kumar, S., Karunakaran, C., & Peng, G. (2017). Evaluating changes in cell-wall components associated with clubroot resistance using fourier transform infrared spectroscopy and RT-PCR. *International Journal of Molecular Sciences*, 18(10): p.2058. doi:10.3390/ ijms18102058

Lammers, K., Arbuckle-Keil, G. & Dighton, J. (2009). FT-IR study of the changes in carbohydrate chemistry of three New Jersey pine barrens leaf litters during simulated control burning. *Soil Biology and Biochemistry*, 41(2): 340-347. doi:10.1016/j.soilbio.2008.11.005.

Lasch, P., Haensch, W., Naumann, D., & Diem, M. (2004). Imaging of colorectal adenocarcinoma using FT-IR microspectroscopy and cluster analysis. *Biochimica et Biophysica Acta (BBA)-Molecular Basis of Disease*, 1688(2): 176-186. doi:10.1016/j.bbadis.2003.12.006.

Le Thanh, T., Thumanu, K., Wongkaew, S., Boonkerd, N., Teaumroong, N., Phansak, P., & Buensanteai, N. (2017). Salicylic acid-induced accumulation of biochemical components associated with resistance against *Xanthomonas oryzae* pv.

oryzae in rice. *Journal of Plant Interactions*, 12(1): 108-120. doi:10.1080/17429145.2017.1291859.

Lee, H. B., Patriarca, A., & Magan, N. (2015). *Alternaria* in food: ecophysiology, mycotoxin production and toxicology. *Mycobiology*, 43(2): 93-106. doi:10.5941/MYCO.2015.43.2.93.

Liu, X., Renard, C. M., Bureau, S., & Le Bourvellec, C. (2021). Revisiting the contribution of ATR-FTIR spectroscopy to characterize plant cell wall polysaccharides. *Carbohydrate Polymers*, 262: p.117935. doi:10.1016/j.carbpol.2021.117935.

Liyanage, S., Dassanayake, R. S., Bouyanfif, A., Rajakaruna, E., Ramalingam, L., Moustaid-Moussa, N., & Abidi, N. (2017). Optimization and validation of cryostat temperature conditions for trans-reflectance mode FTIR microspectroscopic imaging of biological tissues. *MethodsX*, 4: 118-127. doi:10.1016/j.mex.2017.01.006.

Mahatma, M. K., Thawait, L. K., Jadon, K. S., Rathod, K. J., Sodha, K. H., Bishi, S. K., Thirumalaisamy, P. P., & Golakiya, B. A. (2019). Distinguish metabolic profiles and defense enzymes in *Alternaria* leaf blight resistant and susceptible genotypes of groundnut. *Physiology and Molecular Biology of Plants*, 25(6): 1395-1405. doi:10.1007/s12298-019-00708-x.

Maizatul-Suriza, M., Seman, I. A., Madihah, A. Z., & Rusli, M. H. (2017). Detached leaf assay for *in vitro* screening of potential biocontrol agents to control goosegrass weed (*Eleusine indica*). *Journal of Oil Palm Research*, 29(4): 562-569. doi:10.21894/jopr.2017.0003.

Malinovsky, F. G., Fangel, J. U., & Willats, W. G. (2014). The role of the cell wall in plant immunity. *Frontiers in Plant Science*, 5: p.178. doi:10.3389/fpls.2014.00178.

Mallick, S. A., Kumari, P., Gupta, M., & Gupta, S. (2015). Effect of *Alternaria* blight infection on biochemical parameters, quantity and quality of oil of mustard genotypes. *Indian Journal of Plant Physiology*, 20(4): 310-316. doi:10.1007/s40502-015-0178-z.

Manamgoda, D. S., Cai, L., Bahkali, A. H., Chukeatirote, E., & Hyde, K. D. (2011). *Cochliobolus*: an overview and current status of species. *Fungal Diversity*, 51(1): 3-42. doi:10.1007/s13225-011-0139-4.

McCallum, E. J., Anjanappa, R. B., & Gruissem, W. (2017). Tackling agriculturally relevant diseases in the staple crop cassava (*Manihot esculenta*). *Current Opinion in Plant Biology*, 38: 50-58. doi:10.1016/j.pbi.2017.04.008.

Meena, M., & Samal, S. (2019). *Alternaria* host-specific (HSTs) toxins: An overview of chemical characterization, target sites, regulation and their toxic effects. *Toxicology Reports*, 6: 745-758. doi:10.1016/j.toxrep.2019.06.021.

Meena, M., Swapnil, P., & Upadhyay, R. S. (2017). Isolation, characterization and toxicological potential of *Alternaria*-mycotoxins (TeA, AOH and AME) in different *Alternaria* species from various regions of India. *Scientific Reports*, 7(1): 1-19. doi:10.1038/s41598-017-09138-9.

Meena, M., Zehra, A., Dubey, M. K., Aamir, M., Gupta, V. K., & Upadhyay, R. S. (2016). Comparative evaluation of biochemical changes in tomato (*Lycopersicon esculentum* Mill.) infected by *Alternaria alternata* and its toxic metabolites (TeA, AOH, and AME). *Frontiers in Plant Science*, 7: p.1408. doi:10.3389/fpls.2016.01408.

Meena, P. D., Awasthi, R. P., Chattopadhyay, C., Kolte, S. J., & Kumar, A. (2010). *Alternaria* blight: a chronic disease in rapeseed-mustard. *Journal of Oilseed Brassica*, 1(1): 1-11.

Minato, N., Sok, S., Chen, S., Delaquis, E., Phirun, I., Le, V. X., Burra, D. D., Newby, J. C., Wyckhuys, K. A., & de Haan, S. (2019). Surveillance for *Sri Lankan cassava mosaic virus* (SLCMV) in Cambodia and Vietnam one year after its initial detection in a single plantation in 2015. *Plos One*. 14(2): p.e0212780. doi:10.1371/journal.pone.0212780.

Mmbaga, M. T., Shi, A., & Kim, M. S. (2011). Identification of *Alternaria alternata* as a causal agent for leaf blight in Syringa species. *The Plant Pathology Journal*, 27(2): 120-127. doi:10.5423/PPJ.2011.27.2.120.

Mohammadi, A., & Bahramikia, S. (2019). Molecular identification and genetic variation of *Alternaria* species isolated from tomatoes using ITS1 sequencing and inter simple sequence repeat methods. *Current Medical Mycology*, 5(2): 1-8. doi:10.18502/cmm.5.2.1154.

Munir, S., Shahzad, A. N., & Qureshi, M. K. (2020). Acuities into tolerance mechanisms via different bioassay during *Brassicaceae-Alternaria brassicicola* interaction and its impact on yield. *Plos One*, 15(12): p.e0242545. doi:10.1371/ journal.pone.0242545.

Ng'ang, P. W., Miano, D. W., Wagacha, J. M., & Kuria, P. (2019). Identification and characterization of causative agents of brown leaf spot disease of cassava in Kenya. *Journal of Applied Biology and Biotechnology*, 7(6): 1-7. doi: 10.7324/JABB.2019.70601.

Obiazi, C. C., & Ojobor, S. A., 2013. Production challenges of cassava and prospects. *Journal of Biology, Agriculture and Healthcare*, 3(14): 31-35.

Pei, Y. L., Shi, T., Li, C. P., Liu, X. B., Cai, J. M., & Huang, G. X. (2014). Distribution and pathogen identification of cassava brown leaf spot in China. *Genetics and Molecular Research*, 13(2): 3461-3473. doi:10.4238/2014.April.30.7.

Pettitt, T. R., Wainwright, M. F., Wakeham, A. J., & White, J. G. (2011). A simple detached leaf assay provides rapid and inexpensive determination of pathogenicity of *Pythium* isolates to 'all year round'(AYR) chrysanthemum roots. *Plant Pathology*, 60(5): 946-956. doi:10.1111/j.1365-3059.2011.02451.x.

Piasecka, A., Jedrzejczak-Rey, N., & Bednarek, P. (2015). Secondary metabolites in plant innate immunity: conserved function of divergent chemicals. *New Phytologist*, 206(3): 948-964. doi:10.1111/nph.13325.

Pose, G., Patriarca, A., Kyanko, V., Pardo, A., & Pinto, V. F. (2010). Water activity and temperature effects on mycotoxin production by *Alternaria alternata* on a synthetic tomato medium. *International Journal of Food Microbiology*, 142(3): 348-353. doi:10.1016/j.ijfoodmicro.2010.07.017.

Prabakar, K., & Raguchander, T. (2000). Fungicidal control of cassava brown leaf spot caused by *Cercospora henningsii* Allescher. *Madras Agricultural Journal*, 87(7/9), 537-538.

Puttaso, P., Namanusart, W., Thumanu, K., Kamolmanit, B., Brauman, A. & Lawongsa, P. (2020). Assessing the effect of rubber (*Hevea brasiliensis* (Willd. ex A. Juss.) Muell. Arg.) leaf chemical composition on some soil properties of differently aged rubber tree plantations. *Agronomy*, 10(12): p.1871. doi:10.3390/ agronomy10121871.

Reddy, P. P. (2015). Cassava, *Manihot esculenta*. In Reddy, P. P. (Ed.). *Plant Protection in Tropical Root and Tuber Crops* (1st ed, pp. 17-81). New Delhi: Springer India.

Sangpueak, R., Phansak, P., & Buensanteai, N. (2018). Morphological and molecular identification of *Colletotrichum* species associated with cassava anthracnose in Thailand. *Journal of Phytopathology*, 166(2): 129-142. doi:10.1111/jph. 12669.

Sangpueak, R., Phansak, P., Thumanu, K., Siriwong, S., Wongkaew, S., & Buensanteai, N. (2021). Effect of salicylic acid formulations on induced plant defense against cassava anthracnose disease. *The Plant Pathology Journal*, 37(4): p.356. doi:10.5423/PPJ.OA.02.2021.0015.

Siciliano, I., Gilardi, G., Ortu, G., Gisi, U., Gullino, M. L., & Garibaldi, A. (2017). Identification and characterization of *Alternaria* species causing leaf spot on cabbage, cauliflower, wild and cultivated rocket by using molecular and morphological features and mycotoxin production. *European Journal of Plant Pathology*, 149(2): 401-413. doi:10.1007/s10658-017-1190-0.

Siriwong, S., Thepbandit, W., Hoang, N. H., Papathoti, N. K., Teeranitayatarn, K., Saardngen, T., Thumanu, K., Bhavaniramya, S., Baskaralingam, V., Le Thanh, T., & Phansak, P. (2021). Identification of a Chitooligosaccharide mechanism against bacterial leaf blight on rice by *in vitro* and *in silico* studies. *International Journal of Molecular Sciences*, 22(15): 7990. doi:10.3390/ijms22157990.

Skenderidis, P., Mitsagga, C., Giavasis, I., Petrotos, K., Lampakis, D., Leontopoulos, S., Hadjichristodoulou, C., & Tsakalof, A. (2019). The *in vitro* antimicrobial activity assessment of ultrasound assisted *Lycium barbarum* fruit extracts and pomegranate fruit peels. *Journal of Food Measurement and Characterization*, 13(3): 2017-2031. doi:10.1007/s11694-019-00123-6.

Takahashi, Y., Berberich, T., Kanzaki, H., Matsumura, H., Saitoh, H., Kusano, T. & Terauchi, R. (2009). Unraveling the roles of sphingolipids in plant innate immunity. *Plant Signaling & Behavior*, 4(6): 536-538. doi:10.4161/psb.4.6.8583.

Taoutaou, A., Socaciu, C., Pamfil, D., Fetea, F., Balazs, E., Botez, C., Adina, C. H. I. S., Briciu, D., & Briciu, A. (2010). Fourier-Transformed Infrared Spectroscopy Applied for Studying Compatible Interaction in the Pathosystem *Phytophtora infestans-Solanum tuberosum*. *Notulae Botanicae Horti Agrobotanici Cluj-Napoca*, 38(3): 69-75. doi:10.15835/nbha3834851.

Teri, J. M., Thurston, H. D., & Lozano, J. C. (1980). Effect of brown leaf spot and Cercospora leaf blight on cassava productivity. *Tropical Agriculture*, 57(3): 239-243.

Thepbandit, W., Papathoti, N. K., Daddam, J. R., Thumanu, K., Siriwong, S., Thanh, T. L., & Buensanteai, N. (2021). Identification of Salicylic Acid Mechanism against Leaf Blight Disease in *Oryza sativa* by SR-FTIR Microspectroscopic and Docking Studies. *Pathogens*, 10(6): p.652. doi:10.3390/pathogens10060652.

Thumanu, K., Sompong, M., Phansak, P., Nontapot, K., & Buensanteai, N. (2015). Use of infrared microspectroscopy to determine leaf biochemical composition of cassava in response to *Bacillus subtilis* CaSUT007. *Journal of Plant Interactions*, 10(1): 270-279. doi:10.1080/17429145.2015.1059957.

Thumanu, K., Wongchalee, D., Sompong, M., Phansak, P., Le Thanh, T., Namanusart, W., Vechklang, K., Kaewnum, S. & Buensanteai, N. (2017). Synchrotron-based FTIR microspectroscopy of chili resistance induced by *Bacillus subtilis* strain D604 against anthracnose disease. *Journal of Plant Interactions*, 12(1): 255-263. doi:10.1080/17429145.2017.1325523.

Uke, A., Hoat, T. X., Quan, M. V., Liem, N. V., Ugaki, M., & Natsuaki, K. T. (2018). First report of *Sri Lankan cassava mosaic virus* infecting cassava in Vietnam. *Plant Disease*, 102(12): 2669. doi:10.1094/PDIS-05-18-0805-PDN.

van Loon, L. C., Rep, M., & Pieterse, C. M. (2006). Significance of inducible defense-related proteins in infected plants. *Annual Review of Phytopathology*, 44: 135-162. doi:10.1146/annurev.phyto.44.070505.143425.

Wan, J., He, M., Hou, Q., Zou, L., Yang, Y., Wei, Y., & Chen, X. (2021). Cell wall associated immunity in plants. *Stress Biology*, 1(1): 1-15. doi:10.1007/s44154-021-00003-4.

Wang, J., Zhu, J., Huang, R., & Yang, Y. (2012). Investigation of cell wall composition related to stem lodging resistance in wheat (*Triticum aestivum* L.) by FTIR spectroscopy. *Plant Signaling & Behavior*, 7(7): 856-863. doi:10.4161/psb.20468.

White, T. J., Bruns, T., Lee, S. J. W. T., & Taylor, J. (1990). Amplification and direct sequencing of fungal ribosomal RNA genes for phylogenetics. In Innis, M. A., Gelfand, D. H., Sninsky, J. J., & White, T. J. (Eds). *PCR Protocols: A Guide to Methods and Applications* (1st ed, pp. 315-322). California: Academic Press.

Wight, W. D., Labuda, R., & Walton, J. D. (2013). Conservation of the genes for HC-toxin biosynthesis in *Alternaria jesenskae*. *BMC Microbiology*, 13(1): 1-11. doi:10.1186/1471-2180-13-165.

Yu, P. (2005). Molecular chemistry imaging to reveal structural features of various plant feed tissues. *Journal of Structural Biology*, 150(1): 81-89. doi:10.1016/j.jsb.2005.01.005.

Zheng, H. H., Zhao, J., Wang, T. Y., & Wu, X. H. (2015). Characterization of *Alternaria* species associated with potato foliar diseases in China. *Plant Pathology*, 64(2): 425-433. doi:10.1111/ppa.12274.

Zohdi, V., Whelan, D. R., Wood, B. R., Pearson, J. T., Bambery, K. R., & Black, M. J. (2015) Importance of Tissue Preparation Methods in FTIR Micro-Spectroscopical Analysis of Biological Tissues: 'Traps for New Users'. *Plos One*, 10(2): e0116491. doi:10.1371/journal.pone.0116491.

CHAPTER IV
EFFICACY OF CHITOSAN NANOPARTICLE LOADED-SALICYLIC ACID AND -SILVER ON MANAGEMENT OF CASSAVA LEAF SPOT DISEASE

ABSTRACT

In recent years, application of nanotechnology to build sustainable agriculture is a trend. Leaf spot disease is one of the most important cassava diseases. Nano-fungicides, nano-fertilizers, and nano-stimulants can be applied to control diseases and improve plant growth. This study was performed to prepare chitosan (CS) nanoparticle (NP) loaded-salicylic acid (SA) or -silver (Ag) by ionic gelation method, evaluate their effectiveness on reducing leaf spot disease and enhancing growth of cassava plant. The CS (0.4%/ or 0.5%) and pentasodium triphosphate (0.2%/ or 0.5%) were mixed with SA at 0.05, 0.1 and 0.2%/ or silver nitrate at 1, 2, 3 mM to prepare three formulations CS-NP-loaded SA named N1, N2, N3/ or three formulations CS-NP-loaded Ag named N4, N5, N6, respectively. The results showed that three of CS-NP-loaded SA and three of CS-NP-loaded Ag were not toxic to cassava leaves. The CS-NP-loaded SA (N3) and CS-NP-loaded Ag (N6) were more effective than the remaining other formulations (N1, N2, and N4, N5) on reducing disease severity and disease index of leaf spot. Furthermore, the N3 at 400 ppm and N6 at 200, 400, 800 ppm could reduce disease severity (68.9-73.6% or 37.0-37.7% depending on treatment time and pathogen density) and enhance plant growth higher than or equal to commercial fungicide or nano-fungicide products at net house conditions. The study indicates the potential to use CS-NP-loaded SA or Ag as elicitors to manage cassava leaf spot disease.

Keywords: Cassava leaf spot, Chitosan, Ionic gelation method, Nanoparticle

4.1 Introduction

The cassava (*Manihot esculenta* Crantz) plant and its tapioca are an important food source for world food security, especially in developing countries. Cassava is used in the production of food, industry, and animal feed (Uchechukwu-Agua *et al*., 2015). Thailand's cassava acreage and production reached 1.34 million hectares and 30.84 million tons in 2017, which has increased by 1.15 folds over the previous ten years. Although Thailand's acreage and production account for only 5.45 and 11.04% of the world, the quantity and value of Thailand are between 58.5-81.2% and 44.4-56.7% in the world export market, respectively. Furthermore, this is Thailand's key export crop (FAOSTAT, 2021). Cassava can tolerate drought or nutrient-poor soil, so it also has a role in water-deficient farming areas. However, the biotic stress by a living organism leading to plant diseases, insects, weeds, or abiotic stresses such as adverse environmental factors could affect the growth and development of cassava, resulting on loss of yield. Currently, twenty-eight types of diseases on cassava caused by fungi, viruses, bacteria, and phytoplasma have been recorded (Gleadow *et al*., 2016; McCallum *et al*., 2017). Leaf spot disease are one of the most important cassava diseases. The disease causes a loss of up to 30% of cassava yield. However, the serious problem of cassava leaf spot disease is often neglected until a recent outbreak in Brazil (Julião *et al*., 2020). In 2019, *Alternaria* sp. has been reported as a pathogen causal of leaf spot disease on cassava (Ng'ang'a *et al*., 2019). It is now possible to implement cultural methods, chemical methods, and host resistance to achieve effective control or manage diseases. Fungicides containing copper, benomyl, thiophanate, carbendazim, flutriafol, cyproconazole, pyraclostrobin, thiophanate-methyl, tebuconazole, and azoxystrobin can control pathogens with varying degrees of effectiveness. Hence, fungicides are a popular method to reduce the damage of the cassava leaf spot. Also, the cassava cultivars Sri Prakash and Sri Visakam were recommended to resist cassava brown leaf spot disease in India (Prabakar and Raguchander, 2000; Reddy, 2015; Julião *et al*., 2020). Whereas, the resistant cultivar againt leaf spot disease is not present in Thailand. Therefore, it is necessary to look for

a new method to increase the resistance of cassava. Elicitation is one of the most effective tools to enhance plant immune by stimulating the secondary metabolite. In general, the plant has an innate immune system against adverse environmental factors including abiotic and biotic stress, which differed levels depending on the cultivar and adverse factors. The plant's immune system can be artificially induced by the elicitor. Elicitors are biotic or abiotic compounds, which activate defense mechanisms and innate immunity in plants against pathogens and stress conditions. The elicitors may be chemical, microbial, chitosan (CS), plant extracts, algal extracts, composts, and biochar. As such, applying appropriate elicitors could aid plants against pathogens, as well as cassava leaf spot disease (Burketova *et al*., 2015; Corwin and Kliebenstein, 2017).

In recent years, nanotechnology has been applied to many fields in agriculture in-cluding nano fertilizers, nanobiotechnology, nanomaterials, nanosensors, nano pesti-cides, nano elicitors, nano herbicides to enhance plants tolerance with biotic and abiotic stress, improve crop yield and quality, especially to build sustainable agriculture (Shang *et al*., 2019; Paramo *et al*., 2020; Liu *et al*., 2021; Rajput *et al*., 2021). Nanoparticles (NPs) are used as protectants (silver, gold, copper, titanium dioxide, CS) or carriers (CS, silica, solid lipid, layered double hydroxide) of active compounds (insecticides, fungicides, herbicides, RNA-interference) to protect plants against bacteria, fungi, viruses, insects on plants. The advantages of applying pesticide-based NPs in agriculture include improvement of shelf-life, target on site-specific uptake, increase of solubility, and reduction of soil leaching and toxicity (Worrall *et al*., 2018). NPs in the form of nutrients and non-nutrients are provided to plants through leaves or roots to improve plant health as well as control plant diseases. In many recent reviews, NP is considered biosafety-techniques. On the indirect side, the amount of chemical pesticides or fertilizers used for crop production is reduced because it is replaced by NPs (nano fertilizers, nano pesticides, nano elicitors). From a direct perspective, applying NP to soil may have a negative impact on microbial communities but to a low degree when compared to chemical application. Although the risk is low,

the potential toxicity and hazardous effect also needs attention. Usual-ly, the safety-by-design principle is applied to screen potential risk from materials, methods synthesis to NP formulation (Zieliński *et al*., 2020; Elemike *et al*., 2019; Ur Rahim *et al*., 2021; Ashraf *et al*., 2021). CS is a natural polysaccharide, with superior characters including low toxic, cheap, biodegradability, biocompatibility, environmental non-toxicity, absorption abilities that have been applied in crop production for plant disease management and enhance crop yield (Malerba *et al*., 2019; Chakraborty *et al*., 2020). The biogenic Ag-NPs are environmentally safer, with more interest as high potential antifungal and anti-bacterial agents (Rozhin *et al*., 2021). Foliar spray of Ag-NPs at 50-70 ppm on tomato plants reduced disease severity caused by *Tomato mosaic virus* and *Potato virus Y* at 3.9-4.8 and 2.2-4.5 folds, respectively. It increased chlorophyll content, total soluble protein, activities of peroxidase, and polyphenol oxidase (Noha *et al*., 2018). Similarly, CS-NP loaded salicylic acid (SA) at 0.01-0.16% can inhibit *Fusarium verticillioides* mycelium growth by 62.2-100% and spore germination by 48.3-60.5% at *in vitro* conditions. And it acted as an elicitor, able to activate the defense system of the maize plants to reduce post-flowering stalk rot disease by 40.5 to 59.47% and increase yield by 1.3 to 1.5 folds when compared with the control in field conditions (Kumaraswamy *et al*., 2019). CS-NP-loaded Cu at 0.1% has been able to inhibit mycelium growth of *Alternaria alternata*, *Macrophomina phaseolina,* and *Rhizoctonia solani* at 89.5, 63.0 and 60.1%, higher than CS-NP loaded saponin at 0.1%; and CS-NP at 0.06 or 0.1%. are 80.9, 66.2, 27.7% and 78.3, 66.2, 27.7 or 82.2, 87.6, 34.4%, respectively. In addition, both CS-NP, CS-NP loaded Cu and CS-NP loaded saponin at 0.06% inhibited the germination of *A. alternata* by 84.4, 83.3, and 78.3%, respectively (Saharan *et al*., 2013). There are two approaches to synthesize NPs including top-down and bottom-up methods, which result in NPs with different sizes, shapes, and functions. Some synthetic NPs for use as a pesticide are not too difficult to implement, such as sol-gel processes, green synthesis by microorganisms, or plant extracts (Singh *et al*., 2018). The ionic gelation technique for the production of micro-particles or NPs is based on the electrostatic interaction between ions with different

charges which was discovered by Calvo *et al*. (1997a and b). This system can load additional macromolecules or drugs as a delivery system to improve biological activity or efficiency. The method is simple, fast, economical, easy to implement, and does not use organic solvents, but it is important to select materials and optimize the process to produce suitable effective NPs (Du *et al*., 2009; Debnath *et al*., 2011; Koukaras *et al*., 2012; Kunjachan *et al*., 2014; Giri, 2016; Pedroso-Santana and Fleitas-Salazar, 2020).

Control studies of cassava brown leaf spot by synthetic pesticides were performed. However, the application of NPs on cassava plants to control or manage cassava diseases in general and cassava leaf spot in specific is not yet available. Moreover, ionic gelation is an easy and environmentally friendly method of NP production if the materials are properly selected and the process is optimized. In this paper, the study was performed to prepare the CS-NPs loaded SA or Ag by ionic gelation method. Then their effectiveness as nanoelicitors on reducing leaf spot disease and enhancing growth of cassava plant were also evaluated at net-house conditions. More specifically, this paper is approached with a focus on reverse research model from preparing elicitors, toxicity test, screening formulation effectiveness to concentration effectiveness and characterization effective elicitors.

4.2 Materials and methods

4.2.1 Materials

CS low molecular weight (Sigma-Aldrich, Iceland), Penta-Sodium triphosphate (Merck, Germany), SA (HiMedia, India), and silver nitrate (AAA, BBB) were provided by the School of Chemistry, Institute of Science, Suranaree University of Technology, Thailand. The pathogen A. alternata strain H-Vi 7 was provided by the Plant Pathology & Biopesticide Laboratory, Suranaree University of Technology, Thailand. The fungi were cultured from Eppendorf stock on potato dextrose agar medium (200 g potato extract; 20 g dextrose, 18 g agar, 1 L distilled water) at 27 ± 2 °C for 2 days. Then, the mycelium was transferred to a new potato dextrose agar and incubated until the

mycelium grew to the edge of the Petri plate (Pei *et al*., 2014; Poletto *et al*., 2018). Moreover, the surface colony was streaked by the sterile needle to enhance conidia production. The 5 mL of sterilized distilled water was added to each Petri plate to harvest conidia. The mixture was filtered through the fabric to remove mycelium. The concentration of suspension was determined using a hemocytometer and adjusted to 1×104 or 1×105 conidia mL-1 by adding sterilized distilled water (Pei *et al*., 2014).

4.2.2 Synthesis of chitosan nanoparticles loaded-salicylic acid and -silver

CS-NPs loaded -SA was synthesized according to the description of Kamaraswamy *et al*. (2019) with minor modifications. In brief, CS (0.4% w/v) was dissolved in 1% acetic acid in 500 mL distilled water by stirring at 300 rpm overnight, which was followed by filtering through Whatman paper 1 with particle retention of 11 µm (90 mm of diameter). Pentasodium triphosphate (0.2% w/v) was prepared in 500 mL of distilled water. In addition, SA was prepared at various concentrations including 0.05, 0.1, and 0.2% (w/v) in 500 mL distilled water. While CS solution was stirred at 400 rpm, pentasodium triphosphate and SA were added to each drop by a syringe. The mixed system was maintained at 600 rpm for 8 hours. An equal volume ratio between CS, pentasodium triphosphate, and each SA concentration including 0.05, 0.1, and 0.2% was combined to formulate 3 types of CS-NPs loaded SA, which coded as N1, N2, N3, respectively.

The CS-NPs loaded Ag was synthesized with a CS: pentasodium triphosphate mass ratio of 1: 1 based on the description of Ali *et al*. (2011) and Rodriguez *et al*. (2019) with modification. In brief, 500 mL of CS (0.5% w/v) and pentasodium triphosphate (0.5% w/v) were prepared in the same way as CS-NPs loaded -SA. Besides, 500 mL of silver nitrate 1, 2, and 3 mM were prepared in distilled water. Three types of CS-NP-loaded -Ag with different concentrations of silver nitrate including 1, 2, 3 mM were synthesized similarly to CS-NPs loaded SA, which coded as N4, N5, N6, respectively. Each formation NP was harvested by centrifuging the mixture at 9,500

rpm at 4 ℃ for 15 minutes. The pellet was collected and freeze-dried, then stored at 4 ℃ until used.

4.2.3 Characterization of elicitor- nanoparticles

The particle size, zeta potential, and PDI (weight average molecular weight per number average molecular weight) of N3, N6 were measured by Zetasizer-ZS (Malvern Instruments Ltd) at Suranaree University of Technology, Thailand. Similarly, the morphology and size, and interaction groups of N3, N6 were detected by Field Emission Scanning Electron Microscope, and Fourier-transform infrared spectroscopy (FTIR), respectively. In FTIR analysis, the NPs N3 and N6 freeze-dried or bulk CS were homogenous finely ground with KBr with a ratio 1:99. Then the KBr pellet was inserted into the IR sample holder. The spectra were collected with transmission mode in the range 400 and 4000 cm^{-1} wavelengths. The peaks were collected by scanning 32 times and analyzed by OPUS 7.5 (Bruker Optics Ltd., Ettlingen, Germany) (Choudhary *et al*., 2019).

4.2.4 Phytotoxicity test

The phytotoxicity test was conducted to assess the toxic potential of NPs on cassava using the leaf disk assay method according to the description of Tanapichatsakul *et al*. (2020). The disks of mature cassava leaf blades were prepared using a cork borer with a diameter of 8 mm. Formulated NPs including N1, N2, N3, N4, N5, N6 were prepared in distilled water into a series of solutions at 25, 50, 100, 200, 400, 800 ppm. A disk was immersed in 1 mL of NP solution. Fungicides including Headline® (Pyraclostrobin), JOINT® (Flutriafol), and ZONO-S1® (Zinc oxide commercial NP) at 10 ml, 30 ml, and 20 ml per 20 L (recommended dose) were used as a positive control that coded as Pyr, Flu, ZON, respectively. Distilled water was used as a negative control. Besides, SA, CS, silver nitrate at 100 ppm also be used as a control group

(**Table 4.1**). The symptoms of leaf disks were observed visually after they were washed with distilled water at 24 hours after incubation. The assessment scale consists of 4 levels: 0 with non-effect, 1 with an area of necrotic spots <50%, 2 with an area of necrotic spots 50-70%, 3 with the area of necrotic spots 70-90%, and 4 with the area of necrotic spots >90%.

Table 4.1 Treatments used in the study.

Treatments	Concentrations	Note
3 formulated of CS-NPs loaded SA (named **N1**, **N2**, **N3**) 3 formulated of CS-NPs loaded Ag (named **N4**, **N5**, **N6**)	25, 50, 100, 200, 400, 800 ppm	NP elicitor group
SA (Salicylic acid), **CS** (Chitosan) and **SN** (Silver nitrate)	100 ppm	Single chemical group
Pyr (Pyraclostrobin, Headline®) **Flu** (Flutriafol, JOINT®) **ZON** (Zinc oxide commercial NP, ZONO-S1®)	10 ml/20 L (recommend dose) 30 ml/20 L (recommend dose) 20 ml/20 L (recommend dose)	Positive control group
Water	-	Negative control group

4.2.5 Screening elicitor formulations for inducing resistance to cassava leaf spot disease and growth in cassava plants at net house conditions

The experiment was carried out in a completely randomized design with four replications. The stalks of cassava varieties Pirun 2 were soaked for 5 minutes with NPs solutions at 25, 50, 100, 200, 400, 800 ppm, water (negative control), fungicides

(positive control), CS, SA, silver nitrate at 100 ppm (control group) as described in **Table 4.1** before planting in the pot containing sandy soil, which was kept in a net house. At 28 and 42 days after planting (DAP), the cassava plants were treated with elicitors by foliar spray at 5 ml per plant. At 44 DAP, cassava plants are inoculated by spraying the suspension of *A. alternata* strain H-Vi 7 at 1×10^4 conidia mL^{-1}, which were covered by plastic and sprayed water to create relative humidity (>80%) conditions (Beckman and Payne 1983; Pei *et al*., 2014; Sangpueak *et al*., 2021; Kamaraswamy *et al*., 2019). The plants were kept in a net house to monitor disease symptoms. Disease score was assessed at 12 days after inoculation based on the diagrammatic scale (0 to 8) following the description of Perina *et al*. (2019). DS (disease severity) was calculated following formula:

$$\text{DS (\%)} = \frac{\text{Sum of all numerical scoring}}{\text{The number of leaves} \times \text{Maximum score}} \times 100$$

DI (disease index) was calculated following formula:

$$\text{DI (\%)} = \frac{\text{The number of leaves appeared symptom}}{\text{The total leaves}} \times 100$$

The DS and DI were analyzed statistically according to two factors by SPSS software version 20, including 6 NPs formulated and 6 concentrations to select the most effective CS-NP loaded SA and one CS-NP loaded Ag. Then, the DS, DI of N3, N6, and controls treatments were analyzed following Duncan's Multiple Range Test (DMRT). The F value detected the significance of treatments P = 0.05.

The RCLSD (reduction of cassava leaf spot disease) is calculated based on DS with the formula:

$$\text{RCLSD (\%)} = \frac{\text{DS of negative control} - \text{DS of elicitors}}{\text{DS of negative control}} \times 100$$

To assess the ability to maintain a stimulating effect on disease resistance, the cassava leaves without disease of the control group treatments were continued to inocule with *A. alternata* H-Vi 7 conidia suspension (1×10^5 conidia mL^{-1}) at 63 DAP

while N3 at 400 ppm and N6 at 200, 400, 800 ppm is done in the same way. The DS and RCLSD were also calculated and analyzed as described above.

Furthermore, to evaluate the ability on enhancing plant growth, the shoot height, the number of leaves at 28, 42 DAP and the root length, root weight, the largest leaf area at 75 DAP of N3, N6 as well as control treatments were recorded. Of these, the largest leaf area was measured by ImageJ 1.4g software (National Institution of Health, USA) (**Figure 4.1**).

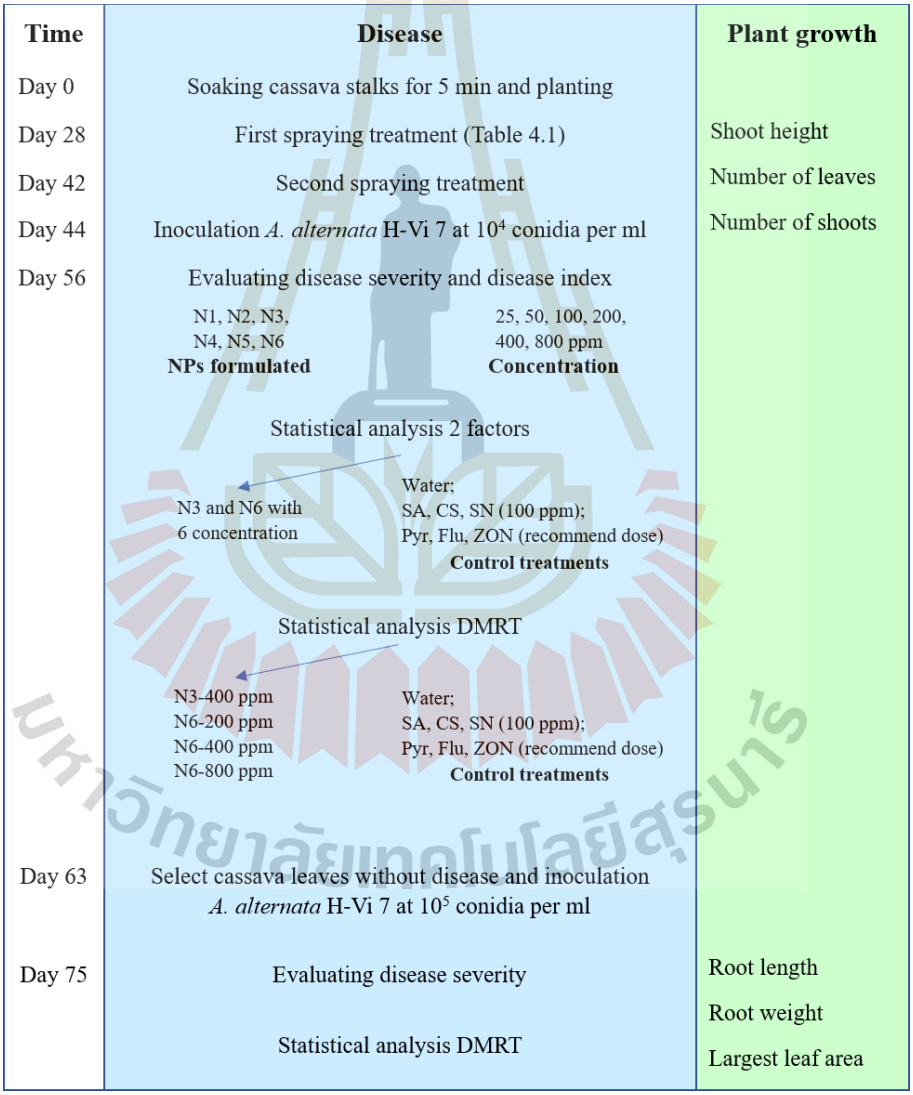

Figure 4.1 The overview of "Screening elicitor formulations for inducing resistance cassava leaf spot disease and growth in cassava plants at net house conditions" experiments.

4.3 Results

4.3.1 Synthesis and characterization chitosan nanoparticles loaded salicylic acid and silver

The hydrodynamic diameter of CS-NP loaded SA (N3) and Ag (N6) was 89.86 ± 9.04 nm and 249.67 ± 23.97 nm with PDI was 0.36 ± 0.02 and 0.53 ± 0.03, the zeta potential was 22.27 ± 1.01 and 13.53 ± 0.74 mV, respectively (**Figure 4.2**). Under the Field Emission Scanning Electron Microscope, the N3 and N6 had spherical forms and porous architecture (**Figure 4.3**). In FTIR test, the peak 3422 (NH_2 stretch - primary amide), 1656 ($CO\text{-}NH_2$ - amide group), 1597 (NH_2 bend - primary amide), 897 (Anhydro glycoside) of bulk CS shifted to 3421, 1640, 1540, 895 cm^{-1} in N3 and 3423, 1643, 1542, 894 cm^{-1} in N6, respectively. That indicated interaction of CS, pentasodium triphosphate, and SA or Ag in the N3 or N6, respectively. Moreover, the shifted to 1314 cm^{-1} in N3 showed interaction of COOH and NH_2 (**Figure 4.4**). The interaction of function groups in N3 and N6 has shown success in the ionic gelation process.

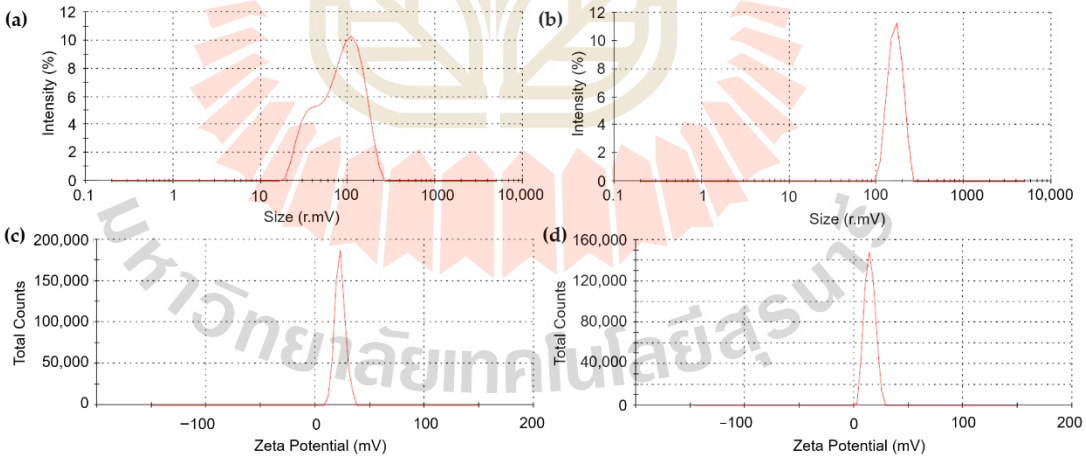

Figure 4.2 The DLS analysis of CS-NP loaded SA (N3) (a) size and (c) zeta potential, CS-NP loaded Ag (N6) (b) size and (d) zeta potential.

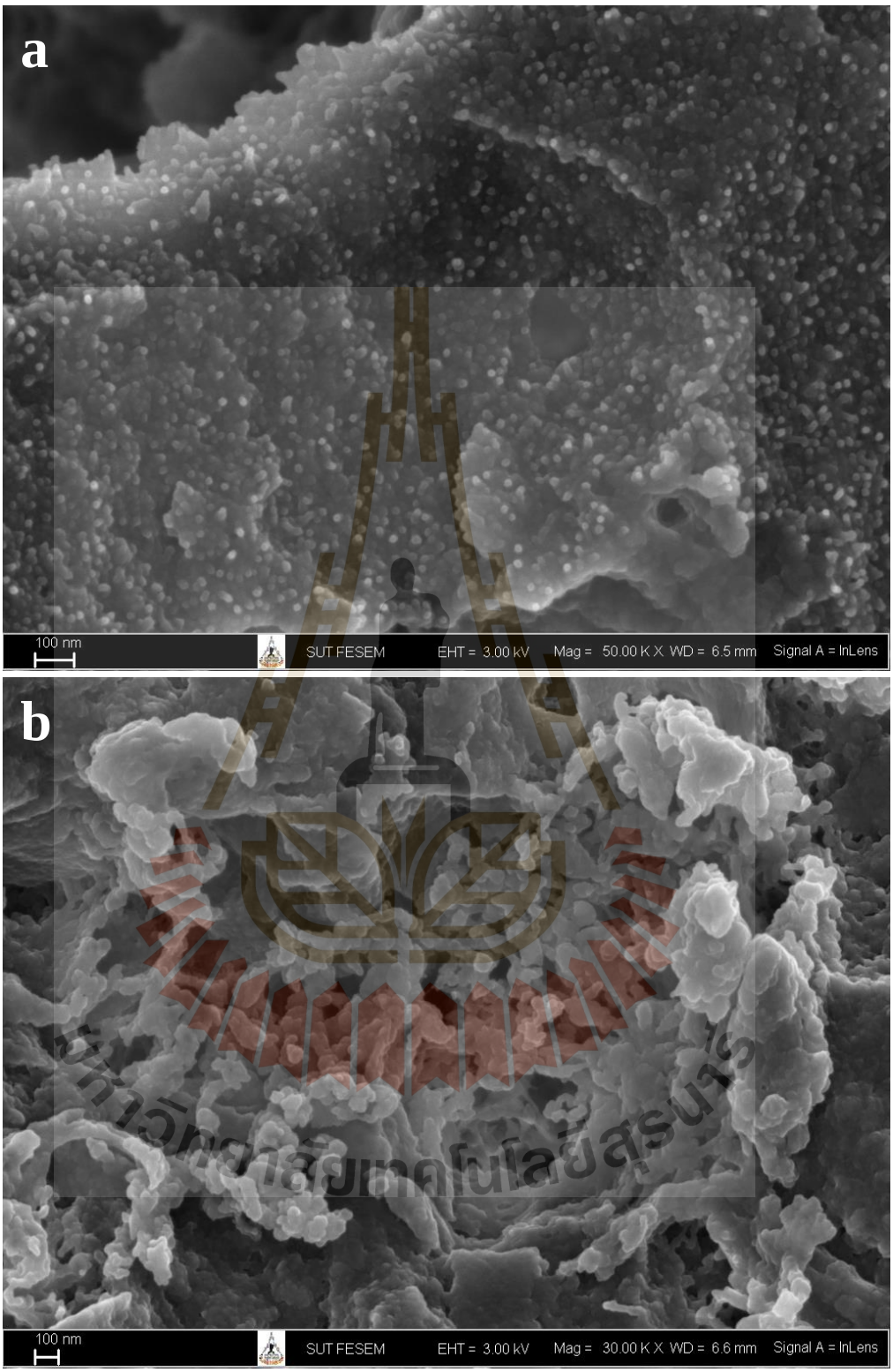

Figure 4.3 The morphology of (**a**) CS-NP loaded SA N3 and (**b**) CS-NP loaded Ag N6 formulations under Field Emission Scanning Electron Microscope.

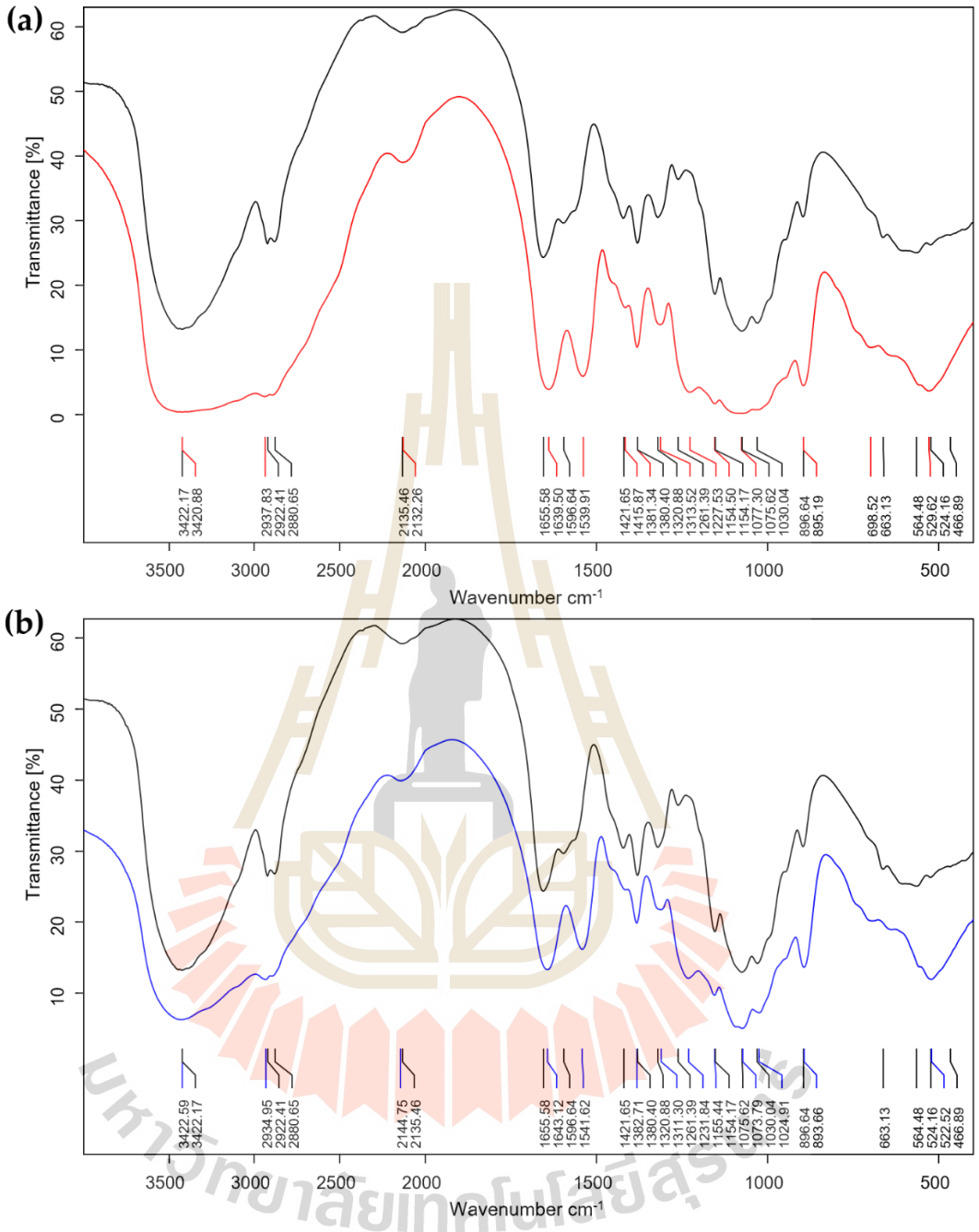

Figure 4.4 The FTIR analysis of CS (black color) compared with (a) CS-NP loaded SA (N3-red color) and (b) CS-NP loaded Ag (N6-blue color).

4.3.2 Phytotoxicity test

The phytotoxicity test was performed to evaluate the potential toxicity of NPs on cassava leaves. Usually, the necrotic spots or the browning around leaves disks margin is the result of toxicity caused by chemical in the leaf disk assay method. The larger the percentage of necrotic or browning area, the greater the toxicity. The results showed that 6 NPs formulations with 6 concentrations did not cause necrotic spots or the browning around leaves disks margin. The leaves disks of control groups did not show toxicity except Pyr treatment turn leaves disk to slight-yellow and SN treatment turn leaves disks margin to brown color – a positive toxicity (Figure 5). That confirmed NP formulation does not cause toxicity on cassava leave (**Figure 4.5**).

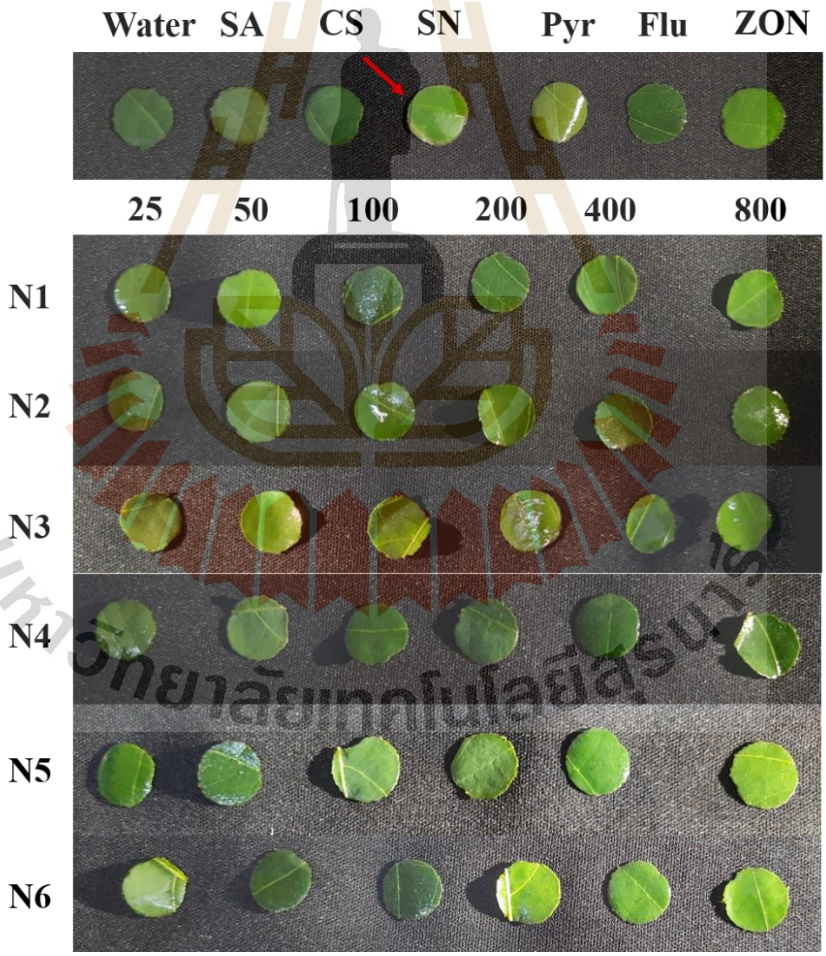

Figure 4.5 Phytotoxicity test of six NP formulations and control groups by leaf disk assay. *Note*: SA-Salicylic acid 100 ppm; CS-Chitosan 100 ppm; SN-Silver nitrate 100 ppm; Pyr-Pyraclostrobin, Headline® 10 ml/20 L; Flu-Flutriafol,

JOINT® 30 ml/20 L; ZON-Zinc oxide NP, ZONO-S1® 20 ml/20 L. The CS (0.4%/ or 0.5%) and pentasodium triphosphate (0.2%/ or 0.5%) were mixed with SA vary at 0.05, 0.1 and 0.2%/ or silver nitrate vary at 1, 2, 3 mM to prepare three formulations CS-NP-loaded SA named N1, N2, N3/ or three formulations CS-NP-loaded Ag named N4, N5, N6, respectively.

4.3.3 Screening elicitor formulations for inducing resistance cassava leaf spot disease and growth in cassava plants at net house conditions

An overview of the experiment to evaluate the effect of CS-NP-loaded SA or Ag formulations on reducing leaf spot and enhance plant growth on cassava is shown in **Figure 4.1**.

Statistic analyze disease severity and disease index data of 6 formulations (N1, N2, N3, N4, N5, N6) by 2 factors including formulation and concentration to select an effective formulation among CS-NPs loaded SA and CS-NPs loaded Ag (**Tables 4.2 and 4.3**). Overall, the disease severity and disease index of CS-NPs loaded Ag were lower than those of CS-NPs loaded SA. The disease severity of N6 was significantly lower than the other formulations with 8.54%. The disease severity of N3 was 10.83% that lower than N1 and N2 but was not significantly different when compared with N4 (10.97%) and N5 (10.40%) (**Table 4.2**). The disease index of N6 was 36.43%, which was also significantly lower than the other formulations, except for N4 with 40.49%. Of the CS-NPs loaded SA, the disease index of N3 was 47.03%, which was significantly lower than N1 (57.71%) and N2 (58.82%) (**Table 4.3**). In addition, concentrations of 200 and 400 ppm were more effective on reducing both disease severity and disease index. Therefore, CS-NP load SA (N3) and CS-NP loaded Ag (N6) were selected for the subsequent analysis.

Table 4.2 The disease severity (%) of cassava leaf spot at 56 days after planting, statistically analyzed by 2 factors.

[1] Nano particles	Concentration (ppm)						[2] Mean
	25	50	100	200	400	800	
N1	9.66	17.19	14.90	13.19	9.47	16.99	13.57 c
N2	11.84	16.11	18.13	17.54	18.10	16.16	16.31 d
N3	10.43	15.20	11.04	10.38	7.81	10.11	10.83 b
N4	11.88	10.86	11.31	8.96	10.93	11.88	10.97 b
N5	10.56	17.01	10.57	10.04	7.39	6.81	10.40 b
N6	10.61	11.86	8.61	6.80	6.62	6.72	8.54 a
[3] **Mean**	10.83 AB	14.70 D	12.43 C	11.15 AB	10.05 A	11.44 BC	**11.77**
CV (%)	16.67						

[1] The CS (0.4%/ or 0.5%) and pentasodium triphosphate (0.2%/ or 0.5%) were mixed with SA vary at 0.05, 0.1 and 0.2%/ or silver nitrate vary at 1, 2, 3 mM to prepare three formulations CS-NP-loaded SA named N1, N2, N3/ or three formulations CS-NP-loaded Ag named N4, N5, N6, respectively.

[2,3] Means followed by the same letter do not differ significantly according to DMRT at $P \leq 0.01$ (**).

Table 4.3 The disease index (%) of cassava leaf spot at 56 days after planting, statistic analyzed by 2 factors.

[1] Nano particles	Concentration (ppm)						[2] Mean
	25	50	100	200	400	800	
N1	36.5	75.0	70.0	53.1	44.1	67.5	57.71 d
N2	44.9	58.1	65.3	61.8	61.6	61.2	58.82 d
N3	55.2	45.2	48.3	48.5	43.0	42.0	47.03 c
N4	37.6	41.3	41.5	39.1	38.4	45.0	40.49 ab
N5	38.8	59.2	46.8	40.2	33.8	28.7	41.26 b
N6	45.0	46.2	34.9	31.4	33.2	27.9	36.43 a
[3] Mean	43.00 A	54.15 B	51.16 B	45.68 A	42.35 A	45.38 A	**46.95**
CV (%)	16.49						

[1] The CS (0.4%/ or 0.5%) and pentasodium triphosphate (0.2%/ or 0.5%) were mixed with SA vary at 0.05, 0.1 and 0.2%/ or silver nitrate vary at 1, 2, 3 mM to prepare three formulations CS-NP-loaded SA named N1, N2, N3/ or three formulations CS-NP-loaded Ag named N4, N5, N6, respectively.

[2,3] Means followed by the same letter do not differ significantly according to DMRT at P ≤ 0.01 (**).

The disease severity and disease index of N3 and N6 with six concentrations including 25, 50, 100, 200, 400, 800 ppm were compared with the control group including water, SA, CS, silver nitrate, pyraclostrobin, flutriafol, zinc oxide commercial NP according to the DMRT model to select the effective concentration and based on this data to calculate the reduction of leaf spot disease severity. In general, the disease severity of water treatment was significantly higher than the others treatments, or in

other words, they can reduce cassava leaf spot disease. The zinc oxide commercial NP was used as a standard that reduces disease severity by 55.7%. The disease severity of CS, silver nitrate, and N3-50 ppm is significantly higher than zinc oxide commercial NPs, which reduces disease severity by 39.4-52.1%. The disease severity of SA, flutriafol and N3-100 ppm was non-significantly with zinc oxide commercial NP treatment. The disease severity of pyraclostrobin, N3 at 25, 200, 800 ppm, and N6 at 25 ppm were significantly slight-lower than zinc oxide commercial NP, which lead to reducing disease severity by 57.7-59.7%. Meanwhile, the disease severity of N3-400 ppm and N6 at 200, 400, 800 ppm were significantly lower than zinc oxide commercial NPs that reduce disease severity by 68.9-73.6%. The disease index of water treatment was 62.9%, which was significantly higher than the other treatments except for slight-significant CS treatment (52.1%) and N3-25 ppm (55.2%). The disease index of N3-50 ppm and N6-25 ppm were non-significantly compared with zinc oxide commercial NPs (44.4%). The disease index of SA, CS, silver nitrate, N3 at 25, 100, 200 ppm, N6 at 50 ppm was significantly higher than zinc oxide commercial NPs. Flutriafol, N3 at 400, 800 ppm, N6 at 100, 400 ppm were similar but with a decreasing trend. Meanwhile, the disease index of N6 at 200 and 800 ppm were 31.4 and 27.9%, which was significantly lower than zinc oxide commercial NP (**Table 4.4, Figure 4.6**). The N3 at 400 ppm and N6 at 200, 400, 800 ppm were effective NPs treatments that were selected to continue to inoculate *A. alternata* H-Vi 7 at 63 DAP (3 weeks after the last time spraying treatment) to assess maintenance effectiveness in stimulating disease resistance. In this testing, the disease severity of water was also significantly higher than the other treatments that indicated reducing disease severity by 14.2-37.7%. The disease severity of pyraclostrobin was 33.9%, which non-significantly compared to zinc oxide commercial NP (34.1%). The disease severity of CS and silver nitrate was slight-significantly lower than zinc oxide commercial NP. The disease severity of SA, flutriafol, N3-400 ppm and N6 at 200, 400, 800 ppm were significantly lower than zinc oxide commercial NP, which can reduce disease severity by 30.9-37.7%. Among them, the NPs treatments slight-significantly lower than SA and flutriafol (**Table 4.5, Figure 4.7**).

Table 4.4 The disease severity, reduction of disease and disease index of cassava leaf spot at 56 days after planting of N3 and N6 treatments compared with control treatments.

[1] Treatment	[2] Disease severity (%)	Reduction of disease severity (%)	[2] Disease index (%)
Control	25.1 f	-	62.9 h
SA 100 ppm	10.9 cd	56.7	51.1 fg
CS 100 ppm	12.0 d	52.1	52.1 f-h
SN 100 ppm	12.3 d	50.8	47.6 e-g
Pyr	10.1 b-d	59.6	38.0 a-e
Flu	11.4 cd	54.7	41.7 b-f
ZON	11.1 cd	55.7	44.4 c-g
N3-25 ppm	10.4 b-d	58.4	55.2 gh
N3-50 ppm	15.2 e	39.4	45.2 c-g
N3-100 ppm	11.0 cd	56.0	48.3 e-g
N3-200 ppm	10.4 b-d	58.6	48.5 e-g
N3-400 ppm	7.8 ab	68.9	43.0 b-g
N3-800 ppm	10.1 b-d	59.7	42.0 b-f
N6-25 ppm	10.6 b-d	57.7	45.0 c-g
N6-50 ppm	11.9 d	52.8	46.2 d-g
N6-100 ppm	8.6 a-c	65.7	34.9 a-d
N6-200 ppm	6.8 a	72.9	31.4 ab
N6-400 ppm	6.6 a	73.6	33.2 a-c
N6-800 ppm	6.7 a	73.2	27.9 a
F-test	**		**
CV (%)	16.41		16.87

[1] SA-Salicylic acid 100 ppm; CS-Chitosan 100 ppm; SN-Silver nitrate 100 ppm; Pyr-Pyraclostrobin, Headline® 10 ml/20 L; Flu-Flutriafol, JOINT® 30 ml/20 L; ZON-Zinc oxide commercial NP, ZONO-S1® 20 ml/20 L; The CS (0.4%/ or 0.5%) and Pentasodium triphosphate (0.2%/ or 0.5%) were mixed with SA 0.2%/ or silver nitrate 3 mM to prepare formulation CS-NP-loaded SA N3/ or formulation CS-NP-loaded Ag N6, respectively.

[2] Means followed by the same letter do not differ significantly according to DMRT at $P \leq 0.01$ (**)

Table 4.5 The disease severity, reduction of disease and disease index of cassava leaf spot at 75 days after planting of N3 and N6 treatments compared with control treatments.

[1] Treatments	[2] Disease severity (%)	Reduction of Disease severity (%)
Control	39.7 e	
SA 100 ppm	27.4 a-c	30.9
CS 100 ppm	32.0 cd	19.3
SN 100 ppm	30.3 b-d	23.8
Pyr	33.9 d	14.7
Flu	25.6 ab	35.4
ZON	34.1 d	14.2
N6-200	24.8 a	37.4
N6-400	25.0 a	37.0
N6-800	24.7 a	37.7
N3-400	25.0 a	37.0
F-test	**	
CV (%)	10.87	

[1] SA-Salicylic acid 100 ppm; CS-Chitosan 100 ppm; SN-Silver nitrate 100 ppm; Pyr-Pyraclostrobin, Headline® 10 ml/20 L; Flu-Flutriafol, JOINT® 30 ml/20 L; ZON-Zinc oxide commercial NP, ZONO-S1® 20 ml/20 L; The CS (0.4%/ or 0.5%) and pentasodium triphosphate (0.2%/ or 0.5%) were mixed with SA 0.2%/ or silver nitrate 3 mM to prepare formulation CS-NP-loaded SA N3/ or formulation CS-NP-loaded Ag N6, respectively.

[2] Means followed by the same letter do not differ significantly according to DMRT at $P \leq 0.01$ (**)

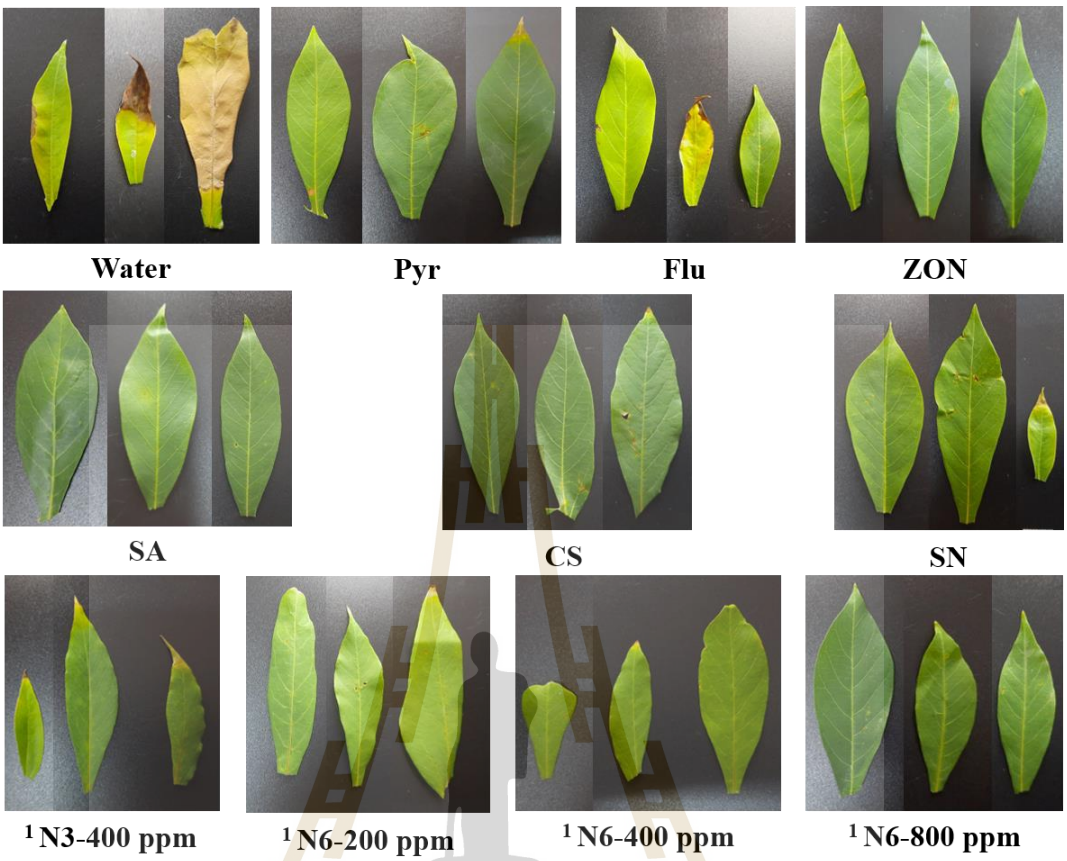

Figure 4.6 The symptom of cassava infected by *A. alternata* H-Vi 7 at 56 DAP. N*ote*: SA-Salicylic acid 100 ppm; CS-Chitosan 100 ppm; SN-Silver nitrate 100 ppm; Pyr-Pyraclostrobin, Headline® 10 ml/20 L; Flu-Flutriafol, JOINT® 30 ml/20 L; ZON- Zinc oxide commercial NP, ZONO-S1® 20 ml/20 L. [1] The CS (0.4%/ or 0.5%) and pentasodium triphosphate (0.2%/ or 0.5%) were mixed with SA 0.2%/ or silver nitrate 3 mM to prepare formulation CS-NP-loaded SA N3/ or formulation CS-NP-loaded Ag N6, respectively.

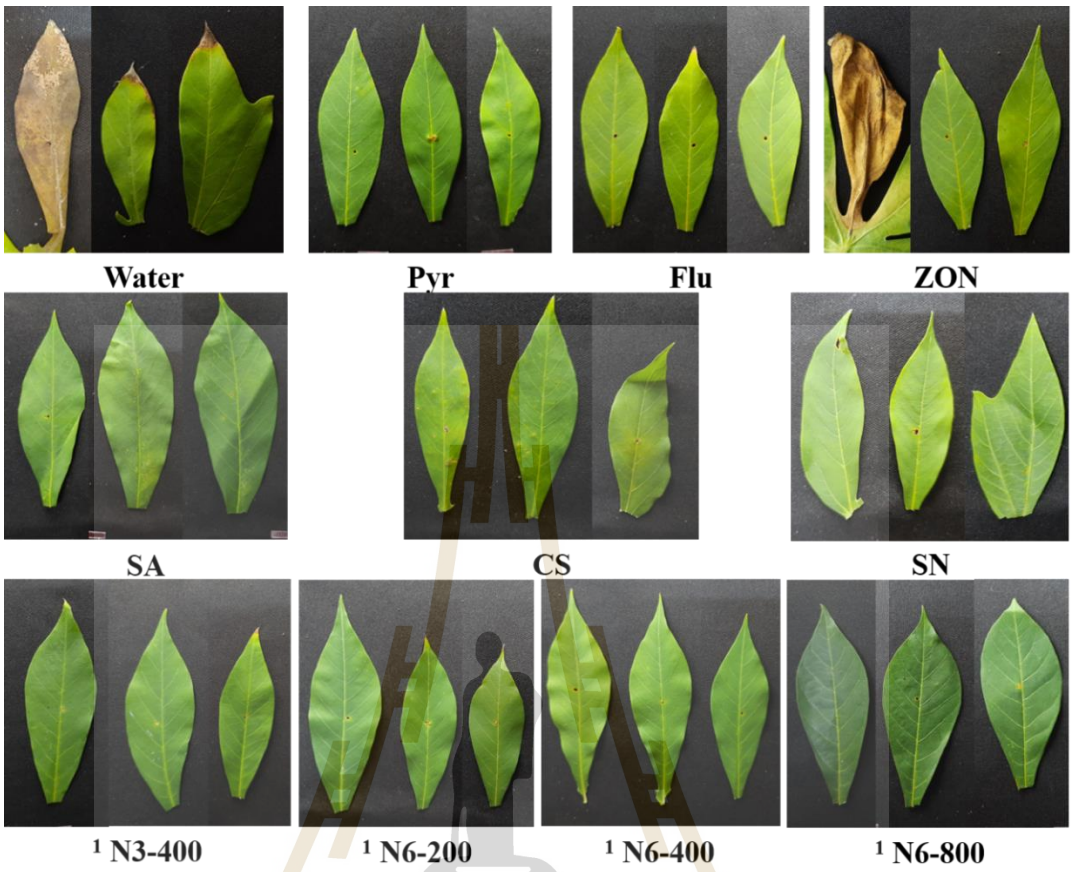

Figure 4.7 The symptom of cassava infected by *A. alternata* H-Vi 7 at 75 DAP. *Note*: SA-Salicylic acid 100 ppm; CS-Chitosan 100 ppm; SN-Silver nitrate 100 ppm; Pyr-Pyraclostrobin, Headline® 10 ml/20 L; Flu-Flutriafol, JOINT® 30 ml/20 L; ZON- Zinc oxide commercial NP, ZONO-S1® 20 ml/20 L. [1] The CS (0.4%/ or 0.5%) and pentasodium triphosphate (0.2%/ or 0.5%) were mixed with SA 0.2%/ or silver nitrate 3 mM to prepare formulation CS-NP-loaded SA N3/ or formulation CS-NP-loaded Ag N6, respectively.

Several concentrations of CS-NP-loaded SA or Ag were able to enhance cassava plant growth including shoot height, the number of leaves, the number of shoots, the largest leaf area, root length, and root weight (**Table 4.6**). The N6-50 ppm treatment was superior to enhance shoot height at 28 and 42 DAP, which increased by 40.7 and

28.2% compared with water treatment, respectively. However, the shoot height was inhibited by N3-200 ppm and N3-50 ppm treatment at 28 and 42 DAP with 30.6 and 26.4%, respectively. Interestingly, N3-200 ppm increased shoot height by 69.4% compared with water treatment was 35.8% within 2 weeks. In addition, N3 at 400 ppm and N6 at 200, 400, 800 ppm was showed non-significantly in enhancing shoot height. Most of the other treatments significantly increased the number of leaves at 28 and 42 DAP when compared with the water treatment. The pyraclostrobin and zinc oxide commercial NP treatment was more effective in increasing the number by 79.2-88.7% and 103.9-123.5% at 28 and 42 DAP, respectively. The N3 and N6 treatments could increase by 20.8-66.0% and 13.2-41.5 at 28 DAP, respectively. In which, N3 at 25, 400, 800 ppm was not significantly different compared with pyraclostrobin and zinc oxide commercial NPs. The N3 and N6 treatments could increase by 43.1-82.4% and 45.1-86.3% at 42 DAP, respectively. Where, N3 at 25, 400 ppm and N6 at 50, 200 were not significantly different compared with pyraclostrobin and zinc oxide commercial NPs. Interestingly, N6 at 50 and 200 ppm treatment increased the number of leaves by 46.2 and 46.8% between 2 weeks that was the highest among the treatments even pyraclostrobin and zinc oxide commercial NPs. The treatments all increased the number of the shoot when compared with water treatment except CS treatment. The N3-400 ppm and N6-50 ppm were higher than the others treatments in increasing the number of the shoot by 64.3 and 76.9% at 28 and 42 DAP, respectively. The N6-200, 400, 800 ppm increased by 14.3 and 38.5-46.2% at 28 and 42 DAP, respectively. Interestingly, the pyraclostrobin, flutriafol, zinc oxide commercial NPs was 28.6-50% and 46.2-61.5% at 28 and 42 DAP, respectively. The treatments except for silver nitrate significantly increased the largest leaf area when compared with water treatment. The N3 and N6 treatments have increased the largest leaf area by 20.2-69.6% and 29.6-86.7%, respectively. In it, the N6-50 was higher than the other treatments. The N3 at 25, 200, 800 ppm was non-significantly when compared with zinc oxide commercial NPs and CS. The N3-400 and the N6 at 200, 400, 800 ppm were increased by 28.8-41.9% compared with the water treatment that similar SA, pyraclostrobin, flutriafol.

The root length and root weight were both increased by treatments when compared with water treatment. However, a few treatments that did not increase significantly included CS, silver nitrate, pyraclostrobin, flutriafol (root length) and SA, CS, pyraclostrobin, flutriafol, N3 treatments, N6-25 ppm (root weight). The N3 and N6 treatments increased the root length by 11.6-27.4 and 20.1-31.7%, root weight by 10.3-27.6%, and 31.0-82.8%, respectively. Interestingly, silver nitrate treatment increased root weight by 70.0%, which was similar to zinc oxide commercial NPs (**Figure 4.8**).

Table 4.6 The plant growth parameters enhanced by N3 and N6 formulations compared with control treatments.

[1] Treatments	[2] Shoot height (cm)		[2] The number of leaves		[2] The number of shoots		[2] Largest leaf area (cm^2)	[2] Root length (cm)	[2] Root weight (g)
	28 DAP	42 DAP	28 DAP	42 DAP	28 DAP	42 DAP			
Control	8.1 bc	11.0 b-e	5.3 f	5.1 d	1.4 de	1.3 d	48.0 e	16.4 g	2.9 f
SA 100 ppm	7.0 cd	10.9 b-e	7.4 b-e	8.2 bc	1.6 a-e	1.6 b-d	62.2 cd	20.1 a-e	3.8 b-f
CS 100 ppm	8.0 bc	11.5 b-d	5.6 ef	7.3 cd	1.2 e	1.2 d	77.8 b	18.1 e-g	4.0 b-f
SN 100 ppm	7.3 cd	11.7 b-d	6.5 d-f	7.2 cd	1.6 b-e	1.6 b-d	48.7 e	16.8 fg	4.9 a-c
Pyr	8.8 b	12.7 ab	9.5 a	10.4 ab	2.1 a-c	2.1 ab	65.1 c	17.1 fg	3.7 c-f
Flu	7.4 b-d	12.7 ab	9.1 ab	8.6 bc	2.1 ab	1.9 a-c	67.9 c	17.4 fg	3.3 ef
ZON	8.9 b	12.3 a-c	10.0 a	11.4 a	1.8 a-e	1.9 a-c	82.8 b	19.0 b-f	4.6 a-d
N3-25 ppm	8.0 bc	11.3 b-e	8.7 a-c	9.3 a-c	1.9 a-d	1.8 a-d	77.2 b	20.0 a-e	3.7 d-f
N3-50 ppm	8.2 bc	8.7 f	6.4 ef	7.6 c	1.6 b-e	1.6 b-d	61.5 cd	18.9 c-f	3.2 ef
N3-100 ppm	8.9 b	11.9 b-d	6.6 d-f	8.1 bc	1.4 de	1.6 b-d	57.7 d	20.9 a-c	3.5 d-f
N3-200 ppm	6.2 d	10.5 c-f	6.9 c-f	7.3 cd	1.7 a-e	1.6 b-d	76.6 b	19.8 a-e	3.5 d-f
N3-400 ppm	7.9 bc	12.0 a-c	8.8 a-c	9.3 a-c	2.3 a	1.9 a-c	62.3 cd	18.3 d-g	3.7 d-f
N3-800 ppm	7.6 bc	12.6 a-c	8.4 a-d	8.8 bc	1.6 a-e	1.8 a-d	81.4 b	20.1 a-e	3.5 d-f

Continue next page

Table 4.6 The plant growth parameers enhanced by N3 and N6 formulations compared with control treatments (**continued**).

[1] Treatments	[2] Shoot height (cm)		[2] The number of leaves		[2] The number of shoots		[2] Largest leaf area (cm^2)	[2] Root length (cm)	[2] Root weight (g)
	28 DAP	42 DAP	28 DAP	42 DAP	28 DAP	42 DAP			
N6-25 ppm	8.8 b	12.0 a-c	6.0 ef	8.3 bc	1.4 c-e	1.5 b-d	67.7 c	20.6 a-d	3.8 b-f
N6-50 ppm	11.4 a	14.1 a	6.5 d-f	9.5 a-c	1.5 b-e	2.3 a	89.6 a	19.8 a-e	4.2 a-e
N6-100 ppm	7.1 cd	9.3 ef	7.4 b-e	8.5 bc	1.5 b-e	1.6 b-d	64.0 cd	21.6 a	4.2 a-e
N6-200 ppm	7.9 bc	11.7 b-d	6.2 ef	9.1 a-c	1.6 b-e	1.9 a-c	64.3 cd	19.7 a-e	4.3 a-e
N6-400 ppm	8.3 bc	9.7 d-f	6.6 d-f	7.4 cd	1.6 a-e	1.9 a-c	68.1 c	21.3 ab	5.0 ab
N6-800 ppm	8.2 bc	10.8 b-e	7.5 b-e	7.6 c	1.6 a-e	1.8 a-d	62.2 cd	20.4 a-d	5.3 a
F-test	**	**	**	**	*	*	**	**	**
CV (%)	10.71	11.14	16.43	17.67	23.24	22.20	6.63	7.21	18.36

[1] SA-Salicylic acid 100 ppm; CS-Chitosan 100 ppm; SN-Silver nitrate 100 ppm; Pyr-Pyraclostrobin, Headline® 10 ml/20 L; Flu-Flutriafol, JOINT® 30 ml/20 L; ZON-Zinc oxide commercial NP, ZONO-S1® 20 ml/20 L; The CS (0.4%/ or 0.5%) and pentasodium triphosphate (0.2%/ or 0.5%) were mixed with SA 0.2%/ or silver nitrate 3 mM to prepare formulation CS-NP-loaded SA N3/ or formulation CS-NP-loaded Ag N6, respectively.

[2] Means followed by the same letter do not differ significantly according to DMRT at $P \leq 0.01$ (**) or $0.01 < P \leq 0.05$ (*); DAP: days after planting

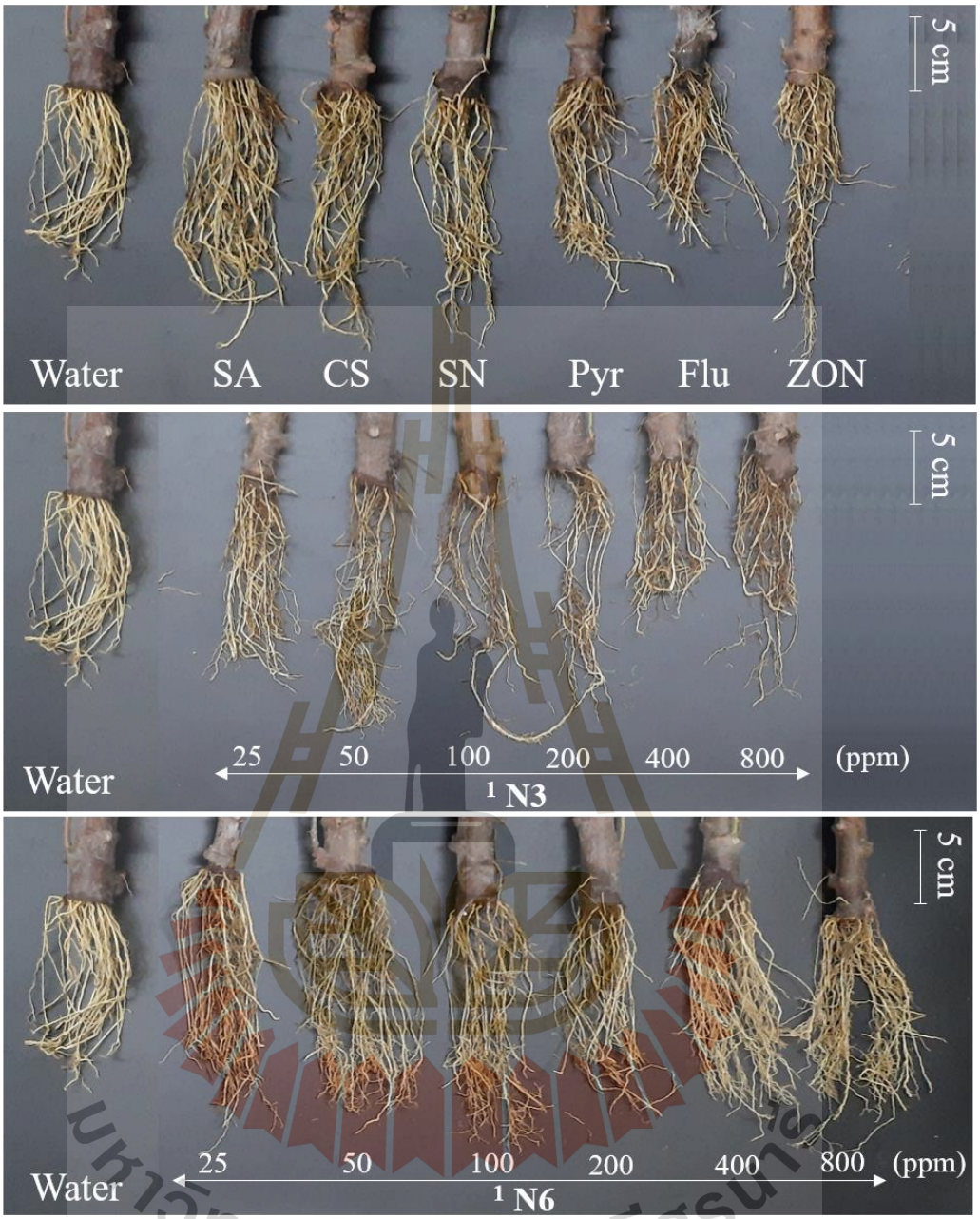

Figure 4.8 The roots of cassava plants at 75 DAP. *Note*: SA-Salicylic acid 100 ppm; CS-Chitosan 100 ppm; SN-Silver nitrate 100 ppm; Pyr-Pyraclostrobin, Headline® 10 ml/20 L; Flu-Flutriafol, JOINT® 30 ml/20 L; ZON-Zinc oxide commercial NP, ZONO-S1® 20 ml/20 L. 1 The CS (0.4%/ or 0.5%) and pentasodium triphosphate (0.2%/ or 0.5%) were mixed with SA 0.2%/ or silver nitrate 3 mM to prepare formulation CS-NP-loaded SA N3/ or formulation CS-NP-loaded Ag N6, respectively.

4.4 Discussion

The hydrodynamic diameter of CS-NP-loaded SA (N3) was 89.86 ± 9.04 nm, which is smaller than the size of CS-NP-loaded SA in the study of Kumaraswamy *et al*. (2019) at 368.7 nm. However, the PDI and zeta potential of N3 are larger and smaller, respectively. Previously, CS-NP-loaded Ag was synthesized by the ionic gelation method with size 90.29 nm and zeta potential +92.05 mV with antibacterial properties that apply in medical (pharmaceutical) (Du *et al*., 2009). In plant disease management, CS-NP-loaded metals are usually Cu and Zn. In these studies, the DLS of CS-NP loaded Cu was 295.4 nm, PDI 0.28, 19.6 mV (Choudhary *et al*., 2017a), 314 nm, PDI 0.48, 19.5 mV (Swati, 2020), 361.3 nm, PDI 0.2, 22.1 mV (Choudhary *et al*., 2017b), 374.3 nm, PDI 0.33, 22.6 mV (Saharan *et al*., 2015), 196.4 nm, PDI 0.5, +88 mV (Saharan *et al*., 2013). And DLS of CS-NP-loaded Zn was 387 nm, PDI 0.22, 34 mV (Choudhary *et al*., 2019). In which, NPs in the studies of Swati (2020), Choudhary *et al*. (2017b), Saharan *et al*. (2015), Choudhary *et al*. (2019) were used as elicitors. The CS-NP loaded Ag (N6) with size 249.67 ± 23.97 nm which was smaller than the size of NPs in these studies. But the PDI and zeta potential of N3 are larger and smaller, respectively. This is also the first case study in plant disease management. The FTIR test was shown the interaction of primary amide, amide group, anhydro glycoside group in CS-NP loaded SA (N3) and CS-NP loaded Ag (N6) formulations compared with CS bulk. The peak 3422 (NH_2 stretch), 1656 ($CO\text{-}NH_2$), 1597 (NH_2 bend), 897 (Anhydro glycoside) of bulk CS shifted to 3421, 1640, 1540, 895 cm^{-1} in N3 and 3423, 1643, 1542, 894 cm^{-1} in N6, respectively. And the shifted to 1314 cm^{-1} in N3 showed interaction of COOH and NH_2. There FTIR peaks are different from previous studies but still in the range that confirms successful synthesis (Ji *et al*., 2011; Choudhary *et al*., 2019, Kumaraswamy *et al*., 2019).

Before application on the cassava plant, the CS-NPs loaded -SA and -Ag were tested phytotoxicity with cassava leaf by leaf disk assay method (Tanapichatsakul *et al*., 2020). In previous, this method has also been used to determine the dose threshold for toxicity of 8-methoxynaphthalen-1-ol – an antifungal compound on

tomato and (±)-botryodiplodin – a phytotoxin produced by *M. phaseolina* caused charcoal rot disease on soybeans (Abbas *et al*., 2020; Tanapichatsakul *et al*., 2020). The results shown that the CS-NPs formulations were not cause necrotic spots or the browning around leaves disks margin. But the SN treatment turn leaves disks margin to brown color (**Figure 4.5**). That confirmed NP formulations has a potential non-toxicity for cassava plant compared with using single chemical (SN). That allowed NP formulations could be treated on the cassava plants. Recent studies also showed that metal NPs (Ag, MgO, ZnO) can directly affect fungal pathogens, a bacterial pathogen, at *in vitro*, greenhouse, and field conditions (Gunalan *et al*., 2012; Chen *et al*., 2020; Ghazy *et al*., 2021). Interestingly, the effectiveness of reducing soft rot disease incidence and enhancing sugar beet growth, sucrose content by Ag-NP treatment was higher than that of *Bacillus subtilis* or algal extract (Ghazy *et al*., 2021). Furthermore, MgO-NPs was able to inhibit spore germination, sporangium formation, and hyphal development of *Phytophthora nicotianae* and *Thielaviopsis basicola*, as well as reduced tobacco black shank and black root rot disease with efficacy control reaching 50.20 and 62.10%, respectively (Chen *et al*., 2020). These CS-NPs continued to further research on the following experiments at net house conditions.

The net house experiment was conducted to select one CS-NP-loaded SA and one CS-NP-loaded Ag as effective formulations with effective concentrations to reduce cassava leaf spot disease as an elicitor (pre-treating before pathogen infection). Through 3 rounds of statistical analysis of disease severity and/or disease index data, the N3 at 400 ppm and N6 at 200, 400, and 800 ppm were shown as high-potential elicitors (**Figure 4.1**). Specifically, six formulations with six concentrations were statistically analyzed by two factors, which showed that CS-NP-loaded SA (N3) and CS-NP-loaded Ag (N6) were effective formulations. The results of the second statistical analysis showed that the N3 at 400 ppm and N6 at 200, 400, 800 ppm were effective concentrations to reduce cassava leaf spot disease by 68.9, 72.9, 73.6, 73.2%, respectively. Therefore, they were selected for further inoculated pathogen at 63 DAP

(3 weeks after the last time spraying treatment). The results showed that they were also effective in reducing disease by 37.0, 37.4, 37.0, 37.7%, respectively. The zinc oxide commercial NPs has the ability to reduce cassava leaf spot disease. Of these, pyraclostrobin was more effective than flutriafol at 56 DAP (59.6 and 54.7%) but lower at 75 DAP (14.7 and 35.4%). The control cassava brown leaf spot disease (*Clarohilum henningsii*) by spraying fungicide at 10 DAI. A study by Julião *et al*. (2020) showed that flutriafol was more effective than pyraclostrobin on reducing the area under the disease progress curve by 68.7 and 11.3%, respectively. In addition, zinc oxide commercial NPs only reduces 55.7 and 14.2% at 56 and 75 DAP, respectively. That is significantly lower than the effective concentrations of N3 and N6. In enhancing cassava growth, the effective concentration usually did not significantly increase the shoot height (-13.4-9.1%) but the opposite was true for the number of leaves (45.1-82.4%) and shoot (38.5-46.2%). Bedides, these treatments significantly increase the largest leaf area (29.6-41.9%), root length (11.6-29.9%), root weight (27.6-82.8%). The zinc oxide commercial NPs is usually higher potential to enhance plant growth because the active ingredient was ZnO that contains the important nutrient element (Zn) for plant growth. Overall, N3 and N6 treatments took the spotlight in reducing leaf spot disease and enhance plant growth on cassava in this study.

In this study, the CS-NPs loaded -SA or -Ag formulations were used as elicitors that can induce plant defense system against pathogens. In previous studies, both CS-NPs and CS-NPs loaded active ingredients were reported to be able to reduce plant diseases. CS-NPs was shown to inhibit the mycelial growth of *A. alternata*, *A. solani* up to 87% at *in vitro* conditions (Saharan *et al*., 2013; Sathiyabama *et al*., 2016; Popova *et al*., 2020). CS-NPs loaded with saponin, copper inhibited mycelial growth and spore germination of *A. alternata* by up to 80.9-89.5% and 82.9-87.4%, respectively (Saharan *et al*., 2013). In the study of Saharan *et al*. (2015), CS-NP-loaded copper inhibited mycelial and spore germination of *A. solani* by up to 84.2% and 60.1%, respectively.

Furthermore, CS-NP-loaded copper could reduce tomato early blight disease up to 87.7% at net house conditions.

CS-NPs at 1000, 1000, and 500 ppm have been reported that reducing rice sheath blight (Divya *et al*., 2020), finger millet blast (Sathiyabama *et al*., 2016b), and wheat *Fusarium* head blight (Kheiri *et al*., 2017) by inducing peroxidase, phenylalanine ammonia-lyase, chitinase, reactive oxygen species, superoxide activity, and H_2O_2 content in plant, respectively. In addition, CS-NPs has been loaded with active ingredients including harpin protein (Nadendla *et al*., 2018), Cu (Choudhary *et al*., 2017b), Zn (Choudhary *et al*., 2019), SA (Kumaraswamy *et al*., 2019), thiamine (Muthukrishnan *et al*., 2019) that can induce plants defense system against the infection of *R. solani* (Tomato), *C. lunata* (Maize), *F. verticillioides* (Maize), *F. oxysporum* (Chickpea) by inducing catalase, chitinase, phenylalanine ammonia-lyase, peroxidase, polyphenol oxidase, protease, superoxide dismutases, β-1,3-glucanase activity, superoxide anion, H_2O_2 content and lignin localization. Moreover, the CS-NP-loaded Cu reduced bacterial pustule disease in soybean by 40.6-49.7% but interestingly, low concentration (0.06%) was more effective than the high concentration (0.16%) (Swati, 2020). In our study, the N3 at 400 ppm was more effective than either 800 ppm or the N3 at 25 ppm was equally effective at 100, 200, and 800 ppm. A mixture of CS-NP (ionic gelation method) and Cu-NPs (chemical reduction method) can also reduce vascular wilt disease in date palm by 16.2-59.3% by inducing total phenol, phenoloxidase, peroxidase (Mohamed *et al*., 2018).

The formulations contain CS, SA, or Ag, so the effectiveness in disease reduction may be due to the synergistic effect of CS and SA or Ag. This is the direct effect of the NP formulations. Besides, NPs can be a good carrier to transport CS, SA, or Ag into plant cells, leading to an indirect effect on increasing plant resistance against plant diseases.

The plant innate immune system has three stages including perception, signal transduction, and defense response. This process could be induced by elicitors (Corwin and Kliebenstein, 2017).

The CS can act as an elicitor that activates a plant's innate immunity including stimulating H_2O_2 production, nitric oxide, generate PR protein, oxidative burst, enzymes, callose, secondary metabolite (phytoalexin, suberin, lignin, phenolic compounds) (Hadwiger, 2013; Kashyap *et al*., 2015; Chakraborty *et al*., 2020). In the study of Jogaiah *et al*. (2020), CS treatment (2.5 mg/ml) increased plant height (39%), stem girth (44%), and reduced powdery mildew (*Erysiphe cichoracearum*) disease (66.6%) on cucumber. Furthermore, this effect was associated with an increase in the production of benzyl aminopurine, indole acetic acid, 1-napthol acetic acid and lignin, callose and H_2O_2, polyphenol oxidase, phenylalanine ammonia-lyase, peroxidase, glucanase in the plant.

SA is a plant hormone that plays a role in plant germination, growth, and immunity. In the cells, endogenous SA is produced by phenylalanine ammonia-lyase and isochorismate pathways. Moreover, when SA concentration is increased, the cellular reduction potential is changed the NPR1 structure changes to a monomer that can enter the nucleus. Here, NPR1 binds to specific TGA transcriptions factors and then expresses defense against pathogen attack (Guilfoyle *et al*., 2015; Maruri-López *et al*., 2019). SA treatment can increase plant defense system in chickpea including enzymes (peroxidase, polyphenol oxidase), total phenol, H_2O_2, protein content (War *et al*., 2011). Previously, Saengchan *et al*. (2021) reported that exogenous SA treatment (1 mM) was able to reduce bacterial leaf blight in rice by 38% with increase superoxide anion production and hypersensitive response, as well as lignin and pectin content in the cell walls. In addition, the formatted SA (Zacha11 at 500 mg/L) has increased stem height, root length, and the number of roots and reduce root rot disease by 53.33% on cassava.

Silver nitrate also has effects on plants depending on the concentration. Murashige and Skoog medium containing silver nitrate (1 mg/L) could increase rooted shoots (63.6%), plant height (78.6%), number of roots (181.3%), root length (508%), and reduced bacterial contamination in *Gentiana lutea* tissue culture (Petrova *et al*.,

2011). Furthermore, Murashige and Skoog medium adding silver nitrate (1 mg/L) could improve the quality shoot and decrease the time required for rooting early than 2 months in 2 cultivars of *Anthurium andraeanum* under tissue culture (Cardoso, 2019). In addition, Ejaz *et al*. (2018) compared the effectiveness of silver nitrate and Ag-NP (green synthesis) on the growth of rice under biotic stress conditions. The results showed that Ag-NP was more effective than silver nitrate at the same 75 mg/L concentration in increasing root length (1.2 and 12.8%), shoot length (21 and 20%), root number (8.1 and 6.8%), fresh weight (6.4 and 5%), dry weight (4.6 and 3.5%), leaf area (58.5 and 57.2%), leaf number (4.3 and 3.7%), lead fresh weight (1.7 and 1.4%), leaf dry weight (0.9 and 0.8%) under *Aspergillus* infection. Furthermore, the aflatoxins of Ag-NP were 3.5±0.1 µg/kg compared with silver nitrate was 3.9±0.3 µg/kg. In Salama, (2012)'s study, Ag-NP (60 ppm) also increased common bean and maize growth including shoot length (47.0 and 27.9%), root length (56.1 and 46.1%), fresh weight (85.9 and 109.2%), dry weight (74.4 and 122.0%), leaf area (56.5 and 70.0%), chlorophyll a (49.0 and 46.0%), chlorophyll b (33.0 and 26.0%), carbohydrate content (57.0 and 62.0%). However, at higher concentrations (100 ppm), growth was reduced. In addition, Ag-NP (50 ppm) in lilies treatment resulted in increased plant height (7.6%), number of leaves (27.2%), greenness index (17.6%), leaf fresh weight (35.1%), bulb fresh weight (73.4%), number of scales (24.3%) but at higher concentrations the effect is not equal or equivalent (Salachna *et al*., 2019).

Why are NP formulations highly effective on reducing plant diseases and enhancing plant growth? In general, the preeminent characteristics of NPs are their small size, large contact surface area, and high reactivity leading to their application on controling disease and enhance growth on plants (Elmer and White, 2018). NPs can be absorbed by plants through foliar, brand, trunk, and root (Mittal *et al*., 2020). CS-NPs with nano size and positive charge lead to them being able to easily penetrate cells or stick to plant surfaces (Chakraborty *et al*., 2020). CS-NPs can enter the plant via leaves (stomata and cuticular pathway) and roots (diffusion and cuticular pathway).

The stomata of cassava leaves from 18.2-24.9 µm × 12.1-16.1 µm (Mondin *et al*., 2018). The hydrodynamic diameter of N3 and N6 was 89.86 ± 9.04 and 249.67 ± 23.97 nm with PDI was 0.36 ± 0.02 and 0.53 ± 0.03, the zeta potential was 22.27 ± 1.01 and 13.53 ± 0.74 mV, respectively. Therefore, these NPs can pass through the stomata or be easily absorbed by the cassava plant. CS-NPs can adjust osmotic pressure in the cell resulting in increased uptake and availability of water and nutrients (Guan *et al*., 2009). In addition, when sticking to plants, the CS-NPs loaded with active ingredients including hexaconazole, Zn, Cu, SA, harpin protein, NPK, silicon can slow-release their active ingredients so that plants can absorb them slowly that reported in the studies (Choudhary *et al*., 2017b; Nadendla *et al*., 2018; Maluin *et al*., 2019; Choudhary *et al*., 2019; Kumaraswamy *et al*., 2019; Ha *et al*., 2019; Kumaraswamy *et al*., 2021). CS is commonly used as a carrier due to solubility in aqueous media and is able to mix with organic or inorganic or copolymer compounds to increase solubility (Das and Pattanayak, 2020). The main component of CS is nitrogen, so the carrier (CS) can act as a source of nitrogen for plants to absorb, or enhance cell division, cell elongation, enzymatic activation, synthesis of protein lead to increase yield (Agarwal *et al*., 2015; Chakraborty *et al*., 2020).

4.5 Conclusion

In this study, three formulations CS-NP-loaded SA (N1, N2, N3) and three formulations CS-NP-loaded Ag (N4, N5, N6) were synthesized by ionic gelation method. The leaf disk assay method confirmed CS-NP formulations does not cause toxicity on cassava leave up to 800 ppm. The CS-NPs formulations at 25-800 ppm were mainly applied as elicitors. The results showed that the CS-NP-loaded SA (N3) and CS-NP-loaded Ag (N6) were more effective than the remaining other formulations (N1, N2, and N4, N5) in reducing disease severity and disease index of leaf spot. The N3 at 400 and N6 at 200, 400, 800 ppm could reduce disease severity 68.9-73.6% and 37.0-37.7% when fungal pathogen was inoculated at 2 and 21 days after spraying elicitor with

density 10^4 and 10^5 conidia per mL, respectively. That was more effective than commercial zinc oxide NP (ZON) was 55.7 and 14.2%, pyraclostropin (Pyr) fungicide was 59.6 and 14.7%, flutriafol (Flu) fungicide was 54.7 and 35.4%, respectively. The N3 and N6 treatments have also enhanced cassava growth including shoot height, the number of leaves, the number of shoots, the largest leaf area, root length, and root weight with a similar effect to the positive control group. That indicates the potential to use CS-NP-loaded SA or Ag at low concentration (200-400 ppm) as elicitors to manage cassava leaf spot disease. The limitation of ionic gelation method is that their NP is difficult to have uniform size, resulting in unstable efficiency. And the effect of size of NP on plant disease management also varied between reports. To solve this problem, the study in this article is approached with a focus on reverse research model from preparing elicitors, toxicity test, screening formulation effectiveness to concentration effectiveness and characterization effective elicitors. This research motif focuses first on the effectiveness in *in-vivo* (net-house) condition after preparing elicitors and toxicity test instead of *in-vitro* condition. Finally, only the high effective formulations were CS-NP loaded SA (N3) and CS-NP loaded Ag (N6) were characterized instead of focusing on all six formulations from the start. In addition, the NP formulations in this research were focused for use as elicitors at low concentrations. Therefore, the effective concentration of NP formulation does not necessarily inhibit fungal pathogens, which are often concentrated in *in-vitro* experiments. This reduces the time and cost of the research process. The field experiment (200 – 400 ppm) is still needed before it is widely recommended. This research motif and CS-NPs based ionic gelation method also holds promise in plant or agricultural disease management, especially in areas where modern techniques are limited.

4.6 Reference

Abbas, H.K., Bellaloui, N., Butler, A.M., Nelson, J.L., Abou-Karam, M. & Shier, W.T. (2020). Phytotoxic responses of soybean (*Glycine max* L.) to botryodiplodin, a toxin produced by the charcoal rot disease fungus, *Macrophomina phaseolina*. *Toxins*, 12(1): p.25. doi:10.3390/toxins12010025.

Agarwal, M., Nagar, D. P., Srivastava, N., & Agarwal, M. K. (2015). Chitosan nanoparticles-based drug delivery: An update. *International Journal of Advanced Multidisciplinary Research,* 2(4): 1-13.

Ali, M. Z., Khan, M. A. A., Rahaman, A. K. M. M., Ahmed, M., & Ahmed, F. (2011). Effect of fungicides on *Cercospora* leaf spot and seed quality of mungbean. *Journal of Experimental Biosciences*, 2(1): 21-26.

Ashraf, S.A., Siddiqui, A.J., Abd Elmoneim, O.E., Khan, M.I., Patel, M., Alreshidi, M., Moin, A., Singh, R., Snoussi, M., & Adnan, M. (2021). Innovations in nanoscience for the sustainable development of food and agriculture with implications on health and environment. *Science of the Total Environment*, 768: p.144990. doi:10.1016/j.scitotenv.2021.144990.

Ayesu-Offei, E. N., & Antwi-Boasiako, C. (1996). Production of microconidia by *Cercospora henningsii* Allesch, cause of brown leaf spot of cassava (*Manihot esculenta* Crantz) and tree cassava (*Manihot glaziovii* Muell.-Arg.). *Annals of Botany*, 78(5): 653-657. doi:10.1006/anbo.1996.0173.

Beckman, P. M., & Payne, G. A. (1983). Cultural techniques and conditions influencing growth and sporulation of *Cercospora zeae-maydis* and lesion development in corn. *Phytopathology*, 73(2): 286-289.

Burketova, L., Trda, L., Ott, P. G., & Valentova, O. (2015). Bio-based resistance inducers for sustainable plant protection against pathogens. *Biotechnology Advances*, 33(6): 994-1004. doi:10.1016/j.biotechadv.2015.01.004.

Calvo, P., Remunan-Lopez, C., Vila-Jato, J. L., & Alonso, M. J. (1997a). Novel hydrophilic chitosan-polyethylene oxide nanoparticles as protein carriers. *Journal of Applied Polymer Science*, 63(1): 125-132. doi:10.1002/(SICI)1097-4628(19970103)63:1<125::AID-APP13>3.0.CO;2-4.

Calvo, P., Remuñan-López, C., Vila-Jato, J. L., & Alonso, M. J. (1997b). Chitosan and chitosan/ethylene oxide-propylene oxide block copolymer nanoparticles as novel carriers for proteins and vaccines. *Pharmaceutical Research*, 14(10): 1431-1436. doi:10.1023/A:1012128907225.

Cardoso, J. C. (2019). Silver nitrate enhances *in vitro* development and quality of shoots of *Anthurium andraeanum*. *Scientia Horticulturae*, 253: 358-363. doi:10.1016/j.scienta.2019.04.054

Chakraborty, M., Hasanuzzaman, M., Rahman, M., Rahman Khan, M., Bhowmik, P., Mahmud, N.U., Tanveer, M. & Islam, T. (2020). Mechanism of plant growth promotion and disease suppression by chitosan biopolymer. *Agriculture*, 10(12): p.624. doi:10.3390/agriculture10120624.

Chen, J., Wu, L., Lu, M., Lu, S., Li, Z., & Ding, W. (2020). Comparative study on the fungicidal activity of metallic MgO nanoparticles and macroscale MgO against soilborne fungal phytopathogens. *Frontiers in Microbiology*, 11: p.365. doi:10.3389/fmicb.2020.00365

Choudhary, M. K., Joshi, A., Sharma, S. S., & Saharan, V. (2017a). Effect of laboratory synthesized Cu-Chitosan nanocomposites on control of PFSR disease of maize caused by *Fusarium verticillioids*. *International Journal of Current Microbiology and Applied Sciences*, 6: 1656-1664. doi:10.20546/ijcmas.2017.608.199.

Choudhary, R. C., Kumaraswamy, R. V., Kumari, S., Sharma, S. S., Pal, A., Raliya, R., Biswas, P., & Saharan, V. (2019). Zinc encapsulated chitosan nanoparticle to promote maize crop yield. *International Journal of Biological Macromolecules*, 127: 126-135. doi:10.1016/j.ijbiomac.2018.12.274.

Choudhary, R. C., Kumaraswamy, R. V., Kumari, S., Sharma, S. S., Pal, A., Raliya, R., Biswas, P., & Saharan, V. (2017b). Cu-chitosan nanoparticle boost defense responses and plant growth in maize (*Zea mays* L.). *Scientific Reports*, 7(1): 1-11. doi:10.1038/s41598-017-08571-0.

Corwin, J. A., & Kliebenstein, D. J. (2017). Quantitative resistance: more than just perception of a pathogen. *The Plant Cell*, 29(4): 655-665. doi:10.1105/tpc.16.00915.

Das, S., & Pattanayak, S. (2020). Nanotechnological approaches in sustainable agriculture and plant disease management. In Das, S. K. (Ed). *Organic Agriculture*. (1 st, 18 pp). London: IntechOpen. doi: 10.5772/intechopen.92463

de Freitas, J. P. X., Diniz, R. P., de Oliveira, S. A. S., da Silva Santos, V., & de Oliveira, E. J. (2017). Inbreeding depression for severity caused by leaf diseases in cassava. *Euphytica*, 213(9): 1-12. doi:10.1007/s10681-017-1995-0.

Debnath, S., Kumar, R. S., & Babu, M. N. (2011). Ionotropic gelation–a novel method to prepare chitosan nanoparticles. *Research Journal of Pharmacy and Technology*, 4(4): 492-495.

Divya, K., Thampi, M., Vijayan, S., Varghese, S., & Jisha, M. S. (2020). Induction of defence response in *Oryza sativa* L. against *Rhizoctonia solani* (Kuhn) by chitosan nanoparticles. *Microbial Pathogenesis*, 149: p.104525. doi:10.1016/j.micpath.2020.104525.

Du, W. L., Niu, S. S., Xu, Y. L., Xu, Z. R., & Fan, C. L. (2009). Antibacterial activity of chitosan tripolyphosphate nanoparticles loaded with various metal ions. *Carbohydrate Polymers*, 75(3): 385-389. doi:10.1016/j.carbpol.2008.07.039.

Ejaz, M., Raja, N. I., Ahmad, M. S., Hussain, M., & Iqbal, M. (2018). Effect of silver nanoparticles and silver nitrate on growth of rice under biotic stress. *IET Nanobiotechnology*, 12(7): 927-932. doi:10.1049/iet-nbt.2018.0057.

Elemike, E. E., Uzoh, I. M., Onwudiwe, D. C., & Babalola, O.O. (2019). The role of nanotechnology in the fortification of plant nutrients and improvement of crop production. *Applied Sciences*, 9(3): p.499. doi:10.3390/app9030499.

Elmer, W., & White, J. C. (2018). The future of nanotechnology in plant pathology. *Annual Review of Phytopathology*, 56: 111-133. doi:10.1146/annurev-phyto-080417-050108.

FAOSTAT, (2021). Rankings. Countries by commodity. Retrieved from https://www.fao.org/faostat/en/#rankings/countries_by_commodity_exports

Ghazy, N. A., Abd El-Hafez, O. A., El-Bakery, A. M., & El-Geddawy, D. I. (2021). Impact of silver nanoparticles and two biological treatments to control soft rot disease in sugar beet (*Beta vulgaris* L). *Egyptian Journal of Biological Pest Control*, 31(1): 1-12. doi:10.1186/s41938-020-00347-5.

Giri, T. K. (2016). Alginate containing nanoarchitectonics for improved cancer therapy. In Holban A. M. & Grumezescu A. M. (Eds.). *Nanoarchitectonics for Smart Delivery and Drug Targeting* (1st ed., pp. 565-588). Oxford: William Andrew.

Gleadow, R., Pegg, A., & Blomstedt, C. K. (2016). Resilience of cassava (*Manihot esculenta* Crantz) to salinity: implications for food security in low-lying regions. *Journal of Experimental Botany*, 67(18): 5403-5413. doi:10.1093/jxb/erw302.

Guan, Y. J., Hu, J., Wang, X. J., & Shao, C. X. (2009). Seed priming with chitosan improves maize germination and seedling growth in relation to physiological changes under low temperature stress. *Journal of Zhejiang University Science B*, 10(6): 427-433. doi:10.1631/jzus.B0820373.

Guilfoyle, T., Hagen, G., Liu, X., Rockett, K. S., Kørner, C. J., & Pajerowska-Mukhtar, K. M. (2015). Salicylic acid signalling: new insights and prospects at a quarter-century milestone. *Essays in Biochemistry*, 58: 101-113. doi:10.1042/bse0580101.

Gunalan, S., Sivaraj, R., & Rajendran, V. (2012). Green synthesized ZnO nanoparticles against bacterial and fungal pathogens. *Progress in Natural Science: Materials International*, 22(6): 693-700. doi:10.1016/j.pnsc.2012.11.015.

Ha, N. M. C., Nguyen, T. H., Wang, S. L., & Nguyen, A. D. (2019). Preparation of NPK nanofertilizer based on chitosan nanoparticles and its effect on biophysical characteristics and growth of coffee in green house. *Research on Chemical Intermediates*, 45(1): 51-63. doi:0.1007/s11164-018-3630-7.

Hadwiger, L. A. (2013). Multiple effects of chitosan on plant systems: Solid science or hype. *Plant Science*, 208: 42-49. doi:10.1016/j.plantsci.2013.03.007.

Hidayat, I., Hastuty, A., & Ramadhani, I. (2020). A molecular phylogenetic study of *Clarohilum henningsii* (Mycosphaerellaceae, Fungi) on cassava from Indonesia based on the ITS rDNA sequence. *Journal of Microbial Systematics and Biotechnology*, 2(1): 40-45. doi:10.37604/jmsb.v2i1.43.

Ji, J., Hao, S., Wu, D., Huang, R., & Xu, Y., 2011. Preparation, characterization and in vitro release of chitosan nanoparticles loaded with gentamicin and salicylic acid. *Carbohydrate Polymers*, 85(4): 803-808. doi:10.1016/j.carbpol.2011.03.051.

Jogaiah, S., Satapute, P., De Britto, S., Konappa, N., & Udayashankar, A. C. (2020). Exogenous priming of chitosan induces upregulation of phytohormones and

resistance against cucumber powdery mildew disease is correlated with localized biosynthesis of defense enzymes. *International Journal of Biological Macromolecules*, 162: 1825-1838. doi:10.1016/j.ijbiomac.2020.08.124.

Julião, E. C., Santana, M. D., Freitas-Lopes, R. D. L., Vieira, A. D. P., de Carvalho, J. S. B., & Lopes, U. P. (2020). Reduction of brown leaf spot and changes in the chlorophyll a content induced by fungicides in cassava plants. *European Journal of Plant Pathology*, 157(2): 433–439. doi:10.1007/s10658-020-02001-0.

Kashyap, P. L., Xiang, X., & Heiden, P. (2015). Chitosan nanoparticle based delivery systems for sustainable agriculture. *International Journal of Biological Macromolecules*, 77: 36-51. doi:10.1016/j.ijbiomac.2015.02.039.

Kheiri, A., Jorf, S. M., Malihipour, A., Saremi, H., & Nikkhah, M. (2017). Synthesis and characterization of chitosan nanoparticles and their effect on Fusarium head blight and oxidative activity in wheat. *International Journal of Biological Macromolecules*, 102: 526-538. doi:10.1016/j.ijbiomac.2017.04.034.

Koukaras, E. N., Papadimitriou, S. A., Bikiaris, D. N., & Froudakis, G. E. (2012). Insight on the formation of chitosan nanoparticles through ionotropic gelation with tripolyphosphate. *Molecular Pharmaceutics*, 9(10): 2856-2862. doi:10.1021/mp300162j.

Kumaraswamy, R. V., Kumari, S., Choudhary, R. C., Sharma, S. S., Pal, A., Raliya, R., Biswas, P., & Saharan, V. (2019). Salicylic acid functionalized chitosan nanoparticle: a sustainable biostimulant for plant. *International Journal of Biological Macromolecules*, 123: 59-69. doi:10.1016/j.ijbiomac.2018.10.202.

Kumaraswamy, R. V., Saharan, V., Kumari, S., Choudhary, R. C., Pal, A., Sharma, S. S., Rakshit, S., Raliya, R., & Biswas, P. (2021). Chitosan-silicon nanofertilizer to enhance plant growth and yield in maize (*Zea mays* L.). *Plant Physiology and Biochemistry*, 159: 53-66. doi:10.1016/j.plaphy.2020.11.054

Kunjachan, S., Jose, S., & Lammers, T. (2014). Understanding the mechanism of ionic gelation for synthesis of chitosan nanoparticles using qualitative techniques. *Asian Journal of Pharmaceutics*, 4(2): 148-153. doi:10.4103/0973-8398.68467.

Liu, C., Zhou, H., & Zhou, J., 2021. The Applications of Nanotechnology in Crop Production. *Molecules*, 26(23): p.7070. doi:10.3390/molecules26237070.

Malerba, M., & Cerana, R. (2019). Recent applications of chitin-and chitosan-based polymers in plants. *Polymers*, 11(5): p.839. doi:10.3390/polym11050839.

Maluin, F. N., Hussein, M. Z., Yusof, N. A., Fakurazi, S., Idris, A. S., Zainol Hilmi, N. H., & Jeffery Daim, L. D. (2019). Preparation of chitosan–hexaconazole nanoparticles as fungicide nanodelivery system for combating Ganoderma disease in oil palm. *Molecules*, 24(13): p.2498. doi:10.3390/molecules24132498.

Maruri-López, I., Aviles-Baltazar, N. Y., Buchala, A., & Serrano, M. (2019). Intra and extracellular journey of the phytohormone salicylic acid. *Frontiers in Plant Science*, 10: p.423. doi:10.3389/fpls.2019.00423.

McCallum, E. J., Anjanappa, R. B., & Gruissem, W. (2017). Tackling agriculturally relevant diseases in the staple crop cassava (*Manihot esculenta*). *Current Opinion in Plant Biology*, 38: 50-58. doi:10.1016/j.pbi.2017.04.008.

Mittal, D., Kaur, G., Singh, P., Yadav, K., & Ali, S. A. (2020). Nanoparticle-based sustainable agriculture and food science: recent advances and future outlook. *Frontiers in Nanotechnology*, 2: p.10. doi:10.3389/fnano.2020.579954.

Mohamed, E. A., Gaber, M. H., & Elsharabasy, S. F. (2018). Evaluating the *in vivo* efficacy of copper-chitosan nanocomposition for treating vascular wilt disease in date palm. *International Journal of Environment, Agriculture and Biotechnology*, 3(2): p.239085. doi:10.22161/ijeab/3.2.17.

Mondin, M., Latado, R. R., & Mourão, F. D. A. A. (2018). *In vitro* induction and regeneration of tetraploids and mixoploids of two cassava cultivars. *Crop Breeding and Applied Biotechnology*, 18: 176-183. doi:10.1590/1984-70332018v18n2a25.

Muthukrishnan, S., Murugan, I., & Selvaraj, M. (2019). Chitosan nanoparticles loaded with thiamine stimulate growth and enhances protection against wilt disease in Chickpea. *Carbohydrate Polymers*, 212: 169-177. doi:10.1016/j.carbpol. 2019.02.037.

Nadendla, S. R., Rani, T. S., Vaikuntapu, P. R., Maddu, R. R., & Podile, A. R., 2018. $Harpin_{Pss}$ encapsulation in chitosan nanoparticles for improved bioavailability and disease resistance in tomato. *Carbohydrate Polymers*, 199: 11-19. doi:10.1016/j.carbpol.2018.06.094.

Ng'ang, P. W., Miano, D. W., Wagacha, J. M., & Kuria, P. (2019). Identification and characterization of causative agents of brown leaf spot disease of cassava in Kenya. *Journal of Applied Biology and Biotechnology*, 7(6): 1-7. doi:10.7324/JABB.2019.70601.

Noha, K., Bondok, A. M., & El-Dougdoug, K. A. (2018). Evaluation of silver nanoparticles as antiviral agent against ToMV and PVY in tomato plants. *Middle East Journal of Applied Sciences*, 8(01): 100-111.

Paramo, L. A., Feregrino-Pérez, A. A., Guevara, R., Mendoza, S., & Esquivel, K. (2020). Nanoparticles in agroindustry: Applications, toxicity, challenges, and trends. *Nanomaterials*, 10(9): p.1654. doi:10.3390/nano10091654.

Pedroso-Santana, S., & Fleitas-Salazar, N. (2020). Ionotropic gelation method in the synthesis of nanoparticles/microparticles for biomedical purposes. *Polymer International*, 69(5): 443-447. doi:10.1002/pi.5970.

Pei, Y. L., Shi, T., Li, C. P., Liu, X. B., Cai, J. M., & Huang, G. X. (2014). Distribution and pathogen identification of cassava brown leaf spot in China. *Genetics and Molecular Research*, 13(2): 3461-3473. doi:10.4238/2014.April.30.7.

Perina, F. J., Belan, L. L., Moreira, S. I., Nery, E. M., Alves, E., & Pozza, E. A. (2019). Diagrammatic scale for assessment of *Alternaria* brown spot severity on tangerine leaves. *Journal of Plant Pathology*, 101(4): 981-990. doi:10.1007/s42161-019-00306-6.

Petrova, M., Zayova, E., & Vitkova, A. (2011). Effect of silver nitrate on in vitro root formation of *Gentiana lutea*. *Romanian Biotechnological Letters*, 16(6): 53-58.

Poletto, T., Muniz, M. F., Fantinel, V. S., Favaretto, R. F., Poletto, I., Reiniger, L. R., & Blume, E. (2018). Culture Medium, Light Regime and Temperature Affect the Development of *Sirosporium diffusum*. *Journal of Agricultural Science*, 10(6): 310-318. doi:10.5539/jas.v10n6p310.

Popova, E. V., Zorin, I. M., Domnina, N. S., Novikova, I. I., & Krasnobaeva, I. L. (2020). Chitosan–tripolyphosphate nanoparticles: Synthesis by the ionic gelation method, properties, and biological activity. *Russian Journal of General Chemistry*, 90(7): 1304-1311. doi:10.1134/S1070363220070178.

Prabakar, K., & Raguchander, T. (2000). Fungicidal control of cassava brown leaf spot caused by *Cercospora henningsii* Allescher. *Madras Agricultural Journal*, 87(7/9), 537-538.

Rajput, V. D., Singh, A., Minkina, T., Rawat, S., Mandzhieva, S., Sushkova, S., Shuvaeva, V., Nazarenko, O., Rajput, P., Verma, K. K., & Singh, A.K. (2021). Nano-Enabled Products: Challenges and Opportunities for Sustainable Agriculture. *Plants*, 10(12): p.2727. doi:10.3390/plants10122727.

Reddy, P. P. (2015). Cassava, *Manihot esculenta*. In P. P. Reddy (Ed.). *Plant Protection in Tropical Root and Tuber Crops* (1st ed, pp. 17-81). New Delhi: Springer India.

Rodriguez, V. A., Bolla, P. K., Kalhapure, R. S., Boddu, S. H. S., Neupane, R., Franco, J., & Renukuntla, J. (2019). Preparation and characterization of furosemide-silver complex loaded chitosan nanoparticles. *Processes*, 7(4): p.206. doi:10.3390/pr7040206.

Rozhin, A., Batasheva, S., Kruychkova, M., Cherednichenko, Y., Rozhina, E., & Fakhrullin, R. (2021). Biogenic Silver Nanoparticles: Synthesis and Application as Antibacterial and Antifungal Agents. *Micromachines*, 12(12): p.1480. doi:10.3390/mi12121480

Saengchan, C., Phansak, P., Le Thanh, T., Papathoti, N. K., & Buensanteai, N. (2021). Efficacy of salicylic acid and a *Bacillus* bioproduct in enhancing growth of cassava and controlling root rot disease. *Journal of Plant Protection Research*, 61(3): 302-310. doi:10.24425/jppr.2021.137952.

Saharan, V., Mehrotra, A., Khatik, R., Rawal, P., Sharma, S. S., & Pal, A. (2013). Synthesis of chitosan based nanoparticles and their *in vitro* evaluation against phytopathogenic fungi. *International Journal of Biological Macromolecules*, 62: 677-683. doi:10.1016/j.ijbiomac.2013.10.012.

Saharan, V., Sharma, G., Yadav, M., Choudhary, M. K., Sharma, S. S., Pal, A., Raliya, R., & Biswas, P. (2015). Synthesis and *in vitro* antifungal efficacy of Cu–chitosan nanoparticles against pathogenic fungi of tomato. *International Journal of Biological Macromolecules*, 75: 346-353. doi:10.1016/j.ijbiomac.2015.01.027.

Salachna, P., Byczyńska, A., Zawadzińska, A., Piechocki, R., & Mizielińska, M. (2019). Stimulatory effect of silver nanoparticles on the growth and flowering of potted oriental lilies. *Agronomy*, 9(10): 610. doi:10.3390/agronomy9100610.

Salama, H. M. (2012). Effects of silver nanoparticles in some crop plants, common bean (*Phaseolus vulgaris* L.) and corn (*Zea mays* L.). *International Research Journal of Biotechnology*, 3(10): 190-197.

Sangpueak, R., Phansak, P., Thumanu, K., Siriwong, S., Wongkaew, S., & Buensanteai, N. (2021. Effect of salicylic acid formulations on induced plant defense against cassava anthracnose disease. *The Plant Pathology Journal*, 37(4): p.356. doi:10.5423/PPJ.OA.02.2021.0015.

Sathiyabama, M. & Parthasarathy, R. (2016a). Biological preparation of chitosan nanoparticles and its *in vitro* antifungal efficacy against some phytopathogenic fungi. *Carbohydrate Polymers*, 151: 321-325. doi:10.1016/j.carbpol.2016.05.033.

Sathiyabama, M., & Manikandan, A. (2016b). Chitosan nanoparticle induced defense responses in fingermillet plants against blast disease caused by *Pyricularia grisea* (Cke.) Sacc. *Carbohydrate Polymers*, 154: 241-246. doi:10.1016/j.carbpol.2016.06.089.

Shang, Y., Hasan, M., Ahammed, G. J., Li, M., Yin, H., & Zhou, J. (2019). Applications of nanotechnology in plant growth and crop protection: a review. *Molecules*, 24(14): 2558. doi:10.3390/molecules24142558.

Singh, J., Dutta, T., Kim, K. H., Rawat, M., Samddar, P., & Kumar, P. (2018). 'Green'synthesis of metals and their oxide nanoparticles: applications for environmental remediation. *Journal of Nanobiotechnology*, 16(1): 1-24. doi:0.1186/s12951-018-0408-4.

Swati, K.J.A.J. (2020). Cu-chitosan nanoparticle induced plant growth and antibacterial activity against bacterial pustule disease in soybean (*Glycine max* (L.)). *Journal of Pharmacognosy and Phytochemistry*, 9(1): 450-455.

Tanapichatsakul, C., Pansanit, A., Monggoot, S., Brooks, S., Prachya, S., Kittakoop, P., Panuwet, P., & Pripdeevech, P. (2020). Antifungal activity of 8-methoxynaphthalen-1-ol isolated from the endophytic fungus *Diatrype*

palmicola MFLUCC 17-0313 against the plant pathogenic fungus *Athelia rolfsii* on tomatoes. *PeerJ*, 8: p.e9103. doi:10.7717/peerj.9103.

Teri, J. M., Thurston, H. D., & Lozano, J. C. (1980). Effect of brown leaf spot and Cercospora leaf blight on cassava productivity. *Tropical Agriculture*, 57(3): 239-243.

Uchechukwu-Agua, A. D., Caleb, O. J., & Opara, U. L. (2015). Postharvest handling and storage of fresh cassava root and products: a review. *Food and Bioprocess Technology*, 8(4): 729-748. doi:10.1007/s11947-015-1478-z.

Ur Rahim, H., Qaswar, M., Uddin, M., Giannini, C., Herrera, M. L., & Rea, G. (2021). Nano-enable materials promoting sustainability and resilience in modern agriculture. *Nanomaterials*, 11(8): p.2068. doi:10.3390/nano11082068.

War, A. R., Paulraj, M. G., War, M. Y., & Ignacimuthu, S. (2011). Role of salicylic acid in induction of plant defense system in chickpea (*Cicer arietinum* L.). *Plant Signaling & Behavior*, 6(11): 1787-1792. doi:10.4161/psb.6.11.17685.

Worrall, E. A., Hamid, A., Mody, K. T., Mitter, N., & Pappu, H. R. (2018). Nanotechnology for plant disease management. *Agronomy*, 8(12): 285. doi:10.3390/agronomy8120285.

Zielińska, A., Costa, B., Ferreira, M.V., Miguéis, D., Louros, J., Durazzo, A., Lucarini, M., Eder, P., V Chaud, M., Morsink, M. & Willemen, N. (2020). Nanotoxicology and nanosafety: Safety-by-design and testing at a glance. *International Journal of Environmental Research and Public Health*, 17(13): p.4657. doi:10.3390/ijerph17134657.

CHAPTER V

EFFICACY OF EFFECTIVE NANOPARTICLES ON LEAF SPOT SEVERITY AND THE PATHOGEN *ALTERNARIA ALTERNATA*

ABSTRACT

Cassava is a major smallholder economic crop in Thailand and recently has severe damage from diseases. The nanoparticles (NPs) are an ecologically promising way to directly inhibit phytopathogens and enhance plant health against leaf spot – an important disease on cassava. This study aims to evaluate (1) the effectiveness of pre- and post-treatments of chitosan (CS)-NP formulations to reduce cassava leaf spot in net-house conditions; (2) assessment of NP efficacy on conidial germination, antifungal activity and fungal viability of pathogen *Alternaria alternata*. The results showed that the mean disease severity of pre- and post-treatment was no significance. While the mean disease severity of CS-NP treatments was 26.77-28.11% similar to flutriafol (28.65%), which significantly lower than commercial zinc oxide NPs (32.58%). The CS-NP loaded salicylic acid 400 ppm and silver 200 ppm treatment could inhibit conidial germination by 32.51 and 23.25%, respectively. The soaking *A. alternata* H-Vi 7 plugs into these two treatments could reduce mycelial growth and their potential virulence causing rot lesions by 42.26 and 51.11%, respectively. Furthermore, these two treatments caused a higher cell death/live rate than commercial zinc oxide NPs but lower than flutriafol. These results indicated CS-NP formulations as a promising solution in cassava leaf spot management.

Keywords: Leaf spot; Chitosan; Fugal virulence; Nanoparticles; Salicylic acid; Silver

5.1 Introduction

Cassava (*Manihot esculenta* Crantz) is an important food crop in the world. Cassava and its product are food for humans, feed for livestock, and raw materials for the industry (Uchechukwu-Agua *et al*., 2015). Thailand's cassava production reached 31.1 million tons in 2019, accounting for 10.24% of the world and 41.52% of Southeast Asia production (FAOSTAT, 2021a). In 2019, the export volume of dried cassava, starch, and flour of Thailand were 1.76, 2.66, and 0.03 million tons, respectively, which always ranked first in the world with a total value of 1.77 billion USD (FAOSTAT, 2021b). The cassava stages are common for 12 months with accumulated leaves, stems, and root biomass. In which, the leaves are formed at the beginning and are maintained until the end (De Souza *et al*., 2017). Through this process, cassava plants or cassava leaves are attacked by many kinds of fungi, viruses, bacteria, and phytoplasma. In which, leaf spot is a common, important disease that broke out recently on cassava, leading to loose yield up to 30% (McCallum *et al*., 2017; Julião *et al*., 2020). In a recent study by Ng'ang'a *et al*. (2019), the cassava leaf spot disease has been reported caused by fungus *Alternaria* sp. The test of fungicide for disease control has been practiced by Julião *et al*. (2020). The results showed that azoxystrobin, cyproconazole, flutrifol, pyraclostrobin, tebuconazole, thiophanate-methyl could all reduce the disease with different degrees of efficacy. The use of fungicide is effective but also toxic to humans, animals, environment, and the potential for degradation in the next generation (Gupta, 2018). An alternative is needed to mitigate these risks as well as build sustainable agriculture.

Each kind of plant has an innate immune system to counteract adverse environmental factors including abiotic and biotic stresses, which varies resistance level depending on the cultivar and stress factors. The plant innate immune system has three stages including perception, signal transduction, and defense response. When pathogens attack plants, the receptors on the plasma membrane recognize damage or microbe/pathogen -associated molecular patterns. Then, signals were formed and

transmitted to the nucleus by mitogen activated protein kinase (MAPK) cascade and transcription factors. Here, defense responses were active including reactive oxygen species production, callose deposition, and camalexin production against the pathogens. This system can be artificially enhanced by elicitors – biotic or abiotic compounds, to against stress factors. The elicitors can be chemical, microbial, chitosan (CS), poly- and oligoglucans, plant extracts, algal extracts, extracts of higher plants, composts, biochar. There are two types of stimulated plant resistance including systemic acquired resistance and induced systemic resistance, depending on the signaling pathway including salicylic acid (SA) for systemic acquired resistance, jasmonic acid and ethylene for induced systemic resistance as well as the elicitors (Burketova *et al*., 2015; Corwin and Kliebenstein, 2017). As such, applying the right elicitors would aid plants against pathogens.

Nanotechnology is a trend in modern agriculture. The particles in nanoscale possess the preeminent property of small size and large surface contact area, high reactivity that has many applications in agriculture as well as in plant science. The nanoparticles (NPs) can be applied in the production of nanopesticides, nanofertilizers, nanosensors, nanobiosensors, nano-carriers to enhance biomass and yield, optimal sources (soil, water, material), to protect the crop, to improve nutrient absorption, to predict pest, to store and transport agri-product (Medina-Pérez *et al*., 2019; Mittal *et al*., 2020; Younas *et al*., 2020). In plant disease management, the NPs can be used as an alternative to agrochemicals to directly inhibit phytopathogen and also enhance plant health to fight diseases. These are safe and sustainable strategies to serve crop production especially in the context of climate change (Elmer and White, 2018; Worrall *et al*., 2018; Sanzari *et al*., 2019).

In previous studies, a treatment of zinc oxide NPs leads to protein leakage and could inhibit many kinds of fungi (*Aspergillus flavus*, *Aspergillus nidulans*, *Rhizopus stolonifera*, and *Trichoderma harzianum*) and bacteria (*Citrobacter freundii*, *Serratia marcescens*, *Staphylococcus aureus*, *Proteus mirabilis*) at *in vitro* conditions (Gunalan

et al., 2012). Silver NP treatment could control soft rot disease on sugar beet at field conditions with efficacy of 76.16-94.11%, which higher than using *Spirulina platensis* extract (47.07-82.36%) and *Bacillus subtilis* (64.71-65.25%) – the bio control agents (Ghazy *et al*., 2021). The magnesium oxide NPs could inhibit *Phytophthora nicotianae* and *Thielaviopsis basicola*, and their root irrigation reduced tobacco black shank and black root rot disease by 50.2 and 62.1% at greenhouse conditions, respectively (Chen *et al*., 2020). CS-NPs showed an excellent antifungal activity with *Alternaria tenuis*, *Aspergillus niger*, *A. flavus*, *Beauveria bassiana*, *Fusarium graminearum*, *Fusarium oxysporum*, *Penicillium* sp. and *Sclerotium rolfsii* (Abdel-Aliem *et al*., 2019). CS-NP loaded -SA (800-1600 ppm) were able to inhibit mycelial growth and spore germination of *Fusarium verticillioides* by 62.2-100% and 48.3-60.5%, respectively. Moreover, this NPs can act as an elicitor to elevate antioxidant-defense, enzyme activities, balance of reactive oxygen species, cell wall reinforcement by lignin deposition, and reduce maize post-flowering stalking rot by 59.4% at field conditions (Kumaraswamy *et al*., 2019). CS-NP, CS-NP loaded saponin and copper could inhibit mycelial growth (65.3-80.1, 70.2-78.3, and 69.3-82.1%, respectively) and conidia germination (68.5-84.4, 73.1-78.3 and 69.3-83.3%, respectively) of *Alternaria alternata* (Saharan *et al*., 2013).

This research was conducted with the aim to evaluate the effectiveness of pre- and post-CS-NP formulations treatment to reduce cassava leaf spot disease at net house conditions. Furthermore, the research also assessed the NP efficacy on conidial germination, antifungal activity and fungal viability of pathogen *A. alternata*.

5.2 Materials and methods

5.2.1 Materials

The two NP formulations were synthesized by ionic gelation method including CS-NP loaded SA and CS-NP loaded silver with hydrodynamic diameter was 89.86 ± 9.04 nm and 249.67 ± 23.97 nm, PDI was 0.36 ± 0.02 and 0.53 ± 0.03, the zeta potential

was 22.27 ± 1.01 and 13.53 ± 0.74 mV, respectively (Chapter IV). These two NP formulations were used on this research.

The virulent fungi *A. alternata* strain H-Vi 7 causing cassava leaf spot disease was provided by the Plant Pathology & Biopesticide Laboratory, Suranaree University of Technology, Thailand. The fungus from the Eppendorf stock was cultured onto potato dextrose agar for 2 weeks. The agar containing fungal colony was cut into pieces to enhance conidia production. The conidia suspension was collected by adding sterilized DI water and filtering through fabric that was adjusted to 1×10^5 conidia mL^{-1} (Pei *et al*., 2014).

5.2.2 Evaluating the application way of effective nanoparticle formulations on reducing cassava leaf spot severity in net-house conditions

The experiment was carried out in a completely randomized design with 11 treatments, 2 factors, four replications. For pre-treatment (factor applying method), the stalks of cassava varieties Pirun 2 were soaked for 5 minutes with water control (T1), SA 100 ppm (T2), CS 100 ppm (T3), silver nitrate 100 ppm (T4), pyraclostrobin (T5, Headline® , BASF Thailand, Bangkok, Thailand, 10 ml/20 L), flutriafol (T6, JOINT®, Sotus International Company Limited, Nonthaburi, Thailand, 30 ml/ 20 L), commercial zinc oxide NP (T7, ZONO-S1®, IRPC Public Company Limited, Rayong, 20 ml/20 L), CS-NP loaded SA 400 ppm (T8), CS-NP loaded silver at 200 ppm (T9), 400 ppm (T10), 800 ppm (T11) (factor treatment). At 28 and 42 days after planting (DAP), the plants were sprayed with treatments at a volume of 5 ml per plant. The net conditions had light regime of 12 light/12 h dark, 28 ± 2°C, RH 80 ± 6%. At 44 DAP, the plants were inoculated with conidia suspension of *A. alternata* H-Vi 7 until the leaves runoff. For post-treatment (factor applying method), the cassava plants were inoculated with the pathogen similar to pre-treatment group at 44 DAP, then sprayed with treatments at 48 DAP. Then, the inoculated plants were incubated with high relative humidity (>80%) conditions by covering plastic, spraying water and keep under black sun shade orchid

net to reduce 50% of light intensity (Pei *et al*., 2014; Kumaraswamy *et al*., 2019; Julião *et al*., 2020; Sangpueak *et al*., 2021). At 56 DAP, the disease score was assessed based on the diagrammatic scale (0 to 8) following the description of Perina *et al*. (2019). The DS (disease severity) was calculated following formula:

$$\text{DS (\%)} = \frac{\text{Sum of all numerical scoring}}{\text{The number of leaves} \times \text{Maximum score}} \times 100\%$$

The control efficacy was calculated based on DS with the formula:

$$\text{Control efficacy (\%)} = \frac{\text{DS of negative control} - \text{DS of the rest treatment}}{\text{DS of negative control}} \times 100\%$$

Where DS of negative control is the disease severity in T1 treatment. DS of the rest treatment is the disease severity in T2-T11 treatments.

5.2.3 Inhibition ability of nanoparticle formulations on conidial germination

The conidia suspension of *A. alternata* H-Vi 7 was prepared as above mentioned. The inhibition of conidial germination was performed according to the description of Chen *et al*. (2020) with modification. Briefly, 500 µL of conidial suspension was mixed with 500 µL of the treatment at 2X concentration to achieve the final concentrations as T1, T6, T7, T8, T9 treatments in Eppendorf. Then, the mixture was incubated for 24 hours. The ratio of the number of germinated conidia to the total number of conidia observed in a 10X objective area was recorded as a percent germination rate. The percent inhibitory rate was calculated based on the formula of Saharan *et al*. (2013) as followed:

$$\text{Inhibitory rate (\%)} = \frac{GR_C - GR_T}{GR_C} \times 100$$

Where GR_c is the percent germination rate in T1 treatment (control), and GR_T is the percent germination rate in T6, T7, T8, T9 treatment. The mean of 50 conidia

was calculated. The experiment was performed in completely randomized design with 3 replications.

5. 2. 4 Evaluation on antifungal activity of nanoparticle formulations in detached leaves

For soaking treatment, the 9 mm-diameter of potato dextrose agar plug containing *A. alternata* H-Vi 7 was cultured in a 30 mL-glass bottle containing a mixture of potato dextrose broth 2X and treatment with ratio 1:1 to obtain the final concentration as treatments (T1, T6, T7, T8, T9). The glass bottle was shaken in an Incubator Shaker at 150 rpm, 28 ± 1 °C for 24 h. The cassava leaves were sterilized with 70% ethanol and placed three layers of tissue paper added sterilized water in the box. Then, the fungi plugs were put into surface cassava leaves and incubated for 5 days to measure the diameter of the rot lesions.

For spraying treatment, the cassava leaves were sprayed with treatments (T1, T6, T7, T8, T9) after preparing as described above. After that, the agar plugs contained fungi without soaking in treatment were put into surface leaves and evaluated as described above. The experiment was carried out in completely randomized design with 4 replications (one agar plug per replication). The percent inhibition percentage (IP) was calculated based on the formula:

$$\text{IP}\ (\%) = \frac{\text{Diameter rot of T1} - \text{Diameter rot of the rest treatment}}{\text{Rot diameter of T1}} \times 100\%$$

Where Diameter rot of the rest treatment is the rot diameter in T6, T7, T8, T9 treatment.

5.2.5 Assessing the viability of fungus by treating nanoparticle formulations

The experiment was performed in completely randomized design with 4 replications. The viability of mycelium was determined by staining them with propidium iodide (PI) as well as SYTO 9 and observed under confocal microscopy. The mixture of PI and SYTO 9 with a ratio 1:1 was prepared before use by LIVE/DEAD™ BacLight™ Bacterial Viability Kit (Invitrogen by Thermo Fisher Scientific). The mycelia from agar plug treatment (T1, T6, T7, T8, T9) was prepared as a soaking treatment part, which was stained with PI and SYTO 9 for 15 min in dark conditions. Then, the mycelia were observed under confocal microscopy (Nikon A1plus with N-SIM, Nikon, Japan) using a filter of 488 nm for SYTO 9 and 561 nm for PI. The red and green fluorescent indicate non-viability and viability mycelial, respectively (Hoque *et al*., 2015).

5.2.6 Data analysis

The DS (disease severity) was analyzed following 2 factor. The percent germination rate and diameter rot were analyzed following Duncan's Multiple Range Test (DMRT). The F value detected the significance of treatments P = 0.05.

5.3 Results

5.3.1 Efficacy of nanoparticle formulations on reducing cassava leaf spot disease

The disease severity and control efficacy on leaf spot disease treated by NP formulations were shown in **Table 5.1, Figure 5.1** and **5.2**.

The mean disease severity of pre- and post-treatment (factor applying method) was no significance. The mean disease severity of factor treatment (T1 to T11) was significant between water control, commercial fungicide, and NP formulation treatments. The mean disease severity of CS-NP treatments (T8 to T11) was 26.77-

28.11% similar to flutriafol (T6) was 28.65%, which significantly lower than the others treatment including water control, SA (T2), CS (T3), silver nitrate (T4), pyraclostrobin (T5) and commercial zinc oxide NP (T7). The mean control efficacy of NP formulation treatments (T8 to T11) and flutriafol (T7) were 40.74-43.54 and 39.61% compared with water control, respectively, while commercial NP (T7) and pyraclostrobin (T5) were 31.34 and 32.58%, respectively. Besides, single chemical (T2 to T4) was 20.61 to 25.27%.

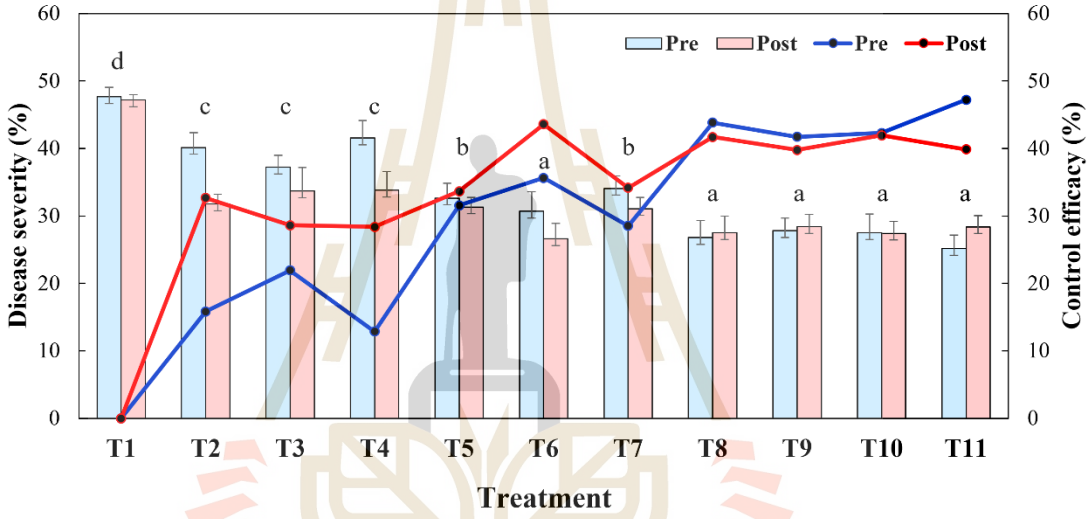

Figure 5.1 The disease severity and control efficacy of leaf spot disease at net house conditions. *Note:* Water control (**T1**), SA 100 ppm (**T2**), CS 100 ppm (**T3**), silver nitrate 100 ppm (**T4**), Pyraclostrobin (**T5**, Headline® 10 ml/20 L), Flutriafol (**T6**, JOINT® 30 ml/ 20 L), commercial zinc oxide NP (**T7**, ZONO-S1®, 20 ml/20 L), CS-NP loaded SA 400 ppm (**T8**), CS-NP loaded silver at 200 ppm (**T9**), 400 ppm (**T10**), 800 ppm (**T11**). For **Pre**, the stalks of cassava varieties Pirun 2 were soaked for 5 minutes before planting and foliar-sprayed at 28 and 42 day after planting (DAP). For **Post**, the cassava plants were planted without treatment and foliar sprayed at 48 DAP. All cassava plants were inoculated with *A. alternata* H-Vi 7 at 44 DAP. Means followed by the same letter do not differ significantly according to DMRT at $P \leq 0.01$ (**).

Table 5.1 The disease severity and control efficacy of leaf spot disease at net house conditions

Treatment[1]	Disease severity (%)			Control efficacy (%)		
	Applying method[2]		Mean[3]	Applying method[2]		Mean
	Pre	Post		Pre	Post	
Water control (T1)	47.67	47.19	47.43 d	0.00	0.00	0.00
SA 100 ppm (T2)	40.13	31.77	35.95 c	15.82	32.67	24.25
CS 100 ppm (T3)	37.23	33.68	35.46 c	21.91	28.62	25.27
Silver nitrate 100 ppm (T4)	41.55	33.80	37.68 c	12.85	28.36	20.61
Pyraclostrobin (T5)	32.64	31.32	31.98 b	31.53	33.63	32.58
Flutriafol (T6)	30.68	26.62	28.65 a	35.63	43.58	39.61
Commercial zinc oxide NP (T7)	34.08	31.07	32.58 b	28.51	34.16	31.34
CS-NP loaded SA 400 ppm (T8)	26.78	27.52	27.15 a	43.82	41.68	42.75
CS-NP loaded silver 200 ppm (T9)	27.79	28.42	28.11 a	41.71	39.76	40.74
CS-NP loaded silver 400 ppm (T10)	27.52	27.41	27.47 a	42.28	41.92	42.10
CS-NP loaded silver 800 ppm (T11)	25.17	28.37	26.77 a	47.21	39.87	43.54
Mean	33.75	31.56				
CV (%)	6.58					

[1] Water control (T1), SA 100 ppm (T2), CS 100 ppm (T3), silver nitrate 100 ppm (T4), Pyraclostrobin (T5, Headline® 10 ml/20 L), Flutriafol (T6, JOINT® 30 ml/ 20 L), commercial zinc oxide NP (T7, ZONO-S1®, 20 ml/20 L), CS-NP loaded SA 400 ppm (T8), CS-NP loaded silver at 200 ppm (T9), 400 ppm (T10), 800 ppm (T11) (Factor Treatment).

[2] For **Pre-treatment**, the stalks of cassava varieties Pirun 2 were soaked for 5 minutes before planting and foliar-sprayed at 28 and 42 day after planting (DAP). For **Post-treatment**, the cassava plants were planted without treatment and foliar sprayed at 48 DAP (Factor Applying method). All cassava plants were inoculated with the conidial suspension of *A. alternata* H-Vi 7 at 44 DAP.

[3] Means followed by the same letter do not differ significantly according to DMRT at $P \leq 0.01$ (**).

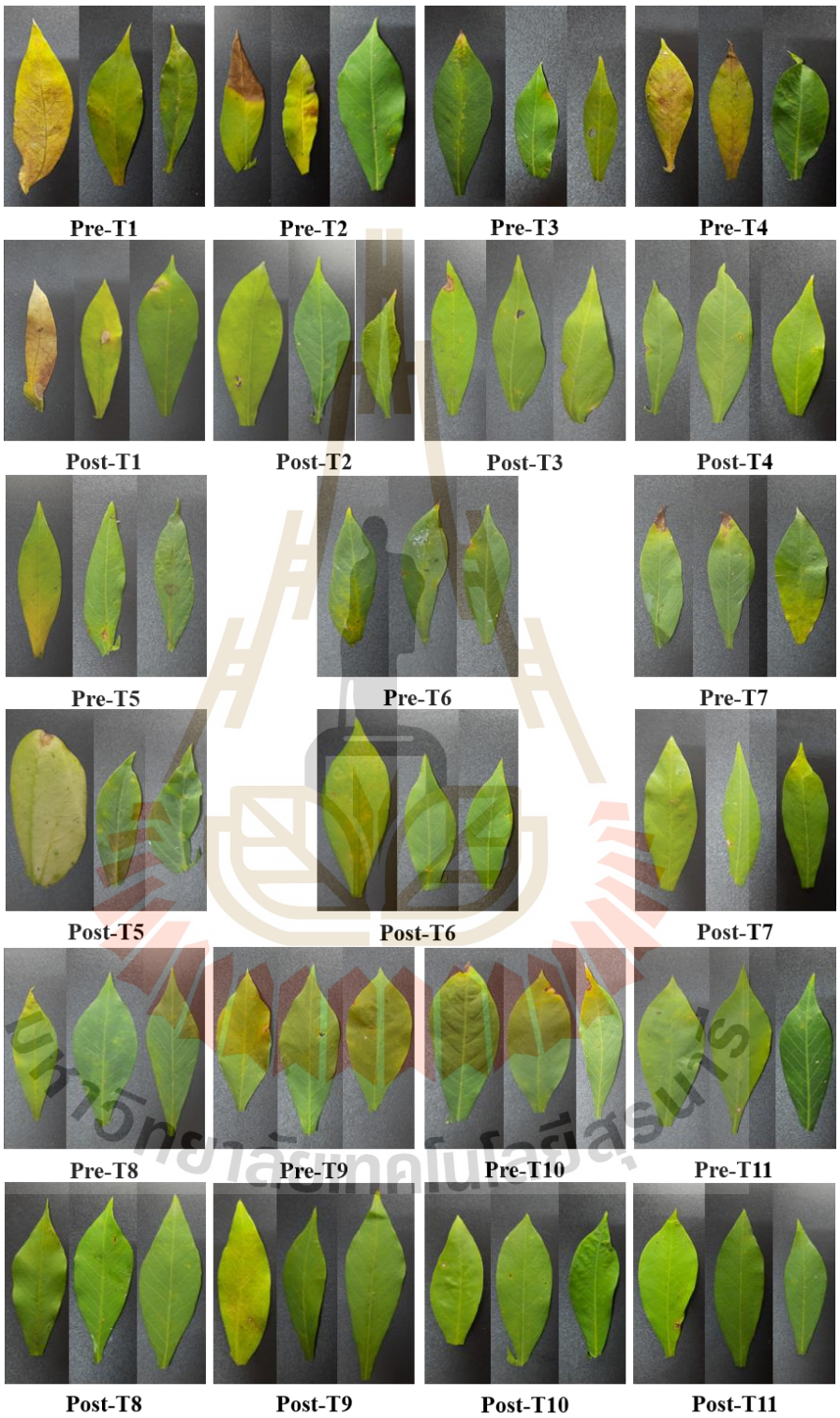

Figure 5.2 The symptom of cassava infected by *A. alternata* H-Vi 7 at net house conditions.

5.3.2 Inhibition ability of nanoparticle formulations on conidial germination

The inhibition ability of nanoparticle formulations on conidial germination *A. alternata* H-Vi 7 were shown in **Figure 5.3**. In overview, the percent inhibitory rate was 15.00 – 32.51%. The CS-NP loaded SA 400 ppm (T8) showed the highest inhibited conidial germination at 32.51% but no significance with flutriafol (T6) and CS-NP loaded silver 200 ppm (T9). The commercial NP (T7) could also inhibit conidial germination by 15.0%, but also no significance with T6 and T7 treatments.

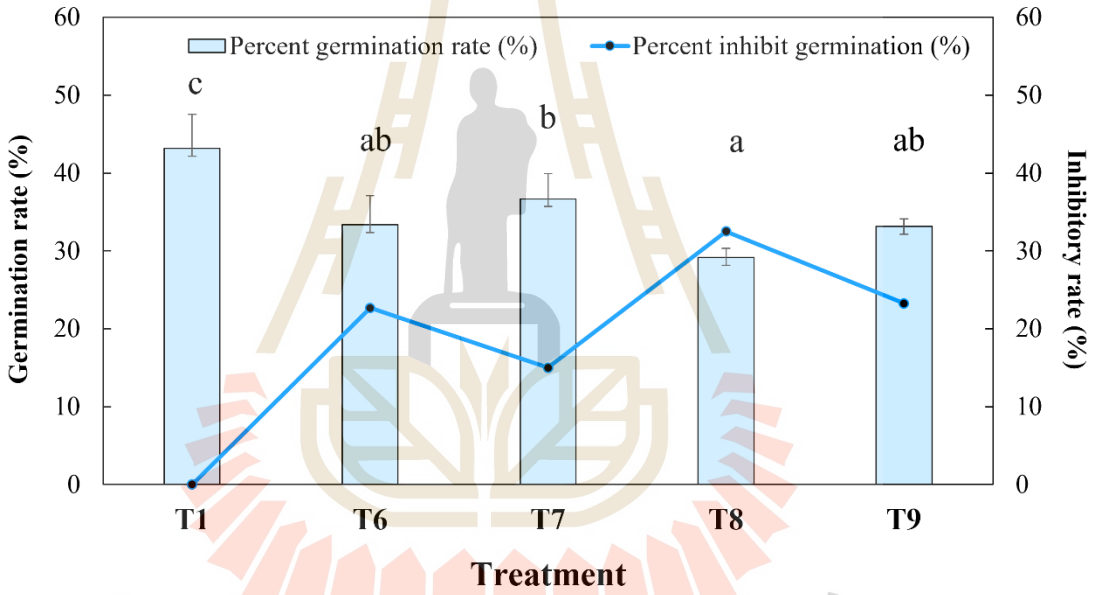

Figure 5.3 The percent germination rate and percent inhibitory rate of *A. alternata* H-Vi 7. *Note*: Water control (T1), Flutriafol (T6, JOINT® 30 ml/ 20 L), commercial zinc oxide NP (T7, ZONO-S1®, 20 ml/20 L), CS-NP loaded SA 400 ppm (T8), CS-NP loaded silver at 200 ppm (T9). Means followed by the same letter do not differ significantly according to DMRT at P ≤ 0.01 (**).

5.3.3 Antifungal efficacy of nanoparticle formulations in detached leaves

The antifungal activity of NP formulations in detached leaves is shown in **Table 5.2**, **Figure 5.4** and **5.5**.

For soaking treatment, the mycelia were grown from fungi plugs with various degrees at 24h after incubation. The mycelia of the water control treatment (T1) grow dense around the fungi plug. In contrast, both flutriafol (T6) and CS-NP loaded SA 400 ppm (T8) inhibited mycelial growth around the fungi plug. However, the surface of CS-NP loaded SA 400 ppm treatment (T8) had a fine gray-white layer indicating mycelium growth. The commercial zinc oxide NP (T7) was similar but mycelia were sparser than the water control treatment (T1). The CS-NP loaded silver 200 ppm (T9) inhibited mycelium growth at the lower surface fungi plug (**Figure 5.4a**).

For soaking treatment, the diameter rot treated by CS-NP loaded silver 200 ppm (T9) was significantly higher than CS-NP loaded SA 400 ppm (T8), commercial zinc oxide NP (T7) as well as control treatment but lower than flutriafol (T6). The inhibition percent of T8 and T9 were 42.26 and 51.11%, respectively, which was higher than T7 (16.95%) but lower than T6 (70.02%) (**Table 5.2, Figure 5.4b, Figure 5.5**).

For spraying treatment, the diameter rot treated by CS-NP formulations (T8, T9) were not significant but still lower than commercial zinc oxide NP (T7), control (T1), and both higher than flutriafol (T6). The inhibition percentages treated by T8 and T9 was 44.95 and 42.79%, respectively, which were higher than T7 (22.60%) but lower than T6 (58.41%) (**Table 5.2, Figure 5.4c, Figure 5.5**).

Table 5.2 The diameter rot and inhibition percentage of *A. alternata* H-Vi 7 by soaking and spraying treatments in detached leaves

Treatment[1]	Soak		Spray	
	Diameter rot[2] (mm)	Inhibition percentage (%)	Diameter rot[2] (mm)	Inhibition percentage (%)
Water control (T1)	40.7 e	-	41.6 d	-
Flutriafol (T6)	12.2 a	70.02	17.3 a	58.41
Commercial zinc oxide NP (T7)	33.8 d	16.95	32.2 c	22.60
CS-NP loaded SA 400 ppm (T8)	23.5 c	42.26	22.9 b	44.95
CS-NP loaded silver 200 ppm (T9)	19.9 b	51.11	23.8 b	42.79
F-test	**		**	
CV (%)	6.98		6.04	

[1] Water control (T1), Flutriafol (T6, JOINT® 30 ml/ 20 L), commercial zinc oxide NP (T7, ZONO-S1®, 20 ml/20 L), CS-NP loaded SA 400 ppm (T8), CS-NP loaded silver at 200 ppm (T9).

[2] Means followed by the same letter do not differ significantly according to DMRT at P ≤ 0.01 (**)

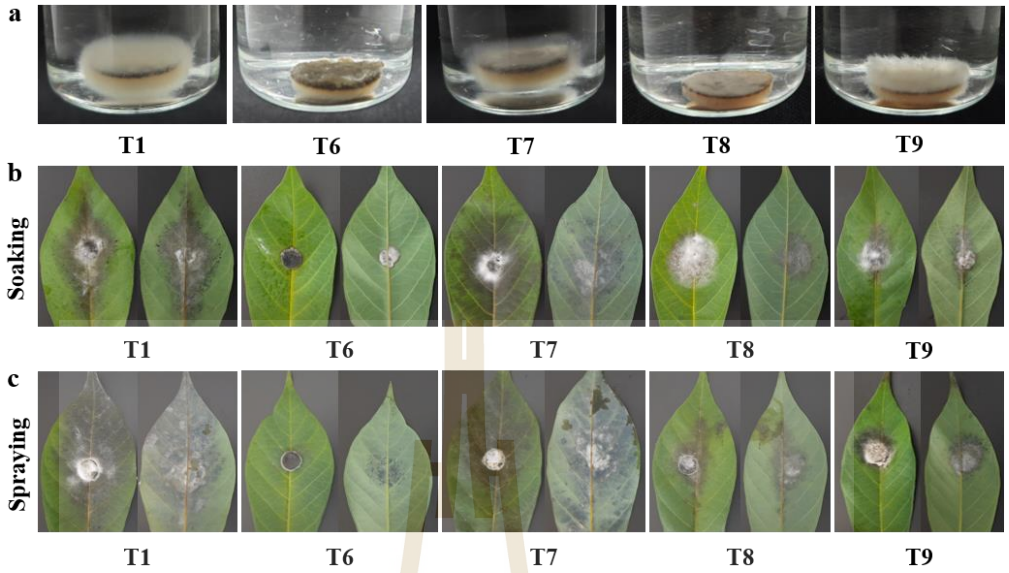

Figure 5.4 The morphology of *A. alternata* H-Vi 7 plug (**a**) and rot lesion (**b**) in soaking treatment, and spraying treatment (**c**).

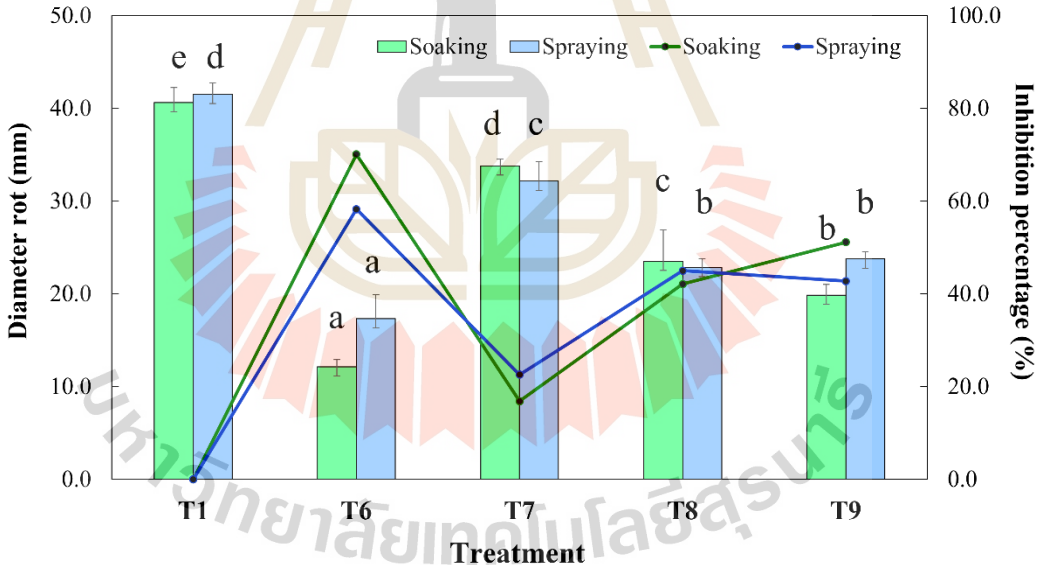

Figure 5.5 The diameter rot and inhibition percentage of *A. alternata* H-Vi 7 in detached leaves. *Note*: Water control (**T1**), Flutriafol (**T6**, JOINT® 30 ml/ 20 L), commercial zinc oxide NP (**T7**, ZONO-S1®, 20 ml/20 L), CS-NP loaded SA 400 ppm (**T8**), CS-NP loaded silver at 200 ppm (**T9**). Means followed by the same letter do not differ significantly according to DMRT at $P \leq 0.01$ (**).

5.3.4 The viability of fungal by treating nanoparticle formulation

Overall, all five treatments affected fungi viability including mycelial cell live and death to various degrees (**Figure 5.6**). The mycelia in the water control (T1) was mostly green fluorescent while flutriafol (T6) showed the majority of the red fluorescent. The CS-NP loaded silver 200 ppm (T9) and CS-NP loaded SA 400 ppm (T8) caused a higher cell death/live ratio than commercial zinc oxide NP (T7) but lower than flutriafol (T6).

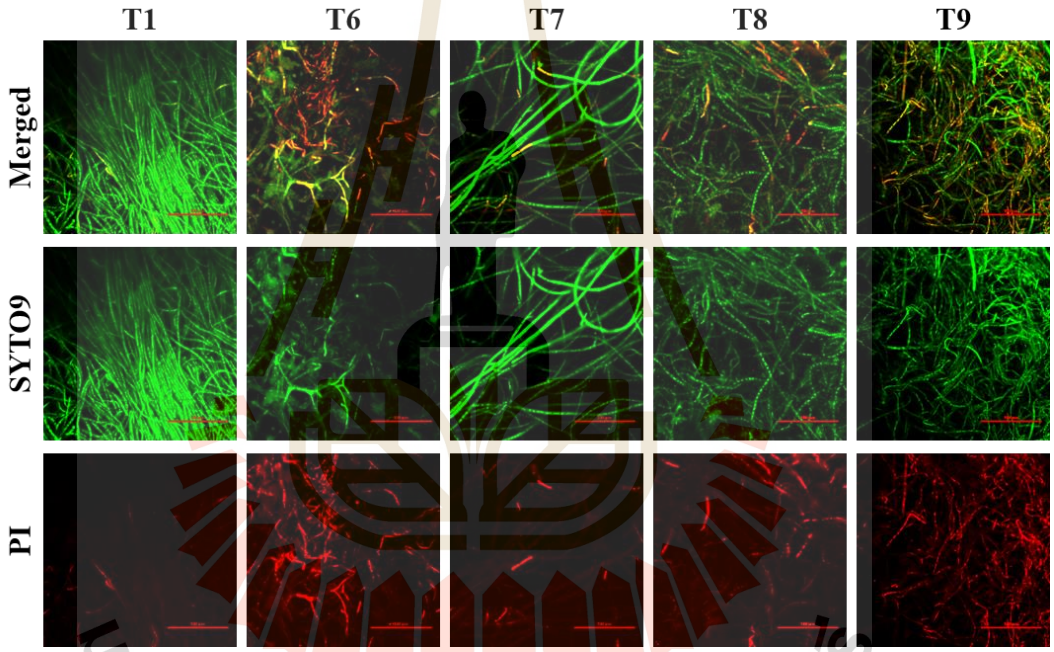

Figure 5.6 The viability of *A. alternata* H-Vi 7 observed under confocal microscopy. *Note*: The green and red color indicated cell live and death, respectively. Water control (**T1**), Flutriafol (**T6**, JOINT® 30 ml/ 20 L), commercial zinc oxide NP (**T7**, ZONO-S1®, 20 ml/20 L), CS-NP loaded SA 400 ppm (**T8**), CS-NP loaded silver at 200 ppm (**T9**).

5.4 Discussion

In this study, a net-house experiment was performed to evaluate the effect of two factors including NP formulations (CS-NP loaded SA 400 ppm, CS-NP loaded silver at 200, 400, 800 ppm) treatment and method (Pre and Post) treatment on reducing cassava leaf spot disease. The Pre and Post-treatment are designed to assess to the indirect and direct mechanisms. In this experiment, both CS-NP treatments (T8 to T11) showed efficacy (40.74-43.54%) similar to flutriafol (T6) but superior to the commercial zinc oxide NP (T7) in reducing leaf spot disease. Then, the lowest concentrations with similar efficacy of CS-NP loaded silver at 200 ppm (T9) and CS-NP loaded SA at 400 ppm (T8) were selected for comparison with commercial zinc oxide NP (T7), flutriafol (T6), water control (T1) for evaluating the ability to inhibit conidial germination, antifungal activity in detached leaves, and fungal viability. Overall, CS-NP loaded silver at 200 ppm (T9) and CS-NP loaded SA at 400 ppm (T8) both had similar and higher efficacy than commercial zinc oxide NP (T7) but lower than flutriafol (T6) treatment in antifungal activity. The CS-NP loaded SA at 400 ppm (T8) and CS-NP loaded silver at 200 ppm (T9) were inhibited conidial germination by 32.51 and 23.25%, respectively. This result is lower than that of CS-NPs, CS-NP loaded saponin and copper (200-600 ppm) reported in the study by Saharan *et al*. (2013) with inhibiting germination of *A. alternata* at 57.3-68.5, 73.1-78.3 and 69.3-83.3%, respectively. Besides, CS-NPs (2000 ppm) also inhibited *Colletotrichum gloeosporioides* conidial germination by 61.2% (Suryadi *et al*., 2019). In addition, a CS-NP loaded with other metals can also inhibit the spore germination of many fungal pathogens. CS-NP loaded copper inhibited conidial germination of *Alternaria solani* and *F. oxysporum* by 73.3 and 79.9% at 1000 ppm, respectively (Saharan *et al*., 2015). Similarly, CS-NP loaded zinc (100-800 ppm) and SA (800-1600 ppm) inhibited *Curvularia lunata* and *F. verticillioides* conidial germination by 50.6-73.3 and 48.3-60.5%, respectively (Choudhary *et al*., 2019; Kumaraswamy *et al*., 2019).

The CS-NP loaded SA at 400 ppm (T8) and CS-NP loaded silver at 200 ppm (T9) were inhibited mycelial growth when cultured the fungal plug into medium containing treatment (**Figure 5.4a**). Moreover, these agar plugs were also reduced in the ability to cause rot lesions on cassava leaves by 42.26 and 51.11%, respectively (**Table 5.2, Figure 5.4b**). This inhibition is related to the viability of fungi as examination under the confocal microscope shows that the ratio of mycelial death/live is similar to that of the rot lesions on cassava leaves (**Figure 5.6**). On the other hand, after spraying this treatment into the leaf surface and inoculated pathogen, the rot lesions were also reduced by 45.01 and 42.75%, respectively (**Table 5.2, Figure 5.4c**). Similar results were indicated on some previous researches. Anthracnose disease in chilli and papaya were inhibited by 75 and 10% when treating fruits with CS-NPs (2000 ppm) together with inoculating *C. gloeosporioides* (Suryadi *et al*., 2019). CS-NPs may inhibit mycelial growth of *A. alternata* (65.53-80.1%), *Rhizoctonia solani* (18.1-32.2%), *Macrophomina phaseolina* (87.3-87.5 %) at 200-600 ppm (Saharan *et al*., 2013), *Pyricularia grisea* (92%), *A. solani* (87%), *F. oxysporum* (72%) with amount of 100 µg (Sathiyabama and Parthasarathy, 2016), *P. grisea* (65%) at 1000 ppm (Sathiyabama and Manikandan, 2016), *A. tenuis* (67.67%), *A. niger* (62.75%), *Aspergillus terreus* (74.67%), *B. bassiana* (76.08%), *F. graminearum* (60.37%), *F. oxysporum* (66.60%), *S. rolfsii* (37.41%) at 800 ppm and the zearalenone produced by *F. graminearum* (Abdel-Aliem at al., 2019), *C. gloeosporioides* (37.8%), *Phytophthora capsica* (50.7%), *Sclerotinia sclerotiorum* (39.5%), *F. oxysporum* (50.3%), *Gibberella fujikuori* (56.3%) at 5000 ppm (Oh *et al*., 2019), *C. gloeosporioides* (85.7%) (Suryadi *et al*., 2019), *A. solani* (10.70%) at 300 and 400 ppm (Popova *et al*., 2020). In addition, CS-NP loaded copper could inhibit mycelial growth of *A. alternata* (69.3-82.1%), *M. phaseolina* (54.3-62.5%), *R. solani* (18.1-32.2%) at 200-600 ppm (Saharan *et al*., 2013), *A. solani* (52.7-68.7%) and *F. oxysporum* (60.3-73.3%) at 800-1000 ppm (Saharan *et al*., 2015), *C. lunata* by 50.0 and 52.7% at 1200 and 1600 ppm (Choudhary *et al*., 2017b), respectively. In addition, the mixture of CS-NPs (ionic gelation) and copper NPs (chemical reduction) could inhibit the mycelial growth of *F. oxysporum* by 61.94-100% at 500-2000 ppm (Mohamed *et al*., 2018). CS-

NP loaded with saponin inhibited the mycelial growth of *A. alternata* by 70.2-78.3% and *R. solani* by 22.8-27.7% at 200-600 ppm (Saharan *et al*., 2013). CS-NPs loaded zinc inhibited mycelial growth of *C. lunata* by 17.04-20.0% and 47.7-65.2% at 100-400 and 800-1600 ppm, respectively (Choudhary *et al*., 2019). CS-NP loaded SA could evade *F. verticillioides* mycelial growth by 62.2-100% at 800-1600 ppm (Kumaraswamy *et al*., 2019). However, in some reports, CS-NPs or CS-NP loaded thiamine did not inhibit mycelial growth, spore germination, sporulation of *P. grisea* or *F. oxysporum* even at high concentration at 1000 ppm (Sathiyabama and Manikandan, 2016; Manikandan and Sathiyabama, 2016; Muthukrishnan *et al*., 2019). This antifungal traits depend on the active ingredient, concentration, and type of fungus. High concentrations tend to be more inhibitory than low concentrations. To achieve 100% inhibition, concentrations should be up to 1600 ppm (CS-NP loaded SA) for *F. verticillioides* or 2000 ppm (CS-NP mixed copper NP) for *F. oxysporum* (Mohamed *et al*., 2018; Kumaraswamy *et al*., 2019). The use of NP treatment at high concentrations can be wasteful if the effectiveness of disease control is not increased at a linear rate. In addition, there are many factors in nature that affect pathogens, so even though the efficiency in *in-vitro* conditions can be up to 100%, the effect could be lower when applied at net house or field conditions. In the past, flutriafol has also shown better disease control than other fungicides including azoxystrobin, cyproconazole, pyraclostrobin, tebuconazole, thiophanate-methyl (Julião *et al*., 2020). At net house conditions, CS-NP and CS-NPs loaded active ingredients have been treated pre and post before inoculating fungal pathogens to reduce many plant diseases. Pre-treatment CS-NP (1000 ppm) could reduce sheath blight disease by 75.01% (Divya *et al*., 2020), decrease disease incidence of finger millet blast by 2.8 folds (Sathiyabama and Manikandan, 2016) by inducing peroxidase, phenylalanine ammonia-lyase, chitinase, peroxidase and reactive oxygen species activity. Interestingly, spraying CS-NP (500 ppm) after *F. graminearum* infected could reduce area under the disease progress curve by 2.2 folds and increase superoxide and H_2O_2 content in wheat (Kheiri *et al*., 2017). Similarly, CS-NP loaded copper and zinc (400-1200 ppm) could reduce maize leaf spot disease (*C. lunata*) by

43.86-46.97% and 46.24-50.72% (Choudhary *et al*., 2017b; Choudhary *et al*., 2019). CS-NP loaded SA (400-1600 ppm) could reduce post-flowering stalk rot at 49.49-49.52% (Kumaraswamy *et al*., 2019). CS-NP loaded thiamine could not inhibit *F. oxysporum* under *in vitro* conditions but pre-treatment at 3 days before fungal infection could reduce cell death in 2 days after inoculation compared with the control (Muthukrishnan *et al*., 2019). The defense system of the plants could elicit enzymes (catalase, chitinase, phenylalanine ammonia-lyase, peroxidase, protease, superoxide dismutases, β-1,3-glucanase, superoxide anion, H_2O_2 content and lignin formulation (Choudhary *et al*., 2017b; Choudhary *et al*., 2019; Kumaraswamy *et al*., 2019; Muthukrishnan *et al*., 2019). Application mixture of CS-NPs and copper NPs (500-2000 ppm) in root zone could increase total phenol, phenoloxidase, peroxidase, which lead to reduce vascular wilt disease in date palm by 16.2-59.3% (Mohamed *et al*., 2018). On the other hand, treating CS-NP loaded copper treatment (1200 ppm) at 3 days after inoculating could reduce tomato early blight and fusarium wilt disease at equivalent degrees to mancozeb fungicide, by 87.7 and 61.1%, respectively (Saharan *et al*., 2015). Furthermore, priming maize seed with this NP (1000 ppm) for 8 hours combined with foliar spraying after infection could reduce post-flowering stalk rot disease by 49.6% that is equivalent to carbendazim fungicide treatment (Choudhary *et al*., 2017a).

The NP formulations are used in this research containing CS, SA or silver, so the disease reduction effect may be due to the synergistic effect of CS or SA or silver to directly anti-fungal pathogen and to induce systemic resistance cassava plants.

In previous reviews, CS was known to act as an elicitor to induce plant innate immunity including stimulating H_2O_2 production, nitric oxide, generate PR protein, oxidative burst, enzyme activity, callose, secondary metabolites (phytoalexin, suberin, lignin, phenolic compounds) (Hadwiger 2013; Kashyap *et al*., 2015; Chakraborty *et al*., 2020). Then, the perception, signal transduction, and defense response of the plant were strongly triggered against phytopathogens (Corwin and Kliebenstein, 2017). In addition, CS was able to suppress fungal mycelium, spore formation, spore viability,

spore germination, and fungal virulence factor (Badawy and Rabea, 2011). The positive charge of CS (polycationic) strong electrostatic interacted with the negative charge of pathogen surfaces such as lipopolysaccharides, protein, metal ions present in the cell walls and plasma membranes, leading to cell damage and leakage of intracellular component, so increase its membrane permeability and then make cell death. Furthermore, when CS penetrated into cells, their cationic binding surface with the negative charge phosphate group of DNA lead to specific modification in protein expression, inhibition of mRNA, and pathogen reproduction. In addition, CS chelates the essential elements (mental ion, mineral, nutrients) and deposits in pathogen surface to form a barrier against extracellular transport of the essential nutrients and metabolites from entering the cells that prevent the normal growth of pathogens (Helander *et al*., 2001; Cruz-Romero *et al*., 2013; Malerba and Cerana, 2015; Xing *et al*., 2015; Malerba and Cerana, 2019; Maluin and Hussein, 2020). In previous studies, CS (low molecular weight) was known to be more effective than CS (high molecular weight) in inhibiting 18 phytopathogens fungi (*A. solani, F. oxysporum, R. solani*, ect.) in tomato, green bean, and potato (El-Mohamedya *et al*., 2019). CS (1250 ppm) significantly inhibited spore germination, mycelial growth with caused damage in the plasma membranes and increase level of the lipid oxidation of *Alternaria tenuissima*. Pre-treatment CS reduced rot lesions in potato at 1.7 folds and increased gene expression including catalase, peroxidase, polyphenol oxidase, chitinase, β-1,3-glucanase, and level of flavonoids, lignin (Liu *et al*., 2019). At 3000 ppm, CS could highly inhibit spore germination (100%), mycelial growth (77.4-88.2%) of *C. gloeosporioides* and *A. alternata,* and reduce decay lesions on apple fruits by 67.2-68.36% (Živković *et al*., 2018). CS (1000 ppm) could reduce disease severity of *Alternaria* leaf blight (*A. solani*) by 50 and 66.7% in tomato and brinjal (Tumpa and Khokon, 2020), and brown leaf spot (*A. alternata*) in potato variety Goldrust and FL1879 at field conditions by 1.3-1.8 and 1.2-2.4 folds, respectively (Soleimani and Kirk, 2012). The commercial CS extract (500 ppm) and SA (100 ppm) could reduce the incidence 64.19% and 58.73% at net house conditions, which is significantly higher

than fungicide (copper hydroxide). The CS extract treatment increased a broad of defense enzyme activity and upregulated the PIN II marker and ETR-cat - the gene Jasmonic acid- inducible and ethylene signal transduction pathways, respectively (Ramkissoon *et al*., 2016).

SA is a plant growth hormone, which produces through phenylalanine ammonia-lyase and the isochorismate pathway, contributing to enhance plant growth and immunity system. When endogenous SA is stimulated, the NPR1 changes to monomer structure and enter the nucleus. Then, the NPR1 binds to a specific TGA transcription factor, leading to an express defense system against phytopathogens (Guilfoyle *et al*., 2015; Maruri-López *et al*., 2019). The artificial supplement SA stimulated chickpea's defense system including enzyme activity (peroxidase, polyphenol oxidase), total phenol, H_2O_2, protein content (War *et al*., 2011). SA (1 mM) could increase total protein and free proline to improve water balance when *A. tenuissima* infected tomato plant, which leads to decrease disease incidence by 2.9 folds and reduced disease index by 55.6% (Agamy *et al*., 2013). The disease bioassays and transcriptomic analysis in Brouwer *et al*.'s study showed that intact SA signaling (not JA signaling) is required in protecting potato plants against an attack by necrotrophic fungi *A. solani* (Brouwer *et al*., 2020). In addition, SA formulation (500 ppm) could increase the endogenous SA level and reduce *Fusarium* root rot disease on cassava by 55.5%. The field test with two varieties including Rayong 72 and CMR-89 showed that the brown leaf spot disease was reduced but non-significant when compared with control treatment (Saengchan *et al*., 2021).

Silver nitrate and silver NPs also have an in-plant and phytopathogenic effect depending on the concentrations. The study by Ejaz *et al*. (2018) showed that at 100 ppm, silver NP was more effective (2.7 folds) than silver nitrate (2.5 folds) in decreasing aflatoxins content in rice infected by *Aspergillus* sp. when compared with control. Silver NP (100 ppm) inhibited *A. brassicicola* mycelial growth by 92.2% (Gupta and Chauhan, 2016). Silver NP (15 ppm) inhibited the mycelial growth of *A. alternata* by

59.4%. The scanning electron microscope test showed that the hyphae was damaged and collapsed, leading to the release of internal cellular material that resulted in shrinkage of hyphae, conidia deformities and low sporulation. In cell filtrate, the total sugar and protein were greatly reduced. Moreover, the sugar, protein, and N-acetyl glucoseamine were reduced in cell wall components while the lipid was distinctively increased (AOuda, 2014).

The efficacy of CS-NP formulations can be enhanced by their small size, large contact area, and high reactivity. That leads to enhanced plant uptake, and increased penetration and penetration into plant tissues or cell membranes of pathogens (Maluin and Hussein, 2020; Mittal *et al*., 2020). Then, both the indirect and direct mechanisms of CS are improved for manage plant diseases. In addition, CS-NPs could easily stick in the plant part surface (Chakraborty *et al*., 2020). Then, the active ingredient (hexaconazole, zinc, copper, SA, Harpin protein, NPK, silicon) could slowly release to the plant, then absorb or attack pathogen (Choudhary *et al*., 2017b; Nadendla *et al*., 2018; Choudhary *et al*., 2019; Kumaraswamy *et al*., 2019; Maluin *et al*., 2019; Ha *et al*., 2019; Kumaraswamy *et al*., 2021).

5.5 Conclusion

In this study, the research started from the efficacy of CS-NP formulations to reduction of leaf spot disease at net house conditions. The mean pre- and post-treatment of CS-NP loaded SA at 400 ppm (T8), CS-NP loaded silver at 200 (T9), 400 (T10), 800 (T11) ppm have able to reduce cassava leaf spot disease by 40.74-43.54%, which similar flutriafol fungicide (T6, 39.61%), but significantly higher than commercial zinc oxide NPs (T7, 31.34%). The CS-NP loaded SA at 400 ppm (T8), CS-NP loaded silver at 200 (T9) could inhibit conidial germination by 32.51 and 23.25%, that also similar flutriafol fungicide (T6, 22.68%) and significantly higher than commercial zinc oxide NPs (T7, 15.00%). Furthermore, the soaking *A. alternata* H-Vi 7 agar plugs into CS-NP loaded SA at 400 ppm (T8), CS-NP loaded silver at 200 ppm (T9) could reduce fungal virulence by inhibiting mycelium growth, viability and their causing rot lesion by 42.26 and

51.11% in detached leaves assay, respectively. Similar, spraying T8 and T9 before inoculation could reduce rot lesions by 44.95 and 42.79%, respectively. The antifungal efficacy of CS-NP loaded SA 400 ppm (T8) and CS-NP loaded silver 200 ppm (T9) in detached leaves assay significantly lower than flutriafol fungicide (T6) but significantly higher than commercial zinc oxide NPs (T7). These results indicate CS-NP formulations as a promising solution in cassava leaf spot disease management.

5.6 Reference

Abdel-Aliem, H. A., Gibriel, A. Y., Rasmy, N. M., Sahab, A. F., El-Nekeety, A. A., & Abdel-Wahhab, M. A. (2019). Antifungal efficacy of chitosan nanoparticles against phytopathogenic fungi and inhibition of zearalenone production by *Fusarium graminearum*. *Comunicata Scientiae*, 10(3): 338-345. doi:10.14295/cs.v10i3.1899.

Agamy, R., Alamri, S., Moustafa, M. F., & Hashem, M. (2013). Management of tomato leaf spot caused by *Alternaria tenuissima* Wiltshire using salicylic acid and agrileen. *International Journal of Agriculture and Biology*, 15(2): 266-272.

AOuda, S. M. (2014). Antifungal activity of silver and copper nanoparticles on two plant pathogens, *Alternaria alternata* and *Botrytis cinerea*. *Research Journal of Microbiology*, 9(1): p.34. doi:10.3923/jm.2014.34.42.

Badawy, M. E., & Rabea, E. I. (2011). A biopolymer chitosan and its derivatives as promising antimicrobial agents against plant pathogens and their applications in crop protection. *International Journal of Carbohydrate Chemistry*, 2011: Article ID 460381.

Brouwer, S. M., Odilbekov, F., Burra, D. D., Lenman, M., Hedley, P. E., Grenville-Briggs, L., Alexandersson, E., Liljeroth, E. & Andreasson, E. (2020). Intact salicylic acid signalling is required for potato defence against the necrotrophic fungus *Alternaria solani*. *Plant Molecular Biology*, 104(1): 1-19. doi:10.1007/s11103-020-01019-6

Burketova, L., Trda, L., Ott, P. G., & Valentova, O. (2015). Bio-based resistance inducers for sustainable plant protection against pathogens. *Biotechnology Advances*, 33(6): 994-1004. doi:10.1016/j.biotechadv.2015.01.004.

Chakraborty, M., Hasanuzzaman, M., Rahman, M., Rahman Khan, M., Bhowmik, P., Mahmud, N.U., Tanveer, M. & Islam, T., 2020. Mechanism of plant growth promotion and disease suppression by chitosan biopolymer. *Agriculture*, 10(12): p.624. doi:10.3390/agriculture10120624.

Chen, J., Wu, L., Lu, M., Lu, S., Li, Z., & Ding, W. (2020). Comparative study on the fungicidal activity of metallic MgO nanoparticles and macroscale MgO against soilborne fungal phytopathogens. *Frontiers in Microbiology*, 11: p.365. doi:10.3389/fmicb.2020.00365

Choudhary, M. K., Joshi, A., Sharma, S. S., & Saharan, V., (2017a). Effect of laboratory synthesized Cu-Chitosan nanocomposites on control of PFSR disease of maize caused by *Fusarium verticillioids*. *International Journal of Current Microbiology and Applied Sciences*, 6: 1656-1664. doi:10.20546/ijcmas.2017.608.199.

Choudhary, R. C., Kumaraswamy, R. V., Kumari, S., Sharma, S. S., Pal, A., Raliya, R., Biswas, P., & Saharan, V., 2019. Zinc encapsulated chitosan nanoparticle to promote maize crop yield. *International Journal of Biological Macromolecules*, 127: 126-135. doi:10.1016/j.ijbiomac.2018.12.274.

Choudhary, R. C., Kumaraswamy, R. V., Kumari, S., Sharma, S. S., Pal, A., Raliya, R., Biswas, P., & Saharan, V., (2017b). Cu-chitosan nanoparticle boost defense responses and plant growth in maize (*Zea mays* L.). *Scientific Reports*, 7(1): 1-11. doi:10.1038/s41598-017-08571-0.

Corwin, J. A., & Kliebenstein, D. J. (2017). Quantitative resistance: more than just perception of a pathogen. *The Plant Cell*, 29(4): 655-665. doi:10.1105/tpc.16.00915.

Cruz-Romero, M., Murphy, T., Morris, M., Cummins, E., & Kerry, J. (2013). Antimicrobial activity of chitosan, organic acids and nano-sized solubilisates for potential use in smart antimicrobially-active packaging for potential food applications. *Food Control*, 34: 393-397. doi:10.1016/j.foodcont.2013.04.042.

De Souza, A. P., Massenburg, L. N., Jaiswal, D., Cheng, S., Shekar, R., & Long, S. P. (2017). Rooting for cassava: insights into photosynthesis and associated physiology as a route to improve yield potential. *New Phytologist*, 213(1): 50-65. doi:10.1111/nph.14250.

Divya, K., Thampi, M., Vijayan, S., Varghese, S., & Jisha, M. S. (2020). Induction of defence response in *Oryza sativa* L. against *Rhizoctonia solani* (Kuhn) by chitosan nanoparticles. *Microbial Pathogenesis*, 149: p.104525. doi:10.1016/j.micpath.2020.104525.

Ejaz, M., Raja, N. I., Ahmad, M. S., Hussain, M., & Iqbal, M. (2018). Effect of silver nanoparticles and silver nitrate on growth of rice under biotic stress. *IET Nanobiotechnology*, 12(7): 927-932. doi:10.1049/iet-nbt.2018.0057.

Elmer, W., & White, J. C. (2018). The future of nanotechnology in plant pathology. *Annual Review of Phytopathology*, 56: 111-133. doi:10.1146/annurev-phyto-080417-050108.

El-Mohamedya, R. S. R., Abd El-Aziz, M. E., & Kamel, S. (2019). Antifungal activity of chitosan nanoparticles against some plant pathogenic fungi *in vitro*. *Agricultural Engineering International: CIGR Journal*, 21: 201-209.

FAOSTAT, (2021a). Crops and livestock products. Retrieved from https://www.fao.org/faostat/en/#data/QCL

FAOSTAT, (2021b). Rankings. Countries by commodity. Retrieved from https://www.fao.org/faostat/en/#rankings/countries_by_commodity_exports

Ghazy, N. A., Abd El-Hafez, O. A., El-Bakery, A. M., & El-Geddawy, D. I. (2021). Impact of silver nanoparticles and two biological treatments to control soft rot disease in sugar beet (*Beta vulgaris* L). *Egyptian Journal of Biological Pest Control*, 31(1): 1-12. doi:10.1186/s41938-020-00347-5.

Guilfoyle, T., Hagen, G., Liu, X., Rockett, K.S., Kørner, C. J., & Pajerowska-Mukhtar, K. M. (2015). Salicylic acid signalling: new insights and prospects at a quarter-century milestone. *Essays in Biochemistry*, 58: 101-113. doi:10.1042/bse0580101.

Gunalan, S., Sivaraj, R., & Rajendran, V. (2012). Green synthesized ZnO nanoparticles against bacterial and fungal pathogens. *Progress in Natural Science: Materials International*, 22(6): 693-700. doi:10.1016/j.pnsc.2012.11.015.

Gupta, D., & Chauhan, P. (2016). Fungicidal activity of silver nanoparticles against *Alternaria brassicicola*. *AIP Conference Proceedings*, 1724(1): p.020031. AIP Publishing LLC. doi:10.1063/1.4945151.

Gupta, P. K. (2018). Toxicity of fungicides. In Gupta, R. C. (Ed.). *Veterinary Toxicology: Basic and Clinical Principles* (3rd ed, pp. 569-580). London: Academic Press.

Ha, N. M. C., Nguyen, T. H., Wang, S. L., & Nguyen, A. D. (2019). Preparation of NPK nanofertilizer based on chitosan nanoparticles and its effect on biophysical characteristics and growth of coffee in green house. *Research on Chemical Intermediates*, 45(1): 51-63. doi:0.1007/s11164-018-3630-7.

Hadwiger, L. A. (2013). Multiple effects of chitosan on plant systems: Solid science or hype. *Plant Science*, 208: 42-49. doi:10.1016/j.plantsci.2013.03.007.

Helander, I. M., Nurmiaho-Lassila, E. L., Ahvenainen, R., Rhoades, J., & Roller, S. (2001). Chitosan disrupts the barrier properties of the outer membrane of Gram-negative bacteria. *International Journal of Food Microbiology*, 71(2-3): 235-244. doi:10.1016/s0168-1605(01)00609-2.

Hoque, J., Akkapeddi, P., Yadav, V., Manjunath, G. B., Uppu, D. S., Konai, M. M., Yarlagadda, V., Sanyal, K., & Haldar, J. (2015). Broad spectrum antibacterial and antifungal polymeric paint materials: synthesis, structure–activity relationship, and membrane-active mode of action. *ACS Applied Materials & Interfaces*, 7(3): 1804-1815. doi:10.1021/am507482y.

Julião, E. C., Santana, M. D., Freitas-Lopes, R. D. L., Vieira, A. D. P., de Carvalho, J. S. B., & Lopes, U. P. (2020). Reduction of brown leaf spot and changes in the chlorophyll a content induced by fungicides in cassava plants. *European Journal of Plant Pathology*, 157(2): 433–439. doi:10.1007/s10658-020-02001-0.

Kashyap, P. L., Xiang, X., & Heiden, P. (2015). Chitosan nanoparticle based delivery systems for sustainable agriculture. *International Journal of Biological Macromolecules*, 77: 36-51. doi:10.1016/j.ijbiomac.2015.02.039.

Kheiri, A., Jorf, S. M., Malihipour, A., Saremi, H., & Nikkhah, M. (2017). Synthesis and characterization of chitosan nanoparticles and their effect on Fusarium head blight and oxidative activity in wheat. *International Journal of Biological Macromolecules*, 102: 526-538. doi:10.1016/j.ijbiomac.2017.04.034.

Kumaraswamy, R. V., Kumari, S., Choudhary, R. C., Sharma, S. S., Pal, A., Raliya, R., Biswas, P., & Saharan, V. (2019). Salicylic acid functionalized chitosan nanoparticle: a sustainable biostimulant for plant. *International Journal of Biological Macromolecules*, 123: 59-69. doi:10.1016/j.ijbiomac.2018.10.202.

Kumaraswamy, R. V., Saharan, V., Kumari, S., Choudhary, R. C., Pal, A., Sharma, S. S., Rakshit, S., Raliya, R., & Biswas, P. (2021). Chitosan-silicon nanofertilizer to enhance plant growth and yield in maize (*Zea mays* L.). *Plant Physiology and Biochemistry*, 159: 53-66. doi:10.1016/j.plaphy.2020.11.054

Liu, J., Zhang, X., Kennedy, J. F., Jiang, M., Cai, Q., & Wu, X. (2019). Chitosan induces resistance to tuber rot in stored potato caused by *Alternaria tenuissima*. *International Journal of Biological Macromolecules*, 140: 851-857. doi:10.1016/j.ijbiomac.2019.08.227.

Malerba, M., & Cerana, R. (2015). Reactive oxygen and nitrogen species in defense/stress responses activated by chitosan in sycamore cultured cells. *International Journal of Molecular Sciences*, 16(2): 3019-3034. doi:10.3390/ijms16023019.

Malerba, M., & Cerana, R. (2019). Recent applications of chitin-and chitosan-based polymers in plants. *Polymers*, 11(5): p.839. doi:10.3390/polym11050839.

Maluin, F. N., & Hussein, M. Z. (2020). Chitosan-based agronanochemicals as a sustainable alternative in crop protection. *Molecules*, 25(7): p.1611. doi:10.3390/molecules25071611.

Maluin, F. N., Hussein, M. Z., Yusof, N. A., Fakurazi, S., Idris, A. S., Zainol Hilmi, N. H., & Jeffery Daim, L. D. (2019). Preparation of chitosan–hexaconazole nanoparticles as fungicide nanodelivery system for combating Ganoderma disease in oil palm. *Molecules*, 24(13): p.2498. doi:10.3390/molecules24132498.

Manikandan, A., & Sathiyabama, M. (2016). Preparation of chitosan nanoparticles and its effect on detached rice leaves infected with *Pyricularia grisea*. *International Journal of Biological Macromolecules*, 84: 58-61. doi:10.1016/j.ijbiomac. 2015.11.083.

Maruri-López, I., Aviles-Baltazar, N. Y., Buchala, A., & Serrano, M. (2019). Intra and extracellular journey of the phytohormone salicylic acid. *Frontiers in Plant Science*, 10: p.423. doi:10.3389/fpls.2019.00423.

McCallum, E. J., Anjanappa, R. B., & Gruissem, W. (2017). Tackling agriculturally relevant diseases in the staple crop cassava (*Manihot esculenta*). *Current Opinion in Plant Biology*, 38: 50-58. doi:10.1016/j.pbi.2017.04.008.

Medina-Pérez, G., Fernández-Luqueño, F., Campos-Montiel, R. G., Sánchez-López, K. B., Afanador-Barajas, L. N., & Prince, L. (2019). Nanotechnology in crop protection: Status and future trends. In Koul, O. (Ed). *Nano-Biopesticides Today and Future Perspectives* (1st ed, pp. 17-45). London: Academic Press.

Mittal, D., Kaur, G., Singh, P., Yadav, K., & Ali, S. A. (2020). Nanoparticle-based sustainable agriculture and food science: recent advances and future outlook. *Frontiers in Nanotechnology*, 2: p.10. doi:10.3389/fnano.2020.579954.

Mohamed, E. A., Gaber, M. H., & Elsharabasy, S. F. (2018). Evaluating the *in vivo* efficacy of copper-chitosan nanocomposition for treating vascular wilt disease in date palm. *International Journal of Environment, Agriculture and Biotechnology*, 3(2): p.239085. doi:10.22161/ijeab/3.2.17.

Muthukrishnan, S., Murugan, I., & Selvaraj, M. (2019). Chitosan nanoparticles loaded with thiamine stimulate growth and enhances protection against wilt disease in Chickpea. *Carbohydrate Polymers*, 212: 169-177. doi:10.1016/j.carbpol. 2019.02.037.

Nadendla, S. R., Rani, T. S., Vaikuntapu, P. R., Maddu, R. R., & Podile, A. R., 2018. $Harpin_{Pss}$ encapsulation in chitosan nanoparticles for improved bioavailability and disease resistance in tomato. *Carbohydrate Polymers*, 199: 11-19. doi:10.1016/j.carbpol.2018.06.094.

Ng'ang, P. W., Miano, D. W., Wagacha, J. M., & Kuria, P. (2019). Identification and characterization of causative agents of brown leaf spot disease of cassava in Kenya. *Journal of Applied Biology and Biotechnology*, 7(6): 1-7. doi: 10.7324/ JABB.2019.70601.

Oh, J. W., Chun, S. C. & Chandrasekaran, M. (2019). Preparation and *in vitro* characterization of chitosan nanoparticles and their broad-spectrum antifungal action compared to antibacterial activities against phytopathogens of tomato. *Agronomy*, 9(1): p.21. doi:10.3390/agronomy9010021.

Pei, Y. L., Shi, T., Li, C. P., Liu, X. B., Cai, J. M., & Huang, G. X. (2014). Distribution and pathogen identification of cassava brown leaf spot in China. *Genetics and Molecular Research*, 13(2): 3461-3473. doi:10.4238/2014.April.30.7.

Perina, F. J., Belan, L. L., Moreira, S. I., Nery, E. M., Alves, E., & Pozza, E. A. (2019). Diagrammatic scale for assessment of *Alternaria* brown spot severity on tangerine leaves. *Journal of Plant Pathology*, 101(4): 981-990. doi:10.1007/s42161-019-00306-6.

Popova, E. V., Zorin, I. M., Domnina, N. S., Novikova, I. I., & Krasnobaeva, I. L. (2020). Chitosan–tripolyphosphate nanoparticles: Synthesis by the ionic gelation method, properties, and biological activity. *Russian Journal of General Chemistry*, 90(7): 1304-1311. doi:10.1134/S1070363220070178.

Ramkissoon, A., Francis, J., Bowrin, V., Ramjegathesh, R., Ramsubhag, A., & Jayaraman, J. (2016). Bio-efficacy of a chitosan based elicitor on *Alternaria solani* and *Xanthomonas vesicatoria* infections in tomato under tropical conditions. *Annals of Applied Biology*, 169(2): 274-283. doi:10.1111/aab.12299.

Saengchan, C., Phansak, P., Le Thanh, T., Papathoti, N. K., & Buensanteai, N. (2021). Efficacy of salicylic acid and a *Bacillus* bioproduct in enhancing growth of cassava and controlling root rot disease. *Journal of Plant Protection Research*, 61(3): 302-310. doi:10.24425/jppr.2021.137952.

Saharan, V., Mehrotra, A., Khatik, R., Rawal, P., Sharma, S. S., & Pal, A. (2013). Synthesis of chitosan based nanoparticles and their *in vitro* evaluation against phytopathogenic fungi. *International Journal of Biological Macromolecules*, 62: 677-683. doi:10.1016/j.ijbiomac.2013.10.012.

Saharan, V., Sharma, G., Yadav, M., Choudhary, M. K., Sharma, S. S., Pal, A., Raliya, R., & Biswas, P. (2015). Synthesis and *in vitro* antifungal efficacy of Cu–chitosan nanoparticles against pathogenic fungi of tomato. *International Journal of Biological Macromolecules*, 75: 346-353. doi:10.1016/j.ijbiomac.2015.01.027.

Sangpueak, R., Phansak, P., Thumanu, K., Siriwong, S., Wongkaew, S., & Buensanteai, N. (2021). Effect of salicylic acid formulations on induced plant defense against cassava anthracnose disease. *The Plant Pathology Journal*, 37(4): p.356. doi:10.5423/PPJ.OA.02.2021.0015.

Sanzari, I., Leone, A., & Ambrosone, A. (2019). Nanotechnology in plant science: to make a long story short. *Frontiers in Bioengineering and Biotechnology*, 7: p.120. doi:10.3389/fbioe.2019.00120.

Sathiyabama, M. & Parthasarathy, R. (2016). Biological preparation of chitosan nanoparticles and its *in vitro* antifungal efficacy against some phytopathogenic fungi. *Carbohydrate Polymers*, 151: 321-325. doi:10.1016/j.carbpol.2016.05.033.

Sathiyabama, M., & Manikandan, A. (2016). Chitosan nanoparticle induced defense responses in fingermillet plants against blast disease caused by *Pyricularia grisea* (Cke.) Sacc. *Carbohydrate Polymers*, 154: 241-246. doi:10.1016/j.carbpol. 2016.06.089.

Soleimani, M. J., & Kirk, W. (2012). Enhance resistence to *Alternaria alternata* causing potato brown leaf spot disease by using some plant defense inducers. *Journal of Plant Protection Research*, 52(1): 83-90. doi:10.2478/v10045-012-0014-7.

Suryadi, Y., Priyatno, T. P., Samudra, I., Susilowati, D. N., Sriharyani, T. S., & Syaefudin, S. (2019). Control of anthracnose disease (*Colletotrichum gloeosporioides*) using nano chitosan hydrolyzed by chitinase derived from *Burkholderia cepacia* Isolate E76. *Jurnal AgroBiogen*, 13(2): 111–122. doi:10.21082/jbio. v13n2.2017.p111-122.

Tumpa, F. H., & Khokon, M. A. R. (2020). Foliar application of chitosan and yeast elicitor facilitate reducing incidence and severity of *Alternaria* leaf blight of tomato and brinjal. *Research Journal of Plant Pathology*, 3(2): p.4.

Uchechukwu-Agua, A. D., Caleb, O. J., & Opara, U. L. (2015). Postharvest handling and storage of fresh cassava root and products: a review. *Food and Bioprocess Technology*, 8(4): 729-748. doi:10.1007/s11947-015-1478-z.

War, A. R., Paulraj, M. G., War, M. Y., & Ignacimuthu, S. (2011). Role of salicylic acid in induction of plant defense system in chickpea (*Cicer arietinum* L.). *Plant Signaling & Behavior*, 6(11): 1787-1792. doi:10.4161/psb.6.11.17685.

Worrall, E. A., Hamid, A., Mody, K. T., Mitter, N., & Pappu, H. R. (2018). Nanotechnology for plant disease management. *Agronomy*, 8(12): 285. doi:10.3390/ agronomy8120285.

Xing, K., Zhu, X., Peng, X., & Qin, S. (2015). Chitosan antimicrobial and eliciting properties for pest control in agriculture: A review. *Agronomy for Sustainable Development*, 35: 569-588. doi:10.1007/s13593-014-0252-3.

Younas, A., Yousaf, Z., Rashid, M., Riaz, N., Fiaz, S., Aftab, A., & Haung, S. (2020). Nanotechnology and plant disease diagnosis and management. In Javad, S. (Ed). *Nanoagronomy* (1st ed, pp. 101-123). Cham: Springer.

Živković, S., Stevanović, M., Đurović, S., Ristić, D., & Stošić, S. (2018). Antifungal activity of chitosan against *Alternaria alternata* and *Colletotrichum gloeosporioides*. *Pesticides and Phytomedicine*, 33(3-4): 197-204. doi:10.2298/PIF1804197Z.

CHAPTER VI

OVERALL DISCUSSION AND CONCLUSION

6.1 Overall discussion

The objectives of this study were (1) to detect fungal pathogen associated with leaf spot disease on cassava in Thailand, (2) to synthesize effective nanoparticle (NP) elicitors against cassava leaf spot disease, (3) to evaluate the application method of NP elicitors on the reduction of cassava leaf spot disease at net house conditions.

First, the fungal pathogen caused leaf spot disease on cassava was detected and identified following Koch's postulates. Next, the biochemical change on *Alternaria alternata* infected tissues was detected by Synchrotron Fourier-transform infrared spectroscopy (SR-FTIR) (**Chapter III**). Then, the chitosan (CS)-NP loaded salicylic acid (SA) and silver formulations were synthesized by ionic gelation method that were evaluated as potential elicitors against leaf spot disease (**Chapter IV**). Lastly, the effectiveness of pre- and post-treatments of CS-NP formulations on reducing cassava leaf spot at net house conditions and the potential virulence of *A. alternata* treated by the CS-NP formulations in detached leaves were evaluated (**Chapter V**). The overall highlight results of this study were shown in **Figure 6.1**.

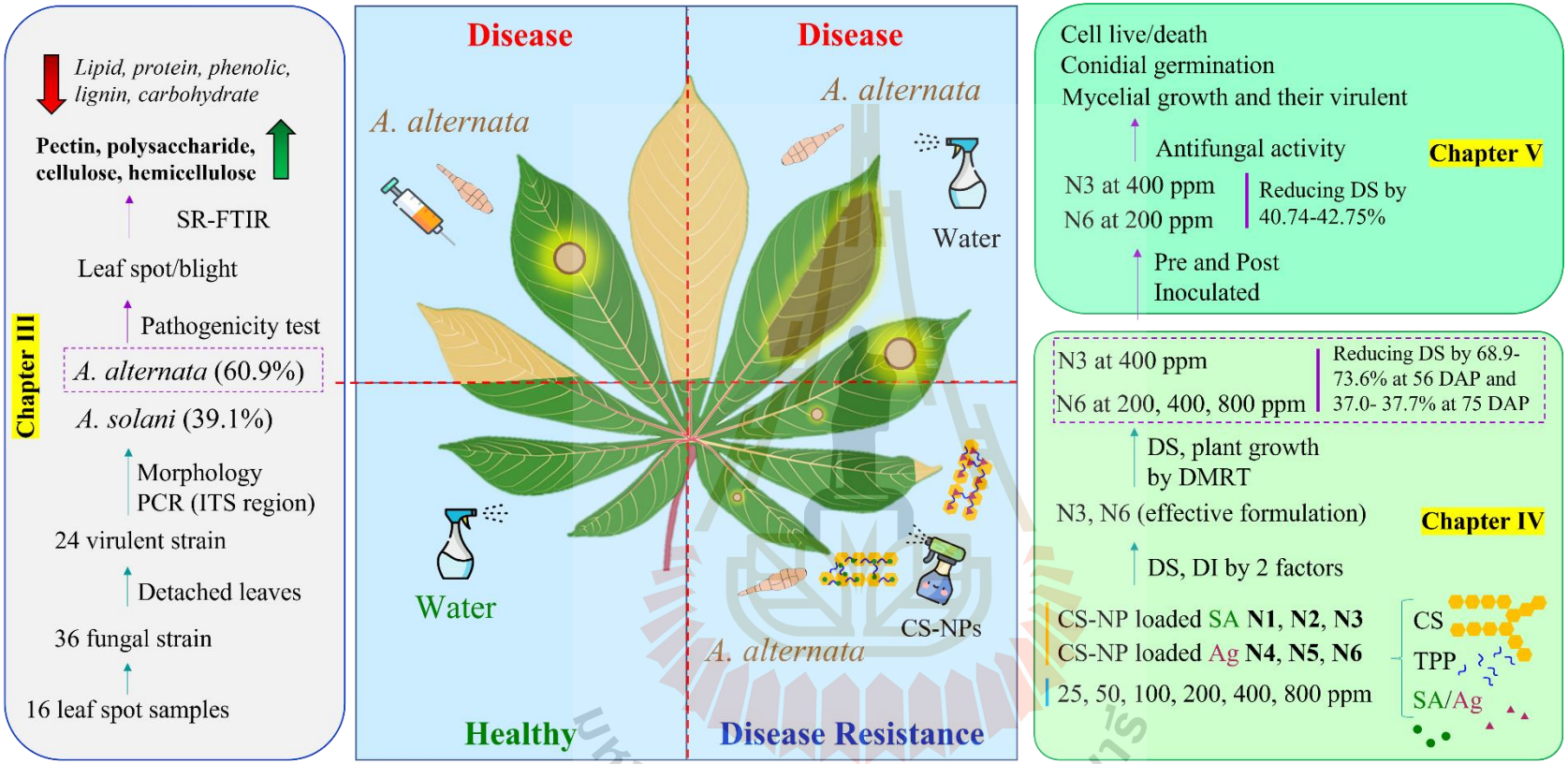

Figure 6.1 The overall results of chapter III, IV and V in this research.

In chapter III, the 36 fungal strains were isolated from 16 leaf spot samples collected from fields at Nakhon Ratchasima, Thailand. Then, the fungal were screened virulent by detached leaves assay method. The 23 virulent fungal including 14 of *A. alternata* and 9 of *Alternaria solani* strains were identified based on morphological colony and conidia combined with sequencing Internal transcribed spacer (ITS) region. In previous research, 48 strains of *Alternaria* spp. isolated from tomato, brinjal, mustard, potato, cauliflower, pea, cabbage, spinach, onion, cicer, eichhornia, lantana, parthenium could cause black sunken necrotic lesions with many crops that are most susceptible to tomato. The high pathogenic group accounted for 27.08% isolates, while moderate and less pathogenic ones were 35.41 and 37.5%, respectively (Meena *et al*., 2017). In our research, the most and highly virulent fungal isolate caused rot lesions with sizes 28.35-32.72 × 25.70-29.70 and 26.86-30.57 × 19.20-24.05 mm, accounting for 30.4 and 34.8%, respectively. The *A. altenata* tend to be more damaging than the *A. solani* isolates. In the research of Zheng *et al*. (2015), *A. alternata*, *A. solani* and *Alternaria tenuissima* accounted for 18.6, 5.9 and 75.5% of the total 511 fungal isolates from potato foliar diseases in China. The fungal isolates also caused rot lesions with yellow halo but virulent was not significantly different between species. *A. alternata* caused small dark brown spots, which enlarged and coalesced to blight symptom on leaves and also sporadic necrotic lesions on petiole carob in Turkey (Basim *et al*., 2018). The *Alternaria* spp. (6 species) caused brown necrotic with concentric ring on detached leaves and moldy core on fruits of apple in Chile (Elfar *et al*., 2018). Besides, 5 species of this genus caused leaf spot disease on cabbage, cauliflower, rocket in Italy (Siciliano *et al*., 2017). Overall, these studies also agree that *A. alternata* could cause necrotic spots lesion on leaves, which could expand to blight symptom with surrounding yellow halo. In both wounding and spraying treatment on pathogenicity test, the *A. alternata* H-Vi 7 caused spot and blight necrotic lesion on cassava leaves. Symptoms vary in size but are all similar including brown with dark brown rims, yellow halos, and dusty black dots as fungal conidia. Previously, the leaf spot disease on cassava has also been reported but is very complex. Brown leaf spot, white leaf spot,

and diffuse or blight leaf spot were three types of spots symptom that have been reported. The commonly known agents are fungi of *Cercospora* (*Mycosphaerella*), and *Passalora* genus (Teri *et al*., 1980; Ayesu-Offei and Antwi-Boasiako, 1996; Prabakar and Raguchander, 2000; Pei *et al*., 2014; Reddy, 2015; de Freitas *et al*., 2017; McCallum *et al*., 2017). In 2018, Ng'ang'a *et al*. reported for the first time that *Alternaria*, *Colletotrichum*, *Cladosporium* caused brown leaf spot disease on cassava in Kenya. In 2020, Hidayat *et al*. and Julião *et al*. recorded *Clarohilum henningsii* causing this disease in Indonesia and Brazil, respectively. The present research is the first to document the damaging effects of *A. alternata* and *A. solani* on cassava in Thailand.

The SR-FTIR was used to determine the biochemical changes in the epidermis and mesophyll tissue when *A. alternata* H-Vi 7 was infected. The researches of Mallick *et al*. (2015), Meena *et al*. (2016), Mahatma *et al*. (2019), Munir *et al*. (2020), Kazerooni *et al*. (2021) shown that the increasing of lipid peroxidation (malondialdehyde), cinnamic acid, hexadecenoic acid, abscisic acid, SA, H_2O_2, 2,2-diphenyl-1-picrylhydrazyl, flavonoid, total phenol, superoxide dismutase, peroxidase, polyphenol oxidase, catalase, phenylalanine ammonia lyase, glutathione reductase, D-mannitol, D-erythropentitol, total amino acid, alpha-D-galactoside, serine, arginine, glycine, lysine, proline, glutamic acid, soluble protein, defense related protein and decreasing of total chlorophyll, carotenoid, total sugar, relative water content in the plant infected by *Alternaria* spp. In SR-FTIR results, The PC1 analysis showed a difference of 22 and 56% between control and *A. alternata* infected tissues in epidermis and mesophyll, respectively. This may be due to the aggressive behavior of this fungi species, which firstly gets inside and secrete mycotoxins. In second derivatives analysis. The results showed an increase in pectin, polysaccharide, cellulose, hemicellulose and a decrease in lipid, protein, phenolic, ligin, carbohydrate component (Yu, 2005; Lammers *et al*., 2009; Wang, 2012; Thumanu *et al*., 2015; Thumanu *et al*., 2017; Lahlali *et al*., 2017; Le Thanh *et al*., 2017; Skenderidis *et al*., 2019; Puttaso *et al*., 2020; Liu *et al*., 2021; Sangpueak *et al*., 2021; Thepbandit *et al*., 2021).

In plant innate immunity, the phenylalanine – an amino acid (amide) is a precursor of the phenylpropanoids, lignins in the phenylalanine ammonia-lyase enzyme pathway (Lahlali *et al*., 2017; Thepbandit *et al*., 2021). When *A. alternata* attacks a plant, the phenylalanine ammonia-lyase is induced (Mallick *et al*., 2015). The polysaccharides including hemicelluloses, celluloses, pectins that is the major constituent in primary plant cell wall, and is increased in *A. alternata* infected tissues. These components can be modified to make plant cells thicker and stronger, and play a crutial role in preventing pathogen infection (Malinovsky *et al*., 2014; Wan *et al*., 2021). On the other hand, the carbohydrate group related sugar decreased in *A. alternata* infected tissue. This is also consistent with previous reports of *A. alternata* attacking plants where sugar provides energy for plant innate defense. And the reduced sugar is also the result of impaired photosynthesis as chlorophyll and carotenoids which are destroyed by mycotoxins (Mallick *et al*., 2015; Meena *et al*., 2016; Munir *et al*., 2020; Kazerooni *et al*., 2021). The changes in biochemical composition in the epidermis and mesophyll identified by SR-FTIR partly explained the infection of *A. alternata* with cassava leaves. Previously, Thumanu *et al*. (2015) and Thumanu *et al*. (2017) used this technique to determine the promotion of plant growth treated by *Bacillus subtilis* or induced systemic resistance in cassava co-inoculated by *B. subtilis* and *Colectotrichum gloeosporioides* related with accumulation of pectin polysaccharides in cell walls.

In chapter IV, the CS (0.4%/ or 0.5%) and pentasodium triphosphate (0.2%/ or 0.5%) were mixed with SA vary at 0.05, 0.1 and 0.2%/ or silver nitrate vary at 1, 2, 3 mM to prepare three formulations CS-NP-loaded SA named N1, N2, N3/ or three formulations CS-NP-loaded silver named N4, N5, N6, respectively. Before use on the cassava plant, the CS-NPs loaded SA and silver were tested phytotoxicity with cassava leaf by leaf disk assay method (Tanapichatsakul *et al*., 2020). The results that the CS-NPs formulations were not toxic to the cassava leaf disk indicated that they could be treated on the cassava plants.

The net house experiment was conducted to select one CS-NP-loaded SA and one CS-NP-loaded silver as effective formulations with effective concentrations to reduce cassava leaf spot disease as an elicitor (pre-treating before pathogen infection). Through three rounds of statistical analysis of disease severity and/or disease index data, the N3 at 400 ppm and N6 at 200, 400, and 800 ppm were shown as high-potential elicitors. Specifically, six formulations with six concentrations were statistically analyzed by two factors, which showed that CS-NP-loaded SA (N3) and CS-NP-loaded silver (N6) were effective formulations. The results of the second statistical analysis showed that the N3 at 400 ppm and N6 at 200, 400, 800 ppm were effective concentrations to reduce cassava leaf spot disease by 68.9, 72.9, 73.6, 73.2%, respectively. Therefore, they were selected for further inoculated pathogen at 63 DAP (3 weeks after the last time spraying treatment). The results showed that they were also effective in reducing disease by 37.0, 37.4, 37.0, 37.7%, respectively. The commercial fungicide also has the ability to reduce cassava leaf spot disease. Of these, pyraclostrobin was more effective than flutriafol at 56 DAP (59.6 and 54.7%) but lower at 75 DAP (14.7 and 35.4%). In addition, zinc oxide commercial NP only reduces 55.7 and 14.2% at 56 and 75 DAP, respectively.

In enhancing cassava growth, the effective concentration usually did not significantly increase the shoot height (-13.4-9.1%) but the opposite was true for the number of leaves (45.1-82.4%) and shoot (38.5-46.2%). And these treatments significantly increase the largest leaf area (29.6-41.9%), root length (11.6-29.9%), root weight (27.6-82.8%). The zinc oxide commercial NP is usually higher potential to enhance plant growth because the active ingredient was ZnO that contains the important nutrient element (Zn) for plant growth.

In this study (chapter), the CS-NPs loaded SA or silver formulation were used as elicitors that can induce plant innate defense system against pathogens. In previous studies, both CS-NPs and CS-NPs loaded active ingredients were reported to be able to reduce plant diseases.

CS-NPs at 1000, 1000 and 500 ppm have been reported that reducing finger millet blast (Sathiyabama and Manikandan, 2016), wheat *Fusarium* head blight (Kheiri *et al*., 2017), and rice sheath blight (Divya *et al*., 2020) by inducing peroxidase, phenylalanine ammonia-lyase, chitinase, reactive oxygen species, superoxide activity, and H_2O_2 content in plant, respectively. In addition, CS-NPs has been loaded with active ingredients including Harpin protein (Nadendla *et al*., 2018), copper (Choudhary *et al*., 2017b), zinc (Choudhary *et al*., 2019), SA (Kumaraswamy *et al*., 2019), thiamine (Muthukrishnan *et al*., 2019) that can induce plants defense system to against infection of *Rhizoctonia solani* (Tomato), *Curvularia lunata* (Maize), *Fusarium verticillioides* (Maize), *Fusarium oxysporum* (Chickpea) by inducing catalase, chitinase, phenylalanine ammonia-lyase, peroxidase, polyphenol oxidase, protease, superoxide dismutases, β-1,3-glucanase activity, superoxide anion, H_2O_2 content and lignin localization. Moreover, the CS-NP-loaded copper also reduced bacterial pustule disease in soybean by 40.6-49.7% but interestingly, low concentration (600 ppm) was more effective than the high concentration (1600 ppm) (Swati *et al*., 2020). In our study, the N3 at 400 ppm was more effective than either 800 ppm or the N3 at 25 ppm was equally effective at 100, 200, and 800 ppm. A mixture of CS-NP (ionic gelation method) and copper-NPs (chemical reduction method) can also reduce vascular wilt disease in date palm by 16.2-59.3% by inducing total phenol, phenoloxidase, peroxidase (Mohamed *et al*., 2018).

Overall, N3 and N6 treatments took the spotlight in reducing leaf spot disease and enhance plant growth on cassava in this study. Among them, CS-NP loaded SA 400 ppm, CS-NP loaded silver at 200, 400, 800 ppm could reduce leaf spot disease by 68.9-73.6% at 56 DAP and 37.0- 37.7% at 75 DAP.

The hydrodynamic diameter of CS-NP-loaded SA (N3) was 89.86 ± 9.04 nm, which is smaller than the size of CS-NP-loaded SA in the study of (Kumaraswamy *et al*., 2019) was 368.7 nm. But the polydispersity index (PDI) and zeta potential of N3 are larger and smaller, respectively. Previously, CS-NP-loaded silver was synthesized by the ionic gelation method with size 90.29 nm and zeta potential +92.05 mV with

antibacterial properties that apply in medical (pharmaceutical) (Du *et al*., 2009). In-plant disease management, CS-NP-loaded metals are usually copper and zinc. In these studies, the dynamic light scattering of CS-NP loaded copper was 295.4 nm, PDI 0.28, 19.6 mV (Choudhary *et al*., 2017a), 361.3 nm, PDI 0.2, 22.1 mV (Choudhary *et al*., 2017b), 314 nm, PDI 0.48, 19.5 mV (Swati *et al*., 2020), 374.3 nm, PDI 0.33, 22.6 mV (Saharan *et al*., 2015), 196.4 nm, PDI 0.5, +88 mV (Saharan *et al*., 2013). And DLS of CS-NP-loaded zinc was 387 nm, PDI 0.22, 34 mV (Choudhary *et al*., 2019). In which, NPs in the studies of Saharan *et al*. (2015), Choudhary *et al*. (2017b), Choudhary *et al*. (2019), Swati *et al*. (2020) were used as elicitors. The CS-NP loaded silver (N6) with size 249.67 ± 23.97 nm which was smaller than the size of NP in these studies. But the PDI and zeta potential of N3 are larger and smaller, respectively. And this is also the first case study in plant disease management. The FTIR peaks are different from previous studies but still in the range that confirms successful synthesis (Ji *et al*., 2011; Choudhary *et al*., 2019; Kumaraswamy *et al*., 2019).

In **Chapter V**, a net-house experiment was performed to evaluate the effect of two factors including NP formulations (CS-NP loaded SA 400 ppm (T8), CS-NP loaded silver at 200 (T9), 400 (T10), 800 (T11) ppm) treatment and method (Pre and Post) treatment on reducing cassava leaf spot disease. The Pre and Post-treatment are designed to assess to the indirect and direct mechanisms. In this experiment, both CS-NP treatments (T8 to T11) showed efficacy (40.74-43.54%) similar to flutriafol (T6) but superior to the commercial zinc oxide NP (T7) in reducing leaf spot disease. Then, the lowest concentrations with similar efficacy of CS-NP loaded silver at 200 ppm (T9) and CS-NP loaded SA at 400 ppm (T8) were selected for comparison with commercial zinc oxide NP (T7), flutriafol (T6), water control (T1) for evaluating the ability to inhibit conidial germination, antifungal activity in detached leaves, and viability fungal. Overall, CS-NP loaded silver at 200 ppm (T9) and CS-NP loaded SA at 400 ppm (T8) both had similar and higher efficacy than commercial zinc oxide NP (T7) but lower than flutriafol (T6) treatment in antifungal activity. The CS-NP loaded SA at 400 ppm (T8) and CS-NP loaded silver at 200 ppm (T9) were inhibited conidial germination by 32.51

and 23.25%, respectively. This result is lower than that of CS-NPs, CS-NP loaded saponin and copper (200-600 ppm) reported in the study by Saharan *et al*. (2013) with inhibiting germination of *A. alternata* were 57.3-68.5, 73.1-78.3 and 69.3-83.3%, respectively. Besides, CS-NPs (2000 ppm) also inhibited *C. gloeosporioides* conidial germination by 61.2% (Suryadi *et al*., 2019). In addition, a CS-NP loaded with other metals can also inhibit the spore germination of many fungal pathogens. CS-NP loaded copper inhibited conidial germination of *A. solani* and *F. oxysporum* by 73.3 and 79.9% at 1000 ppm, respectively (Saharan *et al*., 2015). Similarly, CS-NP loaded zinc (100-800 ppm) and SA (800-1600 ppm) inhibited *C. lunata* and *F. verticillioides* conidial germination by 50.6-73.3 and 48.3-60.5%, respectively (Choudhary *et al*., 2019; Kumaraswamy *et al*., 2019).

The CS-NP loaded SA at 400 ppm (T8) and CS-NP loaded silver at 200 ppm (T9) were inhibited mycelial growth when cultured the plug fungal into medium containing treatment. Moreover, these agar plugs were also reduced in the ability to cause rot lesions on cassava leaves by 42.26 and 51.11%, respectively. This inhibition is related to the viability of fungi as examination under the confocal microscope shows that the ratio of mycelial death/live is similar to that of the rot lesion on cassava leaf. On the other hand, after spraying this treatment into the leaf surface and inoculated pathogen, the rot lesion was also reduced by 45.01 and 42.75%, respectively. Similar results were indicated on some previous researches. Anthracnose disease in chilli and papaya were inhibited by 75 and 10% when treating fruits with CS-NPs (2000 ppm) together with inoculating *C. gloeosporioides* (Suryadi *et al*., 2019). CS-NPs may inhibit mycelial growth of *A. alternata* (65.53-80.1%), *R. solani* (18.1-32.2%), *Macrophomina phaseolina* (87.3-87.5 %) at 200-600 ppm (Saharan *et al*., 2013), *Pyricularia grisea* (92%), *A. solani* (87%), *F. oxysporum* (72%) with amount of 100 µg (Sathiyabama and Parthasarathy, 2016), *P. grisea* (65%) at 1000 ppm (Sathiyabama and Manikandan, 2016), *Alternaria tenuis* (67.67%), *Aspergillus niger* (62.75%), *Aspergillus terreus* (74.67%), *Baeuvaria bassiana* (76.08%), *Fusarium graminearum* (60.37%), *F. oxysporum* (66.60%), *Sclerotium rolfsii* (37.41%) at 800 ppm and the zearalenone produced by *F. graminearum* (Abdel-Aliem

at al., 2019), *C. gloeosporioides* (37.8%), *Phytophthora capsica* (50.7%), *Sclerotinia sclerotiorum* (39.5%), *F. oxysporum* (50.3%), *Gibberella fujikuori* (56.3%) at 5000 ppm (Oh *et al*., 2019), *C. gloeosporioides* (85.7%) (Suryadi *et al*., 2019), *A. solani* (10.70%) at 300 and 400 ppm (Popova *et al*., 2020). In addition, CS-NP loaded copper could inhibit mycelial growth of *A. alternata* (69.3-82.1%), *M. phaseolina* (54.3-62.5%), *R. solani* (18.1-32.2%) at 200-600 ppm (Saharan *et al*., 2013), *A. solani* (52.7-68.7%) and *F. oxysporum* (60.3-73.3%) at 800-1000 ppm (Saharan *et al*., 2015), *C. lunata* by 50.0 and 52.7% at 1200 and 1600 ppm (Choudhary *et al*., 2017b), respectively. In addition, the mixture of CS-NPs (ionic gelation) and copper NPs (chemical reduction) could inhibit the mycelial growth of *F. oxysporum* by 61.94-100% at 500-2000 ppm (Mohamed *et al*., 2018). CS-NP loaded with saponin inhibited the mycelial growth of *A. alternata* by 70.2-78.3% and *R. solani* by 22.8-27.7% at 200-600 ppm (Saharan *et al*., 2013). CS-NPs loaded zinc inhibited mycelial growth of *C. lunata* by 17.04-20.0% and 47.7-65.2% at 100-400 and 800-1600 ppm, respectively (Choudhary *et al*., 2019). CS-NP loaded SA could evade *F. verticillioides* mycelial growth by 62.2-100% at 800-1600 ppm (Kumaraswamy *et al*., 2019). However, in some reports, CS-NPs or CS-NP loaded thiamine did not inhibit mycelial growth, spore germination, sporulation of *P. grisea* or *F. oxysporum* even at high concentration (1000 ppm) (Sathiyabama and Manikandan, 2016; Manikandan and Sathiyabama, 2016; Muthukrishnan *et al*., 2019). This antifungal traits depend on the active ingredient, concentration, and type of fungus. High concentrations tend to be more inhibitory than low concentrations. To achieve 100% inhibition, concentrations should be up to 1600 ppm (CS-NP loaded SA) for *F. verticillioides* or 2000 ppm (CS-NP mixed copper NP) for *F. oxysporum* (Mohamed *et al*., 2018; Kumaraswamy *et al*., 2019). The use of NP treatment at high concentrations can be wasteful if the effectiveness of disease control is not increased at a linear rate. In addition, there are many factors in nature that affect pathogens, so even though the efficiency in *in-vitro* conditions can be up to 100%, the effect could be lower when applied in net-house or field conditions. In the past, flutriafol has also shown better

disease control than other fungicides including azoxystrobin, cyproconazole, pyraclostrobin, tebuconazole, thiophanate-methyl (Julião *et al*., 2020).

The formulations contain CS, SA, or silver, so the effectiveness in disease reduction may be due to the synergistic effect of CS and SA or silver. This is the direct effect of the NP formulations. Besides, NPs can be a good carrier to transport CS, SA, or silver into plant cells, leading to an indirect effect on increasing plant resistance against plant diseases (**Figure 6.2**).

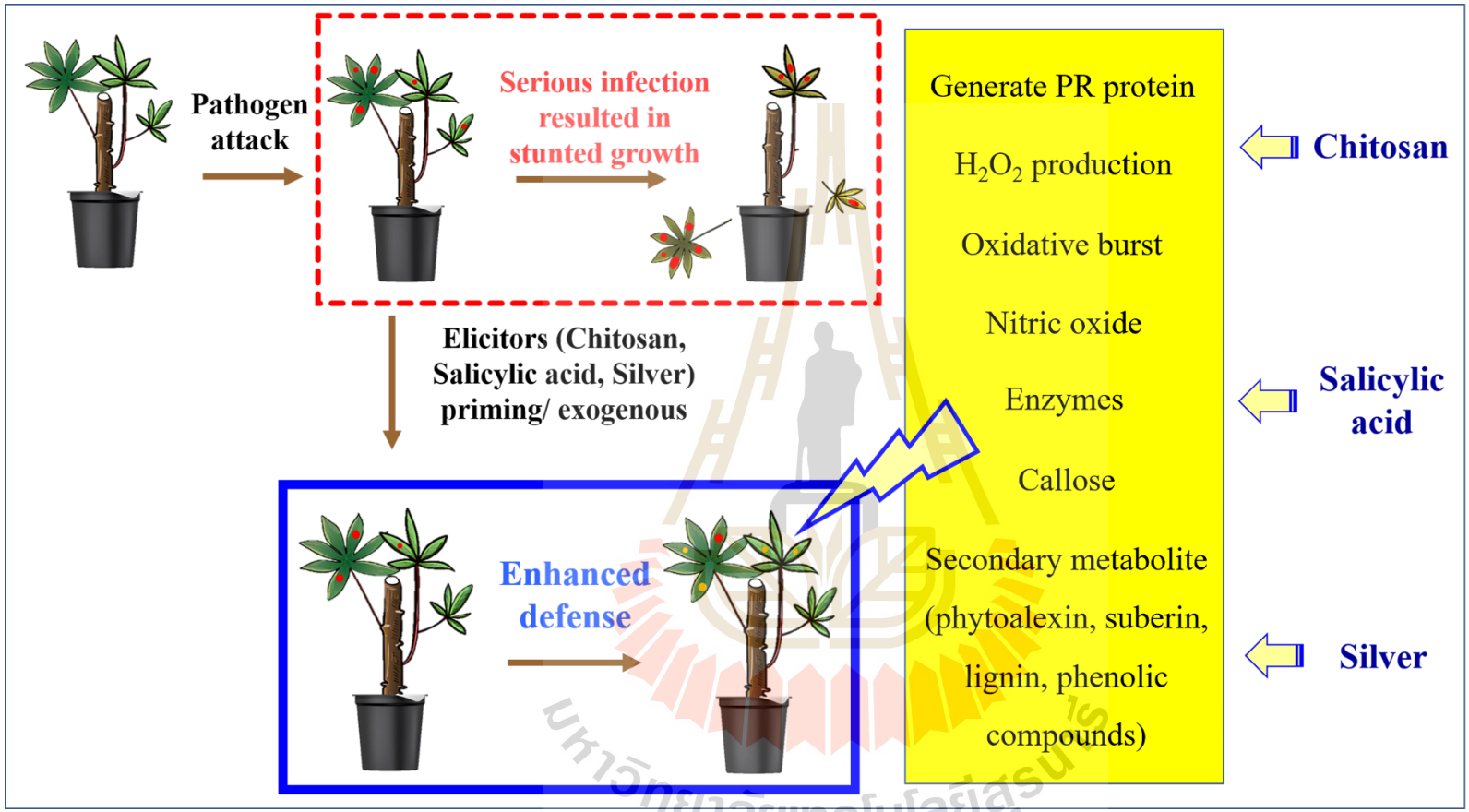

Figure 6.2 The effect of chitosan, salicylic acid and silver on plant defense. Modified from War *et al*. (2011), Hadwiger (2013), Guilfoyle *et al*. (2015), Kashyap *et al*. (2015), Ejaz *et al*. (2018), Maruri-López *et al*. (2019), Chakraborty *et al*. (2020).

The plant innate immune system has three stages including perception, signal transduction, and defense response. This process could be induced by elicitor (Corwin and Kliebenstein, 2017).

The CS can act as an elicitor that activates a plant's innate immunity including stimulating H_2O_2 production, nitric oxide, generate PR protein, oxidative burst, enzymes, callose, secondary metabolite (phytoalexin, suberin, lignin, phenolic compound) (Hadwiger *et al*., 2013; Kashyap *et al*., 2015; Chakraborty *et al*., 2020). In the Jogaiah *et al*. (2020) study's, CS treatment (2.5 mg/ml) increased plant height (39%), stem girth (44%), and reduced powdery mildew (*Erysiphe cichoracearum*) disease (66.6%) on cucumber. Furthermore, this effect was associated with an increase in the production of benzyl aminopurine, indole acetic acid, 1-napthol acetic acid and lignin, callose and H_2O_2, polyphenol oxidase, phenylalanine ammonia-lyase, peroxidase, glucanase in the plant.

SA is a plant hormone that plays a role in plant germination, growth, and immunity. In the cell, endogenous SA is produced by phenylalanine ammonia-lyase and isochorismate pathways. And when SA concentration is increased, the cellular reduction potential is changed the NPR1 structure changes to a monomer that can enter the nucleus. Here, NPR1 binds to specific TGA transcriptions factors and then expresses defense against pathogen attack (Guilfoyle *et al*., 2015; Maruri-López *et al*., 2019). SA treatment can increase plant defense system in chickpea including enzymes (peroxidase, polyphenol oxidase), total phenol, H_2O_2, protein content (War *et al*., 2011). Previously, Le Thanh *et al*. (2017) reported that exogenous SA treatment (1 mM) was able to reduce bacterial leaf blight in rice by 38% with increase superoxide anion production and hypersensitive response, as well as lignin and pectin content in the cell wall. In addition, the formatted SA (Zacha11 at 500 mg/L) has increased stem height, root length, and the number of roots and reduce root rot disease by 53.33% on cassava (Saengchan *et al*., 2021).

Silver nitrate also has effects on plants depending on the concentration. Murashige and Skoog medium containing silver nitrate (1 mg/L) could increase rooted

shoots (63.6%), plant height (78.6%), number of roots (181.3%), root length (508%), and reduced bacterial contamination in *Gentiana lutea* tissue culture (Petrova *et al*., 2011). Furthermore, Murashige and Skoog medium adding silver nitrate (1 mg/L) could improve the quality shoot and decrease the time required for rooting early than 2 months in 2 cultivars of *Anthurium andraeanum* under tissue culture (Cardoso *et al*., 2019). In addition, Ejaz *et al*. (2018) compared the effectiveness of silver nitrate and silver-NP (green synthesis) on the growth of rice under biotic stress conditions. The results showed that silver-NP was more effective than silver nitrate at the same 75 mg/L concentration in increasing root length (1.2 and 12.8%), shoot length (21 and 20%), root number (8.1 and 6.8%), fresh weight (6.4 and 5%), dry weight (4.6 and 3.5%), leaf area (58.5 and 57.2%), leaf number (4.3 and 3.7%), lead fresh weight (1.7 and 1.4%), leaf dry weight (0.9 and 0.8%) under *Aspergillus* infection. Furthermore, the aflatoxins of silver-NP were 3.5±0.1 µg/kg compared with silver nitrate was 3.9±0.3 µg/kg. In Salama (2012) study's, silver-NP (60 ppm) also increased common bean and maize growth including shoot length (47.0 and 27.9%), root length (56.1 and 46.1%), fresh weight (85.9 and 109.2%), dry weight (74.4 and 122.0%), leaf area (56.5 and 70.0%), chlorophyll a (49.0 and 46.0%), chlorophyll b (33.0 and 26.0%), carbohydrate content (57.0 and 62.0%). But at higher concentrations (100 ppm) growth was reduced. In addition, silver-NP (50 ppm) in lilies treatment resulted in increased plant height (7.6%), number of leaves (27.2%), greenness index (17.6%), leaf fresh weight (35.1%), bulb fresh weight (73.4%), number of scales (24.3%) but at higher concentrations the effect is not equal or equivalent (Salachna *et al*., 2019).

Why are NP formulations highly effective in reducing plant diseases and enhance plant growth? In general, the preeminent characteristics of NPs are their small size, large contact surface area, and high reactivity leading to their application in control disease and enhance growth on plants (Elmer and White, 2018). NPs can be absorbed by plants through foliar, brand, trunk, and root (Mittal *et al*., 2020). CS-NPs with nano size and positive charge lead to them being able to easily penetrate cells or stick to plant surfaces (Chakraborty *et al*., 2020). CS-NP can enter the plant via

leaves (stomata and cuticular pathway) and roots (diffusion and cuticular pathway). The stomata of cassava leaves from 18.2-24.9 µm × 12.1-16.1 µm (Mondin *et al*., 2018). The hydrodynamic diameter of N3 and N6 was 89.86 ± 9.04 and 249.67 ± 23.97 nm with PDI was 0.36 ± 0.02 and 0.53 ± 0.03, the zeta potential was 22.27 ± 1.01 and 13.53 ± 0.74 mV, respectively. Therefore, these NPs can pass through the stomata or be easily absorbed by the cassava plant. CS-NP can adjust osmotic pressure in the cell resulting in increased uptake and availability of water and nutrients (Guan *et al*., 2009). In addition, when sticking to plants, the CS-NPs loaded with active ingredients including hexaconazole, zinc, copper, SA, Harpin protein, NPK, silicon can slow-release their active ingredients so that plants can absorb them slowly that reported in the studies (Choudhary *et al*., 2017b; Nadendla *et al*., 2018; Choudhary *et al*., 2019; Ha *et al*., 2019; Kumaraswamy *et al*., 2019; Maluin *et al*., 2019; Kumaraswamy *et al*., 2021). CS is commonly used as a carrier due to solubility in aqueous media and is able to mix with organic or inorganic or copolymer compounds to increase solubility (Das and Pattanayak, 2020). The main component of CS is nitrogen, so the carrier (CS) can act as a source of nitrogen for plants to absorb, or enhance cell division, cell elongation, enzymatic activation, synthesis of protein lead to increase yield (Agarwal *et al*., 2015; Chakraborty *et al*., 2020).

The cost of recommend dose (20 L) of N3 and N6 formulation used chemical analysis grade was higher than the price of commercial products including pyraclostrobin, flutriafol, zinc oxide NP. But the cost of chemical industrial grade was lower (**Figure 6.3** and **6.4**).

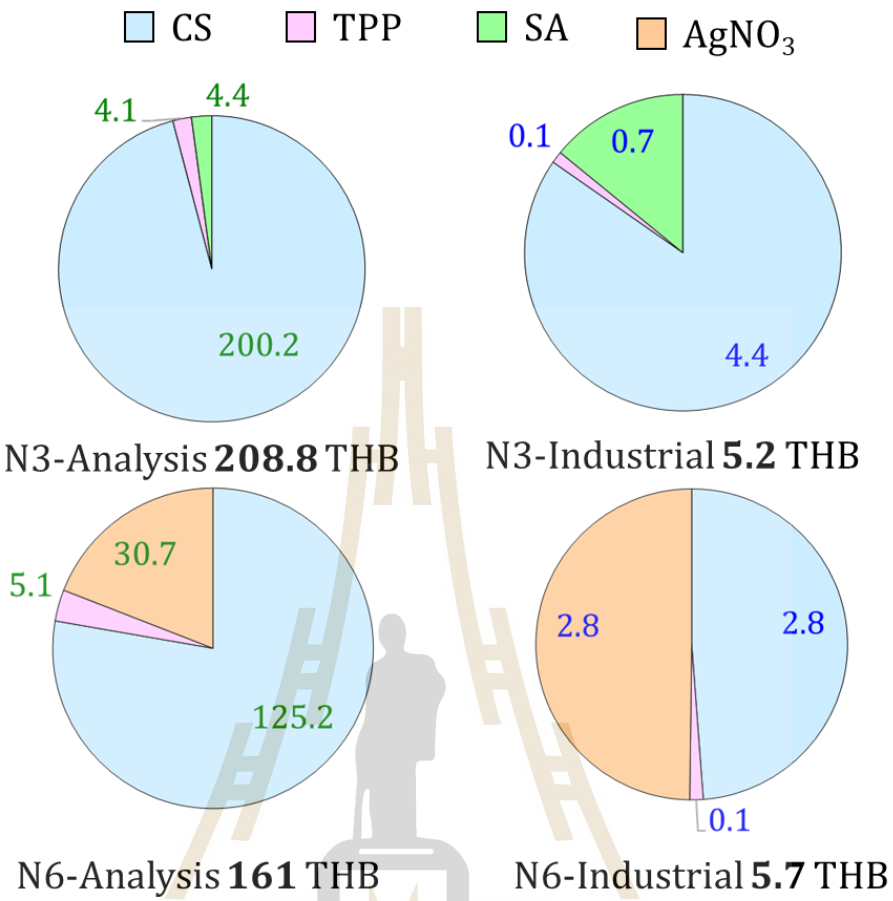

Figure 6.3 The analysis and industrial cost, and their structure of NP formulations for 20 L - recommend dose.

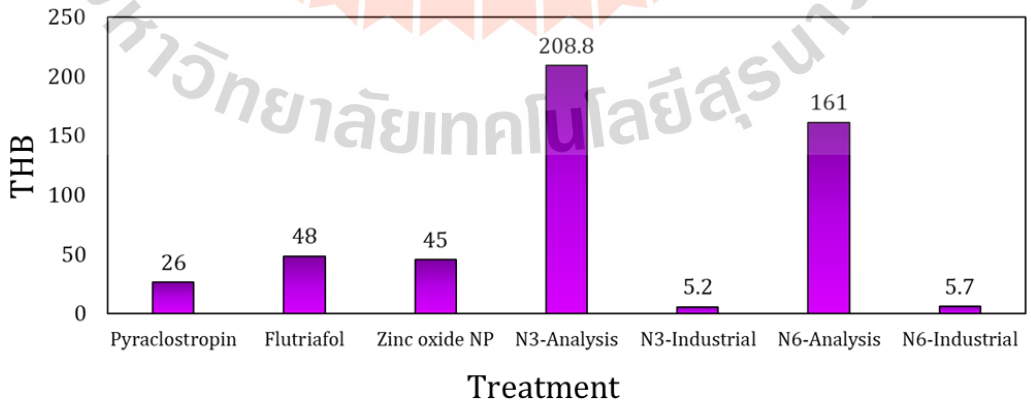

Figure 6.4 The cost of treatments as recommend dose (per 20 L).

6.2 Conclusion

This research was the first report *A. alternata* and *A. solani* associated with leaf spot disease on cassava. CS-NP loaded SA (N3) and silver (N6) synthesized by ionic gelation method were effective solution for management cassava leaf spot disease by pre or post treatment when *A. alternata* infecting. Moreover, the NP treatment also able to enhance cassava growth parameters. Besides, reverse research from net house to laboratory is an effective research way in phytopathology to evaluate the effectiveness of elicitors.

6.3 Suggestion

Although the effectiveness of CS-NP loaded SA and silver was demonstrated in this study, field evaluation is needed. Furthermore, it is interesting if indirect mechanisms involved in the induction of plant disease resistance can be elucidated by experiments. The reverse research model can be applied in many other phytopathology researches.

6.4 References

Abdel-Aliem, H. A., Gibriel, A. Y., Rasmy, N. M., Sahab, A. F., El-Nekeety, A. A., & Abdel-Wahhab, M. A. (2019). Antifungal efficacy of chitosan nanoparticles against phytopathogenic fungi and inhibition of zearalenone production by *Fusarium graminearum*. *Comunicata Scientiae*, 10(3): 338-345. doi:10.14295/cs.v10i3.1899.

Agarwal, M., Nagar, D. P., Srivastava, N., & Agarwal, M. K. (2015). Chitosan nanoparticles-based drug delivery: An update. *International Journal of Advanced Multidisciplinary Research*, 2(4): 1-13.

Ayesu-Offei, E. N., & Antwi-Boasiako, C. (1996). Production of microconidia by *Cercospora henningsii* Allesch, cause of brown leaf spot of cassava (*Manihot esculenta* Crantz) and tree cassava (*Manihot glaziovii* Muell.-Arg.). *Annals of Botany*, 78(5): 653-657. doi:10.1006/anbo.1996.0173.

Basım, H., Basım, E., Baki, D., Abdulai, M., Öztürk, N., & Balkic, R. (2018). Identification and characterization of *Alternaria alternata* (Fr.) Keissler causing Ceratonia Blight disease of carob (*Ceratonia siliqua* L.) in Turkey. *European Journal of Plant Pathology*, 151(1): 73-86. doi:10.1007/s10658-017-1354-y.

Cardoso, J. C. (2019). Silver nitrate enhances in vitro development and quality of shoots of *Anthurium andraeanum*. *Scientia Horticulturae*, 253: 358-363. doi:10.1016/j.scienta.2019.04.054

Chakraborty, M., Hasanuzzaman, M., Rahman, M., Rahman Khan, M., Bhowmik, P., Mahmud, N.U., Tanveer, M. & Islam, T. (2020). Mechanism of plant growth promotion and disease suppression by chitosan biopolymer. *Agriculture*, 10(12): p.624. doi:10.3390/agriculture10120624.

Choudhary, M. K., Joshi, A., Sharma, S. S., & Saharan, V. (2017a). Effect of laboratory synthesized Cu-Chitosan nanocomposites on control of PFSR disease of maize caused by *Fusarium verticillioids*. *International Journal of Current Microbiology and Applied Sciences*, 6: 1656-1664. doi:10.20546/ijcmas.2017.608.199.

Choudhary, R. C., Kumaraswamy, R. V., Kumari, S., Sharma, S. S., Pal, A., Raliya, R., Biswas, P., & Saharan, V. (2019). Zinc encapsulated chitosan nanoparticle to promote maize crop yield. *International Journal of Biological Macromolecules*, 127: 126-135. doi:10.1016/j.ijbiomac.2018.12.274.

Choudhary, R. C., Kumaraswamy, R. V., Kumari, S., Sharma, S. S., Pal, A., Raliya, R., Biswas, P., & Saharan, V. (2017b). Cu-chitosan nanoparticle boost defense responses and plant growth in maize (*Zea mays* L.). *Scientific Reports*, 7(1): 1-11. doi:10.1038/s41598-017-08571-0.

Corwin, J. A., & Kliebenstein, D. J. (2017). Quantitative resistance: more than just perception of a pathogen. *The Plant Cell*, 29(4): 655-665. doi:10.1105/tpc.16.00915.

Das, S., & Pattanayak, S. (2020). Nanotechnological approaches in sustainable agriculture and plant disease management. In Das, S. K. *Organic Agriculture*. (1st ed, 18 pp). London: IntechOpen. doi: 10.5772/intechopen.92463

de Freitas, J. P. X., Diniz, R. P., de Oliveira, S. A. S., da Silva Santos, V., & de Oliveira, E. J. (2017). Inbreeding depression for severity caused by leaf diseases in cassava. *Euphytica*, 213(9): 1-12. doi:10.1007/s10681-017-1995-0.

Divya, K., Thampi, M., Vijayan, S., Varghese, S., & Jisha, M. S. (2020). Induction of defence response in *Oryza sativa* L. against *Rhizoctonia solani* (Kuhn) by chitosan nanoparticles. *Microbial Pathogenesis*, 149: p.104525. doi:10.1016/j.micpath. 2020.104525.

Du, W. L., Niu, S. S., Xu, Y. L., Xu, Z. R., & Fan, C. L. (2009). Antibacterial activity of chitosan tripolyphosphate nanoparticles loaded with various metal ions. *Carbohydrate Polymers*, 75(3): 385-389. doi:10.1016/j.carbpol.2008.07.039.

Ejaz, M., Raja, N. I., Ahmad, M. S., Hussain, M., & Iqbal, M. (2018). Effect of silver nanoparticles and silver nitrate on growth of rice under biotic stress. *IET Nanobiotechnology*, 12(7): 927-932. doi:10.1049/iet-nbt.2018.0057.

Elfar, K., Zoffoli, J. P., & Latorre, B. A. (2018). Identification and characterization of *Alternaria* species associated with moldy core of apple in Chile. *Plant Disease*, 102(11): 2158-2169. doi:10.1094/PDIS-02-18-0282-RE.

Elmer, W., & White, J. C. (2018). The future of nanotechnology in plant pathology. *Annual Review of Phytopathology*, 56: 111-133. doi:10.1146/annurev-phyto-080417-050108.

Guan, Y. J., Hu, J., Wang, X. J., & Shao, C. X. (2009). Seed priming with chitosan improves maize germination and seedling growth in relation to physiological changes under low temperature stress. *Journal of Zhejiang University Science B*, 10(6): 427-433. doi:10.1631/jzus.B0820373.

Guilfoyle, T., Hagen, G., Liu, X., Rockett, K.S., Kørner, C. J., & Pajerowska-Mukhtar, K. M. (2015). Salicylic acid signalling: new insights and prospects at a quarter-century milestone. *Essays in Biochemistry*, 58: 101-113. doi:10.1042/bse0580101.

Ha, N. M. C., Nguyen, T. H., Wang, S. L., & Nguyen, A. D. (2019). Preparation of NPK nanofertilizer based on chitosan nanoparticles and its effect on biophysical characteristics and growth of coffee in green house. *Research on Chemical Intermediates*, 45(1): 51-63. doi:0.1007/s11164-018-3630-7.

Hadwiger, L. A. (2013). Multiple effects of chitosan on plant systems: Solid science or hype. *Plant Science*, 208: 42-49. doi:10.1016/j.plantsci.2013.03.007.

Hidayat, I., Hastuty, A., & Ramadhani, I. (2020). A molecular phylogenetic study of *Clarohilum henningsii* (Mycosphaerellaceae, Fungi) on cassava from Indonesia based on the ITS rDNA sequence. *Journal of Microbial Systematics and Biotechnology*, 2(1): 40-45. doi:10.37604/jmsb.v2i1.43.

Ji, J., Hao, S., Wu, D., Huang, R., & Xu, Y., 2011. Preparation, characterization and in vitro release of chitosan nanoparticles loaded with gentamicin and salicylic acid. *Carbohydrate Polymers*, 85(4): 803-808. doi:10.1016/j.carbpol.2011.03.051.

Jogaiah, S., Satapute, P., De Britto, S., Konappa, N., & Udayashankar, A. C. (2020). Exogenous priming of chitosan induces upregulation of phytohormones and resistance against cucumber powdery mildew disease is correlated with localized biosynthesis of defense enzymes. *International Journal of Biological Macromolecules*, 162: 1825-1838. doi:10.1016/j.ijbiomac.2020.08.124.

Julião, E. C., Santana, M. D., Freitas-Lopes, R. D. L., Vieira, A. D. P., de Carvalho, J. S. B., & Lopes, U. P. (2020). Reduction of brown leaf spot and changes in the chlorophyll a content induced by fungicides in cassava plants. *European Journal of Plant Pathology*, 157(2): 433–439. doi:10.1007/s10658-020-02001-0.

Kashyap, P. L., Xiang, X., & Heiden, P. (2015). Chitosan nanoparticle based delivery systems for sustainable agriculture. *International Journal of Biological Macromolecules*, 77: 36-51. doi:10.1016/j.ijbiomac.2015.02.039.

Kazerooni, E. A., Maharachchikumbura, S. S., Al-Sadi, A. M., Kang, S. M., Yun, B. W., & Lee, I. J. (2021). Biocontrol Potential of *Bacillus amyloliquefaciens* against *Botrytis pelargonii* and *Alternaria alternata* on *Capsicum annuum*. *Journal of Fungi*, 7(6): p.472. doi:10.3390/jof7060472.

Kheiri, A., Jorf, S. M., Malihipour, A., Saremi, H., & Nikkhah, M. (2017). Synthesis and characterization of chitosan nanoparticles and their effect on Fusarium head blight and oxidative activity in wheat. *International Journal of Biological Macromolecules*, 102: 526-538. doi:10.1016/j.ijbiomac.2017.04.034.

Kumaraswamy, R. V., Kumari, S., Choudhary, R. C., Sharma, S. S., Pal, A., Raliya, R., Biswas, P., & Saharan, V. (2019). Salicylic acid functionalized chitosan nanoparticle: a

sustainable biostimulant for plant. *International Journal of Biological Macromolecules*, 123: 59-69. doi:10.1016/j.ijbiomac.2018.10.202.

Kumaraswamy, R. V., Saharan, V., Kumari, S., Choudhary, R. C., Pal, A., Sharma, S. S., Rakshit, S., Raliya, R., & Biswas, P. (2021). Chitosan-silicon nanofertilizer to enhance plant growth and yield in maize (*Zea mays* L.). *Plant Physiology and Biochemistry*, 159: 53-66. doi:10.1016/j.plaphy.2020.11.054

Lahlali, R., Song, T., Chu, M., Yu, F., Kumar, S., Karunakaran, C., & Peng, G. (2017). Evaluating changes in cell-wall components associated with clubroot resistance using fourier transform infrared spectroscopy and RT-PCR. *International Journal of Molecular Sciences*, 18(10): p.2058. doi:10.3390/ijms18102058

Lammers, K., Arbuckle-Keil, G. & Dighton, J. (2009). FT-IR study of the changes in carbohydrate chemistry of three New Jersey pine barrens leaf litters during simulated control burning. *Soil Biology and Biochemistry*, 41(2): 340-347. doi:10.1016/j.soilbio.2008.11.005.

Le Thanh, T., Thumanu, K., Wongkaew, S., Boonkerd, N., Teaumroong, N., Phansak, P., & Buensanteai, N. (2017). Salicylic acid-induced accumulation of biochemical components associated with resistance against *Xanthomonas oryzae* pv. *oryzae* in rice. *Journal of Plant Interactions*, 12(1): 108-120. doi:10.1080/17429145.2017.1291859.

Liu, X., Renard, C. M., Bureau, S., & Le Bourvellec, C. (2021). Revisiting the contribution of ATR-FTIR spectroscopy to characterize plant cell wall polysaccharides. *Carbohydrate Polymers*, 262: p.117935. doi:10.1016/j.carbpol.2021.117935.

Mahatma, M. K., Thawait, L. K., Jadon, K. S., Rathod, K. J., Sodha, K. H., Bishi, S. K., Thirumalaisamy, P. P., & Golakiya, B. A. (2019). Distinguish metabolic profiles and defense enzymes in *Alternaria* leaf blight resistant and susceptible genotypes of groundnut. *Physiology and Molecular Biology of Plants*, 25(6): 1395-1405. doi:10.1007/s12298-019-00708-x.

Malinovsky, F. G., Fangel, J. U., & Willats, W. G. (2014). The role of the cell wall in plant immunity. *Frontiers in Pant Science*, 5: p.178. doi:10.3389/fpls.2014.00178.

Mallick, S. A., Kumari, P., Gupta, M., & Gupta, S. (2015). Effect of *Alternaria* blight infection on biochemical parameters, quantity and quality of oil of mustard genotypes. *Indian Journal of Plant Physiology*, 20(4): 310-316. doi:10.1007/s40502-015-0178-z.

Maluin, F. N., Hussein, M. Z., Yusof, N. A., Fakurazi, S., Idris, A. S., Zainol Hilmi, N. H., & Jeffery Daim, L. D. (2019). Preparation of chitosan–hexaconazole nanoparticles as fungicide nanodelivery system for combating Ganoderma disease in oil palm. *Molecules*, 24(13): p.2498. doi:10.3390/molecules24132498.

Manikandan, A., & Sathiyabama, M. (2016). Preparation of chitosan nanoparticles and its effect on detached rice leaves infected with *Pyricularia grisea*. *International Journal of Biological Macromolecules*, 84: 58-61. doi:10.1016/j.ijbiomac.2015.11.083.

Maruri-López, I., Aviles-Baltazar, N. Y., Buchala, A., & Serrano, M. (2019). Intra and extracellular journey of the phytohormone salicylic acid. *Frontiers in Plant Science*, 10: p.423. doi:10.3389/fpls.2019.00423.

McCallum, E. J., Anjanappa, R. B., & Gruissem, W. (2017). Tackling agriculturally relevant diseases in the staple crop cassava (*Manihot esculenta*). *Current Opinion in Plant Biology*, 38: 50-58. doi:10.1016/j.pbi.2017.04.008.

Meena, M., Swapnil, P., & Upadhyay, R. S. (2017). Isolation, characterization and toxicological potential of *Alternaria*-mycotoxins (TeA, AOH and AME) in different *Alternaria* species from various regions of India. *Scientific Reports*, 7(1): 1-19. doi:10.1038/s41598-017-09138-9.

Meena, M., Zehra, A., Dubey, M. K., Aamir, M., Gupta, V. K., & Upadhyay, R. S. (2016). Comparative evaluation of biochemical changes in tomato (*Lycopersicon esculentum* Mill.) infected by *Alternaria alternata* and its toxic metabolites (TeA, AOH, and AME). *Frontiers in Plant Science*, 7: p.1408. doi:10.3389/fpls.2016.01408.

Mittal, D., Kaur, G., Singh, P., Yadav, K., & Ali, S. A. (2020). Nanoparticle-based sustainable agriculture and food science: recent advances and future outlook. *Frontiers in Nanotechnology*, 2: p.10. doi:10.3389/fnano.2020.579954.

Mohamed, E. A., Gaber, M. H., & Elsharabasy, S. F. (2018). Evaluating the *in vivo* efficacy of copper-chitosan nanocomposition for treating vascular wilt disease in date palm. *International Journal of Environment, Agriculture and Biotechnology*, 3(2): p.239085. doi:10.22161/ijeab/3.2.17.

Mondin, M., Latado, R. R., & Mourão, F. D. A. A. (2018). *In vitro* induction and regeneration of tetraploids and mixoploids of two cassava cultivars. *Crop Breeding and Applied Biotechnology*, 18: 176-183. doi:10.1590/1984-70332018v18n2a25.

Mudgil, M., Gupta, N., Nagpal, M., & Pawar, P. (2012). Nanotechnology: a new approach for ocular drug delivery system. *International Journal of Pharmacy and Pharmaceutical Sciences*, 4(2): 105-112.

Muthukrishnan, S., Murugan, I., & Selvaraj, M. (2019). Chitosan nanoparticles loaded with thiamine stimulate growth and enhances protection against wilt disease in Chickpea. *Carbohydrate Polymers*, 212: 169-177. doi:10.1016/j.carbpol. 2019.02.037.

Nadendla, S. R., Rani, T. S., Vaikuntapu, P. R., Maddu, R. R., & Podile, A. R., 2018. $Harpin_{Pss}$ encapsulation in chitosan nanoparticles for improved bioavailability and disease resistance in tomato. *Carbohydrate Polymers*, 199: 11-19. doi:10.1016/j.carbpol.2018.06.094.

Ng'ang, P. W., Miano, D. W., Wagacha, J. M., & Kuria, P. (2019). Identification and characterization of causative agents of brown leaf spot disease of cassava in Kenya. *Journal of Applied Biology and Biotechnology*, 7(6): 1-7. doi:10.7324/JABB.2019.70601.

Oh, J. W., Chun, S. C. & Chandrasekaran, M. (2019). Preparation and *in vitro* characterization of chitosan nanoparticles and their broad-spectrum antifungal action compared to antibacterial activities against phytopathogens of tomato. *Agronomy*, 9(1): p.21. doi:10.3390/agronomy9010021.

Pei, Y. L., Shi, T., Li, C. P., Liu, X. B., Cai, J. M., & Huang, G. X. (2014). Distribution and pathogen identification of cassava brown leaf spot in China. *Genetics and Molecular Research*, 13(2): 3461-3473. doi:10.4238/2014.April.30.7.

Petrova, M., Zayova, E., & Vitkova, A. (2011). Effect of silver nitrate on in vitro root formation of *Gentiana lutea*. *Romanian Biotechnological Letters*, 16(6): 53-58.

Popova, E. V., Zorin, I. M., Domnina, N. S., Novikova, I. I., & Krasnobaeva, I. L. (2020). Chitosan–tripolyphosphate nanoparticles: Synthesis by the ionic gelation method, properties, and biological activity. *Russian Journal of General Chemistry*, 90(7): 1304-1311. doi:10.1134/S1070363220070178.

Prabakar, K., & Raguchander, T. (2000). Fungicidal control of cassava brown leaf spot caused by *Cercospora henningsii* Allescher. *Madras Agricultural Journal*, 87(7/9), 537-538.

Puttaso, P., Namanusart, W., Thumanu, K., Kamolmanit, B., Brauman, A. & Lawongsa, P. (2020). Assessing the effect of rubber (*Hevea brasiliensis* (Willd. ex A. Juss.) Muell. Arg.) leaf chemical composition on some soil properties of differently aged rubber tree plantations. *Agronomy*, 10(12): p.1871. doi:10.3390/agronomy10121871.

Reddy, P. P. (2015). Cassava, *Manihot esculenta*. In Reddy, P. P. (Ed.). *Plant Protection in Tropical Root and Tuber Crops* (1st ed, pp. 17-81). New Delhi: Springer India.

Saengchan, C., Phansak, P., Le Thanh, T., Papathoti, N. K., & Buensanteai, N. (2021). Efficacy of salicylic acid and a *Bacillus* bioproduct in enhancing growth of cassava and controlling root rot disease. *Journal of Plant Protection Research*, 61(3): 302-310. doi:10.24425/jppr.2021.137952.

Saharan, V., Mehrotra, A., Khatik, R., Rawal, P., Sharma, S. S., & Pal, A. (2013). Synthesis of chitosan based nanoparticles and their *in vitro* evaluation against phytopathogenic fungi. *International Journal of Biological Macromolecules*, 62: 677-683. doi:10.1016/j.ijbiomac.2013.10.012.

Saharan, V., Sharma, G., Yadav, M., Choudhary, M. K., Sharma, S. S., Pal, A., Raliya, R., & Biswas, P. (2015). Synthesis and *in vitro* antifungal efficacy of Cu–chitosan nanoparticles against pathogenic fungi of tomato. *International Journal of Biological Macromolecules*, 75: 346-353. doi:10.1016/j.ijbiomac.2015.01.027.

Salachna, P., Byczyńska, A., Zawadzińska, A., Piechocki, R., & Mizielińska, M. (2019). Stimulatory effect of silver nanoparticles on the growth and flowering of potted oriental lilies. *Agronomy*, 9(10): 610. doi:10.3390/agronomy9100610.

Salama, H. M. (2012). Effects of silver nanoparticles in some crop plants, common bean (*Phaseolus vulgaris* L.) and corn (*Zea mays* L.). *International Research Journal of Biotechnology*, 3(10): 190-197.

Sangpueak, R., Phansak, P., Thumanu, K., Siriwong, S., Wongkaew, S., & Buensanteai, N. (2021. Effect of salicylic acid formulations on induced plant defense against cassava anthracnose disease. *The Plant Pathology Journal*, 37(4): p.356. doi:10.5423/PPJ.OA.02.2021.0015.

Sathiyabama, M., & Manikandan, A. (2016). Chitosan nanoparticle induced defense responses in fingermillet plants against blast disease caused by *Pyricularia grisea* (Cke.) Sacc. *Carbohydrate Polymers*, 154: 241-246. doi:10.1016/j.carbpol. 2016.06.089.

Sathiyabama, M., & Parthasarathy, R. (2016). Biological preparation of chitosan nanoparticles and its *in vitro* antifungal efficacy against some phytopathogenic fungi. *Carbohydrate Polymers*, 151: 321-325. doi:10.1016/j.carbpol.2016.05.033.

Siciliano, I., Gilardi, G., Ortu, G., Gisi, U., Gullino, M. L., & Garibaldi, A. (2017). Identification and characterization of *Alternaria* species causing leaf spot on cabbage, cauliflower, wild and cultivated rocket by using molecular and morphological features and mycotoxin production. *European Journal of Plant Pathology*, 149(2): 401-413. doi:10.1007/s10658-017-1190-0.

Skenderidis, P., Mitsagga, C., Giavasis, I., Petrotos, K., Lampakis, D., Leontopoulos, S., Hadjichristodoulou, C., & Tsakalof, A. (2019). The *in vitro* antimicrobial activity assessment of ultrasound assisted *Lycium barbarum* fruit extracts and pomegranate fruit peels. *Journal of Food Measurement and Characterization*, 13(3): 2017-2031. doi:10.1007/s11694-019-00123-6.

Suryadi, Y., Priyatno, T. P., Samudra, I., Susilowati, D. N., Sriharyani, T. S., & Syaefudin, S. (2019). Control of anthracnose disease (*Colletotrichum gloeosporioides*) using nano chitosan hydrolyzed by chitinase derived from *Burkholderia cepacia* Isolate E76. *Jurnal AgroBiogen*, 13(2): 111–122. doi:10.21082/jbio.v13n2.2017.p111-122.

Swati, K.J.A.J. (2020). Cu-chitosan nanoparticle induced plant growth and antibacterial activity against bacterial pustule disease in soybean (*Glycine max* (L.)). *Journal of Pharmacognosy and Phytochemistry*, 9(1): 450-455.

Tanapichatsakul, C., Pansanit, A., Monggoot, S., Brooks, S., Prachya, S., Kittakoop, P., Panuwet, P., & Pripdeevech, P. (2020). Antifungal activity of 8-methoxynaphthalen-1-ol isolated from the endophytic fungus *Diatrype palmicola* MFLUCC 17-0313 against the plant pathogenic fungus *Athelia rolfsii* on tomatoes. *PeerJ*, 8: p.e9103. doi:10.7717/peerj.9103.

Teri, J. M., Thurston, H. D., & Lozano, J. C. (1980). Effect of brown leaf spot and Cercospora leaf blight on cassava productivity. *Tropical Agriculture*, 57(3): 239-243.

Thepbandit, W., Papathoti, N. K., Daddam, J. R., Thumanu, K., Siriwong, S., Thanh, T. L., & Buensanteai, N. (2021). Identification of Salicylic Acid Mechanism against Leaf Blight Disease in *Oryza sativa* by SR-FTIR Microspectroscopic and Docking Studies. *Pathogens*, 10(6): p.652. doi:10.3390/pathogens10060652.

Thumanu, K., Sompong, M., Phansak, P., Nontapot, K., & Buensanteai, N. (2015). Use of infrared microspectroscopy to determine leaf biochemical composition of cassava in response to *Bacillus subtilis* CaSUT007. *Journal of Plant Interactions*, 10(1): 270-279. doi:10.1080/17429145.2015.1059957.

Thumanu, K., Wongchalee, D., Sompong, M., Phansak, P., Le Thanh, T., Namanusart, W., Vechklang, K., Kaewnum, S. & Buensanteai, N. (2017). Synchrotron-based FTIR microspectroscopy of chili resistance induced by *Bacillus subtilis* strain D604 against anthracnose disease. *Journal of Plant Interactions*, 12(1): 255-263. doi:10.1080/17429145.2017.1325523.

Wan, J., He, M., Hou, Q., Zou, L., Yang, Y., Wei, Y., & Chen, X. (2021). Cell wall associated immunity in plants. *Stress Biology*, 1(1): 1-15. doi:10.1007/s44154-021-00003-4.

Wang, J., Zhu, J., Huang, R., & Yang, Y. (2012). Investigation of cell wall composition related to stem lodging resistance in wheat (*Triticum aestivum* L.) by FTIR spectroscopy. *Plant Signaling & Behavior*, 7(7): 856-863. doi:10.4161/psb.20468.

War, A. R., Paulraj, M. G., War, M. Y., & Ignacimuthu, S. (2011). Role of salicylic acid in induction of plant defense system in chickpea (*Cicer arietinum* L.). *Plant Signaling & Behavior*, 6(11): 1787-1792. doi:10.4161/psb.6.11.17685.

Yu, P. (2005). Molecular chemistry imaging to reveal structural features of various plant feed tissues. *Journal of Structural Biology*, 150(1): 81-89. doi:10.1016/j.jsb.2005.01.005.

Zheng, H. H., Zhao, J., Wang, T. Y., & Wu, X. H. (2015). Characterization of *Alternaria* species associated with potato foliar diseases in China. *Plant Pathology*, 64(2): 425-433. doi:10.1111/ppa.12274.

APPENDIX

I. MEDIUMS

1.1 Water agar

Agar	15 g
Water	1000 mL

The agar was mixed with water and sterilized at 121°C for 20 min.

1.2 Potato Dextrose Agar

Potato	200 g
Dextrose	20 g
Agar	15 g
Water	1000 mL

The potato was extract to both. Then the mixture was added dextrose, agar, water and sterilized at 121°C for 20 min.

1.3 Potato Dextrose Broth

Potato	200 g
Dextrose	20 g
Water	1000 mL

The potato was extract to both. Then the mixture was added dextrose, water and sterilized at 121°C for 20 min.

1.4 Potato Dextrose Broth 2X

Potato	400 g
Dextrose	40 g
Water	1000 mL

The potato was extract to both. Then the mixture was added dextrose, water and sterilized at 121°C for 20 min.

II. CHEMICALS

2.1 20% glycerol

Glycerol	20 mL
DI Water	80 mL

The glycerol was dissolved in DI water and sterilized at 121°C for 20 min.

2.2 Acetyl trimethylammonium bromide (CTAB) buffer

Tris-HCl	15.764 g
NaCl	81.816 g
EDTA	5.8448 g
CTAB	20 g
DI Water	1000 mL
pH	8.0

The Tris-HCl, NaCl, EDTA, CTAB were mixed with DI water and adjusted pH. The the mixture was sterilized at 121°C for 20 min.

2.3 Chloroform: Isoamyl alcohol (24: 1) mixture

Chloroform	96 mL
Isoamyl alcohol	4 mL

The Chloroform was mix with Isoamyl alcohol.

2.4 Tris-EDTA (TE) buffer

Tris-HCl	1.5764 g
EDTA	0.29224 g
DI Water	1000 mL

pH	8.0

The Tris-HCl, EDTA were dissolved in DI water and adjusted pH. Then the mixture was sterilized at 121°C for 20 min.

2.5 0.4% Chitosan* (CS)

Chitosan	4 g
1% acetic acid in sterile DI Water	1000 mL

* 0.5% CS was prepared with a similar amount of linear chemical.

The chitosan was dissolved in 1% acetic acid in sterile DI water by stirring overnight.

2.6 0.2% Penta-Sodium triphosphate*

Penta-Sodium triphosphate	2 g
Sterile DI Water	1000 mL

* 0.5% Penta-Sodium triphosphate was prepared with a similar amount of linear chemical.

The penta-Sodium triphosphate was dissolved in sterile DI Water.

2.7 0.05% Salicylic acid* (SA)

Salicylic acid	0.5 g
Absolute Ethanol	20 mL
Sterile DI Water	980 mL

* 0.1 and 0.2% SA were prepared with a similar amount of linear chemical.

The salicylic acid was dissolved in absolute ethanol. Then the mixture was added sterile DI water.

2.8 Silver nitrate (SN) 1 mM

Silver nitrate	0.17 g
Sterile DI Water	1000 mL

* SN 2 and 3 mM were prepared with a similar amount of linear chemical.

The silver nitrate was dissolved in sterile DI water.

III. ATTACHED FIGURE

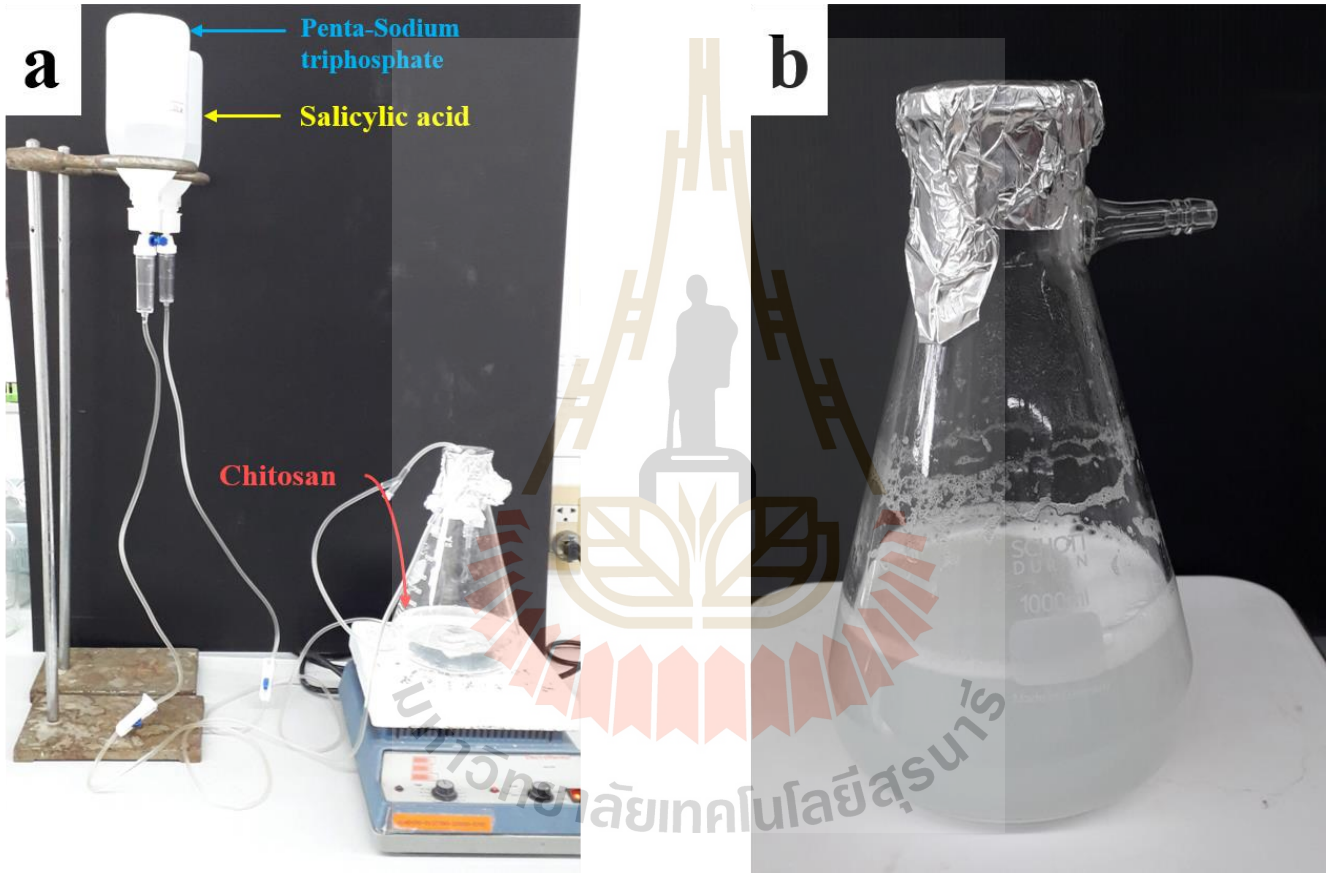

Attached figure 1. (**a**) Synthesis process CS-NP loaded SA and (**b**) their product.

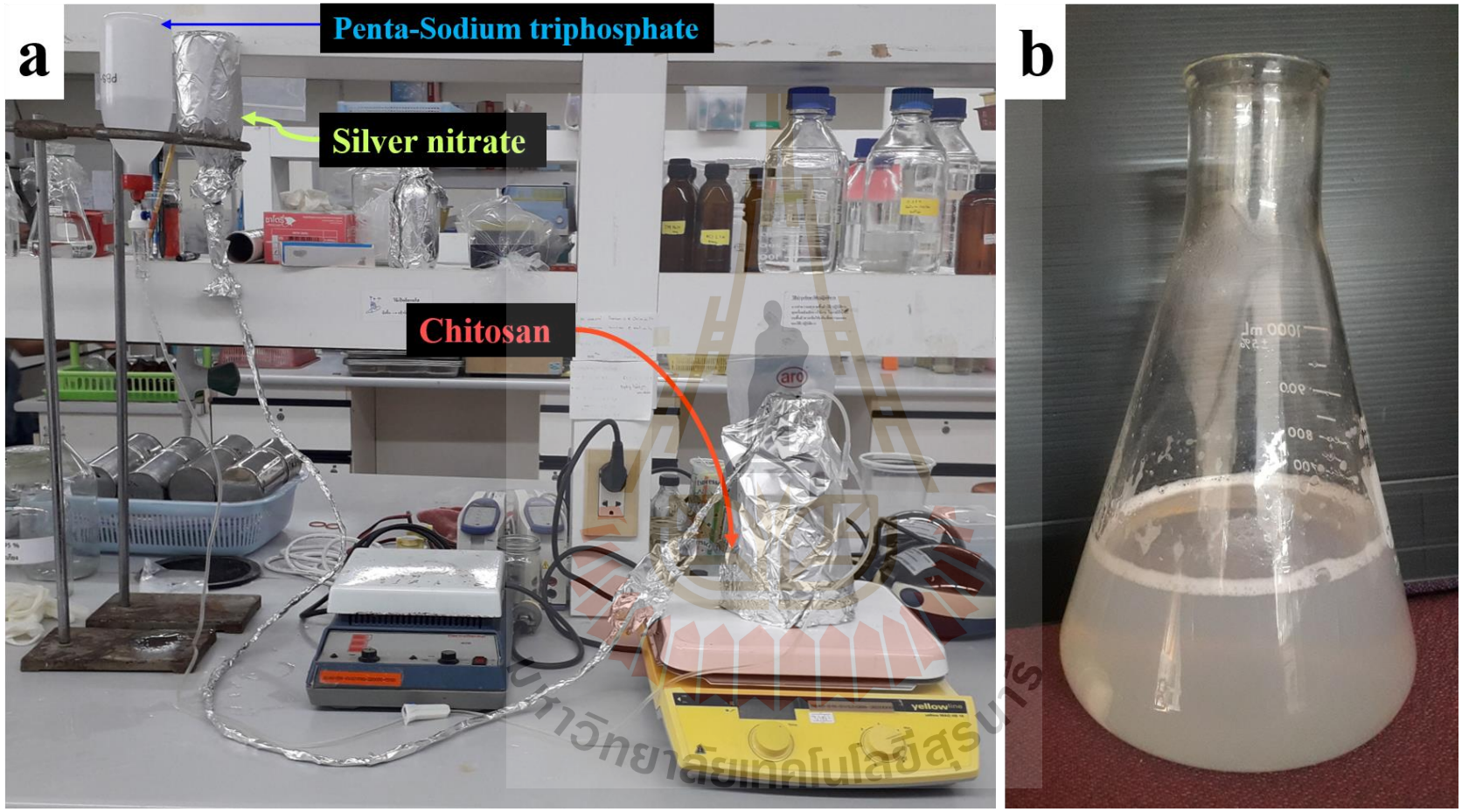

Attached figure 2. (a) Synthesis process CS-NP loaded silver and (b) their product.

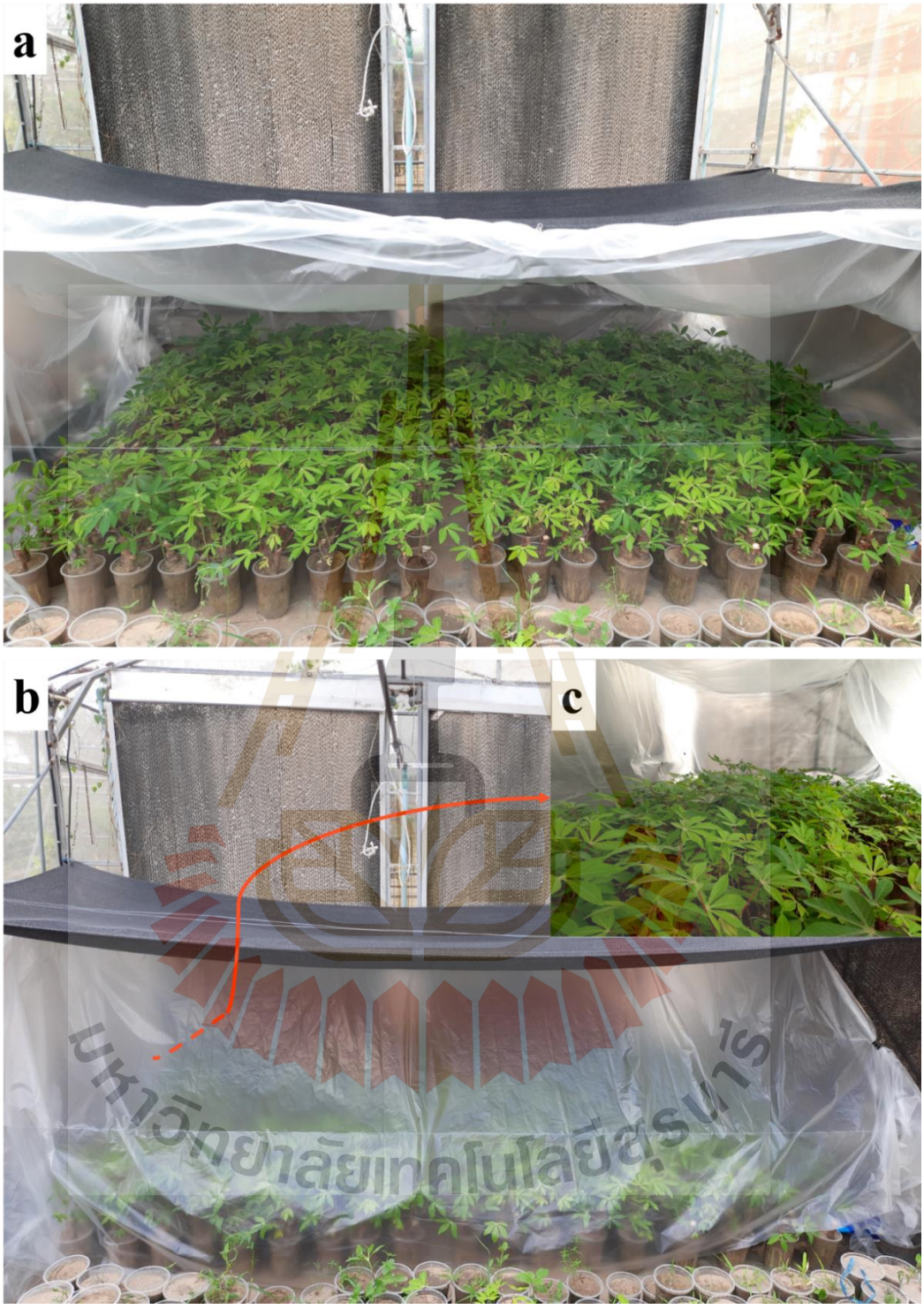

Attached figure 3. The incubation method of inoculation process in experiment at net house conditions. (a) Before and (b) After covered by plastic. (c) Everyday, the plants were sprayed by sterile water to maintain high humidity conditions.

BIOGRAPHY

Mr. Nguyen Huy Hoang was born on March, 1997 in An Hoa village, An Hoa commune, Chau Thanh district, An Giang province, Vietnam. He received his Bachelor of Plant Protection from the Can Tho University, Vietnam in 2019. During May 2018 - Aug 2018, he joins Exchange Student at Suranaree University of Technology, Thailand for 4 months. He started his career as a Research Assistant in The Biological Control Lab, Department of Plant Protection, College of Agriculture, Can Tho University, Vietnam from Dec 2018 - Jun 2019. In July, 2019, he received SUT OROG Scholarship [M6201616; No. 67/2562] to purpose a Master Degree in Suranaree University of Technology, Nakhon Ratchasima, Thailand.

Research output:

Hoang, N.H., Le Thanh, T., Kamkaew, A. and Buensanteai, N., 2021. Study of Nanoparticle Formulations Reduce Leaf Spot Disease and Enhance Plant Growth on Cassava. *The 2nd International Conference on Science and Technology (SUT-IVCST 2021)*. Nakhon-Ratchasima, Thailand, 6th August 2021. (**Full text and Oral**)

Hoang, N.H., Le Thanh, T., Thepbandit, W., Treekoon, J., Saengchan, C., Sangpueak, R., Papathoti, N.K., Kamkaew, A. and Buensanteai, N., 2022. Efficacy of Chitosan Nanoparticle Loaded-Salicylic Acid and-Silver on Management of Cassava Leaf Spot Disease. Polymers, 14(4), p.660. doi: 10.3390/polym14040660 (IF 4.329, Q1)

Hoang, N.H., Le Thanh, T., Sangpueak, R., Treekoon, J., Saengchan, C., Thepbandit, W., Papathoti, N.K., Kamkaew, A. and Buensanteai, N., 2022. Chitosan Nanoparticles-Based Ionic Gelation Method: A Promising Candidate for Plant Disease Management. Polymers, 14(4), p.662. doi: 10.3390/polym14040662 (IF 4.329, Q1)

Two original manuscript in preparation.